INDUCTION OF SECONDARY METABOLISM OF SOME MARINE DERIVED *STREPTOMYCES* SPECIES, AND ISOLATION AND IDENTIFICATION OF THEIR BIOACTIVE SECONDARY METABOLITES

A Thesis Submitted to
the Graduate School of Engineering and Sciences of
İzmir Institute of Technology
in Partial Fulfilment of the Requirements for the Degree of

MASTER OF SCIENCE

in Biotechnology

by
Emre GEZER

December 2020
İZMİR

ACKNOWLEDGEMENT

I am grateful to Prof. Dr. Erdal BEDİR for giving me chance to do this thesis study. His continuous guidance is greatly valuable,

I would like to thank to Eyüp BİLGİ and Melis KÜÇÜKSOLAK sharing their knowledge and experience during my research,

I would like to thank to Gamze DOĞAN, Göklem ÜNER and Ünver KURT for assisting structure elucidation studies,

I also want to thank all Bedir Group members,

I am grateful to Assoc. Prof. Dr. Ali Oğuz BÜYÜKKİLECİ for providing his laboratory to use and sharing valuable knowledge,

I am also grateful to Prof. Dr. Ataç UZEL for providing *S. cacaoi* and *S. rochei* from his microbial collection.

I am appreciated to Lecturers, Evrim PAŞIK and Yekta GÜNAY, and management of BIYOMER for their technical supports,

I am deeply thankful to Menşure ELVAN for her patience and support,

I would like to thank to my friends, Kadir GEZER, Alperay TARIM, Devran DEMİRBAŞ, Aslı KABAŞ and Ezgi DEMİRÖZ for valuable times and their support,

I would like to thank to Mine SARAÇ, Sevim SARAÇ and İbrahim SARAÇ for their valuable support,

Finally, I am deeply grateful to my mother Mevlüde GEZER, my father Mehmet GEZER, my sister Mutlu GEZER, and my brothers Sedat GEZER and Uğur GEZER.

This study was supported by the BAP Project “2019IYTE0273”.

İzmir, December 2020

Emre GEZER

ABSTRACT

INDUCTION OF SECONDARY METABOLISM OF SOME MARINE DERIVED *STREPTOMYCES* SPECIES, AND ISOLATION AND IDENTIFICATION OF THEIR BIOACTIVE SECONDARY METABOLITES

Secondary metabolites are natural products with low molecular weight produced by different organisms. These metabolites have a wide variety of bioactivities because of their adaptive roles in the nature. These properties make secondary metabolites important source in drug discovery studies. *Streptomyces* genus, on the other hand, attracts attention due to their ability to produce many secondary metabolites for the treatment of various diseases, especially infectious diseases and cancer. However, secondary metabolism is not fully expressed under standard laboratory conditions as in nature. This phenomenon limits the discovery of new/novel bioactive molecules from the microbial sources.

In this study, a previously studied marine derived actinobacterium, namely *Streptomyces cacaoi*, was investigated further to discover new antimicrobial metabolites via medium and temperature optimization using Box Behnken design. As a result, GPM medium containing 2.25% glycerol, 1% peptone water, 0.2% $CaCO_3$, 0.1% $MgCl_2$ in distilled water was found to provide the highest chemical diversity with potent bioactivity at 30^oC. In subsequent studies, inductive effects of some microorganisms and inorganic compounds on secondary metabolism were also determined.

Using optimized conditions, a larger fermentation study was undertaken (25 L) followed by extraction and isolation procedures. Sixteen metabolites were purified by chromatographic methods, and structures of the isolates were elucidated by spectral methods. Thirteen compounds, five of which were new, were members of polyketide-type polyether antibiotics. The structures of other molecules were determined as cyclo(Thr-Trp), 6-hydroxy-6-methyloctanoic acid, and 5-hydroxy-1,6-diazacycloundec-5-en-2-one, and all were found to be new. In antimicrobial tests, most polyethers were found to be active against Gram-positive bacteria. In particular, two new polyethers **SC-EG-05** and **SC-EG-07** showed higher antimicrobial activity than widely used antibiotic vancomycin.

ÖZET

BAZI DENİZ KAYNAKLI *STREPTOMYCES* TÜRLERİNİN İKİNCİL METABOLİZMASININ İNDÜKLENMESİ, VE BİYOAKTİF İKİNCİL METABOLİTLERİNİN İZOLASYONU VE TANIMLANMASI

İkincil metabolitler birçok farklı organizma tarafından üretilen düşük molekül ağırlıklı doğal ürünlerdir. Bu moleküller doğada gösterdikleri adaptif rolleri nedeniyle çeşitli biyoaktivitelere sahiptirler. Bu özellikleriyle ikincil metabolitler ilaç keşfi çalışmalarında çok önemli bir kaynak durumundadırlar. *Streptomyces* türü bakteriler ise enfeksiyonlar ve kanser başta olmak üzere çeşitli hastalıkların tedavisi için umut vaat eden biyoaktif metabolitlerin üreticisi olarak ilgi çekmektedirler. Ancak ikincil metabolizma, standart laboratuvar şartlarında tümüyle ifade edilmemektedir. Bu durum mikrobiyal kaynaklardan yeni/özgün biyoaktif moleküllerin keşfini kısıtlamaktadır.

Bu çalışmada, daha önce çalışılmış bir denizel türevli aktinobakteri olan *Streptomyces cacaoi*'den, Box-Behnken tasarım ile besiyeri ve sıcaklık optimizasyonu yapılarak yeni antimikrobiyal metabolitlerin elde edilmesi amaçlanmıştır. Sonuç olarak, distile suda %2.25 gliserol, %1 peptone-water, %0.2 $CaCO_3$, %0.1 $MgCl_2$ içeren GPM besiyerinin 30°C sıcaklıkta en fazla kimyasal çeşitliliği ve en yüksek biyoaktiviteyi sağladığı görülmüştür. İleri çalışmalarda ise bazı mikroorganizmaların ve inorganik bileşiklerin ikincil metabolizma üzerine indükleyici etkileri tespit edilmiştir.

Optimize koşullar kullanılarak büyük ölçekte fermentasyon (25 L) gerçekleştirilmiş, ekstraksiyon ve izolasyon çalışmaları yapılmıştır. Kromatografik yöntemlerle 16 metabolit saflaştırılmış ve spektral yöntemlerle yapıları aydınlatılmıştır. Metabolitlerin 13'ünün poliketit tipi polieter antibiyotik oldukları ve bunların beş tanesinin literatür için yeni oldukları anlaşılmıştır. Diğer üç molekülün yapılarının ise siklo(Thr-Trp), 6-hidroksi-6-metiloktanoik asit ve 5-hidroksi-1,6-diazasikloundek-5-en-2-on olduğu belirlenmiş ve tümünün yeni olduğu anlaşılmıştır. Yapılan antimikrobiyal testlerde polieterlerin Gram-pozitif bakterilere karşı aktif oldukları tespit edilmiştir. Özellikle, yeni oldukları anlaşılan **SC-EG-05** ve **SC-EG-07** kodlu polieterler, antibiyotik olarak sıklıkla kullanılan vankomisinden daha yüksek antimikrobiyal aktivite göstermiştir.

TABLE OF CONTENTS

LIST OF FIGURES

Figure **Page**

Figure	**Page**

LIST OF TABLES

Table	**Page**

Table	**Page**

LIST OF SPECTRA

Spectrum **Page**

Spectrum **Page**

ABBREVIATIONS

- $CHCl_3$ — Chloroform
- EtOH — Ethanol
- DMSO — Dimethyl sulfoxide
- EtOAc — Ethyl acetate
- MeOH — Methanol
- Hex — *n*-Hexane
- ACE — Acetone
- CH_2CI_2 — Dichloromethane
- H_2SO_4 — Sulfuric Acid
- H_2O — Water
- $CDCI_3$ — Deuterated chloroform
- CD_3OD — Deuterated methanol
- UV — Ultraviolet
- TLC — Thin Layer Chromatography
- HPLC — High Performance Liquid Chromatography
- NMR — Nuclear Magnetic Resonance
- 1D-NMR — One-Dimensional Nuclear Magnetic Resonance
- 2D-NMR — Two-Dimensional Nuclear Magnetic Resonance
- ^{1}H-NMR — Proton Nuclear Magnetic Resonance
- ^{13}C-NMR — Carbon Nuclear Magnetic Resonance
- HSQC — Heteronuclear Single Quantum Coherence
- HMBC — Heteronuclear Multiple Bond Coherence
- COSY — Correlation Spectroscopy
- NOESY — Nuclear Overhauser Enhancement Spectroscopy
- *m* — Multiplet
- *s* — Singlet
- *d* — Doublet
- *t* — Triplet
- *dd* — Doublet-doublet

CHAPTER 1

INTRODUCTION

Secondary metabolites, also called natural products, are small organic compounds produced by different organisms.[1,2,3,4] Unlike primary metabolites, they have no direct effect on growth and development of the organisms. However, they have survival functions and give producer organisms important advantages in nature. Secondary metabolites could be toxic agents used against antagonist organisms; agents of symbiosis between bacteria and fungi,[5] plants, insects, and higher animals; chelating or differentiation agents.[6]

The roles of microbial secondary metabolites in nature have not been fully understood. The incredible diversity in their chemical structure gives different functions and specificities. Sunscreen molecules are an example of the different functions that natural products can have. Many marine derived organisms produce mycosporines which protect the producer from high solar radiance by absorbing UV light.[7,8] All these properties have made secondary metabolites important tools in biotechnological uses.

Secondary metabolites are mainly used as a source for therapeutic agents needed in human medicine, animal health, and plant crop protection.[9,10] They are used extensively in the pharmaceutical industry due to their antimicrobial, antiviral, antitumor, cholesterol lowering, immunosuppressant, antiparasitic, herbicide, insecticide and many other effects.[11,12] From January 1981 to September 2019, 441 (23.5%) of the 1881 approved therapeutic agents were natural products.[13] Secondary metabolites are not only directly therapeutic agents, but also a source of inspiration for many synthetic therapeutic agents. With natural product-inspired classification (natural pharmacophore containing synthetic products[14] and natural product mimics[15]) the proportion of approved natural therapeutics rises to 49.2%.[13, 16] Also, natural products are generally less toxic and more biologically friendly because of their co-evolution with the target sites they affect.[17]

There is a growing need for new therapeutic agents. In particular, the multi-drug resistance developed by pathogens,[18] the severe side effects of current anti-cancer drugs,[19] and the emergence of new epidemics at any moment[20] indicate the necessity of drug discovery studies. In this context, secondary metabolites will continue to be an important source for the pharmaceutical industry.

1.1. *Actinobacteria*

Actinobacteria are filamentous Gram-positive bacteria belonging to the *Actinomycetales* order.[21] They also draw attention with their guanine-cytosine ratio, which can exceed 70% in their DNA.[22] *Actinobacteria* are abundant in the soil and play an important role in the carbon cycle by breaking down various dead organisms with extracellular hydrolytic enzymes.[23]

Most of the *actinobacteria* are aerobic and their oxygen needs are very high. Although few thermophilic strains are encountered, most of *actinobacteria* are mesophilic and show optimal growth at the temperature range 25ºC to 30ºC.[24,25] Also, most of them are found in neutral soils and grow maximally in the range of pH 6 and pH 9.[25]

Morphologically, *actinobacteria* have easily recognizable features. They produce two types of mycelium: substrate (vegetative) and aerial mycelium (aerial hyphae). Substrate mycelium causes the formation of submerged colonies, and air mycelium causes the formation of limy colony morphologies by producing reproductive spores, on solid media. The color of the mycelium may be cream, gray, or white as well as yellow, pink, red, orange, green and brown (Figure 1.1). [24,25]

Figure 1.1. Colonies of different *actinobacteria* strains on agar plates; *Streptomyces rochei* (brown), *Streptomyces cacaoi* (white), and *Streptomyces sp.* (pinkish) respectively.

Actinobacteria reproduce by sporulation which is highly correlated process with secondary metabolism.[26,27] Presence of genes that regulate both sporulation and secondary metabolite production has been demonstrated.[28,29] The developmental life cycle of *actinobacteria* begin with a free spore. Hyphae is developed by germination of the spore. Then, the hyphae grows and forms the substrate mycelium by extension and branching. The mycelium continues to grow and most of the secondary metabolites are considered to be produced at this stage (Figure 1.2).[25, 30] However, presence of secondary metabolites produced only in the early stages has been shown.[31]

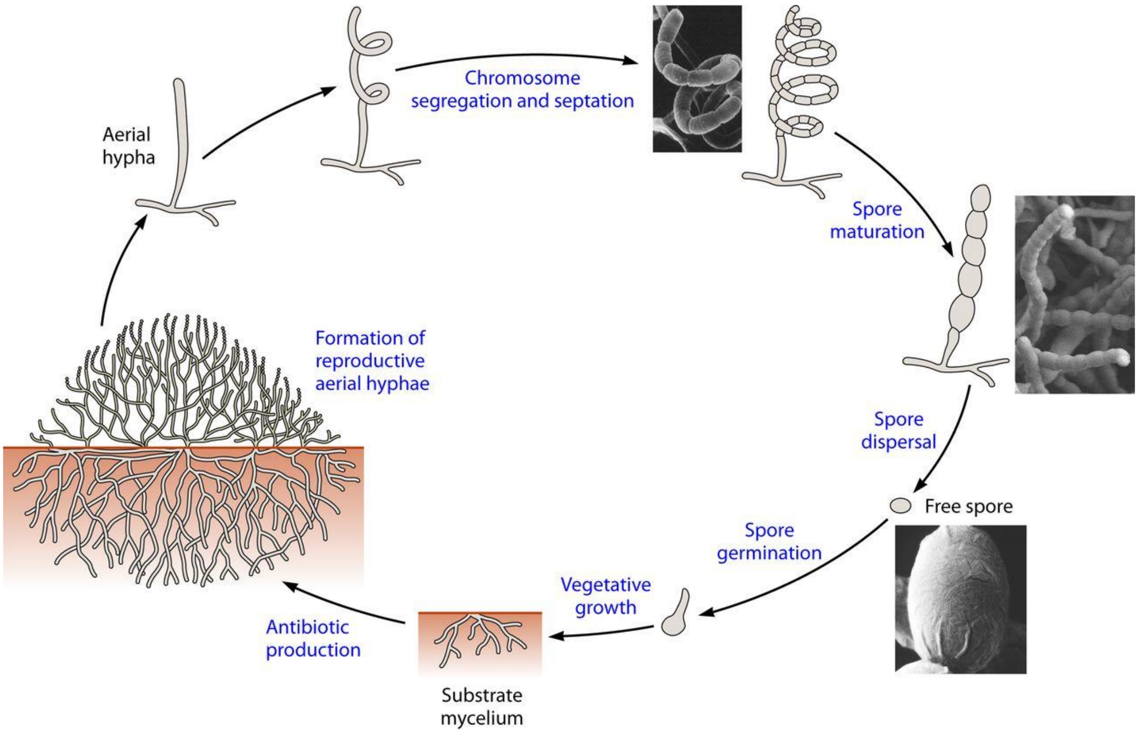

Figure 1.2. Schema of the life cycle of *actinobacteria*[25].

1.1.1. Actinobacterial Secondary Metabolites

Actinobacteria are commercially valuable for their capacity to produce a wide variety of secondary metabolites. Large number of secondary metabolites showing different bioactivity such as antimicrobial, antioxidant, cytotoxic, antitumor, immunosuppressive, and cardiovascular were isolated from *actinobacteria*.[21]

Approximately 500,000 secondary metabolites were obtained from different organisms and 60,000 of them were found to be biologically active. The number of microbial derived secondary metabolites is around 70,000, but ~30,000 of them have activity, which mean half of the total bioactive secondary metabolites. In addition, 0.3%

of all known secondary metabolites marketed as drugs, and this ratio is 0.6% for microbial secondary metabolites.[32] About half of the microbial bioactive secondary metabolites were obtained from *actinobacteria*. All these data make *actinobacteria* important source in drug discovery studies.[33]

1.1.2. *Streptomyces* Genus

Streptomyces is the largest genus of *actinobacteria*, with over 500 identified species.[34] They are producer for 75% of the secondary metabolites of *actinobacteria*.[33] On average, the genome of each strain is capable of producing 15-25 secondary metabolites.[35] These molecules mainly show antimicrobial, antiviral, antitumor, antioxidant and immunosuppressive effects.[36,37] In particular, they constitute the most important source for antibiotic production (Table 1.1).[38]

Table 1.1. Some approved secondary metabolites from *Streptomyces* genus.

Name	**Source**	**Activity**
Daptomycin[39]	*Streptomyces roseosporus*	Antibiotic against Gram-positive bacteria
Ivermectin[40] (Avermectin derivative)	*Streptomyces avermitilis*	Anti-parasite against worm infestations
Lincomycin[41]	*Streptomyces lincolnensis*	Antibiotic against Gram-positive bacteria
Monensin[42]	*Streptomyces cinnamonensis*	Antibiotic, Antiprotozoal
Nystatin[43]	*Streptomyces noursei*	Antibiotic against yeasts and fungi
Pimecrolimus[44] (Ascomycin derivative)	*Streptomyces hygroscopicus*	Immunomodulator for atopic dermatitis

(cont. on next page)

cont. Table 1.1

Ribostamycin[45]	*Streptomyces ribosidificus*	Antibiotic against Gram-negative bacteria
Sirolimus[46,47,48] (Rapamycin)	*Streptomyces hygroscopicus*	Antifungal, Antineoplastic and Immunosuppressant
Streptomycin[49]	*Streptomyces griseus*	Antibiotic against Gram-negative and Gram-posiive bacteria and *Mycobacterium tuberculosis*
Streptozocin[50]	*Stretomyces achromogenes*	Antitumour for metastatic pancreatic islet cell carcinoma
Doxorubicin[51]	*Streptomyces peucetius*	Antitumor agent for neoplastic diseases
Bleomycin[52]	*Streptomyces verticillus*	Antineoplastic for solid tumors

Streptomyces reside in many different terrestrial ecosystems such as mountain and desert, as well as in aquatic ecosystems such as marine and lake. Also, they can be found in/on many different organisms such as plants, ants, insects, bees, fish, and sponges. These environmental variations require *Streptomyces* to adapt to different ecological conditions, making them producers of different secondary metabolites. This phenomenon has made *Streptomyces*, living in extreme ecosystems, promising for the discovery of new/novel secondary metabolites.[30]

1.1.3. Marine Environment and Marine Derived *Streptomyces*

Marine environments harbor high biodiversity such that some marine habitats have more diverse organisms than rainforests.[53] Microorganisms constitute the richest secondary metabolite source among these organisms.[54] They exist freely in seawater and sediments as well as in/on other marine organisms.[55,56] In metagenomic studies on marine, it was observed that approximately 30% of the microbial population were *actinobacteria*.

Also, the presence of *actinobacteria* has been detected in many regions of the oceans, such as 11 km deep and regions with hydrate accumulation.[24] Figure 1.3 shows microbial isolates from sediment samples collected from Aegean Sea.

Marine environments have quite different conditions compared to terrestrial environments, such as high salinity and high pressure. This situation causes the secondary metabolism, which expression is under the control of environmental conditions, to be different from those in terrestrial organisms.[35] In this way, wide range of *actinobacteria*, many of which are *Streptomyces*, have been isolated from the marine in the hope of obtaining new/novel secondary metabolites.[57]

A large number of peptides, quinone, macrolide, terpene, polyketide, alkaloid, flavonoid group secondary metabolites were obtained from marine derived *Streptomyces.*[57] Among them, there are promising molecules with antitumor, antimicrobial, antidiabetic, antioxidant, and antiviral activity. Also, Salinosporamide A, obtained from *Salinispora tropica*, is in clinical trials for use in various types of cancer.[58,59] Marine derived *Streptomyces* continue to be investigated as a natural therapeutic source. In 2018, 167 new secondary metabolites were obtained from the marine derived *Streptomyces* genus, equaled to 69% of bacterial metabolites.[54]

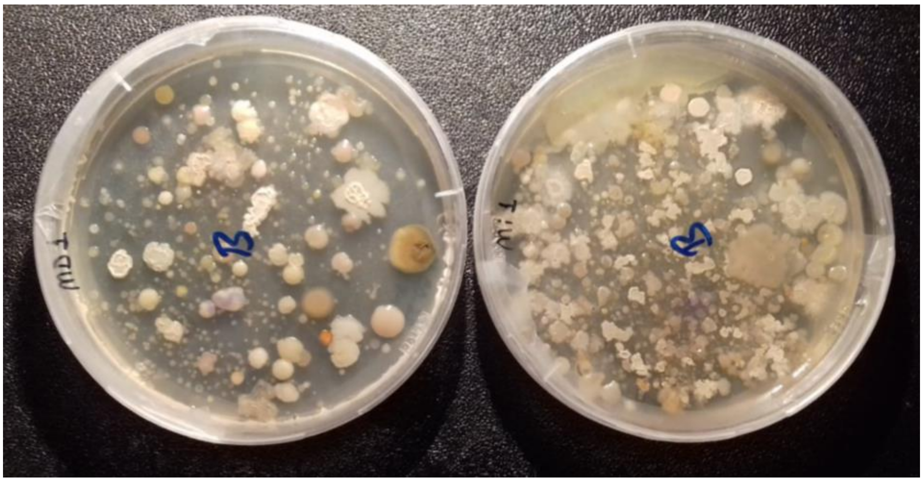

Figure 1.3. Microbial isolates from sediment samples.

Table 1.2. Some novel secondary metabolites from marine derived *Streptomyces*.

Name	Source	Production Medium	Activity
Aureoverticillactam [60]	*Streptomyces aureoverticillatus*	Starch 5 g, Hydro Solubles 4 mL, fish meal 2 g, kelp powder 2 g, and chitosan 2 g in 1 L seawater	Cytotoxicity against various tumor cell lines
Frigocyclinone[61]	*Streptomyces griseus*	Glucose 1%, starch 2%, Bacto peptone 0.3%, meat extract 0.3%, yeast extract 0.5%, and CaCO3 0.3% in tap water	Antibacterial against Gram-positive bacteria
Lajollamycin[62]	*Streptomyces nodosus*	Starch 5 g, Hydro Solubles 4 mL, fish meal 2 g, kelp powder 2 g, and chitosan 2 g in 1L seawater	Antibacterial against Gram-positive bacteria and cytotoxic for B16-F10 tumor cells
Essramycin[63]	*Streptomyces sp.*	Galactose 2.0% galactose, dextrin 2.0% dextrin, 1.0% Bacto-soytone, and 0.5% corn steep liquor in %75 seawater	Antibacterial against Gram-positive and Gram-negative bacteria
Cyclomarin A [64,65]	*Streptomyces sp.*	Starch 10 g, yeast extract 4 g, peptone 2 g in 1000 ml seawater	Antiinflammatory, antimicrobial against *Mycobacterium tuberculosis*
Tirandamycin C [66]	*Streptomyces sp.*	Dextrose 10 g, NZ-Amine A 2 g, yeast extract 1 g, meat extract 0.77 g, NaCl 30 g in seawater	Antimicrobial Vancomycin-resistant *Enterococcus faecalis*
Salinamide A [67]	*Streptomyces sp.*	1% starch, 0.4% yeast extract, 0.2% peptone in 75% seawater	Antiinflammatory
Gutingimycin [68]	*Streptomyces sp.*	Malt extract, yeast extract and glucose	Antibacterial against Gram-positive and Gram-negative bacteria
Komodoquinone A [69]	*Streptomyces sp.*	0.5% glucose and 2% yeast extract and 2.5% rice in artificial seawater	Neurogenic

1.2. Chemistry of Secondary Metabolism

Secondary metabolites are the product of a long series of enzymatically catalyzed reactions. The building blocks forming the skeleton of the secondary metabolite are derived from primary metabolism and most of them are derived from the **acetyl coenzyme A** (acetate pathway), **shikimic acid** (shikimate pathway), **mevalonic acid** (mevalonate pathway), and **methylerythritol phosphate** (methylerythritol phosphate pathway) (Figure 1.4).[70]

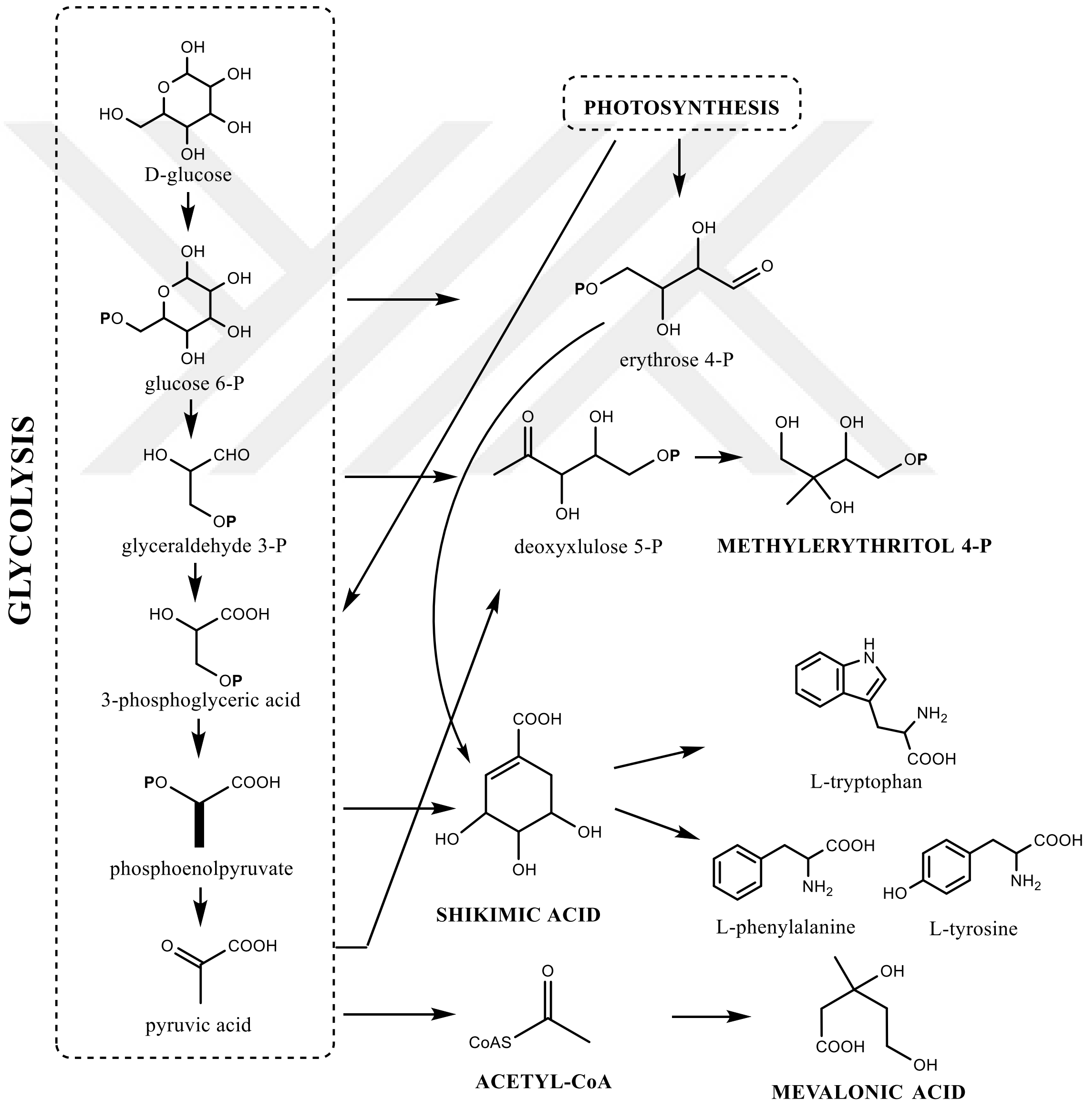

Figure 1.4. Sources of secondary metabolite building blocks.[70]

The **acetate pathway** includes biosynthesis of phenols, prostaglandins, macrolide antibiotics, and polyether antibiotics; the **shikimate pathway** provides the synthesis of phenols, cinnamic acid derivatives, lignans, and alkaloids; and both **mevalonate** and **methylerythritol phosphate pathways** are responsible for a variety of terpenoid and steroid biosynthesis.[70]

1.3. Genetics of Secondary Metabolism

The biosynthesis of a secondary metabolite requires the presence of many different enzymes. The genes of these sequential enzymes can be found clustered on chromosomes.[71] This genome organization, called secondary metabolite gene clusters (SMGCs), contains genes encoding main enzymes involved in the formation of skeletons and tailoring enzymes which modify the skeletons of secondary metabolites.[72] In some cases, SMGCs also contain genes for pathway-specific regulators that control transcription.[73] For example, in the biosynthesis of polyether antibiotic nigericin, 11 genes encoding polyketide synthases (PKSs) module, 6 genes encoding tailoring enzymes, and 2 regulatory genes were identified.[74] These 19 genes are clustered and organized as five operons (Figure 1.5).[75]

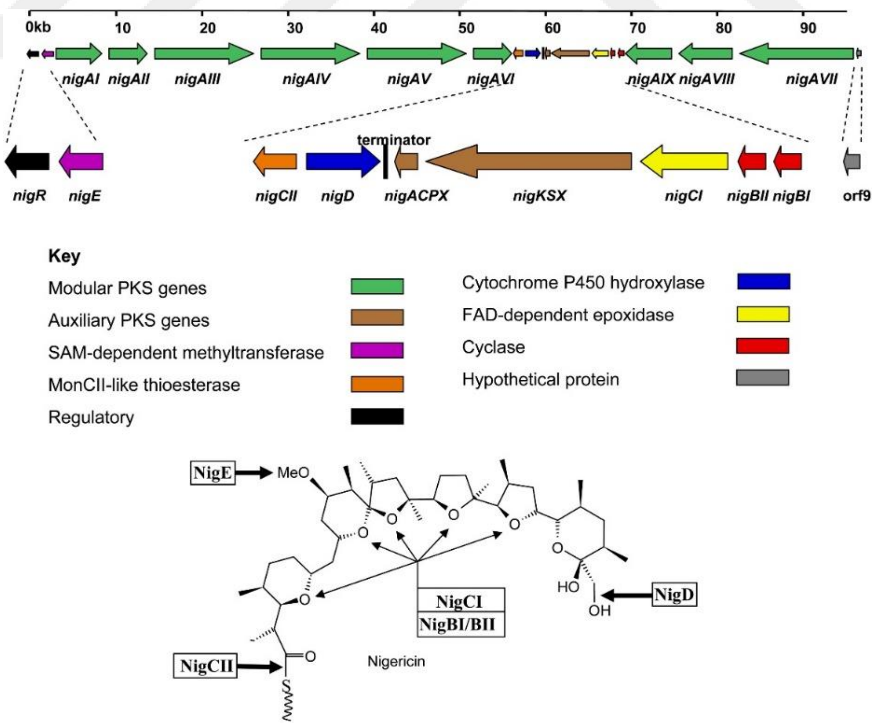

Figure 1.5. Nigericin gene cluster of *Streptomyces* sp. DSM4137.73 Each arrow indicates an open reading frame (ORF) and the direction of transcription.[75]

Two evolutionary advantages are shown as cause for the clustering of secondary metabolite genes: The fact that secondary metabolite genes are functionally related to each other and that they complement each other in the biosynthetic pathway bring the need for physical regulation of these genes; and the need to transfer such genes to other organisms by horizontal gene transfer or to the new generation by vertical gene transfer.[72, 76]

Another feature of secondary metabolite gene clusters is that they are located in the 'arm' region of chromosomes. While genes encoding essential functions for the organism are located in core regions of chromosomes, SMGCs are located close to the ends of chromosomes.[76,77,78] These regions, which are called sub-telomeric in eukaryotic chromosomes, play an important role in adaptive evolution by facilitating different rearrangements such as recombinations, deletions and inversions.[79] Also, the end regions of chromosomes have specific silencing mechanisms. Chromatin remodeling in eukaryotes and histone-like proteins in prokaryotes modulate the biosynthesis of secondary metabolites.[78,80] Clustering of secondary metabolic genes facilitate this modulation process. A chromatin-based silencing can simultaneously suppress the transcription of all genes involved in the cluster. Likewise, histone deacetylation and transcriptional activation can progress throughout the entire cluster to produce relevant secondary metabolite as a rapid response.[72]

These properties of SMGCs make it possible for secondary metabolites to act as adaptive agents. The expression of SMGCs depends on environmental conditions and this adaptive situation provides the organism very important advantages in nature. However, this feature causes many SMGCs to be silent (cryptic) under standard laboratory conditions, and the discovery of new/novel molecules in natural product research becomes difficult.

1.4. Induction of Secondary Metabolism

There are various approaches to activate silent SMGCs in bacteria[81], fungi[82] as well as plants.[83] One of the approaches is manipulation of the cultuvation conditions. The expression of microbial secondary metabolism is entirely dependent on the medium used.[84] Thus, it is very important to determine the appropriate carbon and nitrogen sources for each strain. By changing the incubation conditions, the expression of secondary metabolism can be increased/altered, and the biosynthesis of different secondary metabolites can be achieved. Various metabolic pathways are activated randomly with this approach, which is called one strain many compounds (OSMAC).[85]

Metabolic pathways can be activated by adding various chemicals or solvents to the bacteria. Heavy metals such as scandium and lanthanum have been reported to increase antibiotic production in some *actinobacteria*.[86] DMSO makes qualitative and quantitative changes in the production of secondary metabolites. Three-fold increase in the amount of chloramphenicol and tetracenomycin was observed when *Streptomyces venezuelae* and *Streptomyces glaucescens* were cultured in medium containing DMSO.[87] A marine derived fungus was incubated in a medium containing 1% ethanol and a new antibiotic, pestalone, was obtained. Pestalone has been found to have potent antimicrobial and antitumor effect and is not produced under standard incubation conditions. In addition, it has been shown that the addition of ethanol to the medium at rates varying between 0.2% and 6% significantly increases the production of different antibiotics in some *actinobacteria*.[88]

Another technique of the OSMAC is co-cultivation in which more than one microorganism is cultured together. This coexistence enables microbial communications, and these interactions can activate various metabolic pathways. There are many studies showing that silent SMGCs are activated in *actinobacteria* by co-cultivation with *actinobacteria*, other bacteria or fungi.[86] Co-cuture not only activates the silent SMGCs but also increases the synthesis of metabolites produced in small quantities. For example, co-culture of *Streptomyces griseorubiginosus* with *Pseudomonas maltophilia* increased the production of biphenomycin A, a cyclic peptide antibiotic, 60-fold.[89] There are also several studies using killed microorganisms as the second strain in co-culture. When *Streptomyces coelicolor* was co-cultured with heat killed *Bacillus subtilis* cells, a 256% increase in undecylprodigiosin production was observed.[90]

In this thesis, a marine derived microorganism, viz. *Streptomyces cacaoi*, was investigated to obtain new and bioactive secondary metabolites. In the first phase, a secondary metabolism induction study was performed to increase chemical diversity, amount of metabolites and bioactivity. The design was as follows;

- ✓ compare the efficiency of different growth media on the secondary metabolism and determine the best medium,
- ✓ observe the effects of selected medium contents on secondary metabolism using experimental design approaches.

- ✓ utilize co-culturing with different microorganisms, and supplementing chemicals to induce secondary metabolism,

In the second part, preparative studies to obtain the metabolites were carried out under optimized conditions. In this context, the approach was:

- ✓ purify the secondary metabolites produced and elucidate their chemical structures,
- ✓ determine the antimicrobial effects of the purified molecules,

to prove importance of optimization and induction studies in biosynthesis of secondary metabolites.

CHAPTER 2

MATERIALS AND METHODS

2.1. Materials

Used microorganisms, media, chemicals, and instruments are listed below.

2.1.1. Microorganisms

Streptomyces cacaoi (JX912350.1), which was previously isolated from marine, was used as producer microorganism. Apart from producer, several microorganisms were used as inducer in the fermentation and other several strains were used as test microorganisms in the antimicrobial assays.

For induction studies; *Streptomyces rochei* (JX912315.1), *Bacillus subtilis* ATCC 19659, *Candida albicans* ATCC 64548, *Alternaria alternata* (KU866390.1), *Alternaria eureka* (FR799468.1), *Fusarium solani* (KT583204.1), *Penicillium roseopurpureum* (KJ775658.1), *Penicillium sp.* (JQ781815.1), *Neosartorya hiratsukae* (FR733873.1) *and Camarosporium laburnicola* (JQ781815.1) were used.

For antibacterial assays; *Bacillus subtilis* ATCC 19659, methicillin-resistant *Staphylococcus aureus* (MRSA) ATCC 63300, *Listeria innocua* NRRL-B 33314, *Escherichia coli* O157:H7, *Escherichia coli* JM 109 and *Candida albicans* ATCC 64548 were used.

Figure 2.1. *Streptomyces cacaoi* colonies on agar plate and under light microscope.

2.1.2. Used Culture Media

Used media that are shown in Table 2.1, were sterilized by autoclaving for 15 minutes at 121 ºC (15 psi pressure), except Mannitol Soya Flour (SFM). SFM was sterilized for 20 minutes.

Table 2.1. Used media**.**

Medium	Ingredients	Usage
Tyriptic Soy Agar (TSA)	40 g of the powder (Merck Millipore-105458) dissolved in 1000 ml distilled water.	Activation of the bacterial strains.
Potato Dextrose Agar (PDA)	39 g of the powder (Merck Millipore-110130) dissolved in 1000 ml distilled water.	Activation of the fungal strains.
Mannitol Soya Flour (SFM)	Mannitol 20 g, soya flour 20 g, NaCl 15 g and agar 15 g dissolved in distilled water (Ph 8).	Sporulation of *Streptomyces* strains.
Müller-Hinton Agar (MHA)	38 g of the powder (Merck Millipore-105437) dissolved in 1000 ml distilled water.	Activation and growth of bacterial strains for the antimicrobial assays.
Sabouraud Dextrose Agar (SDA)	65 g of the powder (Merck Millipore-105438) dissolved in 1000 ml distilled water.	Activation and growth of *Candida albicans* for the antimicrobiyal assays.
M1 Broth	Soluble starch 10 g, peptone 2 g, yeast extract 4 g dissolved in 1000 ml distilled water or seawater (pH 7).	Fermentation studies.
Modified M6 Broth	Peptone 8 g, yeast extract 1 g, glucose 10 g dissolved in 1000 ml distilled water or seawater.	Fermentation studies.
Glycerol Peptone Medium (GPM)	2.25% glycerol, 1% peptone water, 0.2% $CaCO_3$, 0.1% $MgCl_2$ dissolved in distilled water (after optimization)	Fermentation studies.

2.1.3. Used Chemicals

The chemicals used in fermentation and isolation-purification studies are listed below.

2.1.3.1. Used Chemicals in Fermentation Studies

- Calcium carbonate: Sigma-Aldrich
- Copper (II) sulfate pentahydrate: Sigma-Aldrich
- Dimethyl Sulfoxide: Sigma-Aldrich
- Ethanol: Merck
- Glucose: Sigma-Aldrich
- Glycerol: Merck
- Iron (II) sulfate heptahydrate: Sigma-Aldrich
- Iron (III) chloride: Sigma-Aldrich
- Lithium carbonate: Sigma-Aldrich
- Lithium chloride: Sigma-Aldrich
- Magnesium chloride: Sigma-Aldrich
- Magnesium sulfate: Sigma-Aldrich
- D-Mannitol: Merck
- Peptone: Merck
- Peptone Water: Merck
- Potassium nitrate: Sigma-Aldrich
- Potassium Phosphate Dibasic: Sigma-Aldrich
- Seawater: Collected from Urla/Gulbahce coast
- Sodium chloride: Sigma-Aldrich
- Soluble starch: Sigma-Aldrich
- Soybean flour: Sigma-Aldrich
- Yeast extract: Merck
- Zinc: Sigma-Aldrich

2.1.3.2. Used Chemicals in Isolation

- Acetonitrile: VWR Chemicals
- Chloroform-d: Merck
- Dimethyl sulfoxide-d_6: Merck
- HPCL Grade Acetonitrile: VWR Chemicals

- Tert-butanol: Sigma-Aldrich
- Chloroform: Sigma-Aldrich
- Ethyl acetate: Sigma-Aldrich
- Formic acid: Sigma-Aldrich
- HCl: Merck, Darmstadt
- *n*-Hexane: Isolab
- *2*-Hexane: Isolab
- Methanol: Merck
- Erhanol: Merck
- HPLC Grade Methanol: Merck
- Methanol-d_4: Merck
- Sulfuric Acid: Merck

2.1.4. Instruments

- Autoclave: Nüve 90L
- Freeze Dryer: Labconco FreeZone Freeze Dry System
- HPLC: Thermo Scientific-Dionex Ultimate 3000
- Mass Spectrometry: Agilent 1200/6530 Instrument – HRTOFMS
- Nuclear Magnetic Resonance Spectrometry: Varian AS400 (400 MHz)
- Rotary Evaporator: Heidolph Laborota 4001; ISOLAB
- Shaking Incubator: SR-JSSI-300C
- SpeedVac Concentrator: Thermo Scientific Savant SPD 121P
- Phase Contrast Microscope: Olympus

2.2. Methods

First of all, the antimicrobial activity of the extracts that obtained from the fermentations of *Streptomyces cacaoi* with different media were compared. A newly developed medium namely glycerol-pepton medium (GPM) was designed with the help of literature and preliminary experiments. Initial contents of GPM (non-optimized) were 2% glycerol, 1% peptone water, 0.1% $CaCO_3$, 0.05% $MgCl_2$ and 0.05% $FeCl_3$ dissolved in distilled water containing 2% NaCl or 50% distilled water/seawater mixture. Once the effectiveness of GPM has been proven, the content of GPM has been further optimized to activate the secondary metabolism of *S. cacaoi*. Next, inducing effects of some chemicals on secondary metabolism were examined, and co-culture experiments were carried out with different microorganisms. After all these induction studies, fermentation of *S. cacaoi* was performed, obtained fermentation broth was extracted and isolation-purification studies were carried out. Finally, the structures of the purified molecules were elucidated and their antimicrobial effects were tested. The methodologies are given in deteail below, and Figure 2.2 shows general methodology used in comparision and induction studies.

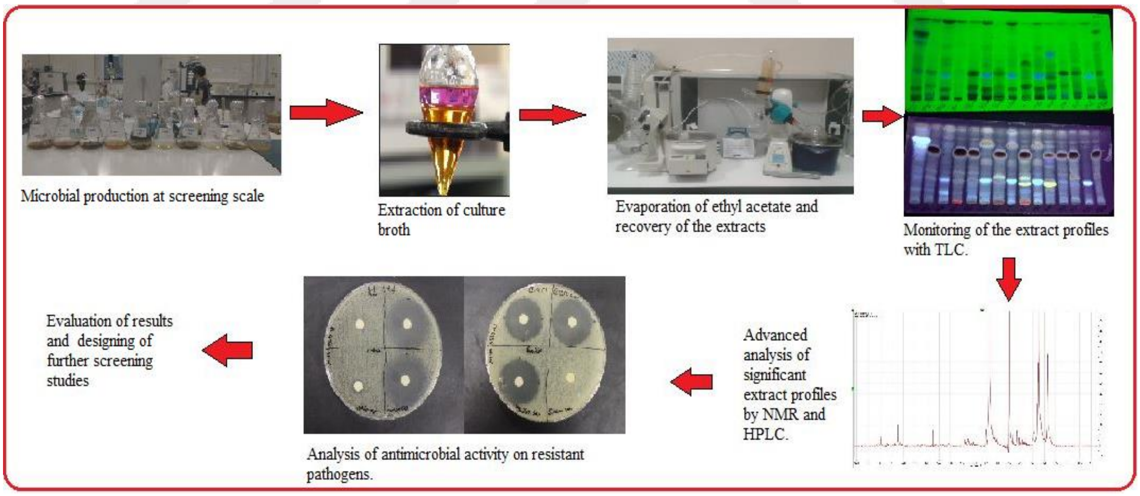

Figure 2.2. Illustration of general methodology.

2.2.1. Comparison of Media

Streptomyces cacaoi was grown in petri dishes containing Mannitol Soya Flour (SFM) at 28 °C for 7 days. SFM medium was used to induce the sporulation and for stock culture preparation. Two stages fermentation was started via transferring one loopful *S. cacaoi* from solid stock culture to 250 ml Erlenmeyer flasks each containing 50 ml of M1, M6 (modıfıed), and GPM which were prepared with either 2% NaCl or 50% seawater (adjusted pH=7.0). In the first stage, the flasks were incubated in a rotary shaker (150 rpm), at 28 °C for 2 days. Then, 1 ml grown samples were transferred to fresh media and incubated for 12 days under the same conditions. As described in detail below, the fermentation broths were extracted, and TLC and HPLC analyses of the extracts were performed followed by antimicrobial effects activity tests.

2.2.1.1. Extraction

After 12 days, fermentation was terminated, and biomass was removed from the fermentation broth using Buchner funnel under vacuum. Each fermentation broth was subjected to liquid-liquid extraction with ethyl acetate (1:1) three times. Relevant media without *S. cacaoi* fermentation were also subjected to the same procedures to be used as negative control (blank extract). The organic phases were collected into flasks and concentrated using rotary evaporator. The extracts were transferred to 20 ml glass vials and the organic phases were evaporated finally using the SpeedVac. All evaporations were carried out at 40 °C and the obtained extracts were stored at 4 °C till further useage.

2.2.1.2. HPLC and TLC Analysis

To see secondary metabolite diversity for each extract, TLC and HPLC analyses were performed. In TLC analysis, MeOH:H_2O (85:15) solvent system was used with reverse phase C-18 plates and *n*-Hex:EtOAc:MeOH (10:10:2) and CHCl3: MeOH (95:5) solvent systems were preferred with normal phase silica gel plates. Each extract was dissolved in ethyl acetate at a concentration of 10 mg/ml and spotted 5 times on the TLC plate. TLC results were examined at 254 nm and 365 nm wavelengths using a UV-lamp. The plates were then sprayed with 1 molar 20% sulfuric acid (aq) and heated (110 °C) to detect metebolites.

For HPLC analysis, Thermo Scientific-Dionex Ultimate 3000 system consisting of automatic sample injection section, quadruple pump, column oven and sequential diode detector (DAD) equipment was used. 10 µL of the samples, which prepared at a concentration of 5000 ppm in HPLC grade methanol, was injected and the peaks were detected at wavelengths of 210, 230, 245, and 365 nm. Table 2.2 shows the HPLC analysis method.

Table 2.2. HPLC Analysis Method.

Time	A (UPW) %	B (MeOH) %
0	90	10
60	0	100
67	0	100
67.1	90	10
75	90	10

The HPLC analysis wwa carried out with Chromolith 4.6X100 mm C18 column, and the mobile phase was containing ultra pure water (A) and HPLC grade methanol (B). Analysis condition was 250 bar max pressure, 25 °C temperature and 1 ml/ min flow rate.

2.2.1.3. Antimicrobial Tests

The antimicrobial effects of the obtained extracts were determined by Kirby-Bauer Disk Diffusion Susceptibility Test. Protocol was carried out according to Jan Hudzicki (2009). On the day of the test, the extracts were dissolved in DMSO to prepare stock solutions at a concentration of 10 mg/ml of which 20 µl were transferred to empty antibiogram discs in a way that 200 µg of the extracts were transferred. Penicillin (40 µg) was used as positive control, and blank extracts -also dissolved in DMSO- (200 µg) of the relevant media were used as negative control. Loaded discs were kept in a sterile cabinet to dry. Meanwhile, fresh cultures of *Candida albicans*, *MRSA*, *Escherichia coli* and *Bacillus subtilis* strains passaged 24 hours before were transferred to tubes containing 0.1% peptone water and adjusted at 0.5 McFarland turbidity. Sabouraud Dextrose Agar (SDA) was used for *Candida albicans* and Müller-Hinton Agar (MHA) for bacteria. The relevant strains were transferred from 0.5 McFarland turbidity stocks to the Petri dishes using a cotton swab by streaking and kept in a sterile cabinet to dry. The dried discs were placed in their respective places in the Petri dishes using sterile tweezers. Finally, the Petri dishes were kept at at 37 °C for 24 hours and diameters of the inhibition zones were measured.

2.2.2. Optimization of Glycerol-Peptone Medium (GPM)

The fermentations performed on GPM, M1 and M2 media were compared in terms of the amount, chemical diversity and bioactivity of the extract, and it was found that GPM medium was as effective as the M1 and M6 media. After these observations, the content of GPM medium was taken into an optimization study, temperature and sea water ratios were used as parameters in addition to medium contents as well.

Response Surface Methodology (RSM) with Box Behnken design was used to determine the effects of GPM contents (glycerol, peptone, $CaCO_3$, $FeCl_3$ and $MgCl_2$), temperature and volume ratio of sea water, and also determine the best conditions for enhanced activity, diversity and amount of ethyl acetate extract. Design-Expert 11 (DOE) was used for the experimental designs and subsequent analysis. The low and high levels of the factors were determined based on literature reviews and preliminary observations (Table 2.3).

Table 2.3. Low and high levels of factors.

Name	Units	Low	High
Temperature	°C	25	35
Sea-water	%	0	100
Glycerol	%	0.75	2.25
Peptone	%	0.5	1.5
$CaCO_3$	%	0	0.2
$FeCl_3$	%	0	0.1
$MgCl_2$	%	0	0.1

The experiment was carried out according to Box-Behnken design matrix with 62 runs with six replicates at the centre point (Table 2.4).

Table 2.4. Box-Behnken design matrix.

	Factor 1	**Factor 2**	**Factor 3**	**Factor 4**	**Factor 5**	**Factor 6**	**Factor 7**
Run	**A:Temperature**	**B: Seawater**	**C: Glycerol**	**D: Peptone**	**E: $CaCO_3$**	**F: $FeCl_3$**	**G: $MgCl_2$**
	°C	%	%	%	%	%	%
1	30	50	1.5	0.5	0	0	0.05
2	30	50	1.5	1.5	0	0	0.05
3	30	50	1.5	0.5	0.2	0	0.05
4	30	50	1.5	1.5	0.2	0	0.05
5	30	50	1.5	0.5	0	0.1	0.05
6	30	50	1.5	1.5	0	0.1	0.05
7	30	50	1.5	0.5	0.2	0.1	0.05
8	30	50	1.5	1.5	0.2	0.1	0.05
9	25	50	1.5	1	0.1	0	0
10	35	50	1.5	1	0.1	0	0
11	25	50	1.5	1	0.1	0.1	0
12	35	50	1.5	1	0.1	0.1	0
13	25	50	1.5	1	0.1	0	0.1
14	35	50	1.5	1	0.1	0	0.1
15	25	50	1.5	1	0.1	0.1	0.1

(cont. on next page)

cont. Table 2.4

16	35	50	1.5	1	0.1	0.1	0.1
17	30	0	1.5	1	0	0.05	0
18	30	100	1.5	1	0	0.05	0
19	30	0	1.5	1	0.2	0.05	0
20	30	100	1.5	1	0.2	0.05	0
21	30	0	1.5	1	0	0.05	0.1
22	30	100	1.5	1	0	0.05	0.1
23	30	0	1.5	1	0.2	0.05	0.1
24	30	100	1.5	1	0.2	0.05	0.1
25	25	0	1.5	0.5	0.1	0.05	0.05
26	35	0	1.5	0.5	0.1	0.05	0.05
27	25	100	1.5	0.5	0.1	0.05	0.05
28	35	100	1.5	0.5	0.1	0.05	0.05
29	25	0	1.5	1.5	0.1	0.05	0.05
30	35	0	1.5	1.5	0.1	0.05	0.05
31	25	100	1.5	1.5	0.1	0.05	0.05
32	35	100	1.5	1.5	0.1	0.05	0.05
33	30	50	0.75	0.5	0.1	0.05	0
34	30	50	2.25	0.5	0.1	0.05	0
35	30	50	0.75	1.5	0.1	0.05	0
36	30	50	2.25	1.5	0.1	0.05	0
37	30	50	0.75	0.5	0.1	0.05	0.1
38	30	50	2.25	0.5	0.1	0.05	0.1
39	30	50	0.75	1.5	0.1	0.05	0.1
40	30	50	2.25	1.5	0.1	0.05	0.1
41	25	50	0.75	1	0	0.05	0.05
42	35	50	0.75	1	0	0.05	0.05
43	25	50	2.25	1	0	0.05	0.05
44	35	50	2.25	1	0	0.05	0.05
45	25	50	0.75	1	0.2	0.05	0.05
46	35	50	0.75	1	0.2	0.05	0.05
47	25	50	2.25	1	0.2	0.05	0.05
48	35	50	2.25	1	0.2	0.05	0.05
49	30	0	0.75	1	0. 1	0	0.05
50	30	100	0.75	1	0.1	0	0.05
51	30	0	2.25	1	0.1	0	0.05
52	30	100	2.25	1	0.1	0	0.05
53	30	0	0.75	1	0.1	0.1	0.05
54	30	100	0.75	1	0.1	0.1	0.05
55	30	0	2.25	1	0.1	0.1	0.05
56	30	100	2.25	1	0.1	0.1	0.05
57	30	50	1.5	1	0.1	0.05	0.05
58	30	50	1.5	1	0.1	0.05	0.05
59	30	50	1.5	1	0.1	0.05	0.05
60	30	50	1.5	1	0.1	0.05	0.05
61	30	50	1.5	1	0.1	0.05	0.05
62	30	50	1.5	1	0.1	0.05	0.05

The statistical significance of the model was verified by applying the analysis of variance (ANOVA). Overall model significance was determined using Fisher's -test. To estimate the model, the lack of fit was also applied.

For two stages fermentation, procedure writen in the section 2.2.1. was used for runs in the design matrix. Each run of which conditions and medium contents were given by the DOE program was prepared in 250 ml erlenmeyer flasks containing 50 ml medium (Figure 2.3) and incubated in the dark, 150 rpm for 10 days.

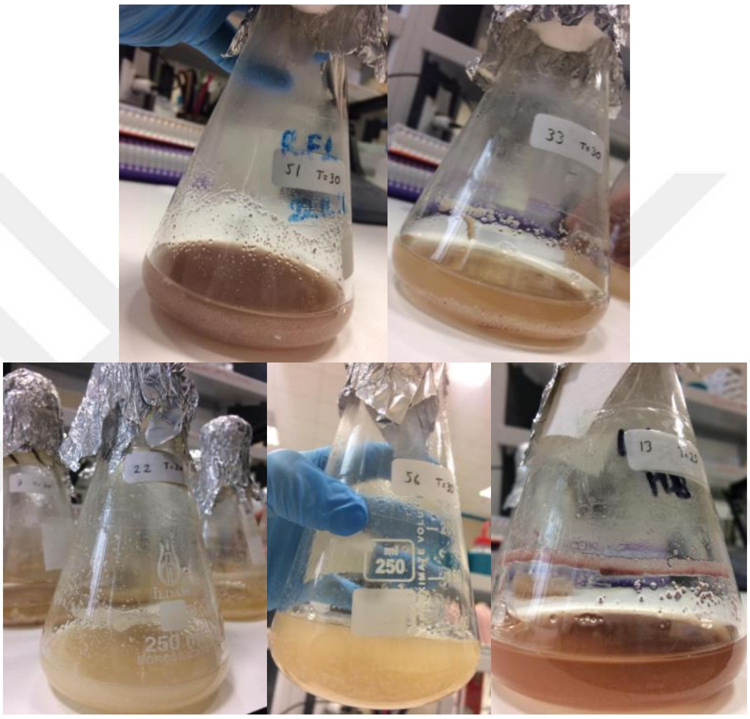

Figure 2.3. Some of runs showing different fermentation color and colony morphology.

After incubation, fermentation broths were extracted, HPLC and TLC analysis were performed as stated in the section 2.2.1.2. HPLC experimental set up was given in Table 2.5. The antibiotic effects of the extracts were determined by the procedure in the section 2.2.1.3. by a minor modification as 100 µg of extract was loaded onto the blank disks instead of 200 µg.

Table 2.5. HPLC method. Analyses were carried out with Chromolith 4.6X100 mm C18 column, and ultra pure water and HPLC grade methanol were used as solvent system. Analysis conditions; 250 bar max pressure, 25 °C tempreture and 1 ml/ min flow rate.

Time (Minute)	**A% (UPW)**	**B% (Methanol)**
0	90	10
35	45	55
50	0	100
55	0	100
55.1	90	10
60	90	10

2.2.3. Biological Induction Studies

Co-culture studies were conducted to examine the effects of different microorganisms on the secondary metabolism of *S. cacaoi*. In this study, the inducer organisms were transferred to the fermentation medium after the log phase (day 3) of *S. cacaoi*, as only the secondary metabolism of *S. cacaoi* was desired to be induced. Thus, the problem of inhibiting the growth of *S. cacaoi* by other microorganisms was overcome and the secondary metabolites of inducer organisms were partially eliminated.

For inducer microorganisms, fungi were planted on petri dishes containing PDA and other inducer organisms on TSA, and grown for a week. To prepare stock inducer solutions, the spores were collected from the petri dishes with the help of tween 80 and transferred into sterile glass tubes. On the 3rd day of *S. cacaoi* fermentation, 1 ml of the each spore stock was transferred to the determined flasks as indicated above (according to design matrix) and the fermentation was continued for another 7 days (Table 2.6 and 2.7).

Multi-cultures were prepared to see the combined effects of more than one inducer microorganisms (Table 2.6). Plackett-Burman design with Design-Expert 11 was employed and 10 microbial strains were screened for their induction capability on secondary metabolism of *S. cacaoi* in 14 trials. Each trial shows different combination of the inducers representing a multi-culture. Each fermentation was carried out in optimized GPM (2.25% glycerol, 1% peptone water, 0.2% $CaCO_3$, 0.1% $MgCl_2$ in distilled water) at 30°C, 150 rpm in the dark. Also, each trial containing the inducer microorganisms without *S. cacaoi* was prepared to be used as a negative control. After fermentation process, ethyl acetate extraction, TLC analysis and antimicrobial analysis were performed as described in section 2.2.1.

Table 2.6. Factors (inducer microorganisms).

Name	Units	Type	Low	High
S. rochei	Ml (5 McFarland)	Numeric	0	1
B. subtilis	Ml (5 McFarland)	Numeric	0	1
C. albicans	Ml (5 McFarland)	Numeric	0	1
A. alternata	Ml (5 McFarland)	Numeric	0	1
A. eureka	Ml (5 McFarland)	Numeric	0	1
F. solani	Ml (5 McFarland)	Numeric	0	1
P. roseopurpureum	Ml (5 McFarland)	Numeric	0	1
Penicillium sp.	Ml (5 McFarland)	Numeric	0	1
Neo	Ml (5 McFarland)	Numeric	0	1
C. laburnicola	Ml (5 McFarland)	Numeric	0	1

Table 2.7. Design matrix of PBD experiments (0: None, 0.5: 0.5 ml and 1: 1 ml stock culture (5 McFarland) of relevant microorganism).

	Factor 1	Factor 2	Factor 3	Factor 4	Factor 5	Factor 6	Factor 7	Factor 8	Factor 9	Factor 10	Factor 11
Run	**A: *S. rochei***	**B: *B. subtilis***	**C: *C. albicans***	**D: *A. alternata***	**E: *A. eureka***	**F: *F. solani***	**G: *P. roseopurpureum***	**H: *Penicillium sp.***	**J: *Neosartarya***	**K: *C. laburnicola***	**L:Dummy 1**
1	1	1	0	1	1	1	0	0	0	1	0
2	0	1	1	0	1	1	1	0	0	0	1
3	1	0	1	1	0	1	1	1	0	0	0
4	0	1	0	1	1	0	1	1	1	0	0
5	0	0	1	0	1	1	0	1	1	1	0
6	0	0	0	1	0	1	1	0	1	1	1
7	1	0	0	0	1	0	1	1	0	1	1
8	1	1	0	0	0	1	0	1	1	0	1
9	1	1	1	0	0	0	1	0	1	1	0
10	0	1	1	1	0	0	0	1	0	1	1
11	1	0	1	1	1	0	0	0	1	0	1
12	0	0	0	0	0	0	0	0	0	0	0
13	0.5	0.5	0.5	0.5	0.5	0.5	0.5	0.5	0.5	0.5	0.5
14	0.5	0.5	0.5	0.5	0.5	0.5	0.5	0.5	0.5	0.5	0.5

2.1.1. Chemical Induction Studies

In order to examine the effects of some inorganic molecules on the secondary metabolism of *S. cacaoi*, an experiment was designed with Placket-Burman design. Ten factors -DMSO, EtOH, Zn^{+2}, K_2HPO_4, $MgSO_4$, KNO_3, Li_2CO_3, LiCl, $CuSO_4$, $FeSO_4$- used for evaluatıon accordıng to lıterature revıews and prelımınary experıments. 12 different runs with a control in which only default version of GPM was used and 3 replicates at the center point were performed acording to the design matrix (Table 2.8).

Each chemical ingredient was added to the medium (GPM) at the ratios specified in the design matrix.

Table 2.8. Placket-Burman design matrix for inorganic inducers (Each chemical was added to the medium as w/v %).

Std	Factors										
	DMSO	EtOH	Zn^{+2}	K_2HPO_4	$MgSO_4$	KNO_3	Li_2CO_3	LiCl	$CuSO_4$	$FeSO_4$	Dummy
	%	%	%	%	%	%	%	%	%	%	
1	1.5	1	0	0.2	0.05	0.2	0	0	0	0.01	0
2	0	1	0.01	0	0.05	0.2	0.01	0	0	0	1
3	1.5	0	0.01	0.2	0	0.2	0.01	0.01	0	0	0
4	0	1	0	0.2	0.05	0	0.01	0.01	0.01	0	0
5	0	0	0.01	0	0.05	0.2	0	0.01	0.01	0.01	0
6	0	0	0	0.2	0	0.2	0.01	0	0.01	0.01	1
7	1.5	0	0	0	0.05	0	0.01	0.01	0	0.01	1
8	1.5	1	0	0	0	0.2	0	0.01	0.01	0	1
9	1.5	1	0.01	0	0	0	0.01	0	0.01	0.01	0
10	0	1	0.01	0.2	0	0	0	0.01	0	0.01	1
11	1.5	0	0.01	0.2	0.05	0	0	0	0.01	0	1
12	0	0	0	0	0	0	0	0	0	0	0
13	0.75	0.5	0.005	0.1	0.025	0.1	0.005	0.005	0.005	0.005	0.5
14	0.75	0.5	0.005	0.1	0.025	0.1	0.005	0.005	0.005	0.005	0.5
15	0.75	0.5	0.005	0.1	0.025	0.1	0.005	0.005	0.005	0.005	0.5

After 10 days of fermentation, the antimicrobial effects of ethyl acetate extracts were examined against *E. coli* following the protocol specified in section 2.2.1. Measured inhibition diameters were evaluated as response in the design matrix. After regression analysis, factors that were significant above 95% confidntial level ($p<0.05$) were considered to have impact on extract amount and synthesis of antimicrobial molecule(s) against *E. coli*. These factors (factor 1, 6 and 7) were further statistically optimized by Box-Behnken design.

In Box-Behnken design, significant factors affecting *E. coli* inhibition were evaluated. Three variables -KNO_3 (Factor 1), Li_2CO_3 (Factor 2) and DMSO (Factor 3)- were used as factors resulted in a combination of 15 runs with 3 replicates at the center point. The responses were extract amount (Response 1), inhibition zone against *B. subtilis* (Response 2) and inhibition zone against *E. coli* (Response 3) (Table 2.9). Ethyl acetate extraction, TLC analysis and antimicrobial analysis were performed as described in section 2.2.1.

The analysis of variance (ANOVA) and the coefficient of R^2 were used to justify the accuracy of the fitted model. By computing the F-value at a probability (value) of

0.05, the significance of all terms in the polynomial model was statistically judged. Also, the regression of the experimental data was made by using Design-Expert 11, and 2D and 3D contour plots were generated by keeping three-variable constants at 0 levels and varying the other variables in the design matrix**.**

Table 2.9. Box-Behnken design matrix for chemical inducers (w/v %)

	Factor 1	Factor 2	Factor 3	Response 1	Response 2	Response 3
Std	A:KNO_3	B:Li_2CO_3	C:DMSO	Extract amount	*B. subtilis*	*E. coli*
	%	%	%	mg	mm	mm
1	0	0	1			
2	0.4	0	1			
3	0	0.04	1			
4	0.4	0.04	1			
5	0	0.02	0			
6	0.4	0.02	0			
7	0	0.02	2			
8	0.4	0.02	2			
9	0.2	0	0			
10	0.2	0.04	0			
11	0.2	0	2			
12	0.2	0.04	2			
13	0.2	0.02	1			
14	0.2	0.02	1			
15	0.2	0.02	1			

The direct bioautography technique was used to determine the induced molecule. 500 µg of the extract showing activity against *E .coli* was applied to the TLC plate and run with the dichloromethane:methanol (85:15) solvent system. This silica layer was placed in a petri dish and TSA medium at about 45 °C was poured over it. When the medium dried, *E. coli* stock culture prepared at 0.5 McFarland turbidity was transferred to the petri dishes by lawn culture method with the help of a cotton swab. Petri dishes were incubated at 37 °C for 24 hours and inhibition region was observed.

2.1.2. Production

With the data obtained from the optimization and induction studies, the conditions providing the most chemical diversity and highest amount in the ethyl acetate extract were determined as 2.25 v/v % glycerol, 1 w/v % peptone water, 0.2 w/v% $CaCO_3$, 0.1 w/v % $MgCl_2$ in distilled water at 30 °C which was validated composition of GPM in Box-

Behnken design. It was determined that *S. cacaoi* could produce a large number of polyether molecules with these fermentation conditions and it was decided that large scale production would be carried out under these conditions.

In order to scale the production properly, production trials were made in both 250 ml, 500 ml, 1 L, 2 L and 5 L volumes of erlenmeyer flasks with the optimized conditions (Figure 2.4). The optimized medium (GPM) was added to each flask at 20% working volume (1/5 v medium/v flask). The first stage of fermentation was initiated by transferring a loopful from the *S. cacaoi* solid culture to a 250 ml flask. They were grown in the dark at 30°C and 150 rpm under the specified conditions for 2 days. Then, these grown cultures were transferred to the relevant flasks at an inoculum ratio of 2 % and they were incubated under the same conditions. After 10 days of fermentation, ethyl acetate extractions, TLC analysis and antimicrobial tests were performed as described in section 2.2.1.

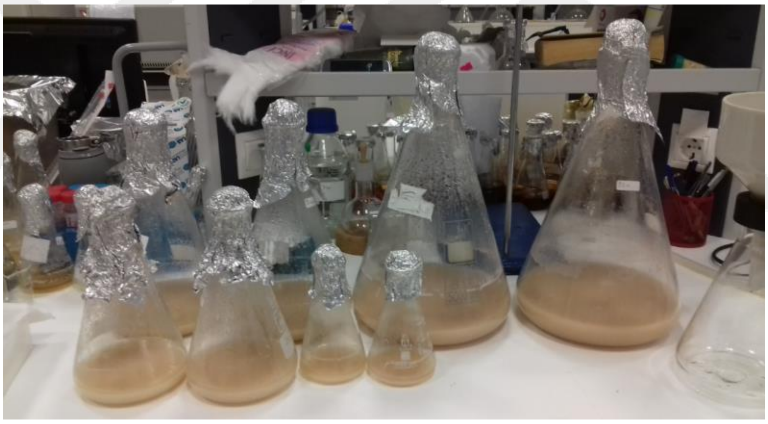

Figure 2.4. Used erlenmeyer flasks in scale up study.

According to results the best volume was determined as 1 L in terms of both the amount and antimicrobial effect of extracts. Thus, further productions were carried out in 1 L flasks with the conditions indicated above. Total of 125 x 1L flasks were used which resulted in a total of 25 L of fermentation broth. *S. cacaoi* colonies were removed from the fermentation broth using Buchner funnel under vacuum and extracted with 1:1 of EtOAce (Figure 2.5). The collected ethyl acetate phase was concentrated in a 20 L volume rotary evaporator under vacuum at 40 °C resulted in 14 g of extract.

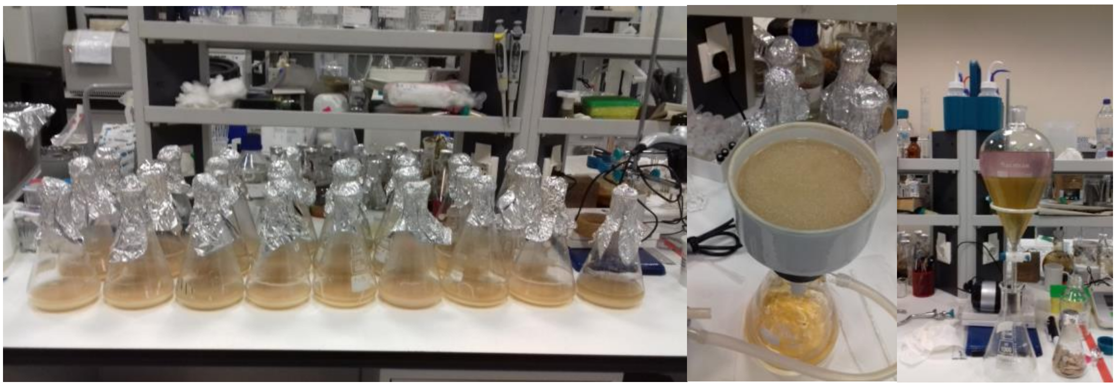

Figure 2.5. *S. cacaoi* broth cultures, filtration and extraction.

2.1.3. Isolation and Purification

Column chromatographies with silica gel 60 (Merck 7734), Li Chroprep RP (C-18, Merck 9303) and sephadex LH-20 (GE Healthcare Life Sciences) were run to obtain pure compounds. TLC was conducted on pre-coated silica gel 60 F254 aluminum sheets (Merck 5554) and RP-18 F254 (Merck) plates. UV-active compounds were detected at 254 and 366, non-UV-active compounds, like K41-A, were visualized by spraying 20% aq.H_2SO_4 onto the TLC plates followed by heating up to 110 °C until the spots became visible.

For column chromatography studies and TLC controls following solvent systems were used with different dilution ratios:

- Chloroform:Methanol ($CHCl_3$:MeOH)
- Iso-hexane:Ethylacetate:Methanol (*2*-Hex:EtOAc:MeOH)
- Hexane:Ethylacetate:Methanol (*n*-Hex:EtOAc:MeOH)
- Hexan:Ethylacetate (*n*-Hex:EtOAc)
- Acetone:Water (ACE:H_2O)
- Dichloromethane:Methanol (DCM:MeOH)
- Acetone:Water (ACN:H_2O)
- Hexane:Ethylacetate:Isopropanol (*n*-Hex:EtOAc:*2*-PrOH)

Isolation studies on the ethyl acetate extract (14 g) started with a 150 g silica gel using open column chromatography (3x60 cm). First, the extract was dissolved in methanol-chloroform mixture and impregnated with 15 g of silica gel and dried. Subsequently, the dried silica containing the extract applied to the silica column equilibrated with chloroform. The column was eluted with $CHCl_3$:MeOH mixtures (100:0

→ 0:100; total of 14 L). Collected fractions showing similar profiles were pooled together, and 23 main fractions were obtained (Figure 2.6).

Figure 2.6. Images of the first column at different elution steps and main fractions collected.

S53-60 (90 mg), one of the main fractions was chromatographed over RP-C18 column (3x12 cm, 30 g RP silica gel) with ACE:H_2O (50:50 → 100:00, total of 410 ml), and six subfractions were obtained. *S53-60_RP12-28* and *S53-60_RP49-51* subfractions were subjected to silica gel columns (1x40 cm, 6,5 g silica gel) with isocratic $_{2-}$Hex-EtOAc-MeOH (8:2:0.25, total of 150 ml) solvent system. *S53-60_RP49-51* column gave **SC-EG-07** (2 mg) and *S53-60_RP12-28_21-30* subfraction wich was further subjected to silica gel column (1x40 cm, 6,5 g silica gel) with isocratic DCM:MeOH (97:3, total of 160 ml) to give **SC-EG-01** (8.4 mg).

S61-71 (250 mg) was submitted to a RP-C18 column (3x12 cm, 30 g RP silica) employing with ACN:H_2O (40:60 → 90:10, total of 620 ml) to give **SC-EG-02** (10 mg) and **SC-EG-03** (42 mg). *S61-71_RP20-37* subfraction was subjected to silica gel column (1x40 cm, 6,5 g silica gel) and eluted with $CHCl_3$:MeOH (99:1 → 90:10, total of 160 ml) to give **SC-EG-04** (3 mg). The other subfraction, *S61-71_RP64-82*, was submitted to the same silica gel column but eluted with DCM:MeOH (99:01 → 85:15, total of 200 ml) to give **SC-EG-05** (3.5 mg).

200 mg of *S72-82* main fraction (980 mg) was subjected to RP-C18 column (3x12 cm, 30 g RP silica). Mixtures of ACN:H_2O (30:70 → 70:30, total of 400 ml) solvent systems were used as mobile phase. Then, *S72-82_RP6-9* subfraction was purified with a silica gel column (1x40 cm, 6,5 g silica gel) using *n*-Hex:EtOAc:MeOH (10:90 → 00:100, total of 140 ml) solvent system and codded as **SC-EG-15** (3.7 mg).

S83-103 (330 mg) was subjected to RP-C18 column (3x12 cm, 30 g RP silica) employing with ACN:H_2O (10:90 → 90:10, total of 1350 ml) to give **SC-EG-16** (13.3 mg) and **SC-EG-17** (17 mg). *S83-103_RP32-35* subfraction was further submitted to silica gel column (1x40 cm, 6,5 g silica gel) with CHCl3:MeOH (95:05 → 85:15, total of 180 ml) and **SC-EG-21** (9 mg) was obtained. The other subfraction, *S83-103_119-126*, was submitted to another silica gel column (2.25x20 cm, 30 g silica gel) employing with *n*-Hex:EtOAc:MeOH (10:10:0.1 → 10:10:1, total of 340 ml) to give **SC-EG-18** (9.8 mg) and **SC-EG-20** (6.6 mg).

S121-148 (310 mg) was subjected to RP-C18 column (3x12 cm, 30 g RP silica) eluting with ACN:H_2O (20:80 → 90:10, total of 1250 ml) to give five promising subfractions. *S121-148_RP9-10* was chromatographed over sephadex column (1x40 cm, 5 g sephadex gel) with 110 ml MeOH and **SC-EG-11** (1.2 mg) was obtained. *S121-148_RP56-67* was submitted to silica gel column (2.25x20 cm, 30 g silica gel) employing with isocratic *n*-Hex:EtOAc:*2*-PrOH (2:8:2, total of 450 ml) to give **SC-EG-12** (12 mg). The other three subfractions, *S121-148_RP75-85*, *S121-148_RP91-94* and *S121-148_RP104-108*, were chromatographed using same silica gel column (1x40 cm, 6,5 g silica gel) with same solvent systems CHCl3:MeOH (90:10 → 85:15, total of ~150 ml for each column) and, **SC-EG-08** (1.7 mg), **SC-EG-13** (2.5 mg) and **SC-EG-14** (3 mg) were obtained, respectively.

S169-180 (100 mg) was chromatographed over RP-C18 column (3x12 cm, 30 g RP silica gel) with ACN:H_2O (20:80 → 100:00, total of 500 ml). *S169-180_RP6-9* subfraction was subjected to silica gel column chromatography (1x40 cm, 6,5 g silica gel) with *n*-Hex:EtOAc:MeOH solvent system mixtures (10:10:0.1 → 10:10:1, total of 150 ml) and **SC-EG-09** (1.2 mg) was obtained. *S169-180_RP11-12* was also submitted to the same column (1x40 cm, 6,5 g silica gel) but employed with CHCl3:MeOH (95:05 → 85:15, total of ~280 ml) to give **SC-EG-10** (13.5 mg).

S7-12 (520 mg) and *S17-19* (1400 mg) main fractions were taken into precipitation studies and total of 1335 mg **SC-EG-19** was crystallized in *n*-hexane. In addition, methanol phase of the *S7-12* (230 mg) was submitted to silica gel column chromatography (60 g) with *n*-Hex:EtOAc solvent system mixtures (30:70 → 50:50, total of 750 ml) and **SC-EG-06** (27.5 mg) was obtained.

It was also observed by TLC analysis that *S13-16* (1300 mg), *S20-22* (2200 mg) and *S23-37* (2240 mg) main fractions contain very high amounts of **SC-EG-19** (Figure 3.25). The isolation steps were illustrated in detail in Figure 2.7, 2.8 and 2.9.

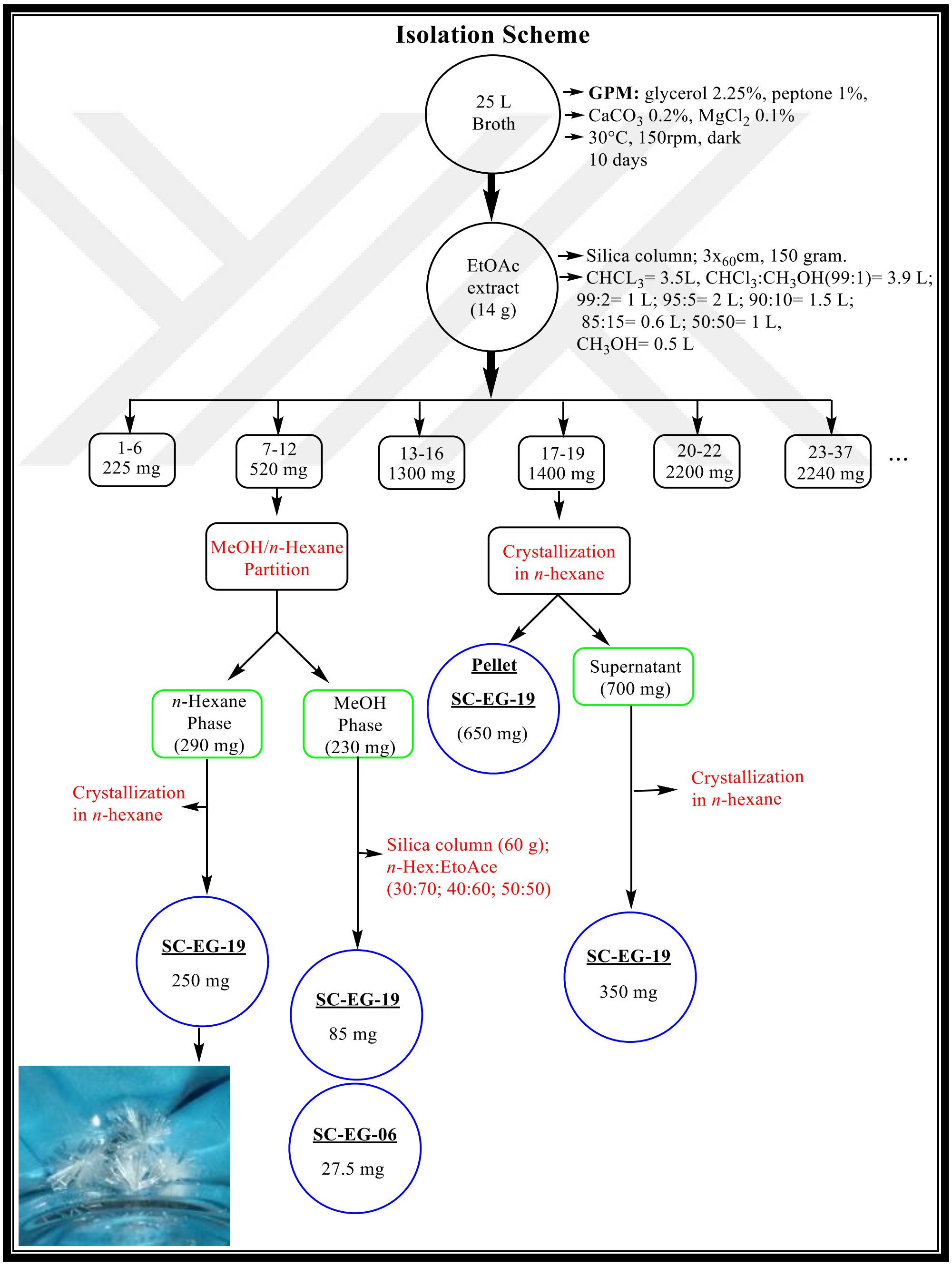

Figure 2.7. Isolation scheme performed on the *S. cacaoi* ethyl acetate extract (Part 1).

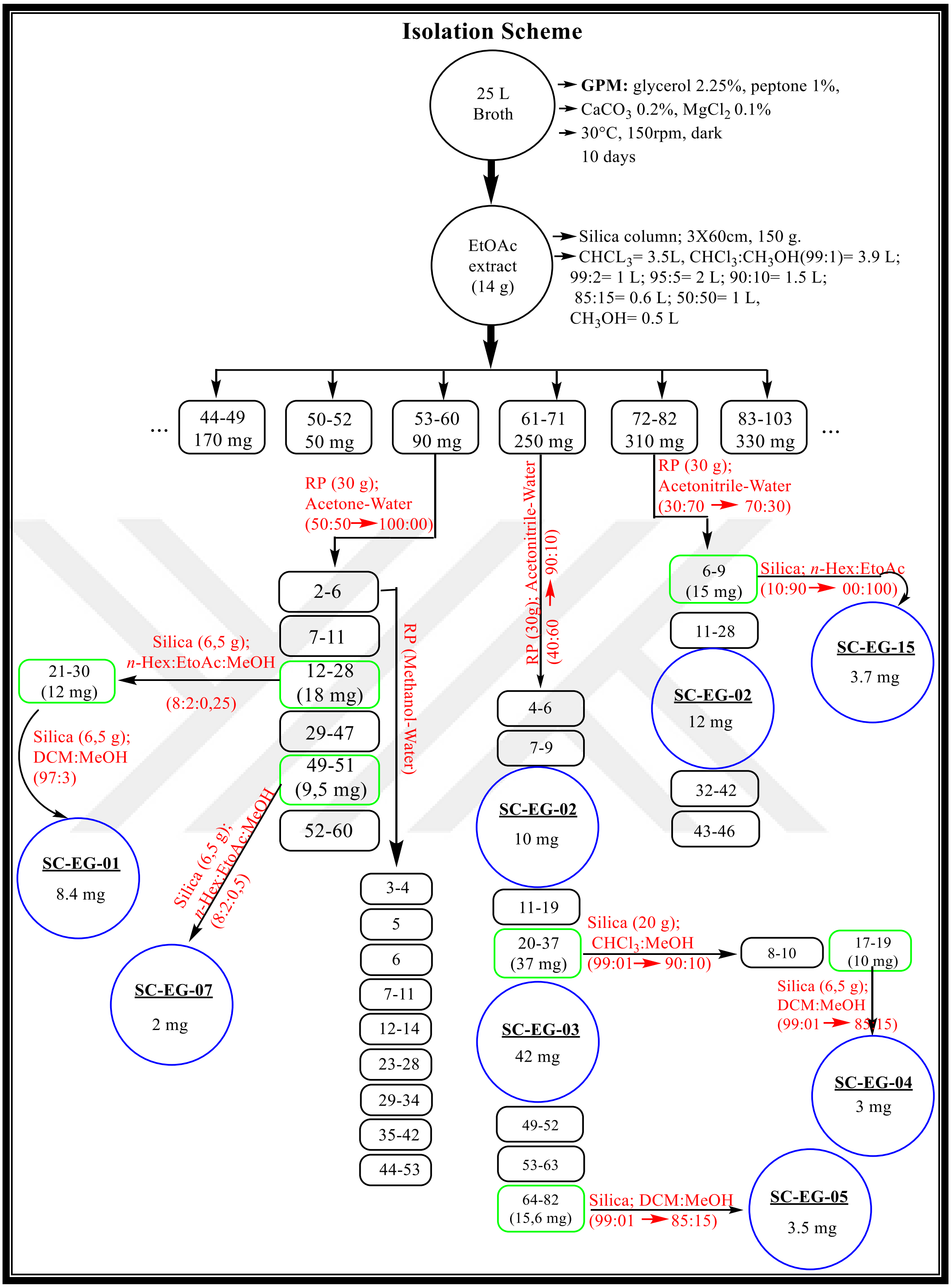

Figure 2.8. Isolation scheme performed on the *S. cacaoi* ethyl acetate extract (Part 2).

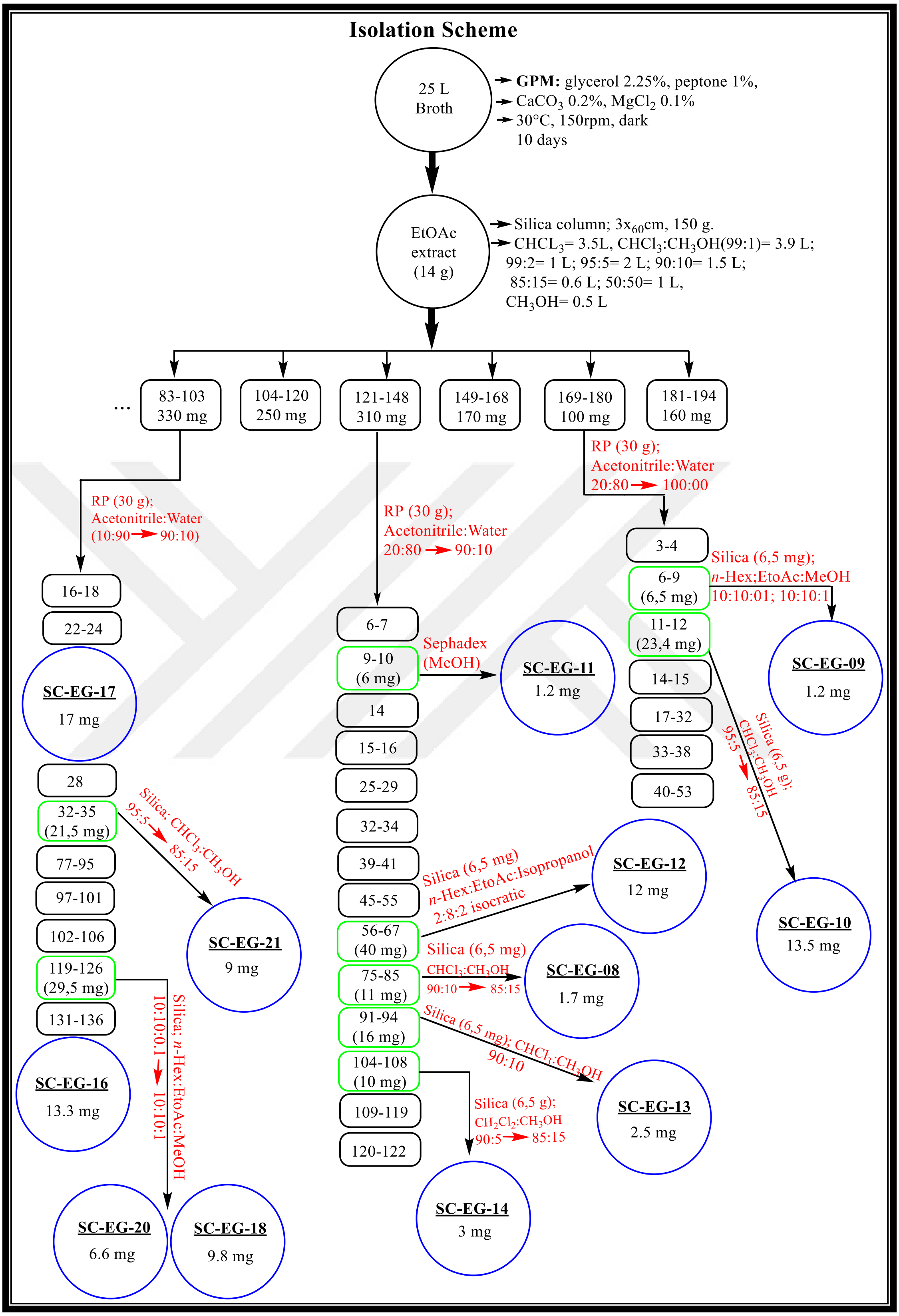

Figure 2.9. Isolation scheme performed on the *S. cacaoi* ethyl acetate extract (Part 3).

CHAPTER 3

RESULTS AND DISCUSSION

3.1. Comparison of Media

M1, M6 (modified) and GPM media were compared for their effects on the secondary metabolism of *S. cacoi*. Fermentation studies were employed for each medium under same conditions (pH 7, 30 °C, 150 rpm, dark). After termination of fermentations, TLC and HPLC analyses were performed on the EtOAc extracts together with antimicrobial activity tests.

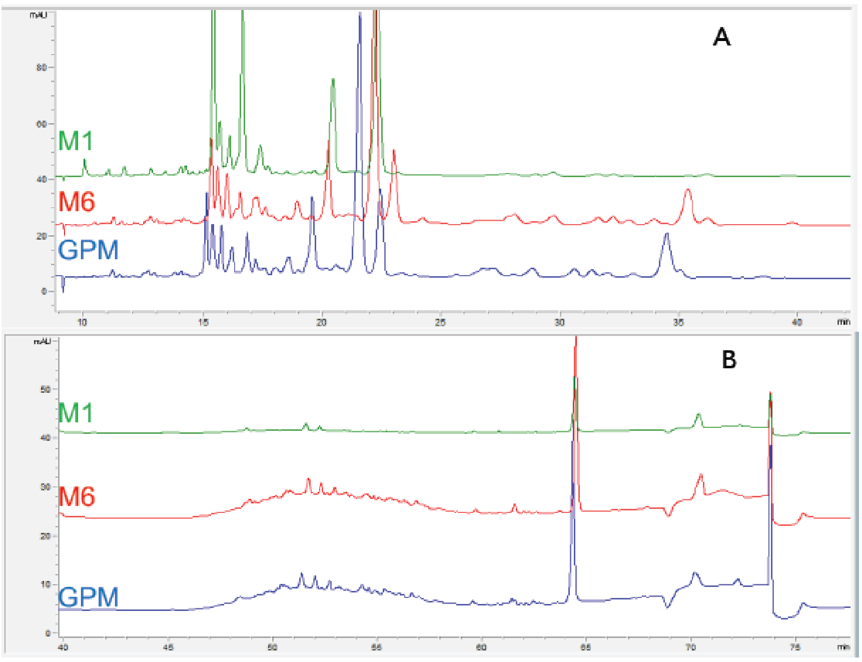

Figure 3.1. HPLC-DAD chromatograms of the EtOAc extracts (at 230 nm). **A:** 0-40 min., **B:** 40-80 min.

When HPLC chromatograms were compared, it was observed that the metabolites produced in M6 and GPM were more diverse than M1 (Figure 3.1). A higher metabolite diversity was noticed in the GPM samples compared to the other media based on the TLC chromatograms, particularly under 254 nm. In addition, the GPM samples had the least amount of default impurities (molecules originating from medium content) bringing an advantage in the isolation and purification studies (Figure 3.2).

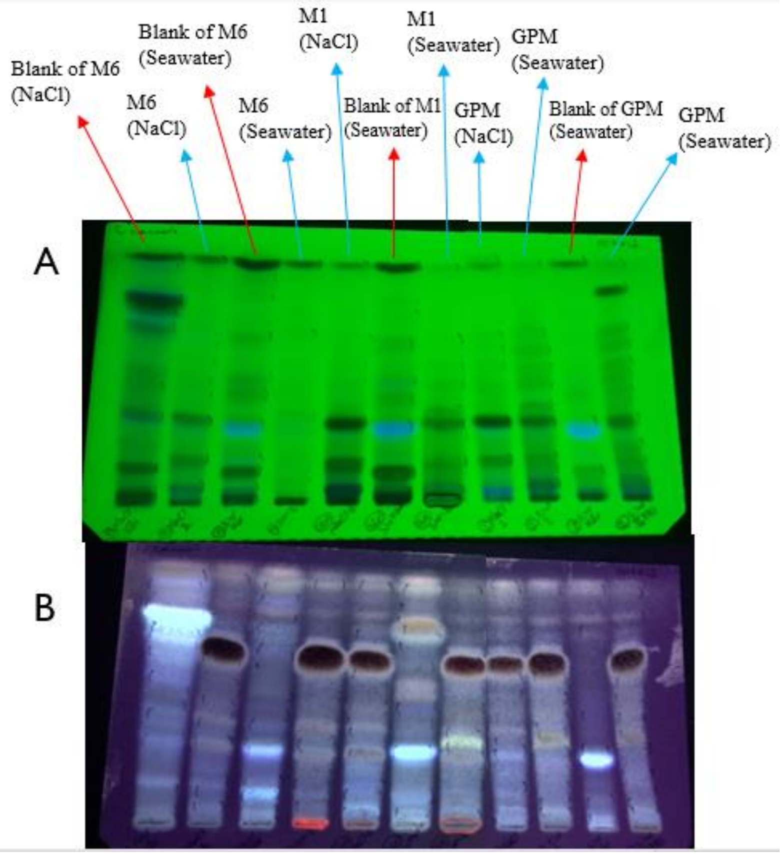

Figure 3.2. TLC chromatograms of the EtOAc extracts of test media; each extract was applied on TLC plate at same concentration. (A) 254 nm before H_2SO_4 treatment, (B) 365 nm after H_2SO_4 treatment [Mobile phase: 10:10:2 (*n*-Hex:EtOAc:MeOH)].

On the other hand, each extract showed potent antimicrobial activity versus *Bacillus subtilis* and methicillin-resistant *Staphylococcus aureus* (*MRSA*) and low activity against *Candida albicans*. However, no inhibition was detected for Gram-negative *Escherichia coli*. In addition, GPM medium was also prepared in %50 seawater-distilled water mixture. While the extract obtained from GPM in 50% seawater showed higher activity against *B. subtilis,* extract obtained from GPM in seawater showed higher activity against *C. albicans* (Table 3.1 and Figure 3.3). These results indicate that secondary metabolism of *S. cacaoi* is affected by seawater-distilled water ratio.

Table 3.1. Amount of the extracts and results of Disc Diffusion Test; 200 µg of extract were loaded to discs for each trial; as positive control cefazolin (100 µg) was used.

Extract	**Amount of Obtained Extract**	**Amount of Extract/Disc**	**Diameter of Inhibition Zones (mm)**		
			Bacillus subtilis	*MRSA*	*Candida albicans*
M1 (NaCl)	8.2 mg	200 µg	29	34	11
M1 (Seawater)	9.5 mg	200 µg	29	33	10
M6 (NaCl)	6 mg	200 µg	31	34	12
M6 (Seawater)	5.3 mg	200 µg	31	35	15
GPM (NaCl)	8 mg	200 µg	28	33	12
GPM (Seawater)	7.1 mg	200 µg	28	34	17
GPM (50% Seawater)	6.6 mg	200 µg	30	34	11
Cefazolin	-	100 µg	0	0	32

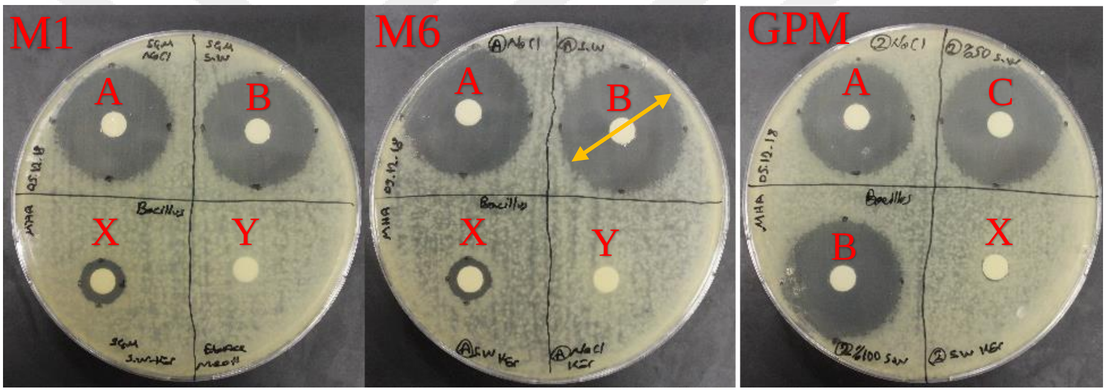

Figure 3.3. Inhibition zones against B. subtilis of extracts produced in M1, M6 and GPM, respectively. Orange arrow is an example of the measurement of the diameter of inhibition zones. (A= in distilled water with 2% NaCl, B= in seawater, C= in 50% distilled water-seawater mixture, X= blank of media in seawater, Y= blank of media in distilled water with 2% NaCl).

3.2. Optimization of GPM

GPM medium was undertaken further optimization studies after medium selection experiments performed in section 3.1. To determine optimum incubation time in a manner of inhibition diameter and biomass production, the fermentation in GPM medium was continued for 16 days till it reached to steady state for both responses. For every two days, incubation finished for two flasks of 50/250 ml (v/v) GPM. TLC profiles of the extracts, antimicrobial activity, also amount of dried biomass were compared for each sample.

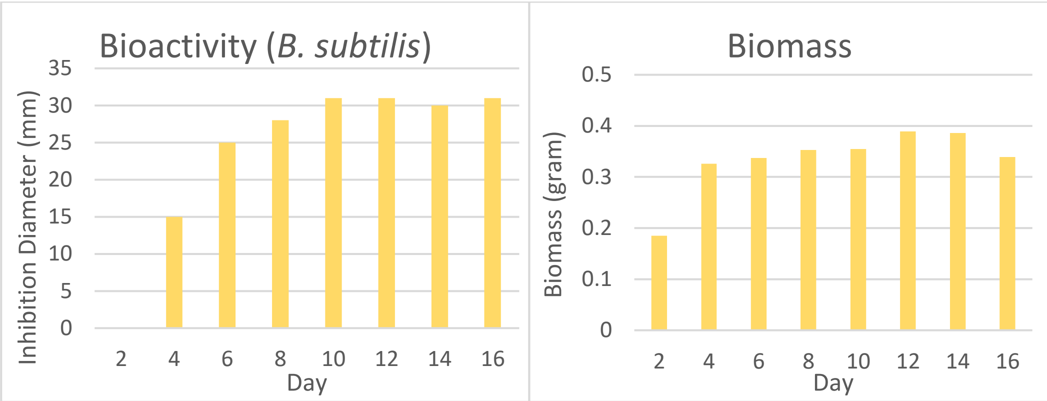

Figure 3.4. Time course of bioactivities of the EtOAc extracts and amount of dried biomasses.

The biomass obtained as 0.185 g/flask on day 2 increased up to 0.33 g/flask on day 4 and no significant biomass increase was observed on the following days. When bioactivity results were examined, no activity was observed until the 4^{th} day on which 15 mm inhibition zone was detected, and the activity continued to increase until day 10 (approx. 31mm) (Figure 3.4). Thus, it was revealed that the bioactive metabolites began to be synthesized in the stationary phase and this trend sustained up to day 10 in the fermentation broth.

After determining incubation time, based on both literature and our preliminary studies, the content of GPM (peptone-water, glycerol, $CaCO_3$, $FeCl_3$, $MgCl_2$), temperature and seawater ratio were selected as factors for further optimization studies. An experimental design was set using Box-Behnken. Sixty-two different combinations of factors given by the design matrix were prepared to carry out 10-day fermentation of *S. cacaoi*. At the end of fermentation, the amount of EtOAc extracts, diameters of inhibition zones against *Bacillus subtilis* and amount of dry biomass were recorded as responses (Table 3.2).

Table 3.2. Design matrix with responses.

Std	Factor 1	Factor 2	Factor 3	Factor 4	Factor 5	Factor 6	Factor 7	Responses		
	A:Temperature	**B:**Seawater	**C:**Glycerol	**D:**Peptone-W	**E:**$CaCO_3$	**F:**$FeCl_3$	**G:**$MgCl_2$	Activity (100 µg)	Biomass	Extract Amount
	°C	%	%	%	%	%	%	mm	g	mg
~~1~~	~~30~~	~~50~~	~~1.5~~	~~0.5~~	~~0~~	~~0~~	~~0.05~~	-	-	-
2	30	50	1.5	1.5	0	0	0.05	20.5	0.156	0.7
~~3~~	~~30~~	~~50~~	~~1.5~~	~~0.5~~	~~0.2~~	~~0~~	~~0.05~~	-	-	-
~~4~~	~~30~~	~~50~~	~~1.5~~	~~1.5~~	~~0.2~~	~~0~~	~~0.05~~	-	-	-
5	30	50	1.5	0.5	0	0.1	0.05	11.5	0.101	1.1
6	30	50	1.5	1.5	0	0.1	0.05	22.5	0.279	3.4
7	30	50	1.5	0.5	0.2	0.1	0.05	22	0.161	4.7
8	30	50	1.5	1.5	0.2	0.1	0.05	23.5	0.422	4.1
9	25	50	1.5	1	0.1	0	0	25.5	0.148	4.9
10	35	50	1.5	1	0.1	0	0	22	0.201	4.9
11	25	50	1.5	1	0.1	0.1	0	21	0.236	1.7
12	35	50	1.5	1	0.1	0.1	0	21	0.286	4.5
13	25	50	1.5	1	0.1	0	0.1	23.5	0.184	5.5
14	35	50	1.5	1	0.1	0	0.1	23	0.14	4.3
15	25	50	1.5	1	0.1	0.1	0.1	21	0.25	5.8
16	35	50	1.5	1	0.1	0.1	0.1	20	0.28	4.7
~~17~~	~~30~~	~~0~~	~~1.5~~	~~1~~	~~0~~	~~0.05~~	~~0~~	-	-	-
18	30	100	1.5	1	0	0.05	0	16	0.181	7.9
~~19~~	~~30~~	~~0~~	~~1.5~~	~~1~~	~~0.2~~	~~0.05~~	~~0~~	-	-	-
20	30	100	1.5	1	0.2	0.05	0	20	0.314	7.2
21	30	0	1.5	1	0	0.05	0.1	19	0.152	4.8
22	30	100	1.5	1	0	0.05	0.1	18.5	0.19	7.3
23	30	0	1.5	1	0.2	0.05	0.1	23	0.221	4.2
24	30	100	1.5	1	0.2	0.05	0.1	21	0.281	5.2
25	25	0	1.5	0.5	0.1	0.05	0.05	20	0.115	6.4
26	35	0	1.5	0.5	0.1	0.05	0.05	12.5	0.122	5.8
27	25	100	1.5	0.5	0.1	0.05	0.05	16	0.149	8.6
28	35	100	1.5	0.5	0.1	0.05	0.05	20	0.171	7.2
29	25	0	1.5	1.5	0.1	0.05	0.05	23	0.261	3.6
30	35	0	1.5	1.5	0.1	0.05	0.05	17	0.257	5
~~31~~	~~25~~	~~100~~	~~1.5~~	~~1.5~~	~~0.1~~	~~0.05~~	~~0.05~~	-	-	-
32	35	100	1.5	1.5	0.1	0.05	0.05	19	0.426	5.5
33	30	50	0.75	0.5	0.1	0.05	0	22	0.105	2.2
34	30	50	2.25	0.5	0.1	0.05	0	18	0.113	10
35	30	50	0.75	1.5	0.1	0.05	0	21	0.368	3.8
36	30	50	2.25	1.5	0.1	0.05	0	21	0.335	5.5
37	30	50	0.75	0.5	0.1	0.05	0.1	21.5	0.115	3.6
38	30	50	2.25	0.5	0.1	0.05	0.1	19	0.119	6.2
39	30	50	0.75	1.5	0.1	0.05	0.1	20	0.394	2.7
40	30	50	2.25	1.5	0.1	0.05	0.1	21.5	0.347	4.7
41	25	50	0.75	1	0	0.05	0.05	21	0.205	2.3
42	35	50	0.75	1	0	0.05	0.05	20	0.21	3.7
43	25	50	2.25	1	0	0.05	0.05	20.5	0.178	8.7
44	35	50	2.25	1	0	0.05	0.05	17	0.214	7.3
45	25	50	0.75	1	0.2	0.05	0.05	23	0.342	2.4
~~46~~	~~35~~	~~50~~	~~0.75~~	~~1~~	~~0.2~~	~~0.05~~	~~0.05~~	-	-	-
47	25	50	2.25	1	0.2	0.05	0.05	20	0.319	10.4

(cont. on next page)

cont. Table 3.2

48	35	50	2.25	1	0.2	0.05	0.05	22	0.348	9.3
49	30	0	0.75	1	0.1	0	0.05	26	0.178	3.7
50	30	100	0.75	1	0.1	0	0.05	23	0.161	4.1
51	30	0	2.25	1	0.1	0	0.05	23.5	0.145	7.3
52	30	100	2.25	1	0.1	0	0.05	18	0.143	7.6
53	30	0	0.75	1	0.1	0.1	0.05	23	0.225	3.9
54	30	100	0.75	1	0.1	0.1	0.05	20	0.297	4.1
55	30	0	2.25	1	0.1	0.1	0.05	21	0.202	3
~~56~~	~~30~~	~~100~~	~~2.25~~	~~1~~	~~0.1~~	~~0.1~~	~~0.05~~	-	-	-
57	30	50	1.5	1	0.1	0.05	0.05	23	0.229	4.5
58	30	50	1.5	1	0.1	0.05	0.05	22.5	0.253	4.3
59	30	50	1.5	1	0.1	0.05	0.05	22	0.185	5
60	30	50	1.5	1	0.1	0.05	0.05	23	0.2	4.7
61	30	50	1.5	1	0.1	0.05	0.05	23.5	0.222	4.2
~~62~~	~~30~~	~~50~~	~~1.5~~	~~1~~	~~0.1~~	~~0.05~~	~~0.05~~	-	-	-

Also, different colony morphologies and broth colors were observed in runs (Figure 3.5). The EtOAc extractions were performed three times for each run. The extracts were dissolved in EtOAc at 5 mg/ml concentration, applied on the TLC plates and developed using *n*-Hex:EtOAc:MeOH (10:10:3) mobile system. The extracts were found to have quite different chemical profiles (Figure 3.6, 3.7 and 3.8). Also, each extract caused different diameter inhibition zone (Figure 3.9).

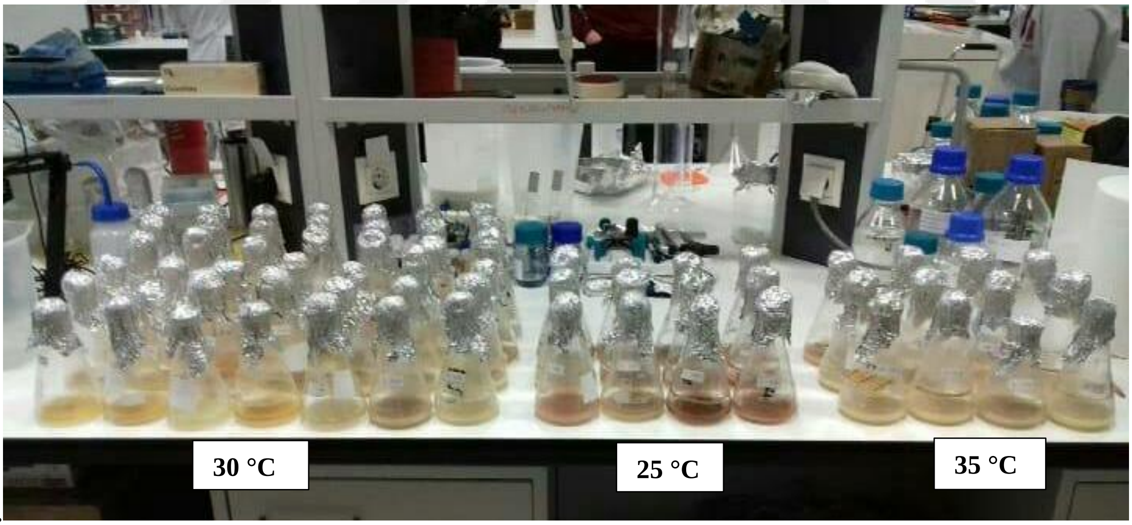

Figure 3.5. Runs of design matrix after 10 days fermentation.

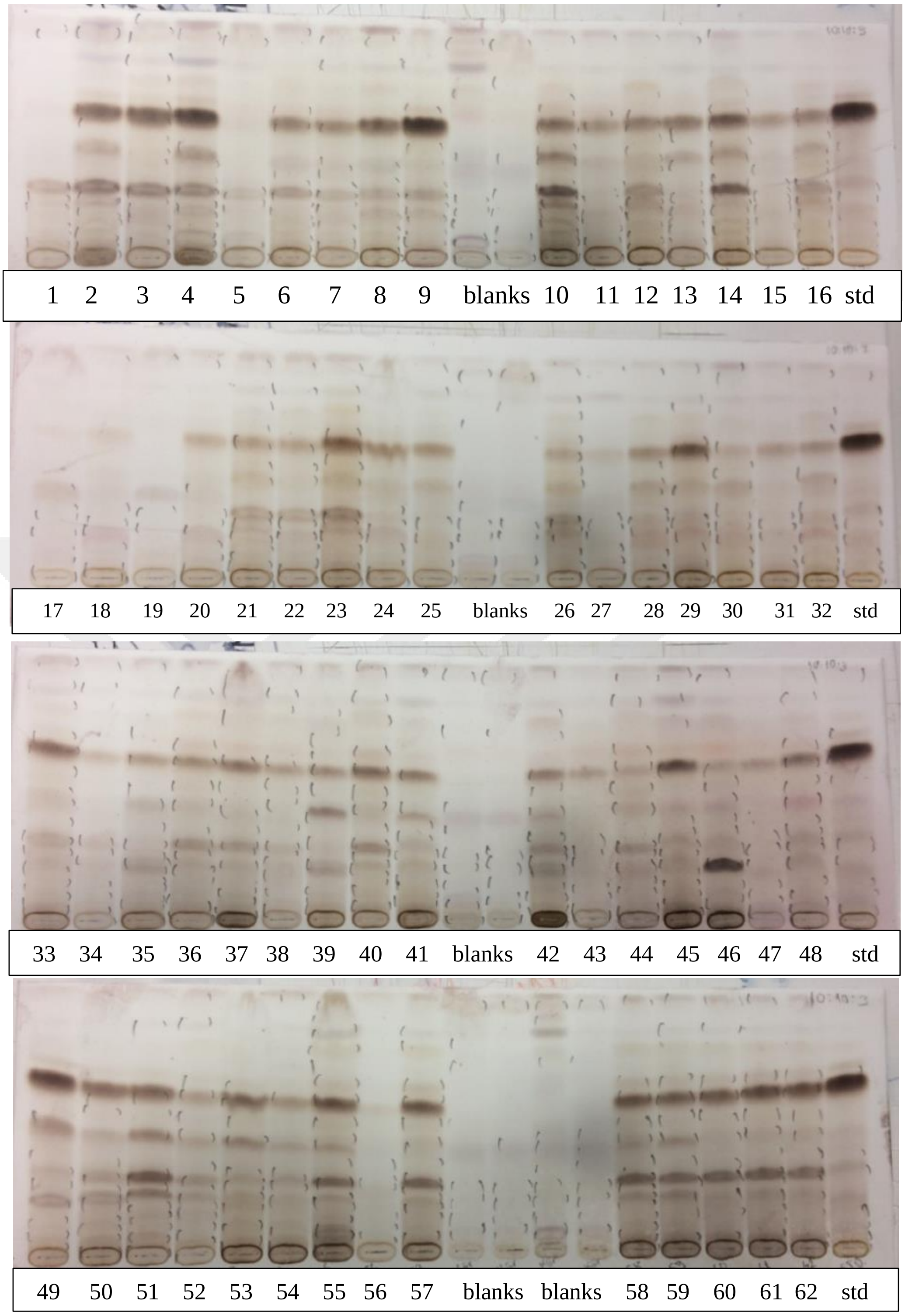

Figure 3.6. TLC chromatograms of the EtOAc extracts after H_2SO_4 treatment. Blanks are the extracts of different runs without organism.

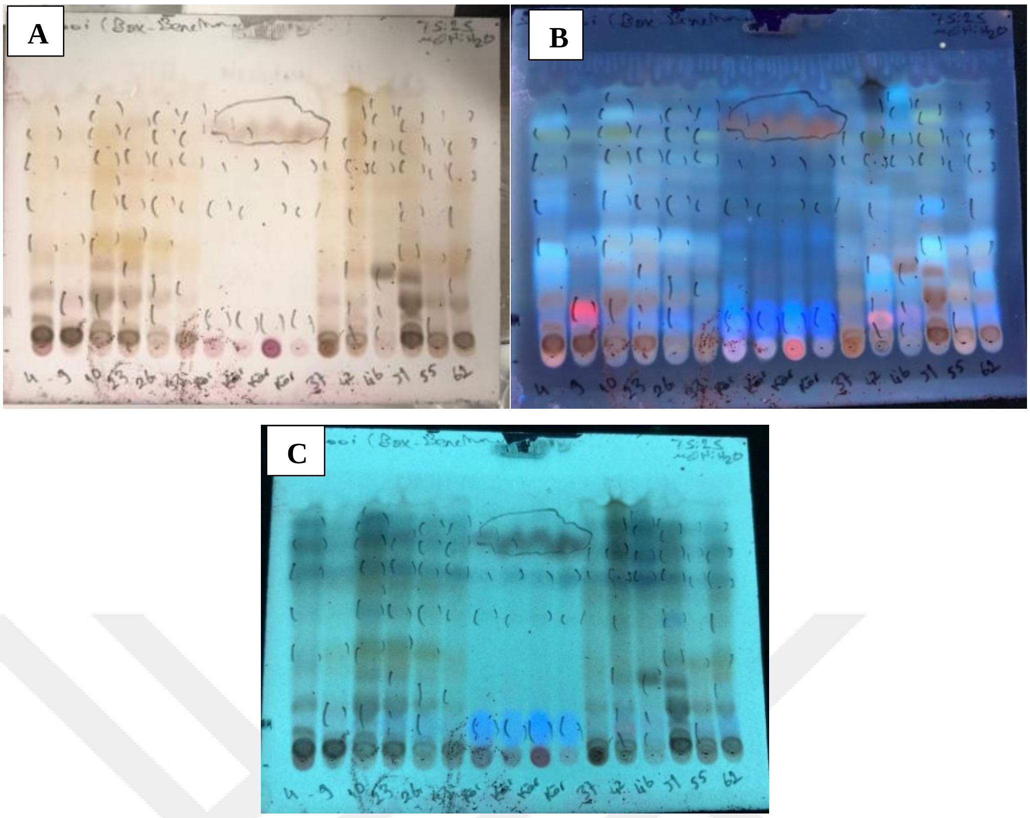

Figure 3.7. RP-TLC chromatograms of the extracts displaying different chemical profiles (runs: 4, 9, 10, 23, 26, 36, four different blanks, 37, 46, 51, 55, 62 respectively). Images of RP-TLC plates after H_2SO_4 treatment; **(A)** under day light after, **(B)** under 365 nm, **(C)** under 254 nm.

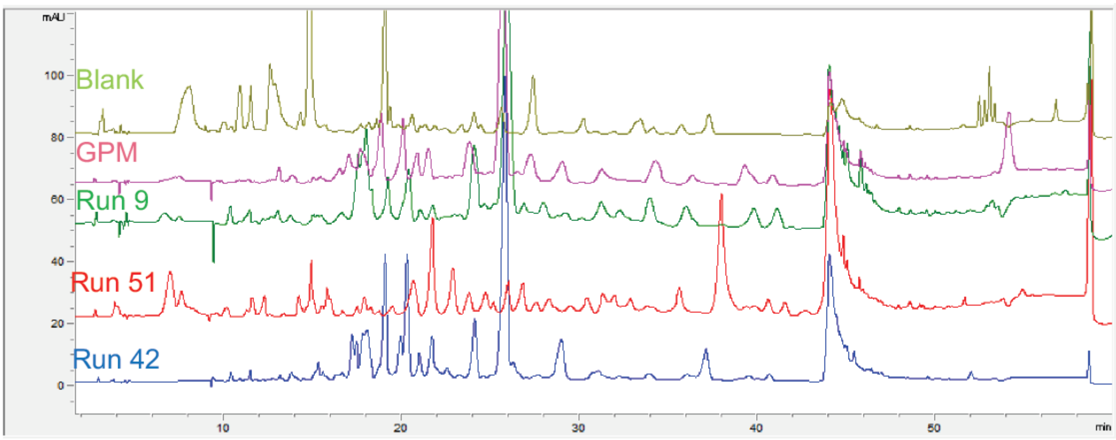

Figure 3.8. HPLC-DAD chromatograms (at 230 nm) of selected runs displaying different chemical profiles in the TLC analysis (9, 42, 51). GPM is non-optimized production sample.

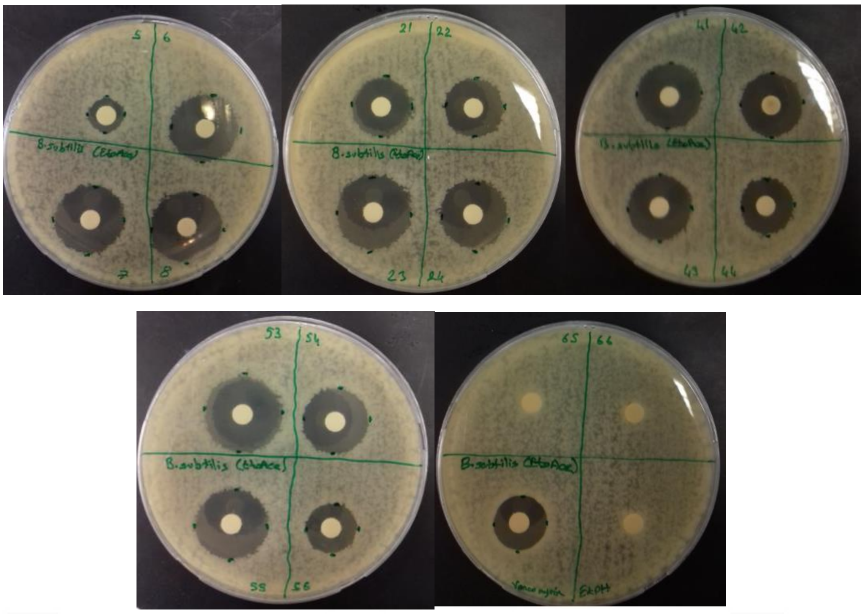

Figure 3.9. Inhibition zones of some extracts showing different chemical profiles in the TLC analysis. 100 µg were loaded to empty discs for each extract and *Bacillus subtilis* was used as test organism. 65 and 66 is blank of GPM as negative control; Vancomycin (V) (50 µg) is positive control

Since Box-Behnken design is suitable for statistical analysis even if there are some missing data, not to repeat whole experiments, some of the trials (1, 3, 4, 17, 19, 31, 46, 56 and 62 runs) that possess experimental errors (break of the flask, contamination of the culture etc.) were ignored (strikeout trials in Table 3.2). Then, the final model found to be statistically significant ($p<0.0001$) for all responses (Table 3.4, Table 3.6, and Table 3.8).

Table 3.3. Summary statistics for response 1 (Antimicrobial activity).

Std. Dev.	0.8311	**R^2**	0.9513
Mean	20.72	**Adjusted R^2**	0.9096
C.V. %	4.01	**Predicted R^2**	0.8060
		Adeq Precision	25.7242

The **R^2** value close to 1 indicates that the predicted and experimental data show a good correlation. In the relevant model, this value was calculated as 0.9513, and this result is quite satisfactory for biological models. **The Predicted R^2** of 0.8060 is in reasonable agreement with the Adjusted R^2 of 0.9096; the difference is less than 0.2. **Adeq Precision** measures the signal to noise ratio. A ratio greater than 4 is desirable.[91] Ratio of 25.724 indicates an adequate signal. Thus, this model can be used to navigate the design space (Table 3.3).

Table 3.4. ANOVA for Reduced Quadratic model (Response 1: Antimicrobial Activity).

Source	Sum of Squares	df	Mean Square	F-value	p-value	
Model	377.91	24	15.75	22.79	< 0.0001	significant
A-Temperature	2.16	1	2.16	3.12	0.0880	
B-Seawater	26.95	1	26.95	39.02	< 0.0001	
C-Glycerol	19.76	1	19.76	28.61	< 0.0001	
D-Peptone	0.7432	1	0.7432	1.08	0.3085	
E-$CaCO_3$	34.76	1	34.76	50.32	< 0.0001	
F-$FeCl_3$	18.15	1	18.15	26.27	< 0.0001	
G-$MgCl_2$	0.1058	1	0.1058	0.1532	0.6985	
AB	60.00	1	60.00	86.85	< 0.0001	
AD	2.81	1	2.81	4.07	0.0532	
AE	5.94	1	5.94	8.60	0.0066	
BD	16.85	1	16.85	24.39	< 0.0001	
BF	1.56	1	1.56	2.26	0.1438	
BG	3.47	1	3.47	5.02	0.0332	
CD	8.00	1	8.00	11.58	0.0020	
CF	2.45	1	2.45	3.55	0.0700	
CG	1.13	1	1.13	1.63	0.2124	
DE	22.47	1	22.47	32.52	< 0.0001	
DF	33.92	1	33.92	49.10	< 0.0001	
EF	5.25	1	5.25	7.60	0.0102	
A^2	21.31	1	21.31	30.85	< 0.0001	
B^2	37.07	1	37.07	53.67	< 0.0001	
D^2	49.43	1	49.43	71.56	< 0.0001	
E^2	2.23	1	2.23	3.22	0.0833	
F^2	6.37	1	6.37	9.22	0.0051	
Residual	19.34	28	0.6908			
Lack of Fit	18.04	24	0.7518	2.31	0.2161	not significant
Pure Error	1.30	4	0.3250			
Cor Total	397.25	52				

The **Model F-value** of 22.79 implies the model is significant. There is only a 0.01% chance that an F-value this large could occur due to noise.

P-values less than 0.05 indicate model terms are significant.[92] In this case B, C, E, F, AB, AE, BD, BG, CD, DE, DF, EF, A^2, B^2, D^2, F^2 are significant model terms. Values greater than 0.1 indicate the model terms were not significant. D, G, BF and CG are not significant model terms (Table 3.4).

The **Lack of Fit F-value** of 2.31 implies the Lack of Fit is not significant relative to the pure error. There is a 21.61% chance that a Lack of Fit F-value this large could occur due to noise. Significant Lack of Fit Value indicates that the model cannot express the relationship between terms. Thus, non-significant Lack of Fit is desired for the model to fit.[93]

Equation for the prediction of antimicrobial activity:

$$\begin{aligned} The\ antimicrobial\ activity &= 22.7655 + -0.329331 * A + -1.30558 * B + -0.983916 \\ &* C + 0.222291 * D + 1.57003 * E + -1.06545 * F \\ &+ -0.0732076 * G + 3.19118 * AB + 0.691185 * AD \\ &+ 0.945823 * AE + -1.69118 * BD + 0.494075 * BF \\ &+ 0.844623 * BG + 1 * CD + 0.619075 * CF + 0.375 * CG \\ &+ -2.26077 * DE + 3.01694 * DF + 1.19074 * EF \\ &+ -1.36624 * A^2 + -1.8573 * B^2 + -2.24393 * D^2 \\ &+ -0.503112 * E^2 + 0.786202 * F^2 \end{aligned}$$

Table 3.5. Summary statistics for response 2 (Biomass).

Std. Dev.	0.0207	**R^2**	0.9717
Mean	0.2233	**Adjusted R^2**	0.9411
C.V. %	9.26	**Predicted R^2**	0.8721
		Adeq Precision	21.5676

The **R^2** value of 0.9717 showed that the predicted and experimental data show a very good correlation. The **Predicted R^2** of 0.8721 is in reasonable agreement with the **Adjusted R^2** of 0.9411; the difference is less than 0.2. Reasonable agreement between adjusted R^2 and predicted R^2 indicates that this model can be used to estimate the behavior of the production with different parameter values for biomass. **Adeq Precision** ratio of 21.568 indicates an adequate signal. Thus, this model can be used to navigate the design space (Table 3.5).

Table 3.6. ANOVA for Reduced Quadratic model (Response 2: Biomass).

Source	Sum of Squares	df	Mean Square	F-value	p-value	
Model	0.3668	27	0.0136	31.74	< 0.0001	significant
A-Temperature	0.0015	1	0.0015	3.50	0.0733	
B-Seawater	0.0205	1	0.0205	47.96	< 0.0001	
C-Glycerol	0.0006	1	0.0006	1.42	0.2451	
D-Peptone	0.2289	1	0.2289	534.83	< 0.0001	
E-CaCO3	0.0526	1	0.0526	123.01	< 0.0001	
F-FeCl3	0.0435	1	0.0435	101.75	< 0.0001	
G-MgCl2	0.0002	1	0.0002	0.3873	0.5393	

(cont. on next page)

cont. Table 3.6

AB	0.0002	1	0.0002	0.5290	0.4738	
AC	0.0005	1	0.0005	1.07	0.3101	
AF	0.0006	1	0.0006	1.47	0.2363	
AG	0.0017	1	0.0017	4.00	0.0565	
BC	0.0006	1	0.0006	1.38	0.2515	
BD	0.0050	1	0.0050	11.65	0.0022	
BF	0.0048	1	0.0048	11.28	0.0025	
BG	0.0005	1	0.0005	1.15	0.2934	
CD	0.0011	1	0.0011	2.47	0.1284	
CE	0.0000	1	0.0000	0.0441	0.8355	
CF	0.0005	1	0.0005	1.05	0.3146	
DE	0.0020	1	0.0020	4.71	0.0398	
EF	0.0005	1	0.0005	1.19	0.2864	
EG	0.0015	1	0.0015	3.46	0.0747	
FG	0.0001	1	0.0001	0.3181	0.5778	
A^2	0.0084	1	0.0084	19.59	0.0002	
B^2	0.0003	1	0.0003	0.7760	0.3868	
C^2	0.0066	1	0.0066	15.48	0.0006	
F^2	0.0069	1	0.0069	16.12	0.0005	
G^2	0.0002	1	0.0002	0.3542	0.5571	
Residual	0.0107	25	0.0004			
Lack of Fit	0.0079	21	0.0004	0.5439	0.8409	not significant
Pure Error	0.0028	4	0.0007			
Cor Total	0.3775	52				

The **Model F-value** of 31.74 implies that the model is significant. There is only a 0.01% chance that an F-value this large could occur due to noise.

P-values less than 0.05 indicate model terms are significant. In this case B, D, E, F, BD, BF, DE, A^2, C^2, F^2 are significant model terms. Values greater than 0.1 indicate the model terms were not significant. C, G, AB, AC, AF, BC, BG, CD, CE, CF, EF, FG, B^2 and G^2 are not significant model terms (Table 3.6).

The **Lack of Fit F-value** of 0.54 implies the Lack of Fit is not significant relative to the pure error. There is an 84.09% chance that a Lack of Fit F-value this large could occur due to noise. Non-significant lack of fit is good for the model to fit.[93]

Equation for the prediction of dry biomass amount:

$$Biomass\ amount = 0.2178 + 0.00812389 * A + 0.0358707 * B + -0.00505385 * C + 0.111012 * D + 0.0610679 * E + 0.0512826 * F + 0.00292413 * G + 0.00568527 * AB + 0.0094386 * AC + -0.000814735 * AD + -0.0034386 * AE + 0.008875 * AF + -0.014625 * AG + 0.0103999 * BC + 0.0280647 * BD + 0.000216062 * BE + 0.0288999 * BF + -0.0101474 * BG + -0.0115 * CD + 0.0026886 * CE + 0.00914986 * CF + -0.00225 * CG + 0.0210404 * DE + -0.00097175 * DF + 0.00275 * DG + -0.0106083 * EF + -0.0157839 * EG + 0.004125 * FG + 0.0269538 * A^2 + -0.00551316 * B^2 + 0.0246839 * C^2 + -0.00167592 * D^2 + -0.00162628 * E^2 + -0.0253209 * F^2 + -0.00380796 * G^2$$

Table 3.7. Summary statistics for response 3 (amount of the extracts).

Std. Dev.	1.10	**R^2**	0.8525
Mean	5.06	**Adjusted R^2**	0.7355
C.V. %	21.80	**Predicted R^2**	0.4116
		Adeq Precision	11.2879

The **R^2** value of 0.8525 showed that the predicted and experimental data show a good correlation for biological design. However, the **Predicted R^2** of 0.4116 is not as close to the **Adjusted R^2** of 0.7355 as one might normally expect; the difference is more than 0.2. This may indicate a large block effect or a possible problem with the model and/or data. Things to consider are model reduction, response transformation, outliers, etc. All empirical models should be tested by doing confirmation runs. **Adeq Precision** ratio of 11.288 indicates an adequate signal (Table 3.7). Thus, this model can be used to navigate the design space.

Among the responses, not only the amounts of extracts but also the antimicrobial effects were evaluated for further studies. In addition to these statistical results, the chemical diversities observed in TLC and HPLC analysis of the extracts were considered. In this context, ongoing studies were planned by evaluating all results together to obtain the bioactive metabolites in maximum variety.

Table 3.8. ANOVA for Reduced Quadratic model (Response 3: Extract amount).

Source	Sum of Squares	df	Mean Square	F-value	p-value	
Model	203.91	23	8.87	7.29	< 0.0001	significant
A-Temperature	0.0885	1	0.0885	0.0728	0.7893	
B-Seawater	17.18	1	17.18	14.12	0.0008	
C-Glycerol	81.51	1	81.51	67.00	< 0.0001	
D-Peptone	13.11	1	13.11	10.78	0.0027	
E-CaCO3	5.13	1	5.13	4.22	0.0492	
F-FeCl3	0.7109	1	0.7109	0.5843	0.4508	
G-MgCl2	0.4272	1	0.4272	0.3511	0.5581	
AC	5.45	1	5.45	4.48	0.0430	
AG	3.25	1	3.25	2.67	0.1129	
BC	4.26	1	4.26	3.50	0.0714	
BE	3.36	1	3.36	2.77	0.1071	
BF	4.00	1	4.00	3.29	0.0801	
CD	5.61	1	5.61	4.61	0.0402	
CG	3.00	1	3.00	2.47	0.1271	
DE	1.65	1	1.65	1.35	0.2543	
DF	8.20	1	8.20	6.74	0.0147	
EG	3.16	1	3.16	2.60	0.1176	
FG	2.31	1	2.31	1.90	0.1786	
A^2	7.75	1	7.75	6.37	0.0174	
B^2	12.44	1	12.44	10.23	0.0033	
C^2	5.17	1	5.17	4.25	0.0483	
D^2	2.49	1	2.49	2.05	0.1628	
F^2	9.21	1	9.21	7.57	0.0101	
Residual	35.28	29	1.22			
Lack of Fit	34.87	25	1.39	13.54	0.0105	significant
Pure Error	0.4120	4	0.1030			
Cor Total	239.19	52				

The **Model F-value** of 7.29 implies that the model is significant. There is only a 0.01% chance that an F-value this large could occur due to noise.

P-values less than 0.050 indicate model terms are significant. In this case B, C, D, E, AC, CD, DF, A^2, B^2, C^2, F^2 are significant model terms. Values greater than 0.1 indicate the model terms were not significant. A, F, G, AG, CG, DE, EG, FG and D^2 are not significant model terms (Table 3.8).

The **Lack of Fit F-value** of 13.54 implies the Lack of Fit is significant. There is only a 1.05% chance that a Lack of Fit F-value this large could occur due to noise.

Equation for the prediction of EtOAc extract amount:

$$
\begin{aligned}
Amount\ of\ EtOAc\ extract &= 4.66589 + 0.0644921 * A + 0.962978 * B + 1.98354 * C \\
&+ -0.880908 * D + 0.58213 * E + -0.203263 * F + -0.141668 \\
&* G + -0.903393 * AC + -0.6375 * AG + 0.81652 * BC \\
&+ -0.828565 * BE + 0.79152 * BF + -0.8375 * CD + -0.6125 \\
&* CG + -0.603266 * DE + 1.42764 * DF + -0.803565 * EG \\
&+ 0.5375 * FG + 0.817615 * A\hat{}2 + 1.05543 * B\hat{}2 + 0.677166 \\
&* C\hat{}2 + -0.477178 * D\hat{}2 + -0.917626 * F\hat{}2
\end{aligned}
$$

When the results were analyzed on graphs, it was seen that all factors except $MgCl_2$ were effective on responses (Figure 3.10). It is noteworthy that the increase of $CaCO_3$ causes an increment for all responses (Figure 3.10-E). While the increase in seawater/distilled water ratio enhanced the biomass and amount of the extract, it caused a serious decrease in the activity of the extract at a rate of over 50% (Figure 3.10-B). The increase in peptone-water caused a continuous increment in biomass and a partial decrease in the amount of extract (Figure 3.10-D). On the contrary to peptone-water, increase in the amount of glycerol did not cause an increment in biomass but caused an increment in the amount of extract (Figure 3.10-C). Therefore, we deduced that peptone-water was a source for primary metabolism, whereas glycerol was a source for secondary metabolism. However, it was observed that the excessive increase in the amount of glycerol could be misleading because of accumulation of glycerol in the ethyl acetate phase, not being consumed completely by *S. cacaoi* (observed by NMR analysis of some extracts which were not part of the design matrix). $FeCl_3$ showed positive effect only on the biomass (Figure 3.10-F). The blue lines on the graphs are 95% confidence limits, and all results are at 95% confidence interval for all graphs.

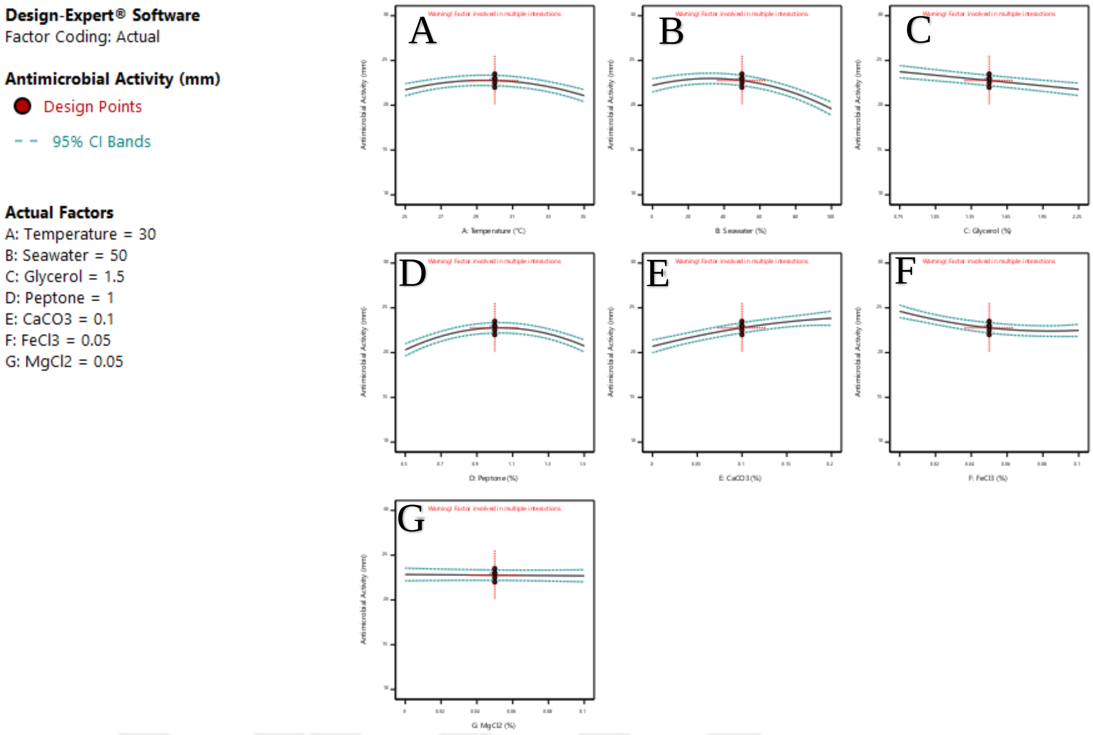

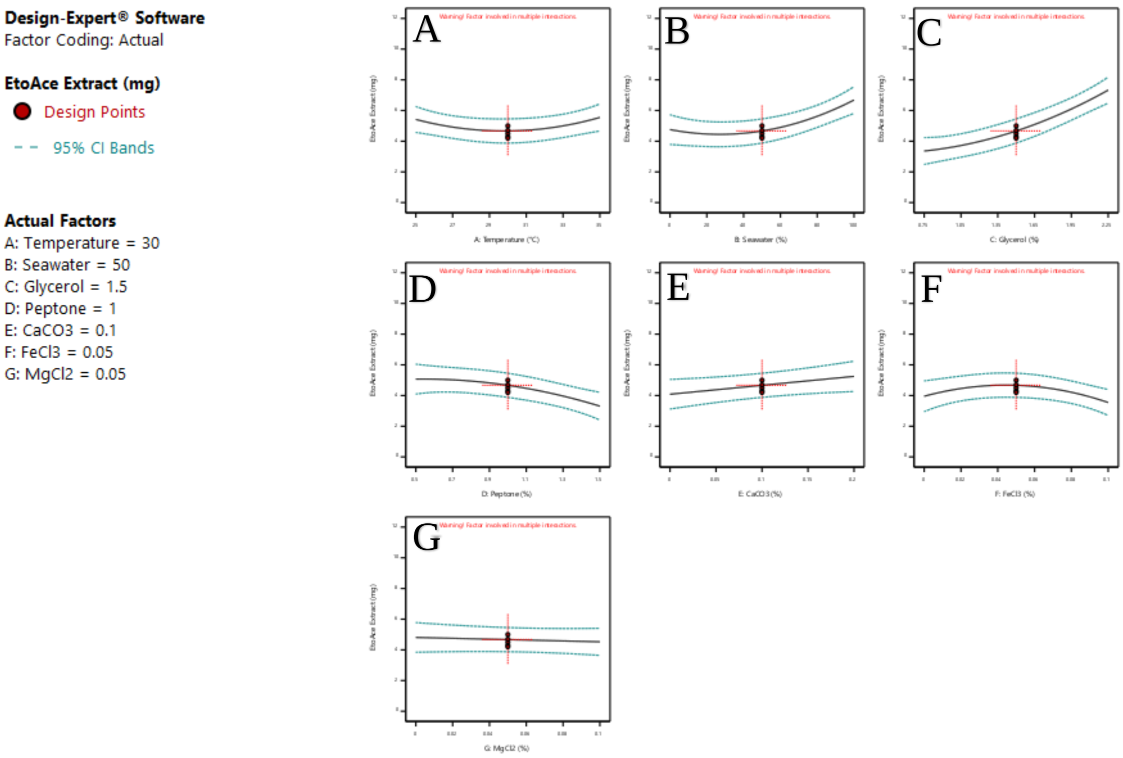

(cont. on next page)

Figure 3.10. Effects of the factors on antimicrobial activity, extract amount and biomass amount, respectively. **A:** Temperature, **B:** Seawater-distilled water ratio, **C:** Glycerol, **D:** Peptone water, **E:** $CaCO_3$, **F:** $FeCl_3$, **G:** $MgCl_2$

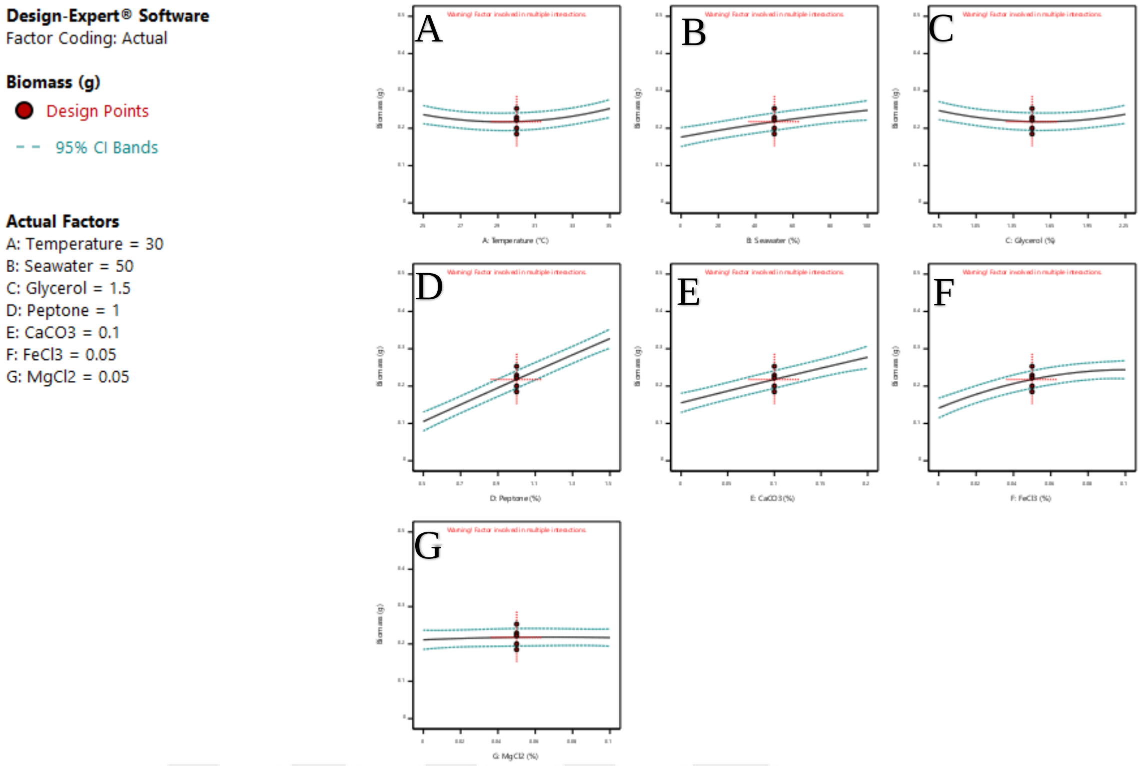

Figure 3.10 (cont.)

One factor effect evaluation gives us important insights how this factor effects a response. Yet since factors may involve in multiple interactions, to determine the correlation between response with multiple factors must be investigated. One of the major advantages of statistical experimental design like Box-Behnken -which is used in this thesis- on one factor at a time approach is allowing observation of multiple factors together on a response rather than analysis them individually. This analysis can be made between all terms that are found significant. For example, according to Figure 3.11, an increase in seawater ratio at 25°C leads to a decrease in antimicrobial activity, whereas an increase in seawater concentration at 35°C causes an increase in antimicrobial activity. This observation allows us to understand the effects of factors on each other and to provide the most suitable conditions for the desired production.

Non-optimized contents of GPM were 2% glycerol, 1% peptone water, 0.1% $CaCO_3$, 0.05% $MgCl_2$ and 0.05% $FeCl_3$ in distilled water containing 2% NaCl or in seawater. Statistical analysis of these contents and incubation temperature was performed using the Box-Behnken design. The results given above were examined in detail and it was revealed that the maximum bioactivity and chemical diversity in the EtOAc extract could be obtained without seawater and $FeCl_3$. Thus, it was decided to prepare the GPM in distilled water and to remove $FeCl_3$ from the composition. Validation studies, in which

Factor 2 and Factor 6 were determined as '0', were initiated. After these studies, the content of GPM and temperature was optimized as 2.25% glycerol, 1% peptone water, 0.2% $CaCO_3$, 0.1% $MgCl_2$ in distilled water and at 30°C, respectively. These values were used for all subsequent studies.

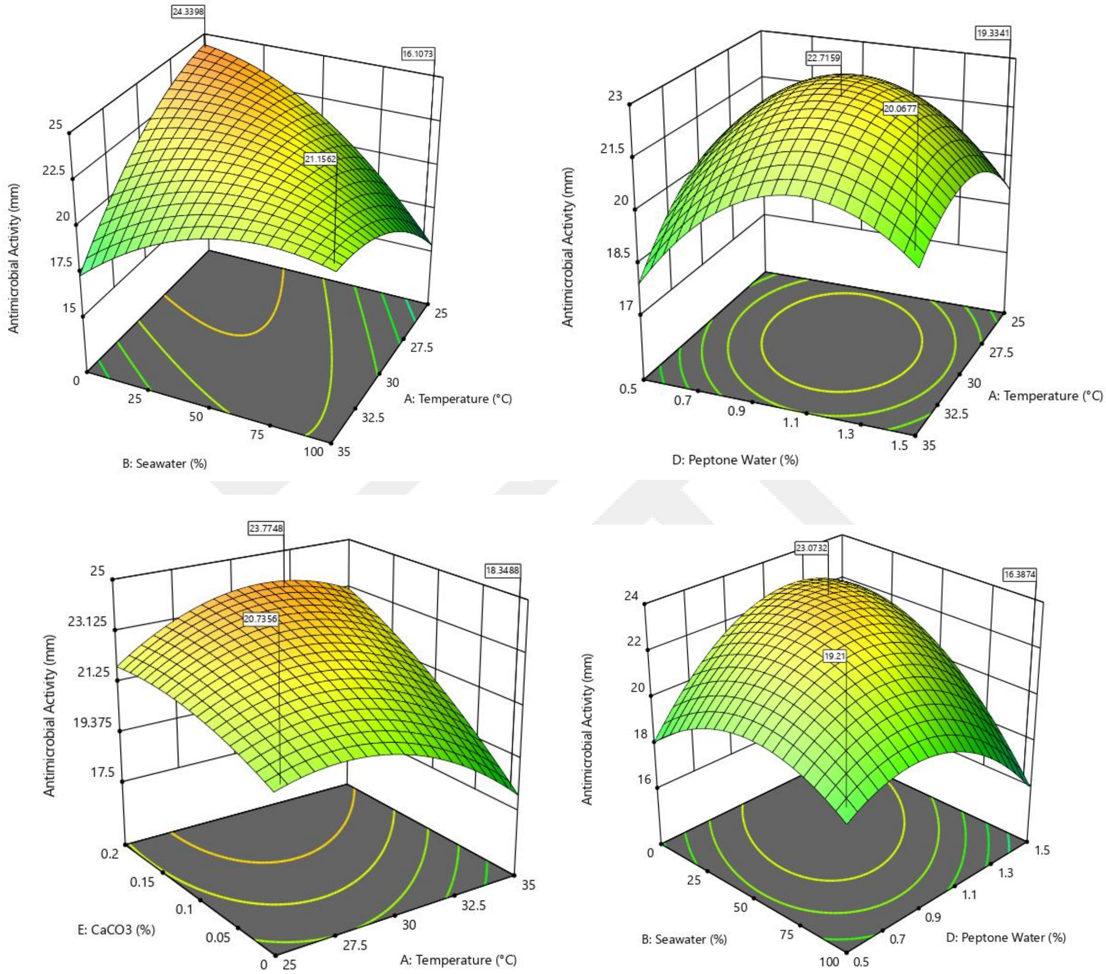

Figure 3.11. 3D Surface graphics for the effects of factors on bioactivity (Part 1).

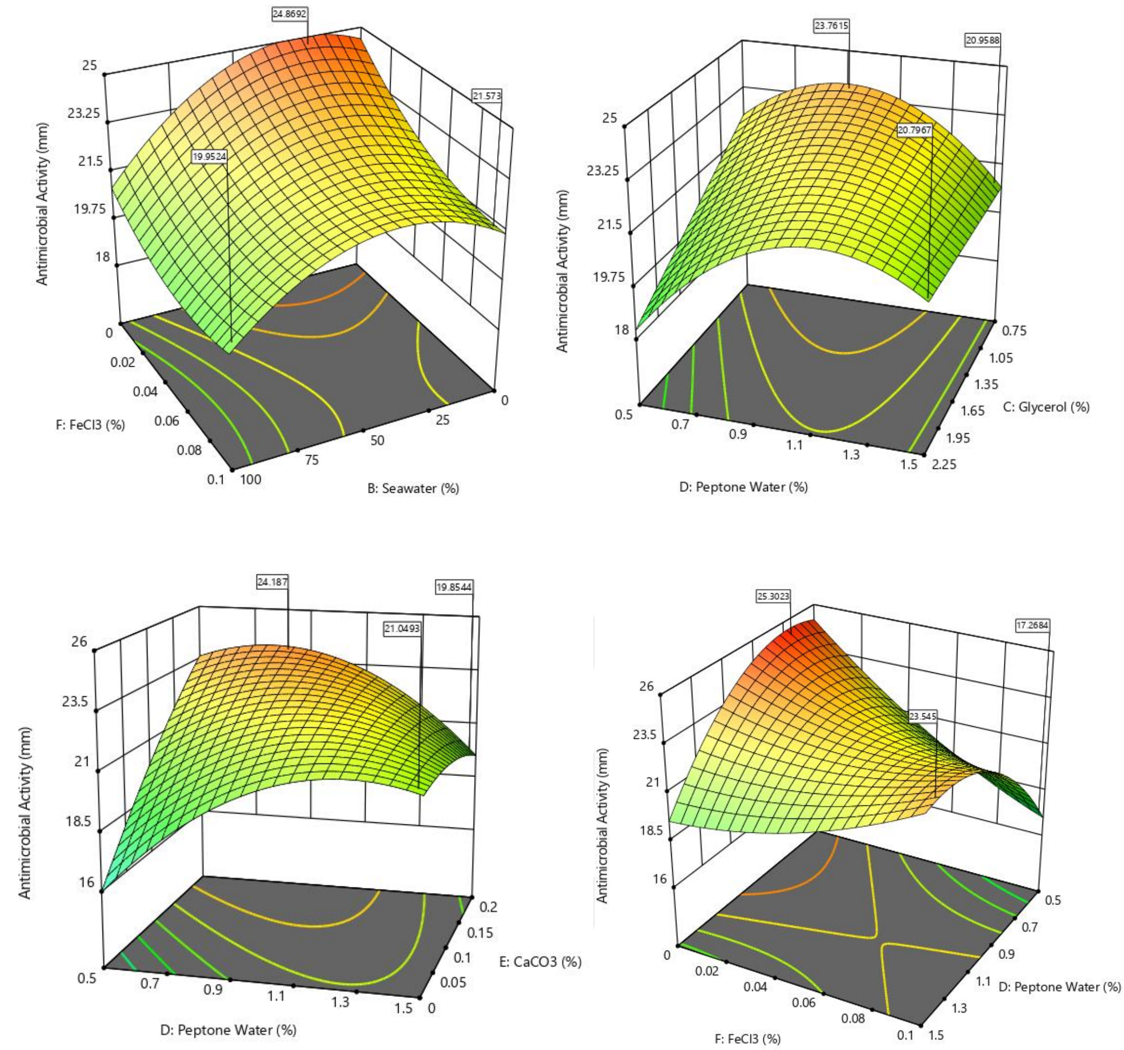

Figure 3.12. 3D Surface graphics for the effects of factors on bioactivity (Part 2).

3.3.Biological Induction Studies

A number of co-culture studies were employed to induce secondary metabolism of *Streptomyces cacaoi*. The approach and procedures described in section 2.2.3 were followed in the preparation of multi-culture fermentations and subsequent analysis. The alterations in morphology and color indicate that co-cultivation was successfully performed (Figure 2.13 and 2.14). Further analysis done via TLC showed that metabolite profiles of *S. cacaoi* were also changed by the inducer microorganisms (Figure 3.15 and 3.16).

Figure 3.13. Multi-cultures after fermentation.

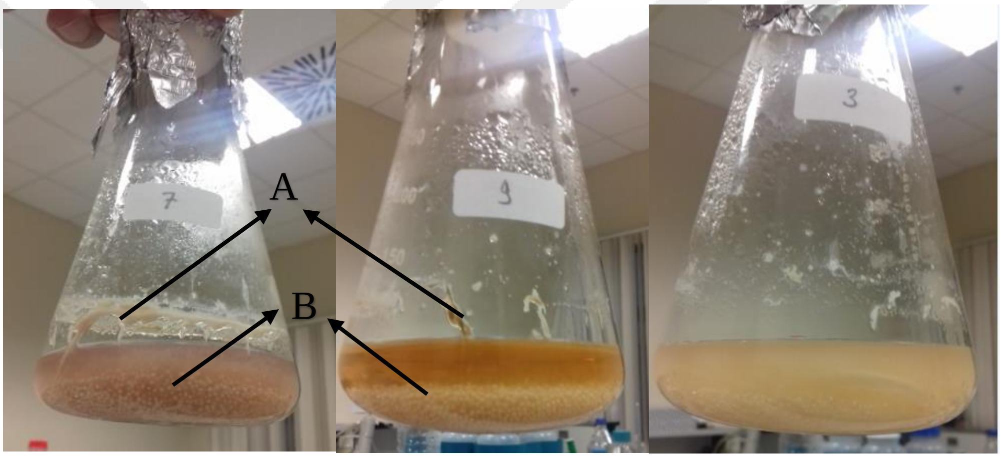

Figure 3.14. Different fermentation colors and different colonial morphologies grown in multi-cultures; **A:** Fungal colonies; **B**: *Streptomyces* colonies.

When the antimicrobial activity (against *B. subtilis*) and the amounts of extracts were evaluated, differences were observed for both responses (there was no correlation between two responses). It was observed that there was an increase for the amount of extract in some runs, but in terms of antimicrobial effect, all the changes were in the direction of activity decrease (Table 3.9). The extracts were also subjected to disc diffusion against *E. coli* to see whether the new procedure resulted in activity gain, which was not the case in optimized culture conditions. Even some antimicrobial activity (8 mm) was detected, the same activity was also present in negative controls of Run-1, in which instead of *S. cacaoi* all other four inducer microorganisms were inoculated and *S. rochei* used for induction. Therefore, it was concluded that the reason behind this activity was not the metabolites produced by *S. cacoi*.

Table 3.9. Placket-Burman design matrix for biological inducers; The inducers contained in the multi-culture are shown in the table as 1 (1 ml/50ml medium). Run-13 and run-14 are controls at the center point. Also, amount and bioactivity results of the ethyl acetate extracts are in the responses; Disc diffusion assay was made with 100 µg extracts for each run.

Runs	**Factors**										**Responses**		
	S. rochei (ml)	*B. subtilis* (ml)	*C. albicans* (ml)	*A. alternata* (ml)	*A. eureka* (ml)	*F. solani* (ml)	*P.roseopurpureum* (ml)	*Penicillium sp.* (ml)	*N. hiratsukae* (ml)	*C. laburnicola* (ml)	Extract amount (mg)	Zone (*B. subtilis)* (mm)	Zone (E. coli) (mm)
1	1	1	0	1	1	1	0	0	0	1	13.9	25	8
2	0	1	1	0	1	1	1	0	0	0	22.1	26	0
3	1	0	1	1	0	1	1	1	0	0	32.6	24	0
4	0	1	0	1	1	0	1	1	1	0	32.2	25	0
5	0	0	1	0	1	1	0	1	1	1	36.7	23	0
6	0	0	0	1	0	1	1	0	1	1	19.5	27	0
7	1	0	0	0	1	0	1	1	0	1	24.8	25	0
8	1	1	0	0	0	1	0	1	1	0	27.3	25	0
9	1	1	1	0	0	0	1	0	1	1	28.3	27	0
10	0	1	1	1	0	0	0	1	0	1	21.9	25	0
11	1	0	1	1	1	0	0	0	1	0	27.5	27	0
12	0	0	0	0	0	0	0	0	0	0	26.6	27	0
13	0.5	0.5	0.5	0.5	0.5	0.5	0.5	0.5	0.5	0.5	26.7	25	0
14	0.5	0.5	0.5	0.5	0.5	0.5	0.5	0.5	0.5	0.5	31.8	24	0

Chemical profiles of the extracts were examined by TLC, and the presence of different spots were observed in run-4 and run-7. Spots were visible under 254 nm UV light, and they were not seen in the blank cultures (Figure 3.15). Also, run-4 and mono-cultures of the inducer microorganisms were examined in detail with RP-TLC; two induced spots appeared yellow under 365 nm UV light were also observed (Figure 3.16). All TLC analyses were made by solving the extracts at same concentration.

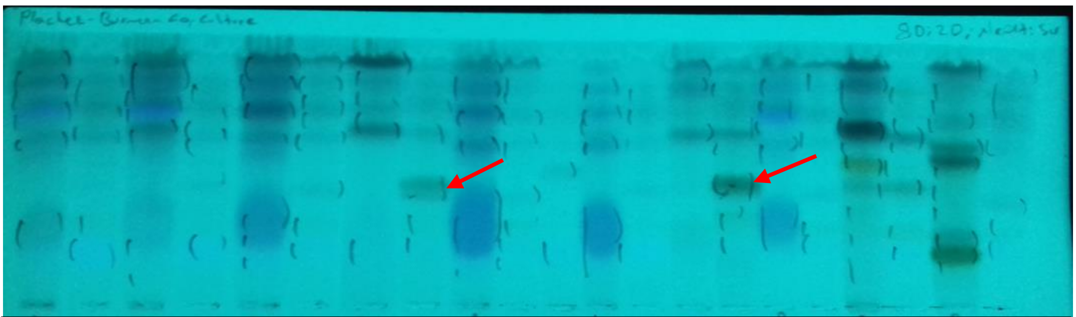

B1 1 B2 2 B3 3 B4 4 B5 5 S B6 6 B7 7 B8 8 B9 9 B10 10

Figure 3.15. RP-TLC of the multi-culture extracts; The numbers written on the TLC's are the numbers of the runs in the design matrix, and the corresponding blanks are indicated by 'B'. 'S' is the extract of mono-culture of *S. cacaoi*. Solvent system is Methanol-Water (80:20 v/v).

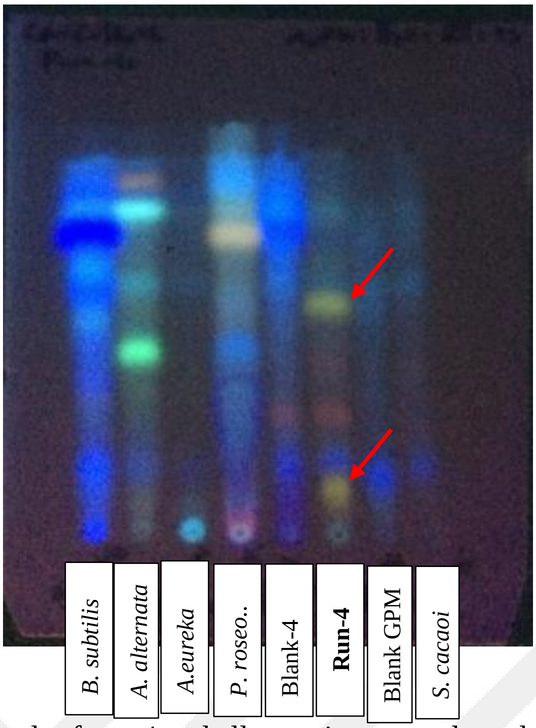

Figure 3.16. RP-TLC result of run-4 and all negative controls under UV 365 nm. On TLC; axenic culture of each microorganism used as inducer in Run-4 (*B. subtilis, A. alternata, A. eureka, P. roseopurpureum*), blank of run-4, run-4, blank of GPM and axenic culture of *S. cacaoi*, respectively. Solvent system is Methanol-Water (85:15 v/v).

3.4. Chemical Induction Studies

Different inorganic compounds were added to GPM and their effects on the secondary metabolism of *S. cacaoi* were examined. Placket-Burman design was used to create different combinations of the chemicals. The antimicrobial effects of the obtained ethyl acetate extracts were tested against *Bacillus subtilis*, *Candida albicans* and *E. coli*.

It was noteworthy that run-2, run-3, and run-8 showed activity against *E. coli* (Figure 3.17). Observation of the activities was done by disc diffusion test by loading 200 µg extract into empty discs. In terms of *C. albicans*, none of the extracts was found active. On the other hand, significant differences were observed in the amounts of extracts. Even some runs (Runs 2, 3, and 8) exerting activity against *E. coli*, the amount of extract decreased significantly (Table 3.10).

The models, in which the amount of extract and activity against *E. coli* and *B. subtilis* were recorded as a response, were found statistically significant (model p-value was 0.0195 for bioactivity and 0.0015 for extract amount). When the coefficient calculations were made, it was seen that KNO_3 and Li_2CO_3 had a positive effect on the activity against *E. coli*, while DMSO provied a positive effect and KNO_3 had a negative effect on the amount of extract (Table 3.11 and Table 3.12).

Table 3.10. Placket-Burman design matrix for chemical induction; The inducers used, and their amounts added to the GPM medium are given in the factors section. In response column, the amount of ethyl acetate extracts and the disc diffusion test results were recorded. **Factors=** A: DMSO, B:EtOH, C: Zn^{+2}, D: K_2HPO_4, E: $MgSO_4$, F: KNO_3, G: Li_2CO_3, H: LiCl, I: $CuSO_4$, J: $FeSO_4$

	Factors										Responses		
Run	A	B	C	D	E	F	G	H	I	J	Extract Amount	Zone (*B. subtilis*)	Zone (*E. coli*)
	%	%	%	%	%	%	%	%	%	%	mg	mm	mm
1	1.5	1	0	0.2	0.05	0.2	0	0	0	0.01	10.9	26	0
2	0	1	0.01	0	0.05	0.2	0.01	0	0	0	6	26	16
3	1.5	0	0.01	0.2	0	0.2	0.01	0.01	0	0	16.6	20	9
4	0	1	0	0.2	0.05	0	0.01	0.01	0.01	0	12.1	23	0
5	0	0	0.01	0	0.05	0.2	0	0.01	0.01	0.01	11.3	28	0
~~**6**~~	~~0~~	~~0~~	~~0~~	~~0.2~~	~~0~~	~~0.2~~	~~0.01~~	~~0~~	~~0.01~~	~~0.01~~	~~17.8~~	~~0~~	~~0~~
7	1.5	0	0	0	0.05	0	0.01	0.01	0	0.01	23.4	26	0
8	1.5	1	0	0	0	0.2	0	0.01	0.01	0	13.7	24	9
9	1.5	1	0.01	0	0	0	0.01	0	0.01	0.01	17.7	16	0
10	0	1	0.01	0.2	0	0	0	0.01	0	0.01	11.7	25	0
11	1.5	0	0.01	0.2	0.05	0	0	0	0.01	0	22.6	25	0
12	0	0	0	0	0	0	0	0	0	0	14.9	27	0
13	0.75	0.5	0.005	0.1	0.025	0.1	0.005	0.005	0.005	0.005	15.9	12	0
14	0.75	0.5	0.005	0.1	0.025	0.1	0.005	0.005	0.005	0.005	18.1	23	0
15	0.75	0.5	0.005	0.1	0.025	0.1	0.005	0.005	0.005	0.005	13	21	0

*Run 6 removed from model and did not included into calculation due to experimental error.

Table 3.11. Coefficient estimate for extract amount.

Factor	**Coefficient Estimate**	**df**	**Standard Error**	**95% CI Low**	**95% CI High**	**VIF**
Intercept	14.04	1	0.8364	12.18	15.90	
DMSO	3.44	1	0.8364	1.58	5.31	1.01
KNO_3	-3.03	1	0.8364	-4.89	-1.16	1.01
Ctr Pt 1	1.63	1	1.79			

Table 3.12. Coefficient estimate for inhibition zone against *E. coli*.

Factor	**Coefficient Estimate**	**df**	**Standard Error**	**95% CI Low**	**95% CI High**	**VIF**
Intercept	3.61	1	1.13	1.09	6.14	
KNO_3	3.61	1	1.13	1.09	6.14	1.01
Li_2CO_3	2.11	1	1.13	-0.4136	4.64	1.01
Ctr Pt 1	-3.61	1	2.43			

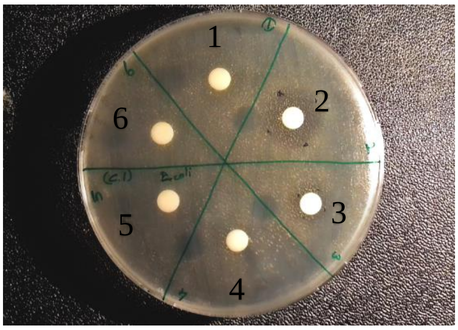

Figure 3.17. Inhibition zones against *E. coli* for run-2 and run-3.

DMSO, KNO_3 and Li_2CO_3 factors were selected to employ further analysis with Box-Behnken design. The combinations indicated in the design matrix were prepared. Totally 12 different runs and 3 center point runs were employed. In addition, as a control, production was also carried out in GPM medium containing none of the factors. As responses, the amounts of extracts and inhibition zones against *E. coli* and *B. subtilis* were recorded. When Table 3.13 is analyzed, it is seen that there are significant differences in all three responses. Every run that shows activity against *E. coli* (2, 4, 6, 8, 9. 11, 12, 15) containing KNO_3. It is also remarkable that these runs, which have activity against *E. coli*, decreased in terms of both the amounts of extracts and their activity against *Bacillus subtilis*. Also, when the runs were examined morphologically, bead-like colonies were observed in runs 1, 3, 5, and 7 while the colonies were much smaller in other runs (Figure 3.18), and in those runs KNO_3 was present while it was not in the others. Thus, it can be concluded that KNO_3 prevents colony formation. Taking all these observations into consideration, it should be kept in mind that KNO_3 may not directly affect the secondary metabolism but may have an indirect effect on secondary metabolism by affecting the morphology of *S. cacaoi*.

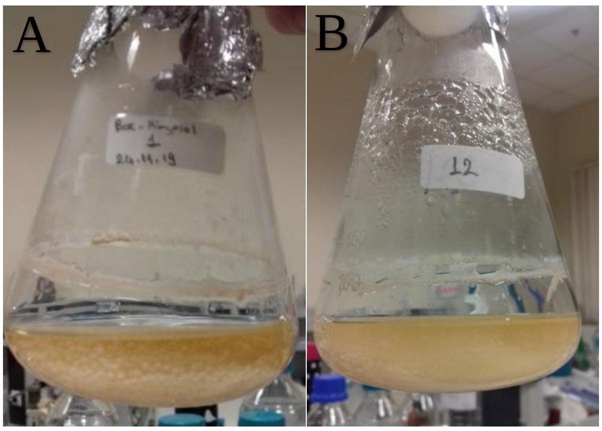

Figure 3.18. *S. cacaoi* morphologies after 10-days of fermentation. **A:** Culturing in GPM without KNO_3, and **B:** Culturing in GPM with KNO_3.

Table 3.13. Box-Behnken design matrix for chemical inducers. The results of the GPM control (without inducer) were highlighted in yellow.

Std	Factors			Responses		
	A: KNO_3	B: Li_2CO_3	C: DMSO	Extract Amount	Inhibition zone (*B. subtilis*)	Inhibition zone (*E. coli*)
	%	%	%	mg	mm	mm
1	0	0	1	32.9	30	0
2	0.4	0	1	17	20	6
3	0	0.04	1	28.6	30	0
4	0.4	0.04	1	14.6	25	9
5	0	0.02	0	21.8	30.5	0
6	0.4	0.02	0	15.2	22.5	6
7	0	0.02	2	30.1	30.5	0
8	0.4	0.02	2	12.3	26	10
9	0.2	0	0	9.1	24	11
10	0.2	0.04	0	11.2	21	0
11	0.2	0	2	16.8	22	9.5
12	0.2	0.04	2	14.3	24	9
13	0.2	0.02	1	14.6	23	0
14	0.2	0.02	1	17	22	0
15	0.2	0.02	1	14.8	26	7
GPM	-	-	-	25	29	0

In terms of the statistical calculations, quadratic model was used for the amounts of extracts and the inhibition zones observed against *Bacillus subtilis*, and reduced quadratic model was used for the observed inhibition zones against *E. coli*. ANOVA calculations were made, and all three models were found to be statistically significant $p<0.05$ (Table 3.14, 3.15 and 3.16).

Table 3.14. ANOVA for Quadratic model; Response 1: extract amount.

Source	Sum of Squares	df	Mean Square	F-value	p-value	
Model	695.55	9	77.28	24.25	0.0013	significant
A-KNO_3	368.56	1	368.56	115.65	0.0001	
B-Li_2CO_3	6.30	1	6.30	1.98	0.2187	
C-DMSO	32.81	1	32.81	10.29	0.0238	
AB	0.9025	1	0.9025	0.2832	0.6174	
AC	31.36	1	31.36	9.84	0.0258	
BC	5.29	1	5.29	1.66	0.2540	
A^2	202.42	1	202.42	63.52	0.0005	
B^2	0.6031	1	0.6031	0.1893	0.6817	
C^2	33.69	1	33.69	10.57	0.0227	
Residual	15.93	5	3.19			
Lack of Fit	12.39	3	4.13	2.33	0.3145	not significant
Pure Error	3.55	2	1.77			
Cor Total	711.48	14				

Table 3.15. ANOVA for Quadratic model; Response 2: Activity against *B. subtilis.*

Source	Sum of Squares	df	Mean Square	F-value	p-value	
Model	168.87	9	18.76	6.37	0.0277	significant
A-KNO_3	94.53	1	94.53	32.09	0.0024	
B-Li_2CO_3	2.00	1	2.00	0.6789	0.4475	
C-DMSO	2.53	1	2.53	0.8593	0.3965	
AB	6.25	1	6.25	2.12	0.2050	
AC	3.06	1	3.06	1.04	0.3547	
BC	6.25	1	6.25	2.12	0.2050	
A^2	47.96	1	47.96	16.28	0.0100	
B^2	3.85	1	3.85	1.31	0.3048	
C^2	0.0401	1	0.0401	0.0136	0.9117	
Residual	14.73	5	2.95			
Lack of Fit	6.06	3	2.02	0.4663	0.7359	not significant
Pure Error	8.67	2	4.33			
Cor Total	183.60	14				

Table 3.16. ANOVA for Reduced Quadratic model; Response 3: Activity against *E. coli.*

Source	Sum of Squares	df	Mean Square	F-value	p-value	
Model	220.11	6	36.68	4.17	0.0337	significant
A-KNO_3	120.13	1	120.13	13.65	0.0061	
B-Li_2CO_3	9.03	1	9.03	1.03	0.3407	
C-DMSO	16.53	1	16.53	1.88	0.2077	
BC	27.56	1	27.56	3.13	0.1147	
B^2	22.68	1	22.68	2.58	0.1470	
C^2	27.50	1	27.50	3.13	0.1150	
Residual	70.39	8	8.80			
Lack of Fit	37.73	6	6.29	0.3850	0.8461	not significant
Pure Error	32.67	2	16.33			
Cor Total	290.50	14				

When the results were examined on the graphs, it was seen that KNO_3 showed negative effect on the amount of extract and activity against *B. subtilis*, while positive effect on activity against *E. coli* was the case. DMSO showed positive effect on the amount of extract. However, Li_2CO_3 had no significant effect on any factor (Figure 3.19, 3.20 and 3.21).

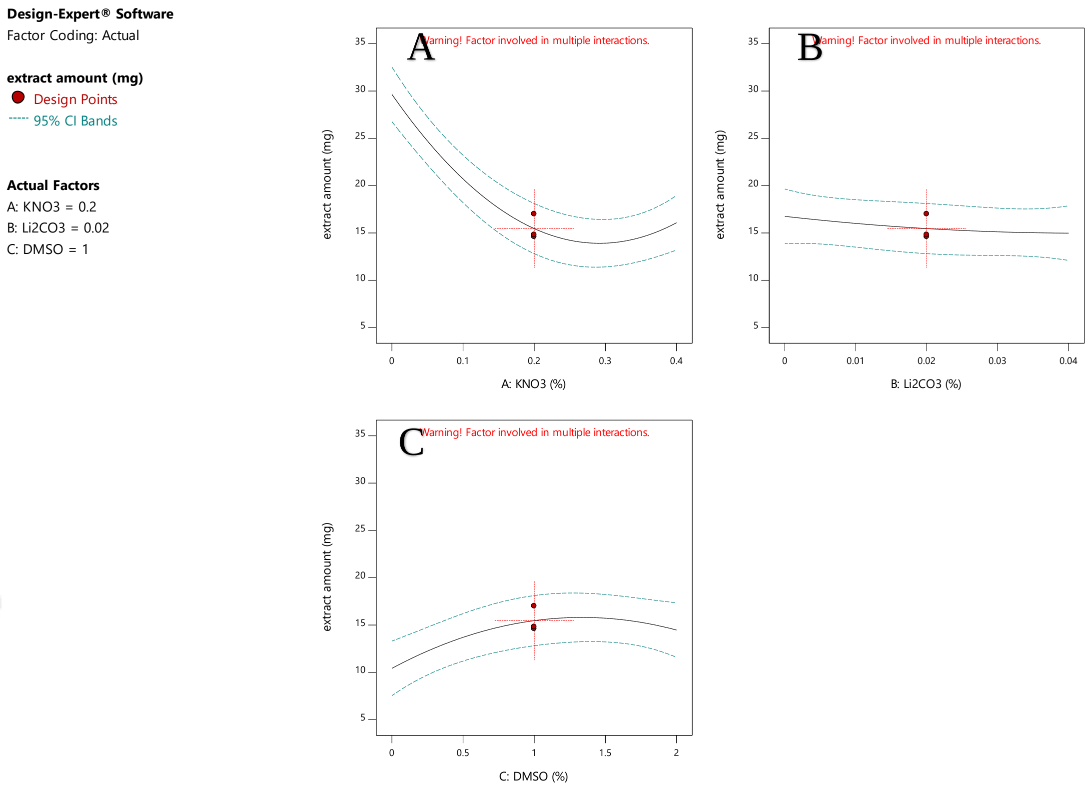

Figure 3.19. Effect of factors (A: KNO_3, B:Li_2CO_3, C: DMSO) on extract amount.

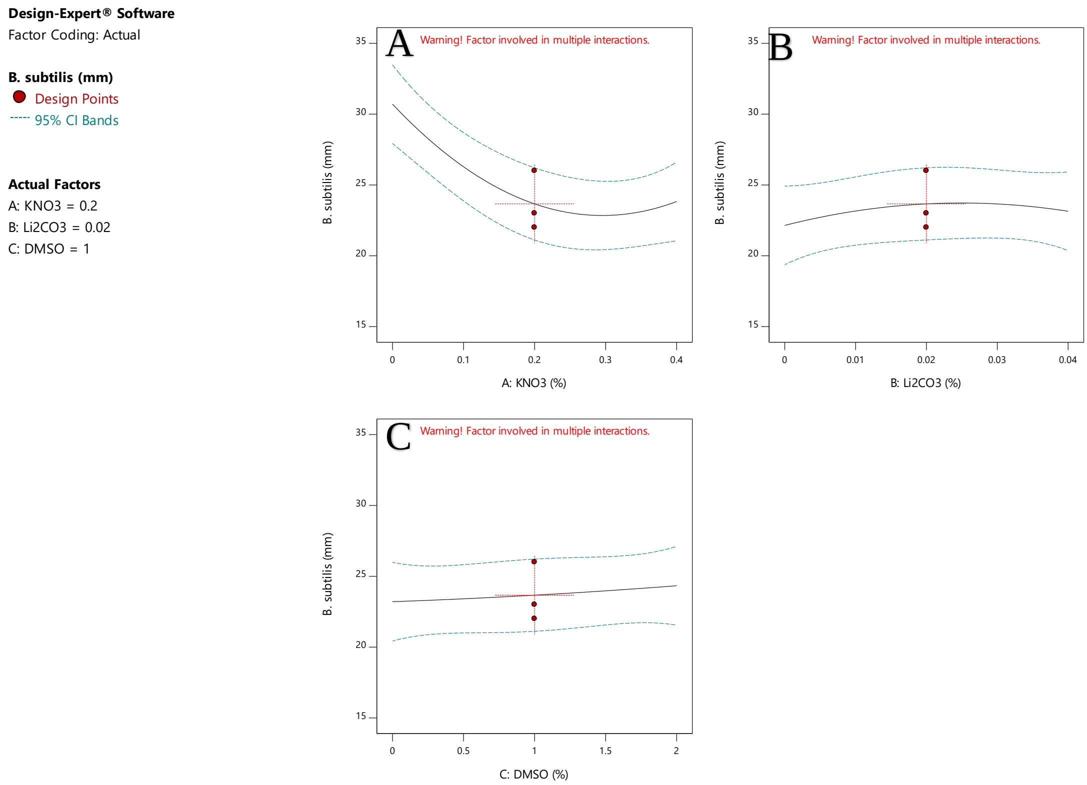

Figure 3.20. Effect of factors (A: KNO_3, B:Li_2CO_3, C: DMSO) on antimicrobial activity against *B. subtilis.*

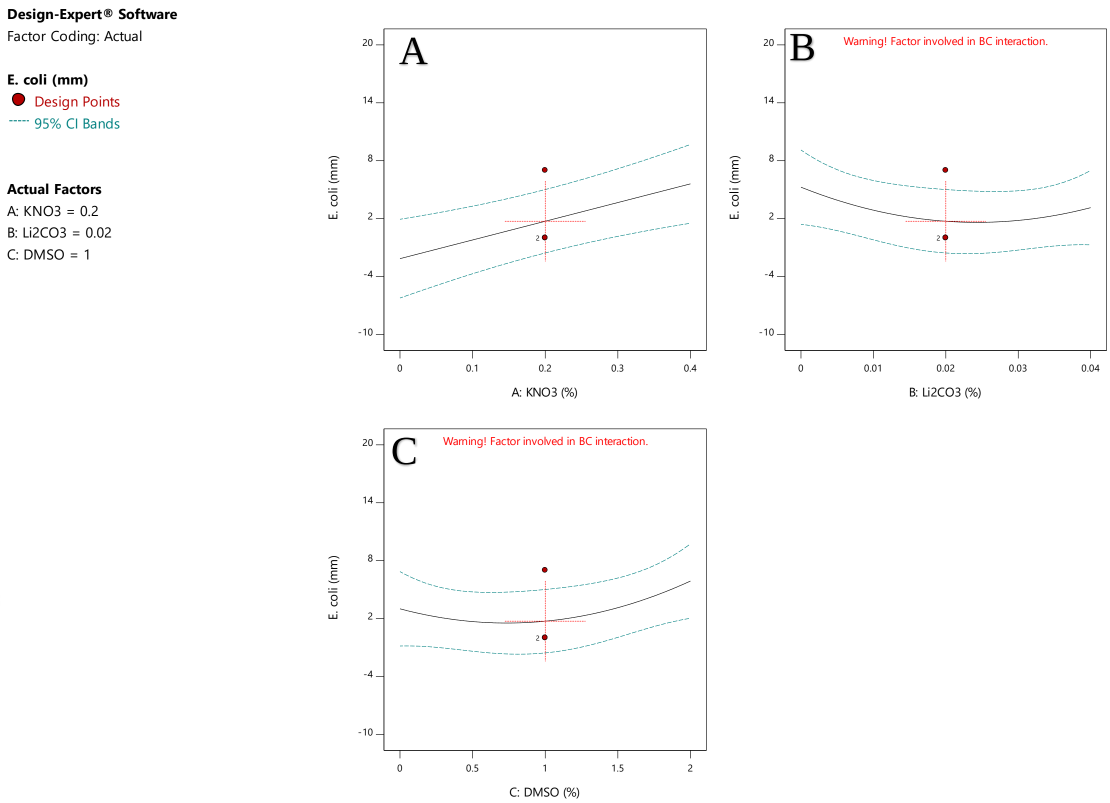

Figure 3.21. Effect of factors (A: KNO_3, B:Li_2CO_3, C: DMSO) on antimicrobial activity against *E. coli*.

Also, multiple interactions of KNO_3 and DMSO were examined, and it was found that the positive effect of DMSO on the amount of extract was observed only when KNO_3 was absent or low. On the other hand, the effect of KNO_3 on the extract amount and antimicrobial activity against *E. coli* was not affected via DMSO existence in culture medium (Figure 3.22).

Polyether antibiotics appear dark brown on the silica plate after H_2SO_4 treatment. As a result of TLC analysis, it was revealed that the production of polyether antibiotics was highly suppressed in media containing KNO_3. On the other hand, 254 nm UV active metabolites were observed in the KNO_3 containing runs (2,4,6,8, R-2, 9, 10, 11, 12, 13, 14, 15) (Figure 3.23).

Unlike KNO_3, DMSO did not enhance the diversity (Figure 3.23), it only caused an increase in the amount of extract, and this effect was only present when polyethers were produced (KNO_3 was not in the medium) (Figure 3.22). These observations allowed us to deduce that DMSO had positive effects on the production of polyether type molecules, while KNO_3 led to biosynthesis of different types of compounds.

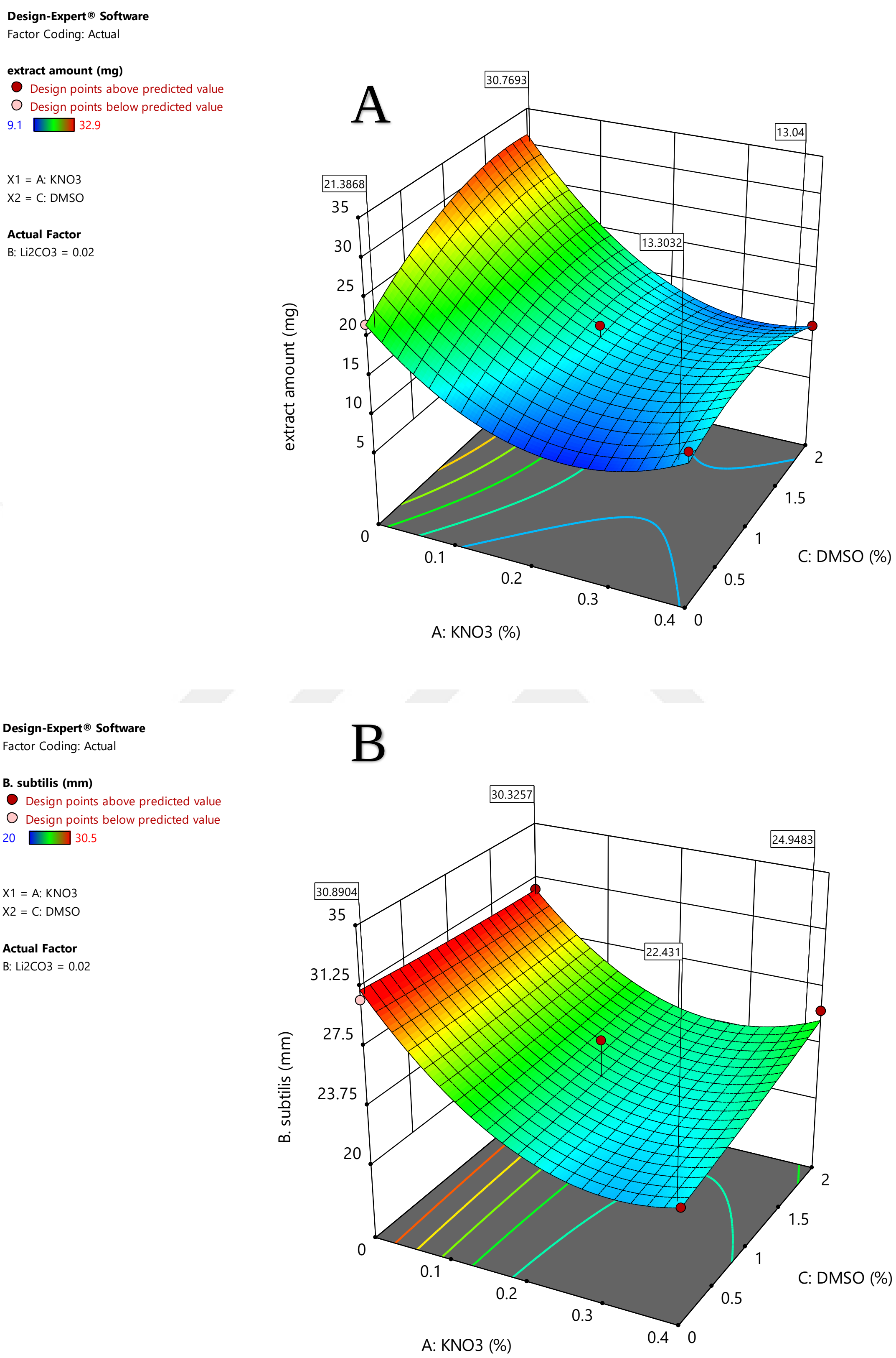

Figure 3.22. Multiple interactions of KNO_3 and DMSO on extract amount (A) and antimicrobial activity against *B. subtilis* (B).

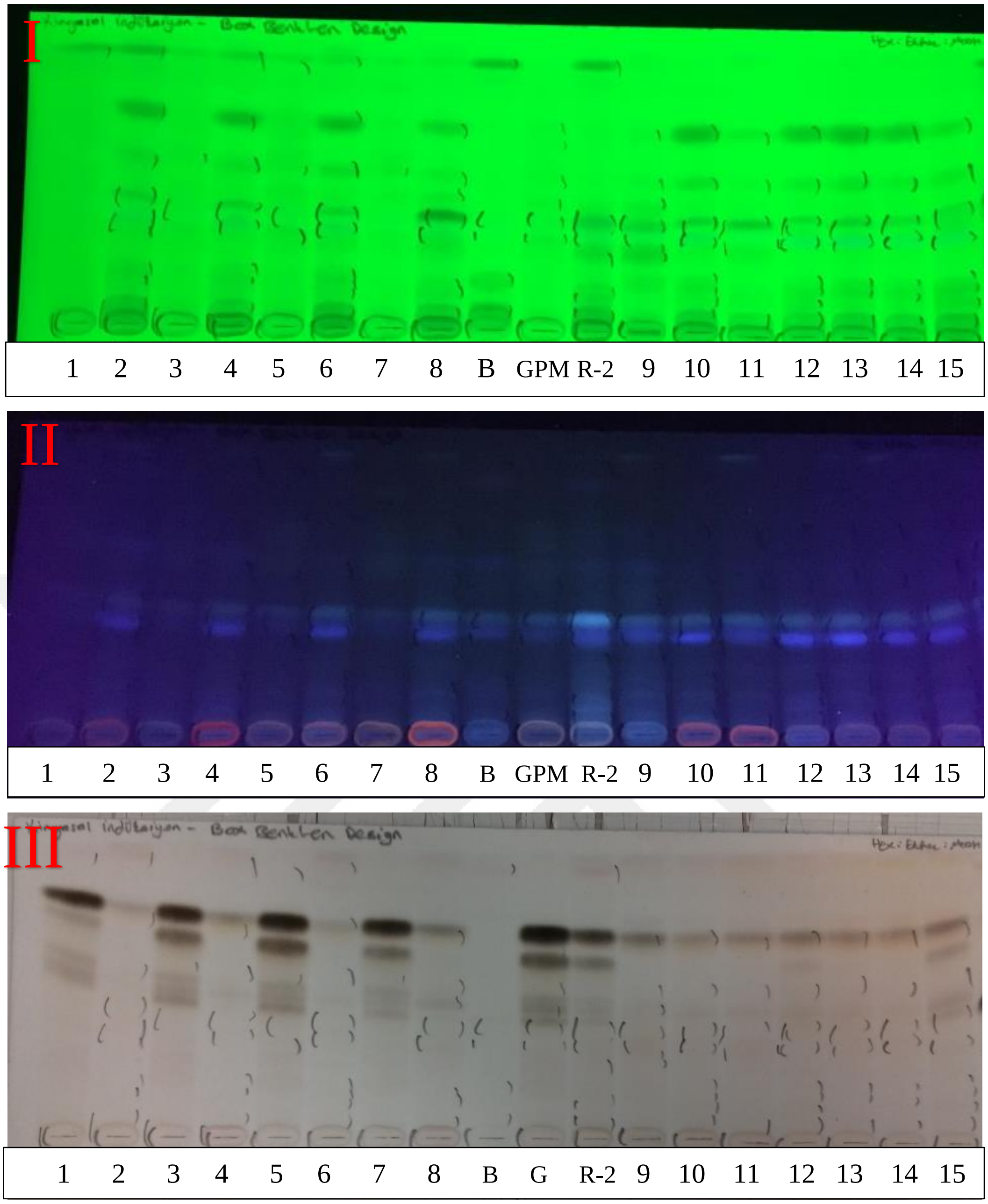

Figure 3.23. TLC results for the extracts obtained according to Box-Behnken design matrix with *n*-Hex:EtOAc:MeOH (10:10:3). **I:** under 254 nm UV, **II:** under 365 nm UV, **III:** under day light after H_2SO_4 (aq.) treatment. **B:** Blank GPM containing KNO_3, Li_2CO_3 and DMSO, **G:** the extract obtained from GPM without KNO_3, Li_2CO_3 and DMSO, **R-2:** Run-2 of Placket-Burman design matrix. Numbers from 1 to 15 indicate the corresponding runs in the Box-Behnken design matrix.

The direct bioautography technique, as described in section 2.2.4, was used to determine the bioactive molecule against *E. coli*. 500 µg of Run-2 extract was loaded onto the TLC plate and the growth of *E. coli* was inhibited in the region of a band visible under UV 254 nm (Figure 3.24).

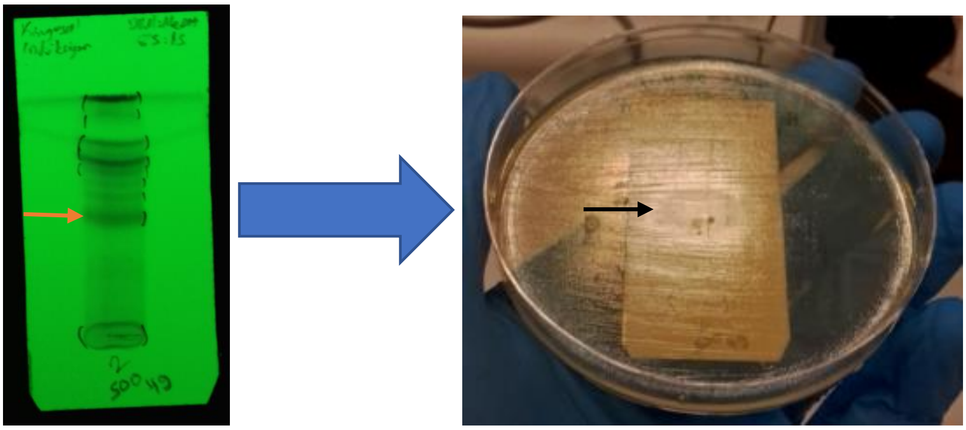

Figure 3.24. TLC image of Run-2 under 254 nm UV and the result of direct bioautography.

3.5. Production, Isolation and Purification

With the data obtained, the conditions providing the best activity, the most chemical diversity and the highest amount for the ethyl acetate extract were determined as 2.25% glycerol, 1% peptone water, 0.2% $CaCO_3$, 0.1% $MgCl_2$ in distilled water at 30 °C. Eventually, it was decided to employ large scale production under these conditions.

Production trials were made in 250 ml, 500 ml, 1000 ml, 2000 ml, and 5000 ml volumes of Erlenmeyer flasks as described in section 2.2.5. It was observed that the different volumes of the flasks greatly affected the extract amounts. Also, there was a decrease in the antimicrobial effect of the extracts obtained from flasks with a volume greater than 1 L (Table 3.17).

Table 3.17. Amounts of the extracts obtained, average amount of the extract per liter of medium, and inhibition zones of 75 µg extracts against *Bacillus subtilis.*

Working Volume/Flask volume (ml/ml)	Obtained Extract Amount	Extract Amount/Liter	Inhibition Zone
1000/5000-a 1000/5000-b	79.8 mg 77.3 mg	78.75 mg, ±1.25	20 mm
400/2000-a 400/2000-b	95.6 mg 99.8 mg	244 mg, ±2.1	21 mm
200/1000-a 200/1000-b	124 mg 127.8 mg	629 mg, ±1.9	25 mm
100/500-a 100/500-b	51 mg 50.1 mg	505 mg, ±0.45	24 mm
50/250-a 50/250-b	27.2 mg 27.1 mg	543 mg, ±0.05	25 mm

Production was made using 1 L flasks containing 200 ml medium as described in section 2.2.5. In total, 25 L of fermentation broth were produced, and 14 grams of EtOAc extract was obtained. Figure 2.25 is showed the main fractions obtained from the first column. Sixteen metabolites were purified by using column chromatography fractionations .and crystallization methods as described in section 2.2.6.

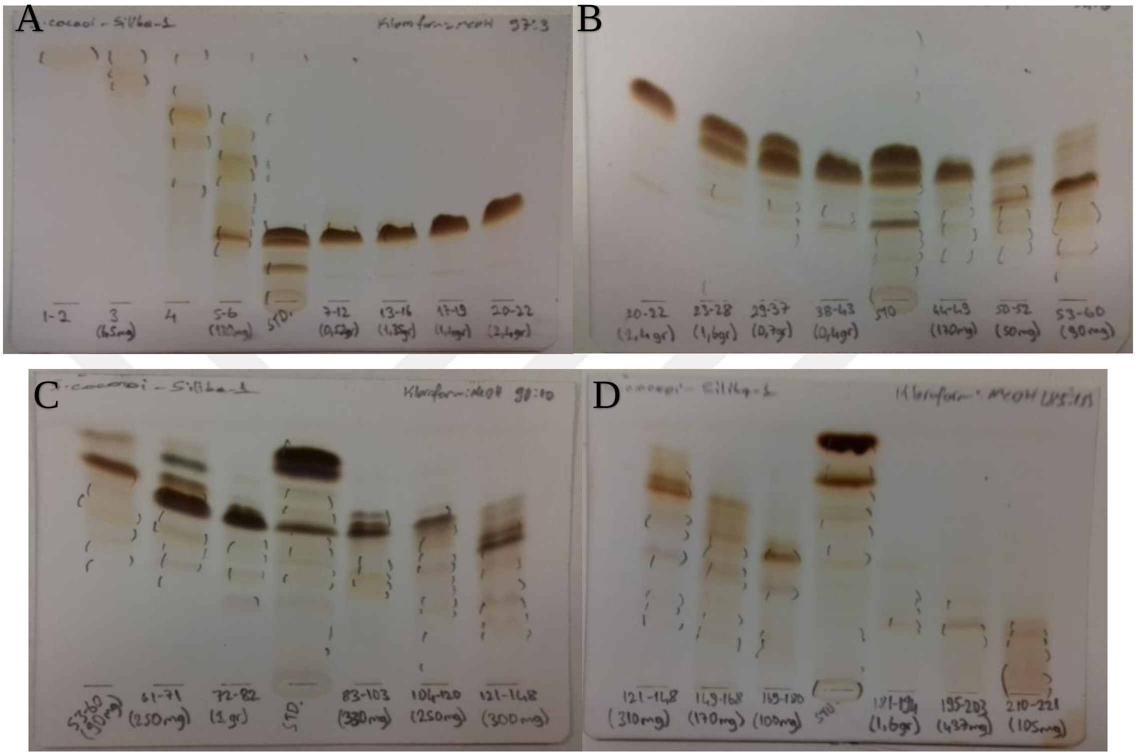

Figure 3.25. TLC images of the main fractions. Chloroform-methanol solvent system was used as mobile phase for both column and TLC analyses (100:0 → 0:100 gradient for column, and **A;** 97:3, **B;** 94:6, **C;** 90:10, **D;** 85:15 mixtures for TLC). Fraction numbers and amounts are written at the bottom of the silica plates, and STD is the ethyl acetate extract that are not subjected to columns. Each fraction was applied onto the TLC plates at same concentration.

Figure 3.26. Some main fractions after evaporation.

3.6. Structure Identification

The chemical structures of purified metabolites were elucidated using spectral methods (MS and NMR). Totally, 16 molecules were structuraly identified and 8 of them were found as new molecule.

3.6.1. Structure Identification of Polyethers

Thirteen molecules were identified as polyether-type polyketides. Among these molecules, **SC-EG-05**, **SC-EG-07**, **SC-EG-13**, **SC-EG-14** and **SC-EG-20** were found as new molecules.

3.6.1.1. Structure Elucidation of SC-EG-19

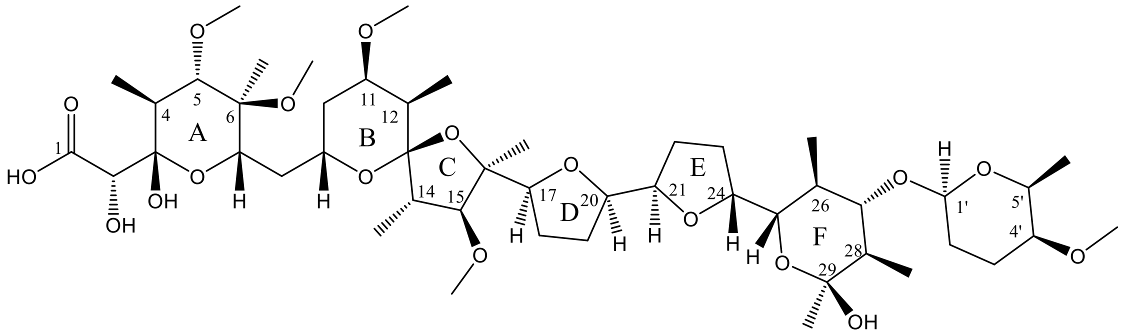

Chemical Formula: $C_{48}H_{82}O_{18}$
Exact Mass: 946.55012

Figure 3.27. Chemical structure of **SC-EG-19** (K41-A).

It is noted in our previous studies that *Streptomyces cacaoi* (JX912350.1) is a producer of polyether K41-A.[94] Eventually, the isolate coded **SC-EG-19**, obtained as a major compound (4.8 g – 192 mg/L) and its structure was verified as K41-A by spectral methods.

The NMR data (Spectrum 3.1-3.6 and Table 3.18) of **SC-EG-19** was fully consistent with the literature.[95] Initial inspection of the ^{1}H and ^{13}C NMR spectra revealed the presence of 14 oxymethines, 5 methoxy groups, and 9 methyl resonances (6 secondary and 3 tertiary). Five spin systems; a) Me-4 to H-5, b) H-7 to Me-12, c) Me-14 to H-15, d) H-17 to Me-28, e) H-1′ to Me-5′, were identified by interpreting COSY and HSQC spectra. Interrelations of the spin systems, quaternary carbons, methoxy groups and tertiary methyls were established based on the HMBC correlations, and the structure was confirmed as K41-A ((2*R*)-2-hydroxy-2-[(2*S*,3*S*,4*S*,5*S*,6*S*)-2-hydroxy-6-[[(2*R*,3*R*,4*R*,5*S*,6*R*,7*R*,9*S*)-2-[(2*R*,5*S*)-5-[(2*R*,5*R*)-5-[(2*S*,3*S*,4*S*,5*R*,6*S*)-6-hydroxy-4-[(2*R*,5*S*,6*R*)-5-methoxy-6-methyloxan-2-yl]oxy-3,5,6-trimethyloxan-2-yl]oxolan-2-yl]oxolan-2-yl]-3,7-dimethoxy-2,4,6-trimethyl-1,10-dioxaspiro[4.5]decan-9-yl]methyl]-4,5-dimethoxy-3,5-dimethyloxan-2-yl]acetic acid).[95]

Table 3.18. ^{1}H and ^{13}C NMR spectroscopic data of **SC-EG-19** (in $CDCl_3$, ^{1}H: 400 MHz, ^{13}C:100 MHz)

H/C	δ_C (ppm)	δ_H (ppm), J (Hz)
1	179.0 s	-
2	72.0 d	3.87 m
3	99.1 d	-
4	38.8 d	2.13 m
5	85.6 d	3.30 m
6	78.4 s	-
7	66.8 d	3.79 m
8	32.5 t	1.53 m
9	61.5 d	3.96 m
10	31.2 t	1.14 m, 2.07 m
11	79.9 d	3.36 m
12	37.0 d	1.82 m
13	107.0 s	-
14	46.3 d	2.12 m
15	94.8 d	3.52 m
16	83.5 s	-
17	83.8 d	3.74 m
18	25.7 t	1.80 m, 1.94 m
19	23.2 t	1.76 m
20	79.4 d	3.90 m
21	79.5 d	4.52 dd (11.0, 5.3, 1.8)
22	29.3 t	1.45 m, 1.98
23	24.3 t	1.82 m, 2.16 m
24	80.9 d	4.36 ddd (8.5, 7.0, 2.7)
25	74.4 d	3.88 m
26	39.2 d	1.26 m
27	83.1 d	3.36 m
28	47.0 d	1.48 m
29	98.5 s	-
1’	102.8 d	4.43 dd (9.5, 2.0)
2’	30.6 t	1.47 m, 1.97 m
3’	27.5 t	1.3 m, 2.18 m
4’	80.5 d	2.78 ddd (10.7, 8.9, 4.5)
5’	74.6 d	3.26 m
4-Me	12.3 q	1.07 d (6.6)
6-Me	11.1 q	1.15 s
5-O-Me	61.2 q	3.54 s
6-O-Me	51 q	3.36 s
11-O-Me	59.4 q	3.44 s
12-Me	12.8 q	0.98 d (7.1)
14-Me	11.7	1.02 s
15-O-Me	60.4 q	3.40 s
16-Me	28.6 q	1.60 s
26-Me	13.5 q	1.03 d (6.2)
28-Me	12.9 q	1.00 d (6.2)
29-Me	27.0 q	1.27 s
4’-O-Me	56.9 q	3.34 s
5’-Me	18.4 q	1.22 d (6.1)

*Assignments were confirmed by COSY, HSQC, and HMBC experiments.

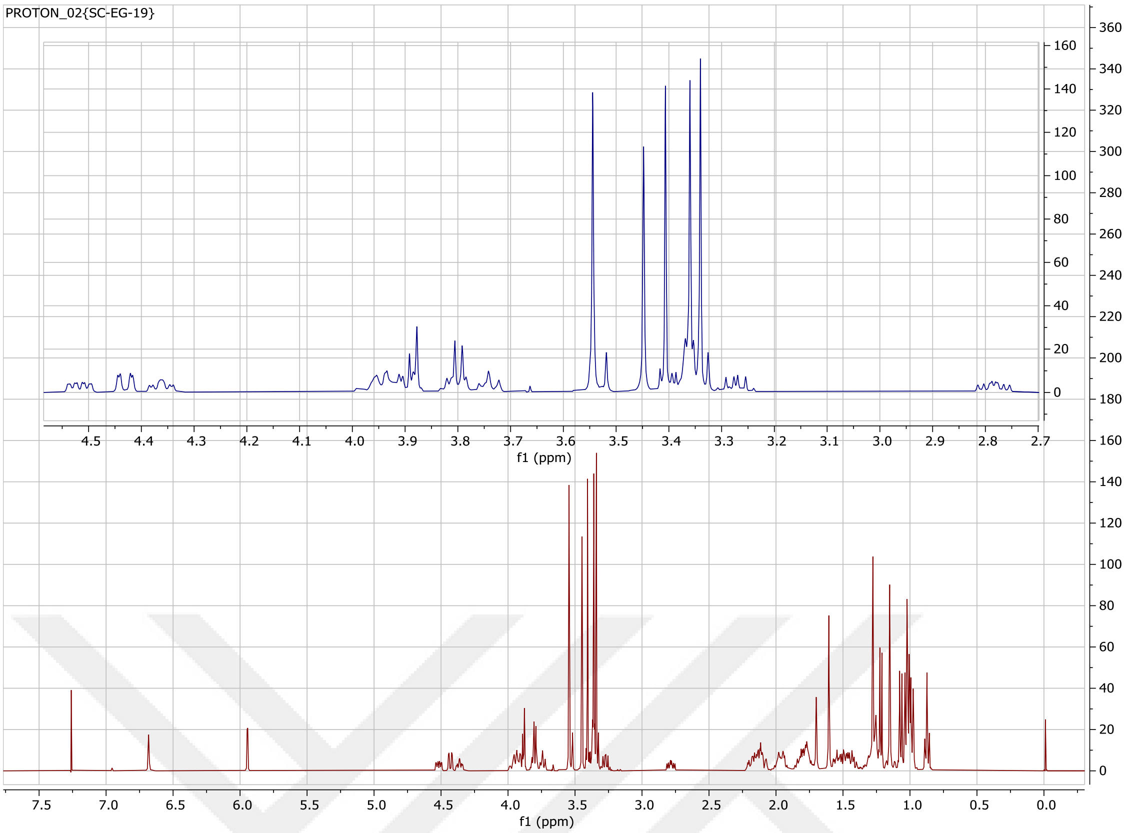

Spectrum 3.1. ^{1}H-NMR spectrum of **SC-EG-19** (in $CDCl_3$, ^{1}H: 400 MHz, ^{13}C:100 MHz)

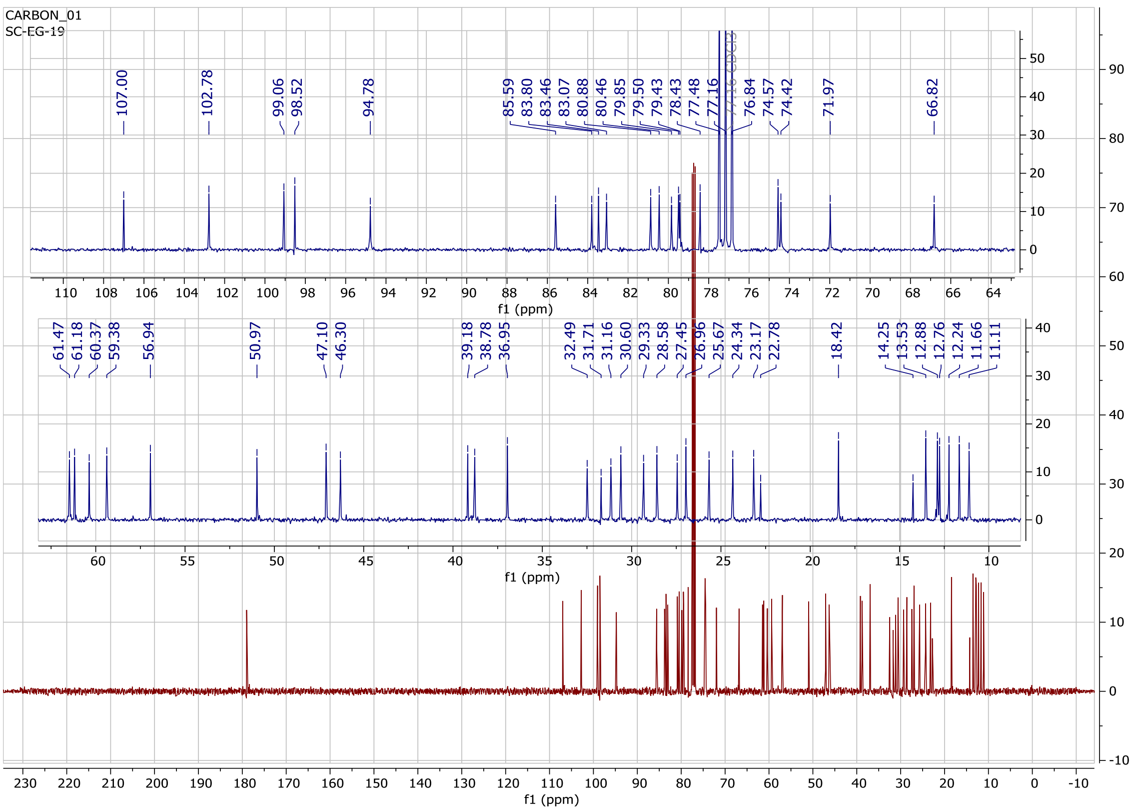

Spectrum 3.2. ^{13}C-NMR spectrum of **SC-EG-19** (in $CDCl_3$, ^{1}H: 400 MHz, ^{13}C:100 MHz)

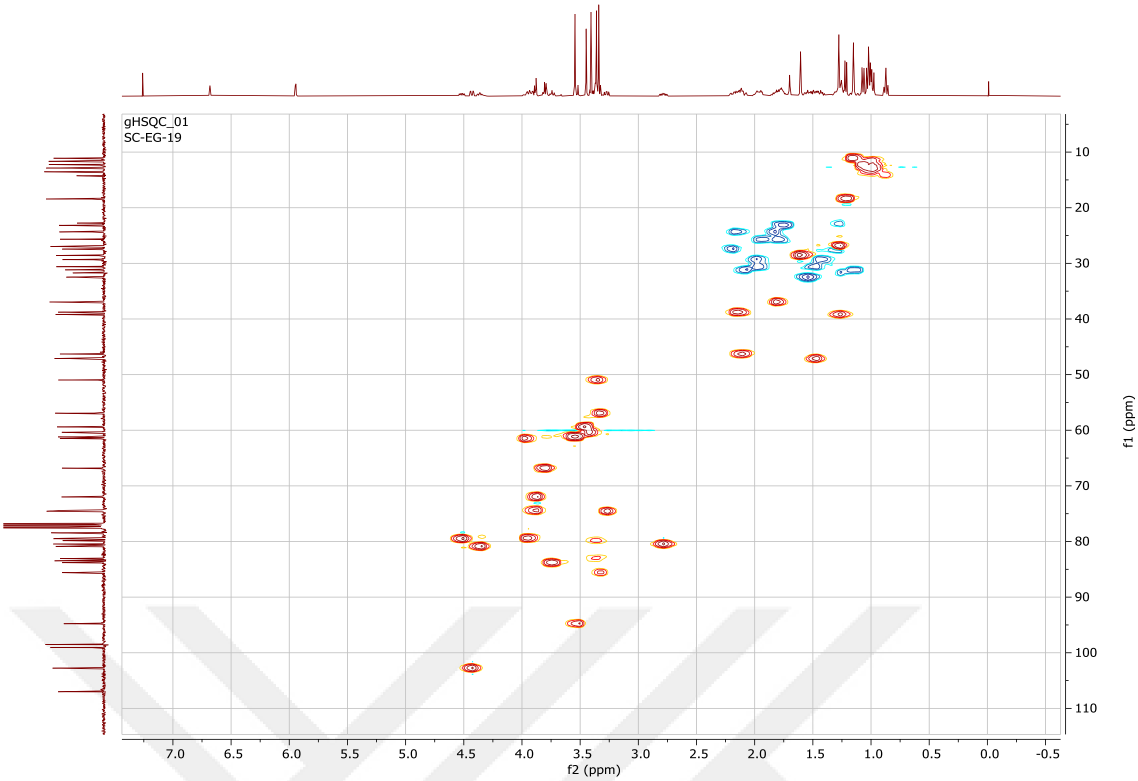

Spectrum 3.3. HSQC spectrum of **SC-EG-19** (in $CDCl_3$, ^1H: 400 MHz, ^{13}C:100 MHz)

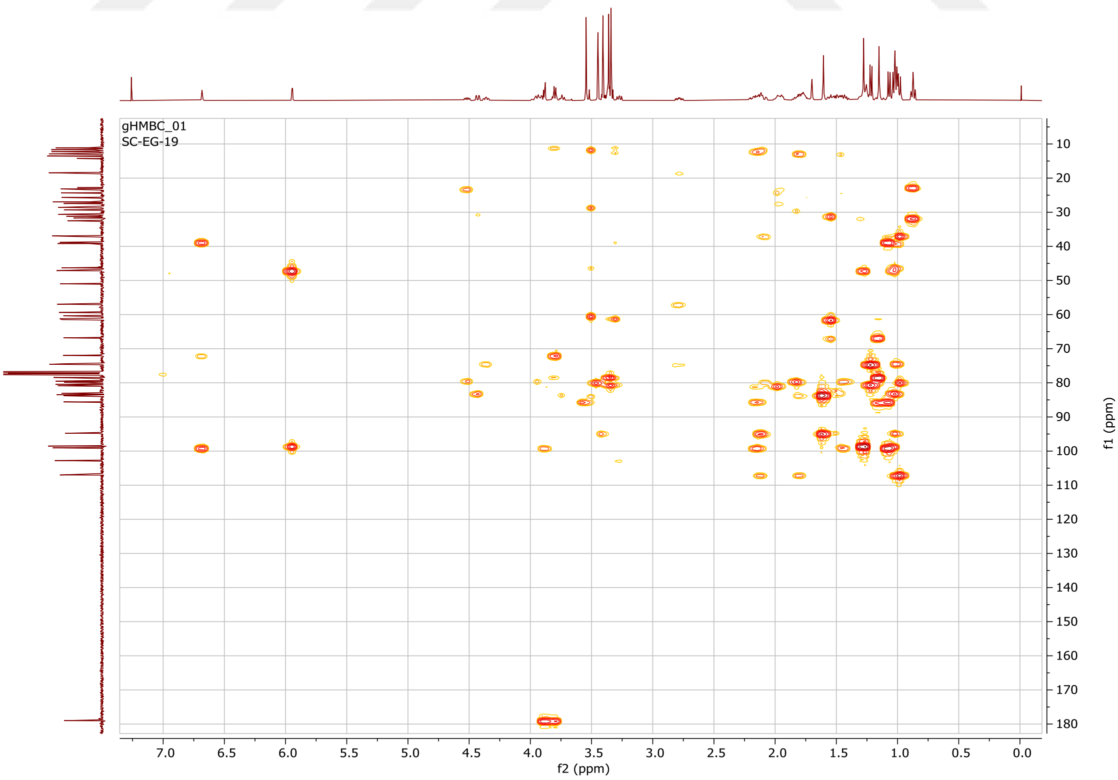

Spectrum 3.4. HMBC spectrum of **SC-EG-19** (in $CDCl_3$, ^1H: 400 MHz, ^{13}C:100 MHz)

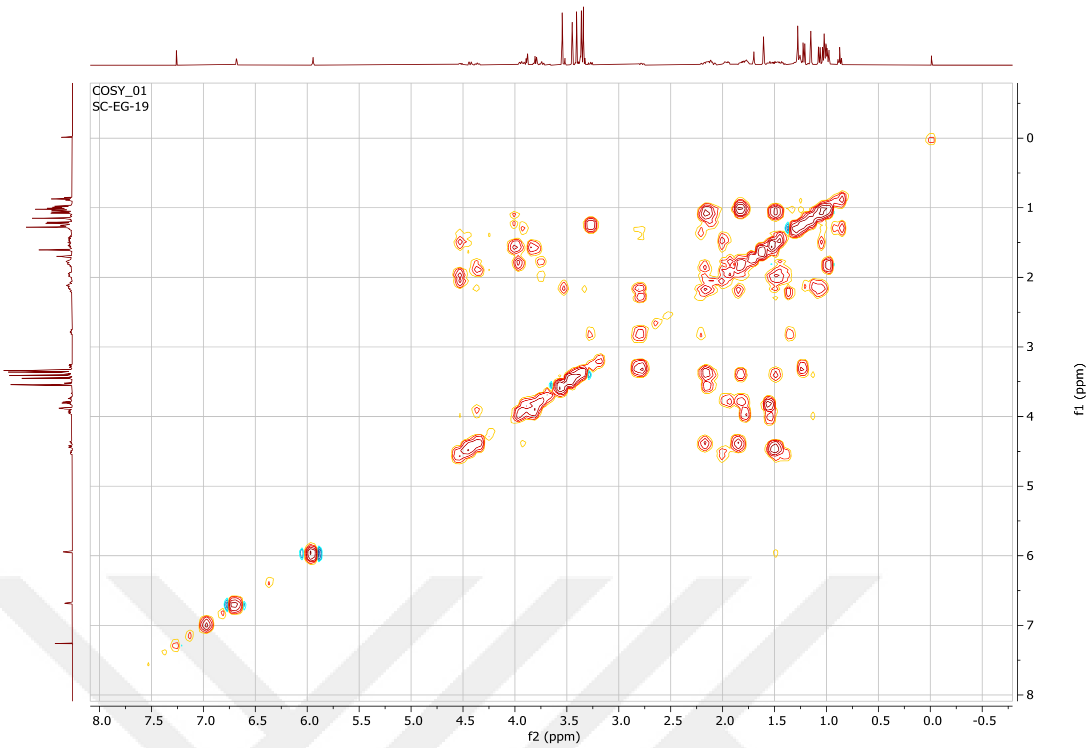

Spectrum 3.5. COSY spectrum of **SC-EG-19** (in $CDCl_3$, ^{1}H: 400 MHz, ^{13}C:100 MHz)

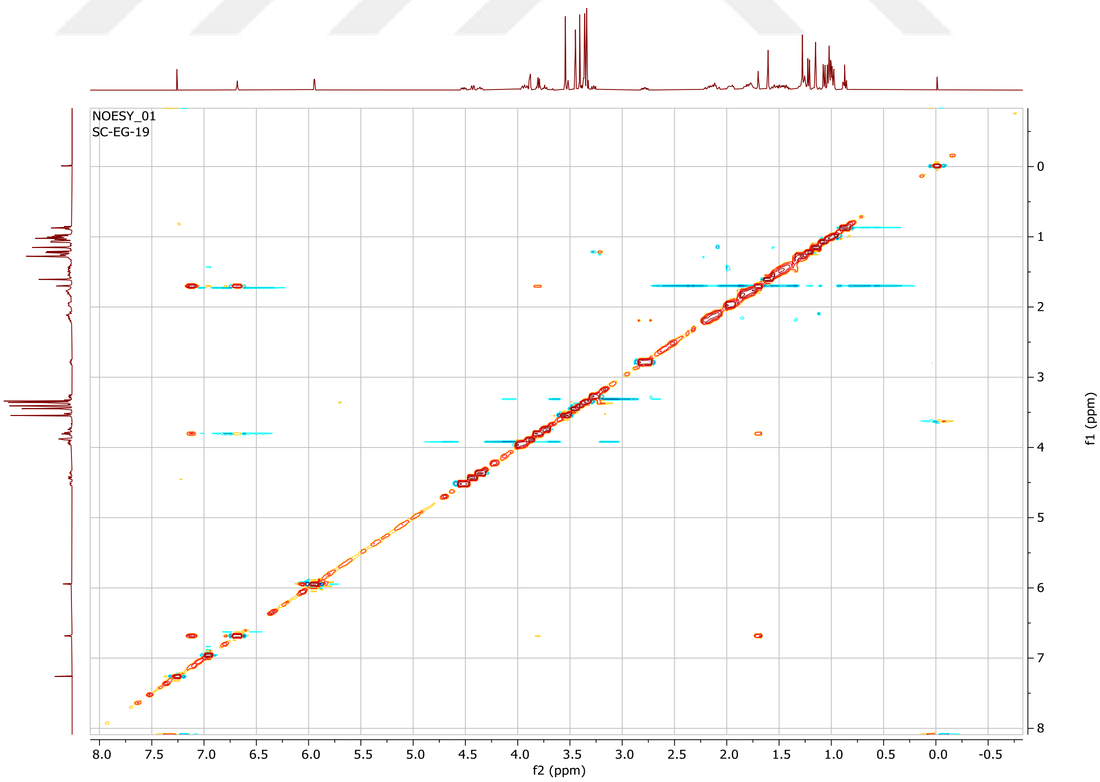

Spectrum 3.6. NOESY spectrum of **SC-EG-19** (in $CDCl_3$, ^{1}H: 400 MHz, ^{13}C:100 MHz)

3.6.1.2. Structure Elucidation of SC-EG-14

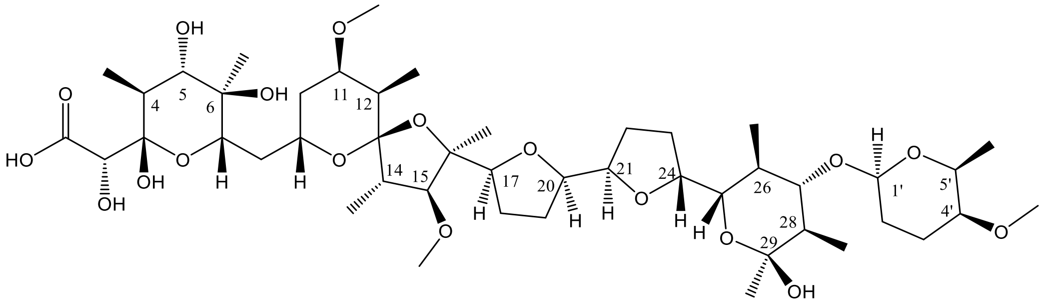

Chemical Formula: $C_{46}H_{78}O_{18}$
Exact Mass: 918.51882

Figure 3.28. Structure of **SC-EG-14.**

In the HR-ESI-MS analysis of **SC-EG-14,** a major ion peak was observed at *m/z* 917.50820 $[M-H]^-$ (calculated: 917.51099) indicating the molecular formula as $C_{46}H_{78}O_{18}$.

Comparison of the ^1H and ^{13}C NMR spectra of **SC-EG-14** with those of **SC-EG-19** revealed the absence of two *O*-methyl signals, which was explaining the mass difference of 28 amu between the compounds. The resonances of 11-*O*-methyl [δ_H 3.45, s; δ_C 59.4], 15-*O*-methyl [δ_H 3.42, s; δ_C 60.3], and 4'-*O*-methyl [δ_H 3.35, s; δ_C 57.0] groups were unambiguously assigned via interpreting 1D- and 2D NMR spectra. Thus, the positions of *O*-demethylations were suggested to be C-5 and C-6. Also, significant low-field shifts observed for C-5 and C-6 resonances were evident for demethylation positions. Consequently, the structure of **SC-EG-14** was elucidated as C5,6-di-*O*-demethyl derivative of **SC-EG-19** (K41-A).

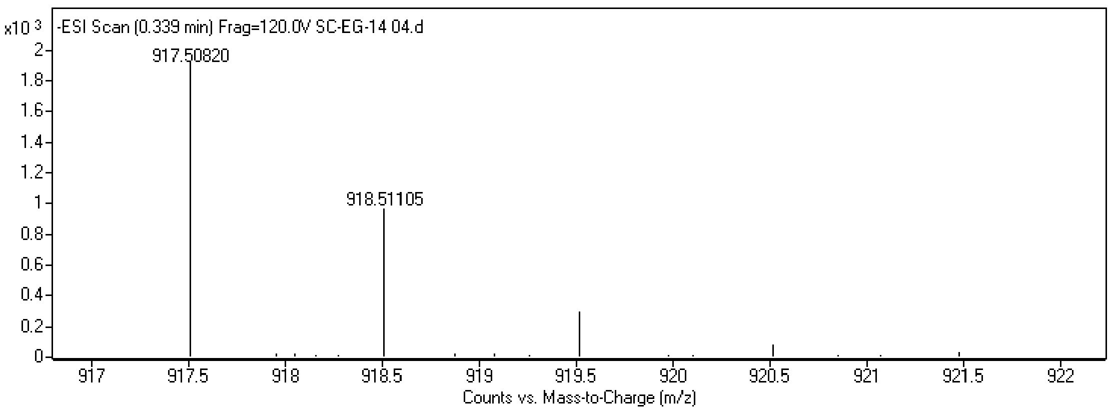

Spectrum 3.7. HR-ESI-MS spectrum of **SC-EG-14** (negative mode).

Table 3.19. ^{1}H and ^{13}C NMR spectroscopic data of **SC-EG-14**. a) (in $CDCl_3$, ^{1}H: 400 MHz, ^{13}C:100 MHz)

H/C	δ_C (ppm)	δ_H (ppm), J (Hz)
1	178.9 s	-
2	72.0 d	3.90 s
3	99.3 s	-
4	38.2 d	2.15 dd (11.1, 6.6)
5	78.5 d	3.59 d (11.1)
6	74.0 s	-
7	68.8 d	3.72 b)
8	32.4 t	1.62 b)
9	61.4 d	3.97 b)
10	31.2 t	2.10 b); 1.10 b)
11	79.8 d	3.39 b)
12	36.9 d	1.83 b)
13	107.1 s	-
14	46.3 d	2.13 dd (9.2, 6.4)
15	94.8 d	3.54 d (9.2)
16	83.5 s	-
17	83.8 d	3.77 b)
18	25.7 t	1.96 b); 1.79 b)
19	23.2 t	1.77 b)
20	79.5 d	3.96 b)
21	79.5 d	4.53 dd (11.1, 5.2)
22	30.6 t	1.98 b); 1.50 b)
23	24.4 t	2.17 b); 1.82 b)
24	80.9 d	4.37 t (7.9)
25	74.4 d	3.91 b)
26	39.2 d	1.27 b)
27	83.1 d	3.35 b)
28	47.1 d	1.49 b)
29	98.6 s	-
1’	102.8 d	4.44 d (9.3)
2’	29.4 t	1.98 b); 1.43 b)
3’	27.4 t	2.21 b); 1.32 b)
4’	80.5 d	2.79 td (9.8, 4.3)
5’	74.6 d	3.28 dd (9.8, 6.0)
4-Me	12.1 q	1.10 d (6.6)
6-Me	13.8 q	1.15 s
11-OMe	59.4 q	3.46 s
12-Me	12.8 q	0.99 d (6.5)
14-Me	11.6 q	1.02 d (6.4)
15-OMe	60.4 q	3.42 s
16-Me	28.6 q	1.62 s
26-Me	13.5 q	1.02 d (6.4)
28-Me	12.9 q	1.04 d (6.0)
29-Me	27.0 q	1.29 s
4’-OMe	57.0 q	3.35 s
5’-Me	18.4 q	1.21 d (6.0)
3-OH	-	6.75 s
29-OH	-	5.92 s

a) Assignments were confirmed by COSY, HSQC, and HMBC experiments.
b) Signal pattern was unclear due to overlapping.

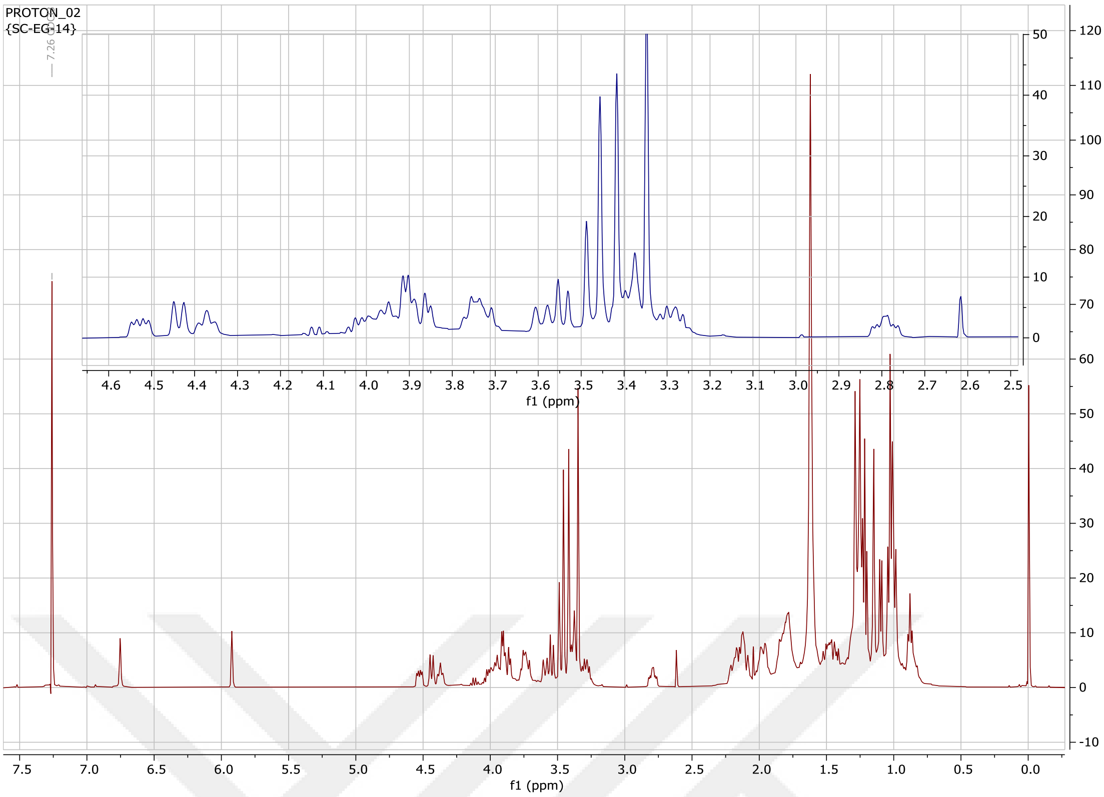

Spectrum 3.8. ^{1}H-NMR spectrum of **SC-EG-14** (in $CDCl_3$, ^{1}H: 400 MHz, ^{13}C:100 MHz)

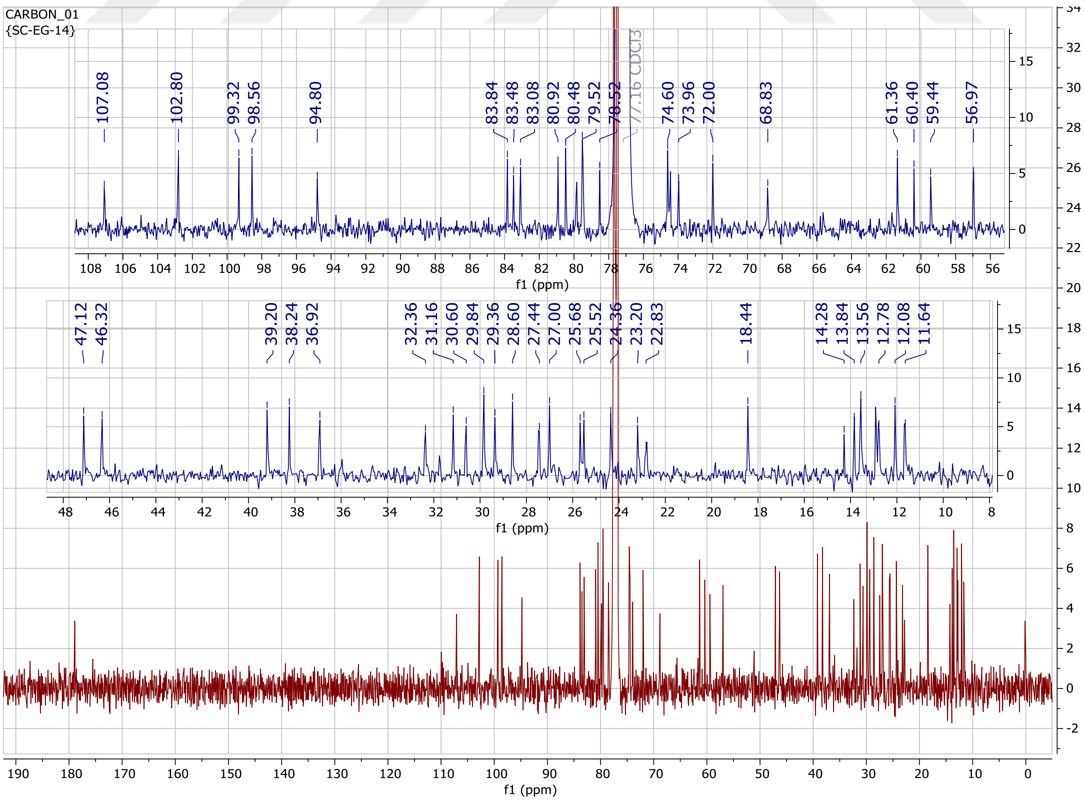

Spectrum 3.9. ^{13}C-NMR spectrum of **SC-EG-14** (in $CDCl_3$, ^{1}H: 400 MHz, ^{13}C:100 MHz)

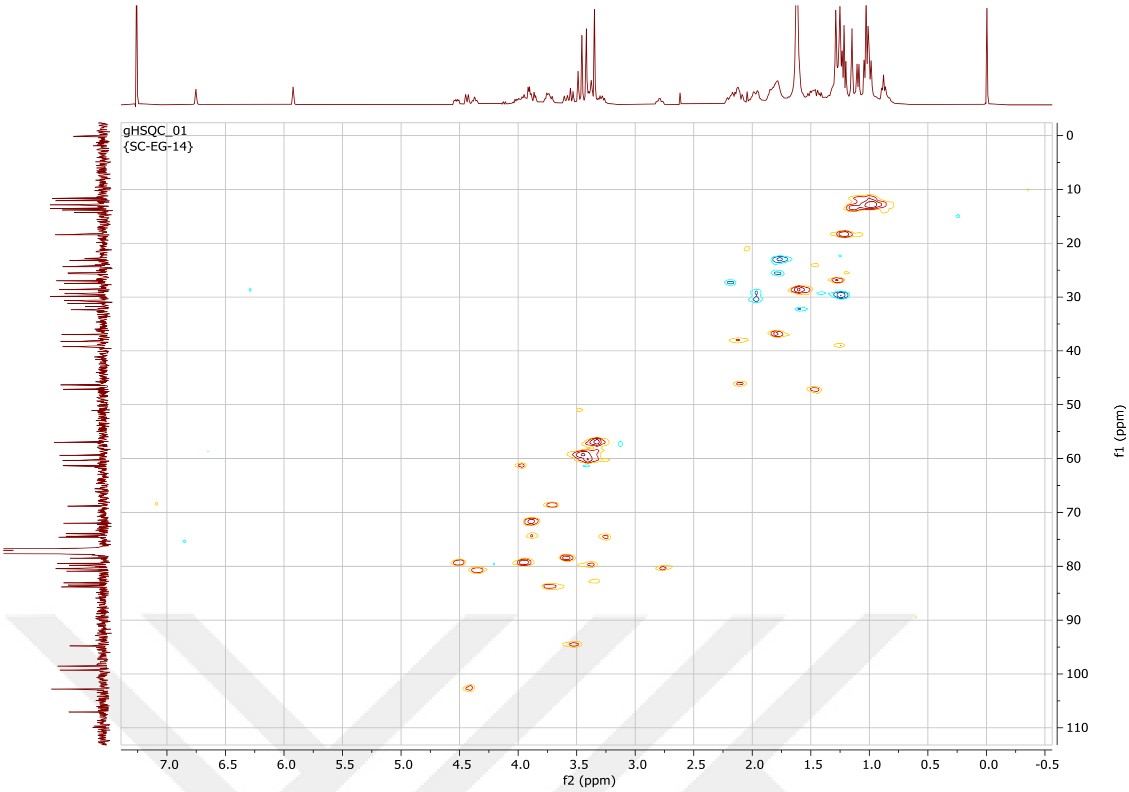

Spectrum 3.10. HSQC spectrum of **SC-EG-14** (in $CDCl_3$, ^1H: 400 MHz, ^{13}C:100 MHz)

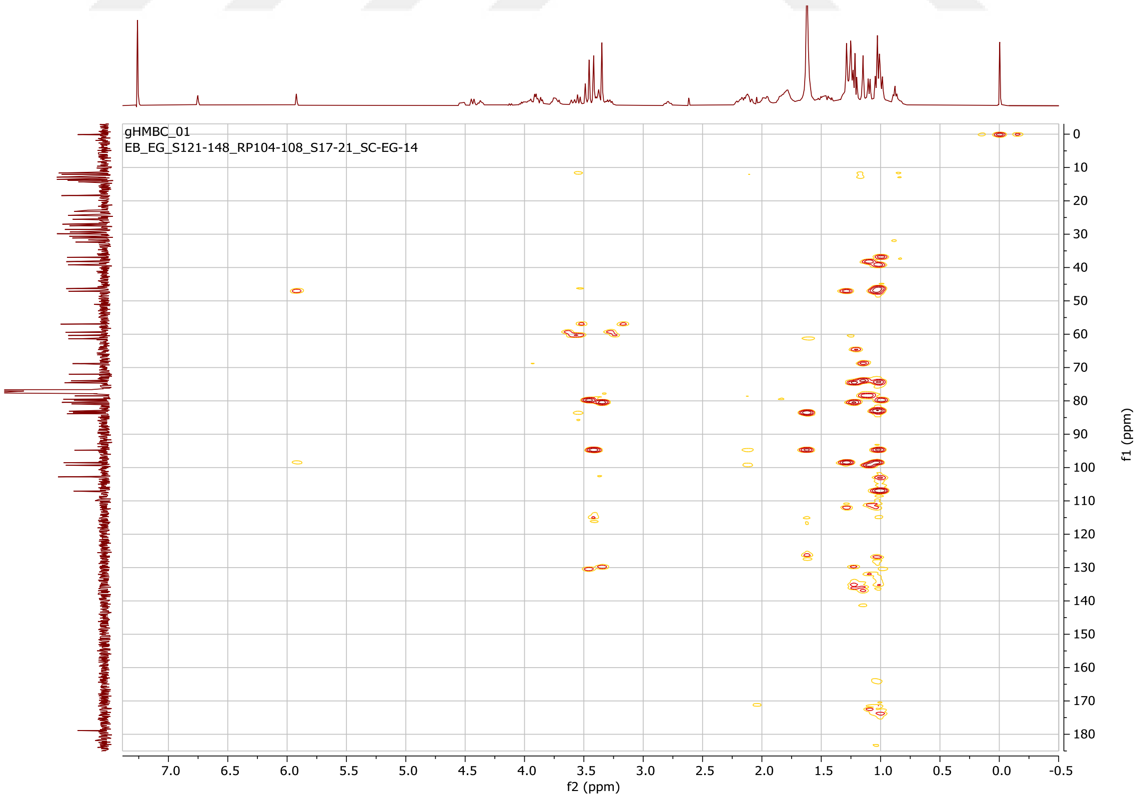

Spectrum 3.11. HMBC spectrum of **SC-EG-14** (in $CDCl_3$, ^1H: 400 MHz, ^{13}C:100 MHz)

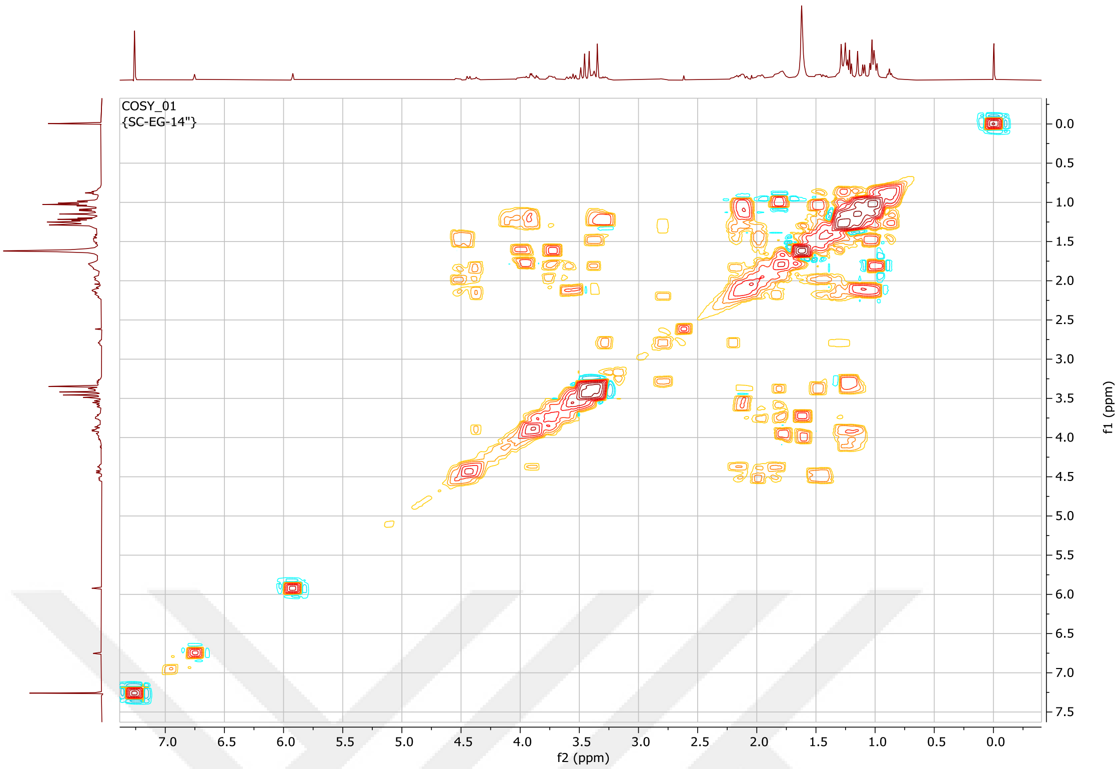

Spectrum 3.12. COSY spectrum of **SC-EG-14** (in $CDCl_3$, ^{1}H: 400 MHz, ^{13}C:100 MHz)

3.6.1.3. Structure Elucidation of SC-EG-05

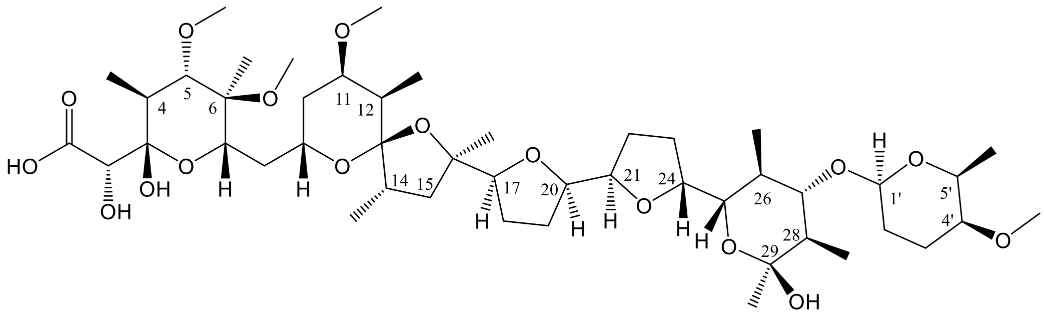

Chemical Formula: $C_{47}H_{80}O_{17}$
Exact Mass: 916.53955

Figure 3.29. Structure of **SC-EG-05.**

In the HR-ESI-MS analysis of **SC-EG-05,** a major peak was observed at *m/z* 939.53224 $[M+Na]^+$ (calculated: 939.52932) indicating the molecular formula as $C_{47}H_{80}O_{17}$.

Comparison of 1D NMR spectra of **SC-EG-05** with those of **SC-EG-19** revealed an additional up-field carbon at δ 40.9 and two up-field protons (δ 1.52 and 1.82). As well the absence of the characteristic C-15 resonance (δ_C 94.5 for **SC-EG-19**) in the ^{13}C NMR spectrum implied a demethoxylation, which was also consistent with the 30 amu mass difference. The HSQC spectrum revealed $^1J_{C\text{-}H}$ correlations between the new carbon (δ 40.9) and protons (δ 1.52 and 1.82). Long-range cross peaks from δ 40.9 to Me-14 (δ 0.92) and Me-16 (δ 1.5) in the HMBC spectrum substantiated demethoxylation at C-15. Thus, the structure of **SC-EG-05** was elucidated as C15-demethoxy derivative of K41-A.

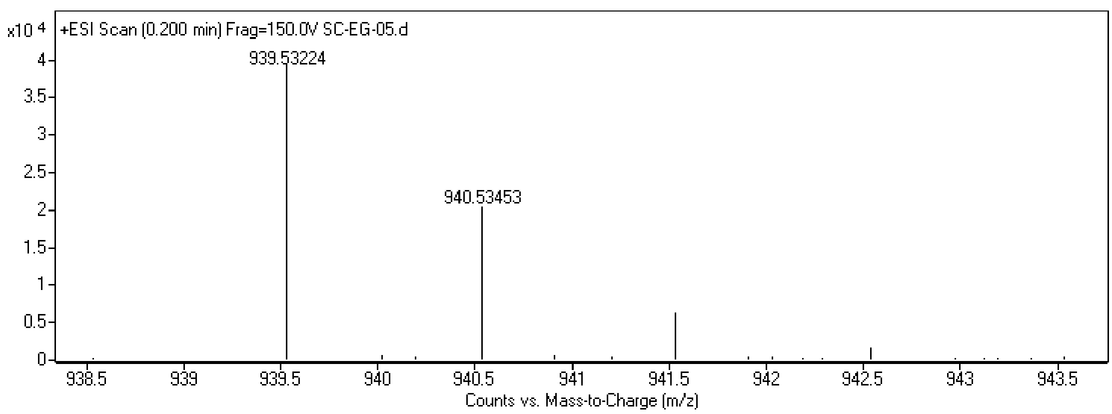

Spectrum 3.13. HR-ESI-MS spectrum of **SC-EG-05** (positive mode)

Table 3.20. ^{1}H and ^{13}C NMR spectroscopic data of **SC-EG-05** (in $CDCl_3$, ^{1}H: 400 MHz, ^{13}C:100 MHz)

H/C	δ_C (ppm)	δ_H (ppm), J (Hz)
1	178.8 s	-
2	71.8 d	3.88 m
3	98.9 s	-
4	38.6 d	2.12 m
5	85.35 d	3.33 m
6	78.30 s	-
7	66.7 d	3.78 m
8	32.3 t	1.56 m
9	61.1 d	3.95 m
10	31.1 t	1.14 m, 2.07 m
11	79.9 d	3.35 m
12	36.8 d	1.8 m
13	108.1 s	-
14	39.5 d	2.2 m
15	40.9 t	1.52 m, 1.82 m
16	82.8 s	-
17	85.7 d	3.73 m
18	24.1	1.82 m
19	22.7	1.77 m
20	80.3 t	4 m
21	79.3 t	4.49 dd (10.8, 5.1)
22	30.4 t	1.46 m, 1.96 m
23	24.2 t	1.83 m, 2.11 m
24	80.6 d	4.35 m
25	74.4 d	3.88 n
26	38.9 d	1.25 m
27	82.9 d	3.26 m
28	46.8 s	1.44 m
29	98.3 s	-
1’	102.6 d	4.42 d (9.2)
2’	29.1 t	1.39 m, 1.95 m
3’	27.3 t	1.32 m, 2.19 m
4’	80.3 d	2.77 td (10.1, 4.3)
5’	74.4 d	3.25 m
4-Me	12.1 q	1.06 d (6.6)
5-OMe	61.1 q	3.53 s
6-Me	11 q	1.14 s
6-O-Me	50.8 q	3.35
11-O-Me	59.1 q	3.44
12-Me	12.8 q	0.96 d (7)
14-Me	13.2 q	0.92 d (6.7)
16-Me	28.2 q	1.5 s
26-Me	13.4 q	1 d (6.7)
28-Me	12.7 q	1.02 d (7)
29-Me	26.8 q	1.26 s
4’-O-Me	56.8 q	3.34 s
5’-Me	18 q	1.21 d (6)

*Assignments were confirmed by COSY, HSQC, and HMBC experiments.

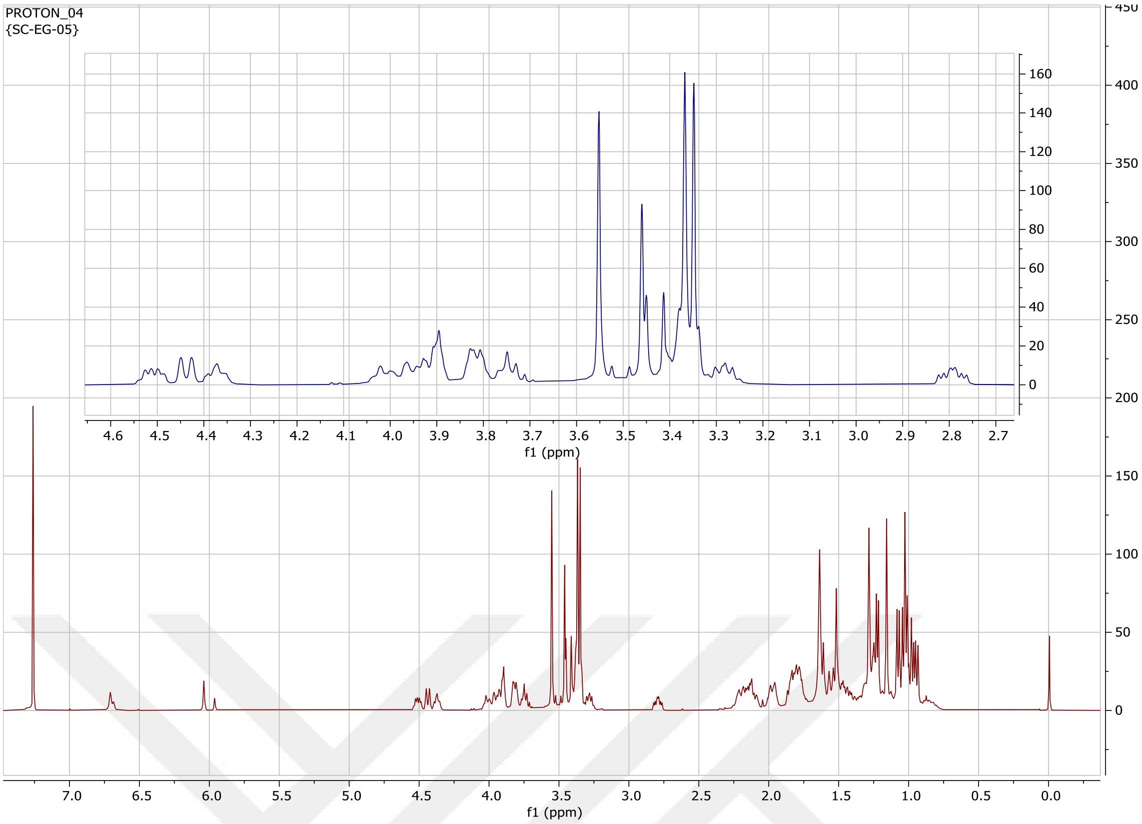

Spectrum 3.14. ^{1}H-NMR spectrum of **SC-EG-05** (in $CDCl_3$, ^{1}H: 400 MHz, ^{13}C:100 MHz)

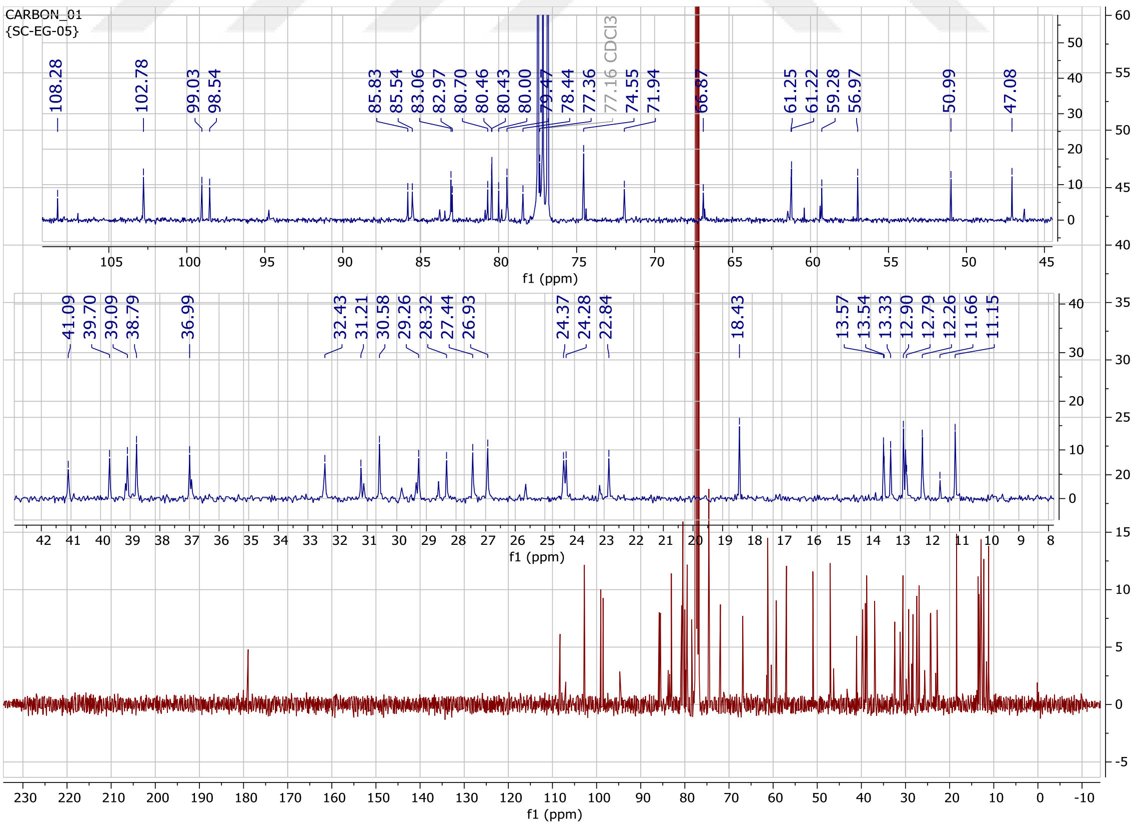

Spectrum 3.15. ^{13}C-NMR spectrum of **SC-EG-05** (in $CDCl_3$, ^{1}H: 400 MHz, ^{13}C:100 MHz)

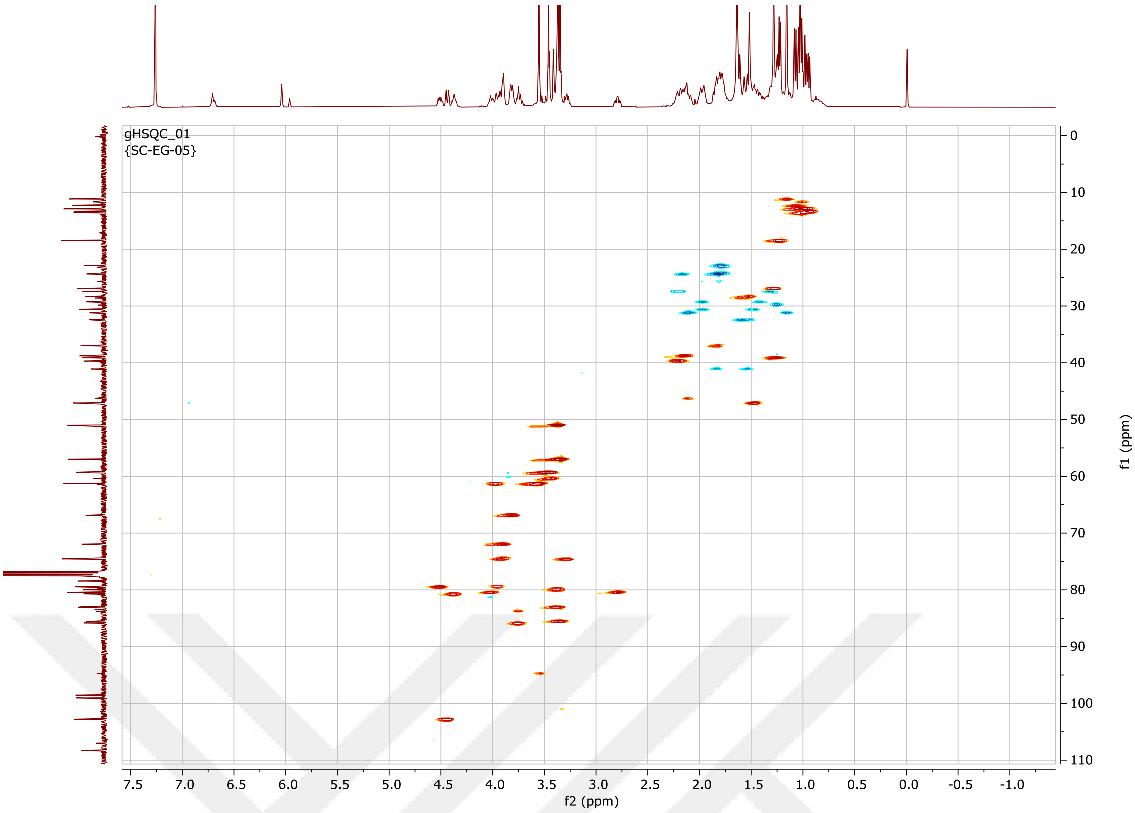

Spectrum 3.16. HSQC spectrum of **SC-EG-05** (in $CDCl_3$, ^1H: 400 MHz, ^{13}C:100 MHz)

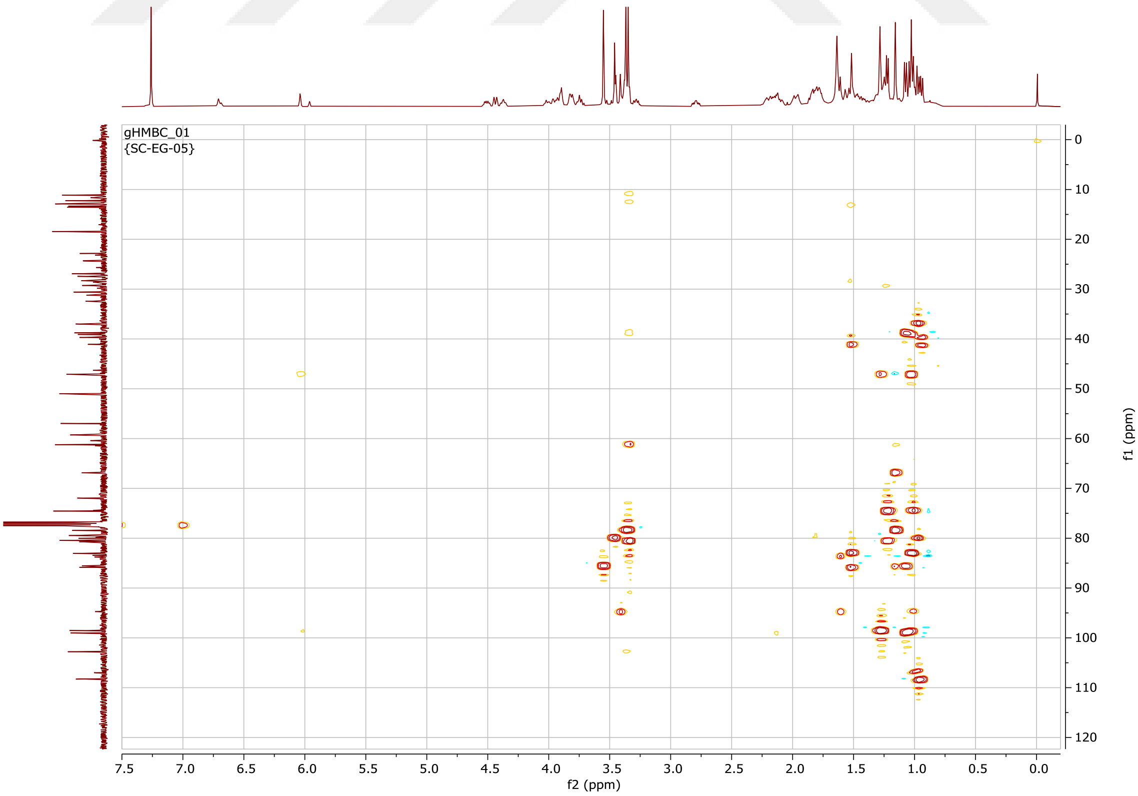

Spectrum 3.17. HMBC spectrum of **SC-EG-05** (in $CDCl_3$, ^1H: 400 MHz, ^{13}C:100 MHz)

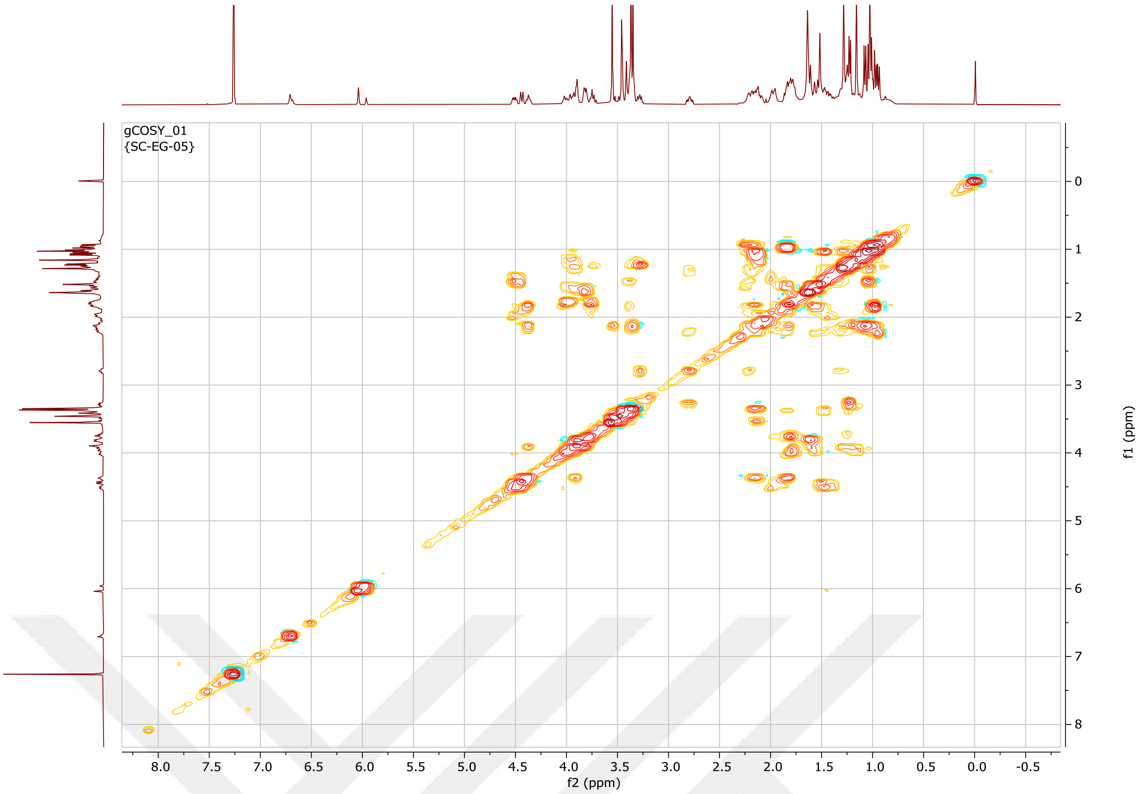

Spectrum 3.18. COSY spectrum of **SC-EG-05** (in $CDCl_3$, ^{1}H: 400 MHz, ^{13}C:100 MHz)

3.6.1.4. Structure Elucidation of SC-EG-20

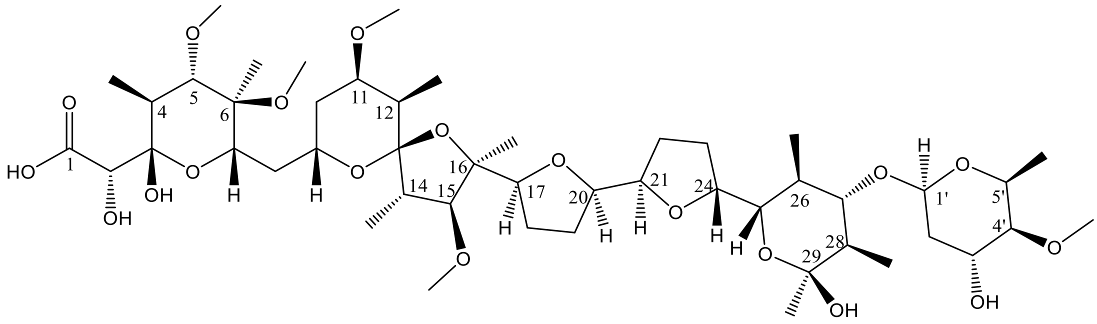

Chemical Formula: $C_{48}H_{82}O_{19}$
Exact Mass: 962.54503

Figure 3.30. Chemical structure of **SC-EG-20.**

The HR-ESI-MS analysis of **SC-EG-20** gave a major ion peak at *m/z* 961.54333 $[M-H]^-$ (calculated: 961.53721) revealing the molecular formula as $C_{48}H_{82}O_{19}$. Sixteen amu increase compared to the molecular weight of **SC-EG-19** (K41-A) implied a monooxygenated derivative.

Inspection of the ^1H and ^{13}C NMR spectra showed that **SC-EG-20** and **SC-EG-19** had superimposable signals except the sugar unit. The characteristic signals of five *O*-methyl groups ([δ_H 3.56, s; δ_C 61.2], [δ_H 3.37, s; δ_C 51.0], [δ_H 3.45, s; δ_C 59.4], [δ_H 3.41, s; δ_C 60.4], [δ_H 3.55, s; δ_C 61.0]) were readily assigned using HSQC and HMBC spectra together with the resonances belonging to polyether framework. Examination of the ^{13}C NMR spectrum of **SC-EG-20** revealed the lack of C-3' methylene carbon (δ_C 27.3 t) in the sugar residue, as well appearance of an additional down-field signal (δ_C 71.5) was noted. Also, the HSQC spectrum revealed a proton resonance at δ 3.61 displaying a $^1J_{C-H}$ correlation with the δ 71.5 carbon. The COSY and HSQC spectra provided a spin system [O–(O)CH-1'-CH_2-2'-(O)CH-3'-(O)CH-4'-(O)CH-5'-CH_3-6'] for the sugar moiety. The long-range correlations from H-1' (δ 4.47) to C-27 (δ 83.5), and (O)C$\underline{H}_3$ (δ 3.55) to C-4' (δ 87.8) in the HMBC spectrum not only helped us to locate the sugar residue on the polyether skeleton but also finalize the structure except the relative stereochemistry of C3'-(OH) and identity of the sugar residue. The ^1H and ^{13}C NMR data of the sugar moiety were consistent with those of β-D-olivose reported for several *Streptomyces* derived metabolites.[111, 112, 113] Thus, **SC-EG-20** was identified as C27-*O*-β-olivose derivative of K41-A.

Table 3.21. ^{1}H and ^{13}C NMR spectroscopic data of **SC-EG-20** (in $CDCl_3$, ^{1}H: 400 MHz, ^{13}C:100 MHz)

H/C	δ_C (ppm)	δ_H (ppm), J (Hz)
1	179.0 s	-
2	72.0 d	3.88 s
3	99.1 s	-
4	38.8 d	2.14 dd (8.5, 6.6)
5	85.7 d	3.34 d (8.5)
6	78.4 s	-
7	66.9 d	3.80 [b)]
8	32.5 t	1.54 dd (10.0, 3.6)
9	61.5 d	3.97 [b)]
10	31.2 t	2.09 [b)]; 1.15 [b)]
11	79.9 d	3.38 [b)]
12	37.0 d	1.80 [b)]
13	107.0 s	-
14	46.3 d	2.11 dd (10.8, 6.3)
15	94.8 d	3.53 d (10.8)
16	83.5 s	-
17	83.8 d	3.74 [b)]
18	25.7 t	1.95 [b)]; 1.78 [b)]
19	23.2 t	1.76 [b)]
20	79.4 d	3.92 dd (11.0, 6.2)
21	79.5 d	4.52 dd (11.0, 5.3)
22	29.3 t	1.99 [b)]; 1.42 [b)]
23	24.4 t	2.16 [b)]; 1.84 [b)]
24	80.9 d	4.36 [b)]
25	74.4 d	3.89 [b)]
26	39.1 d	1.27 [b)]
27	83.5 d	3.38 [b)]
28	47.0 d	1.48 [b)]
29	98.5 s	-
1’	100.7 d	4.47 dd (9.7, 1.8)
2’	38.9 t	2.27 dd (12.3, 5.0); 1.58 dd (8.8, 5.0)
3’	71.5 d	3.61 [b)]
4’	87.8 d	2.69 t (8.9)
5’	71.0 d	3.21 dd (8.9, 6.5)
4-Me	12.2 q	1.07 d (6.6)
5-OMe	61.2 q	3.56 s
6-Me	11.1 q	1.16 s
6-OMe	51.0 q	3.37 s
11-OMe	59.4 q	3.45 s
12-Me	12.8 q	0.99 d (6.9)
14-Me	11.7 q	1.02 d (6.3)
15-OMe	60.4 q	3.41 s
16-Me	28.6 q	1.61 s
26-Me	13.5 q	1.00 d (6.1)
28-Me	12.9 q	1.03 d (6.0)
29-Me	26.9 q	1.28 s
4’-OMe	61.0 q	3.55 s
5’-Me	18.3 q	1.28 d (6.5)
3-OH	-	6.69 s
27-OH	-	5.97 s

a) Assignments were confirmed by COSY, HSQC, and HMBC experiments.
b) Signal pattern was unclear due to overlapping

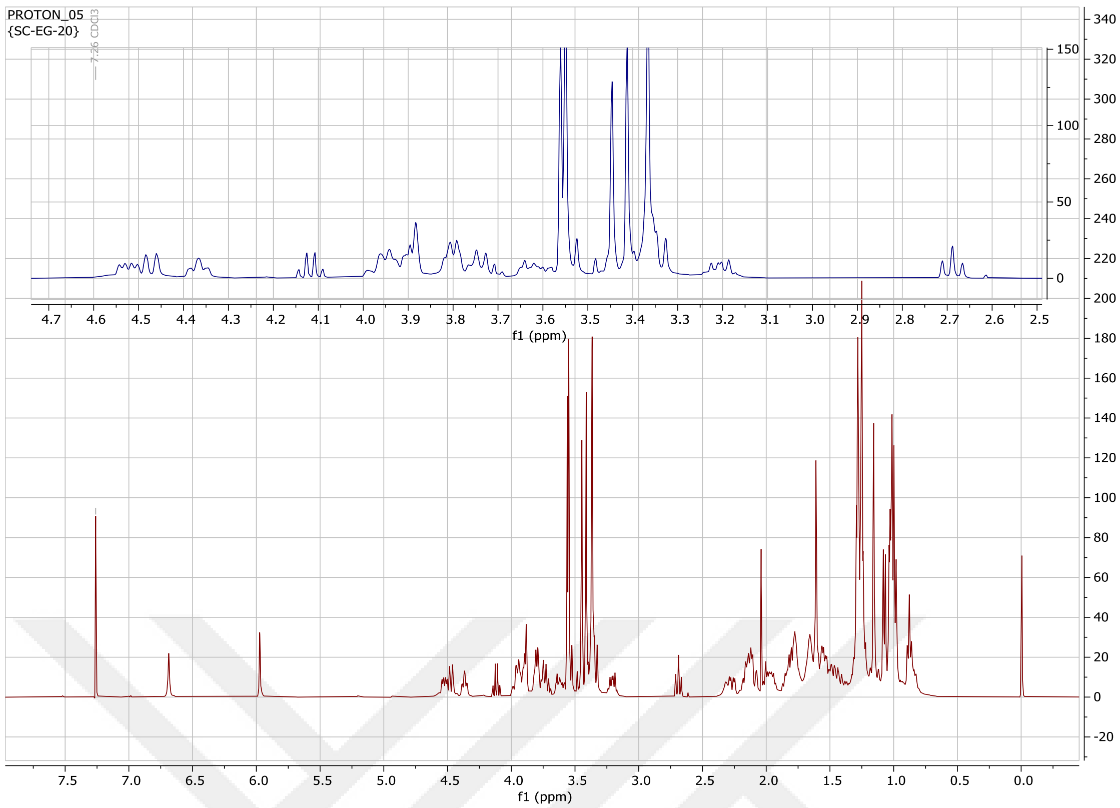

Spectrum 3.19. ^{1}H-NMR spectrum of **SC-EG-20** (in $CDCl_3$, ^{1}H: 400 MHz, ^{13}C:100 MHz)

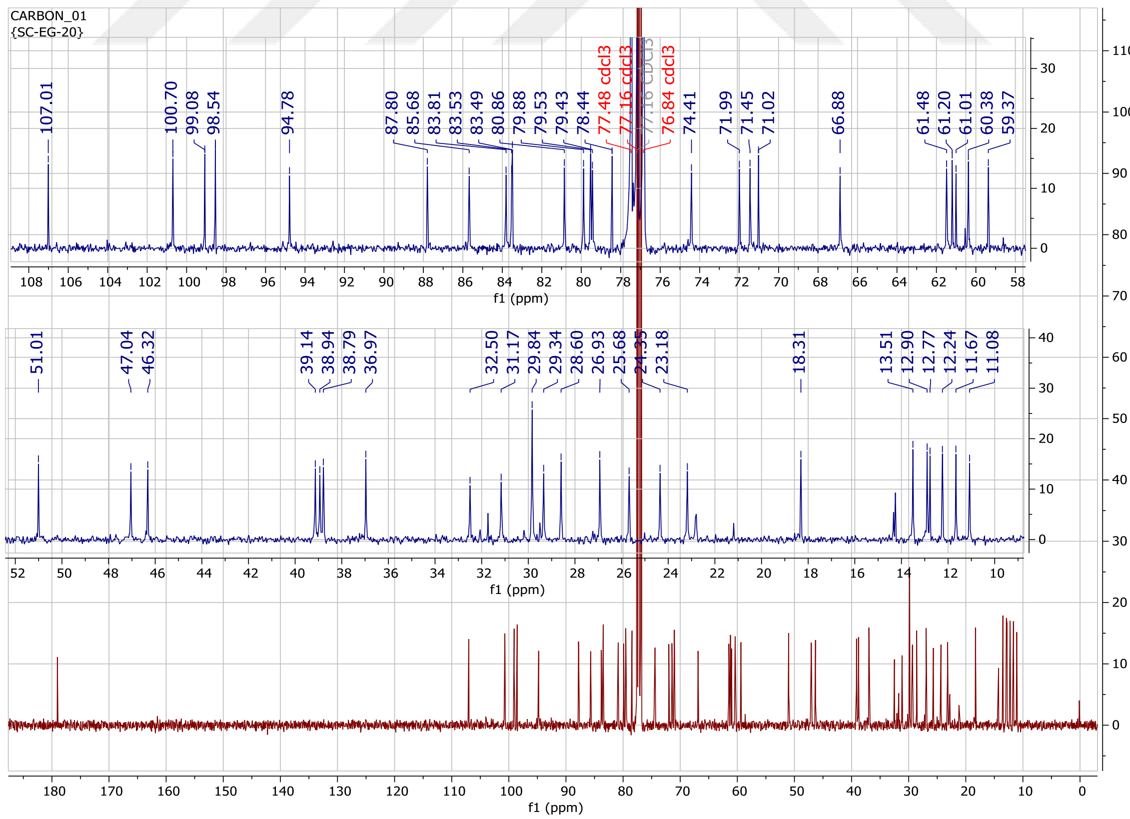

Spectrum 3.20. ^{13}C-NMR spectrum of **SC-EG-20** (in $CDCl_3$, ^{1}H: 400 MHz, ^{13}C:100 MHz)

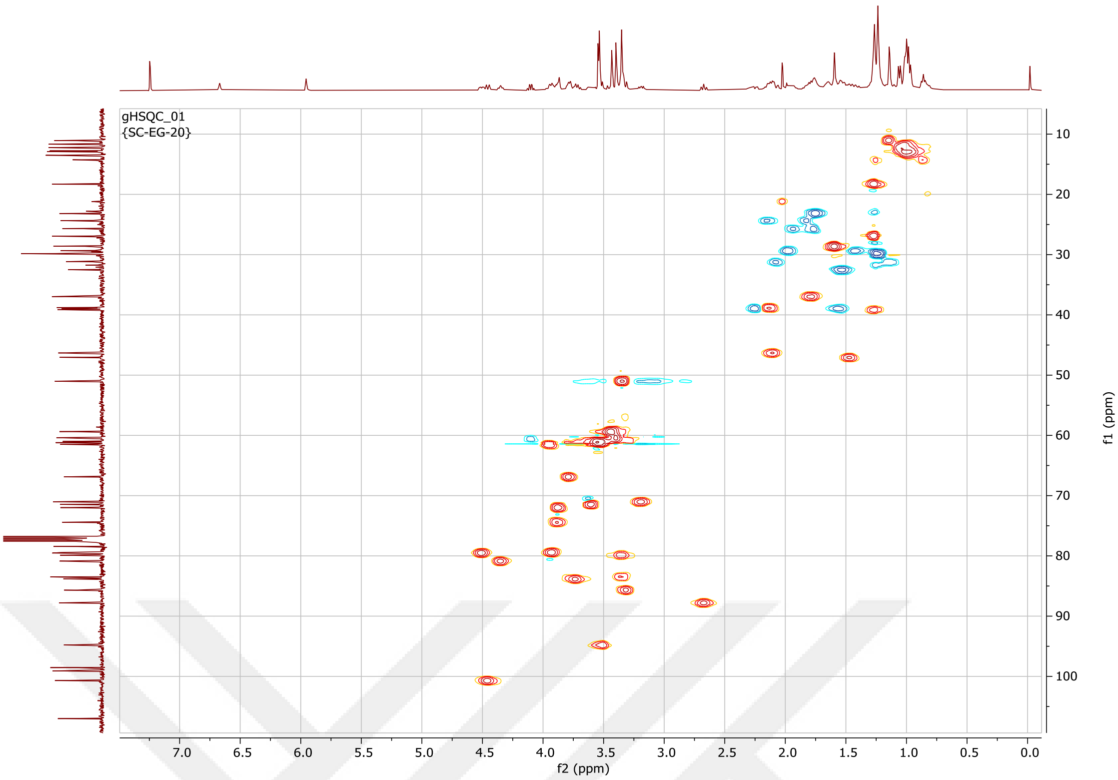

Spectrum 3.21. HSQC spectrum of **SC-EG-20** (in $CDCl_3$, ^{1}H: 400 MHz, ^{13}C:100 MHz)

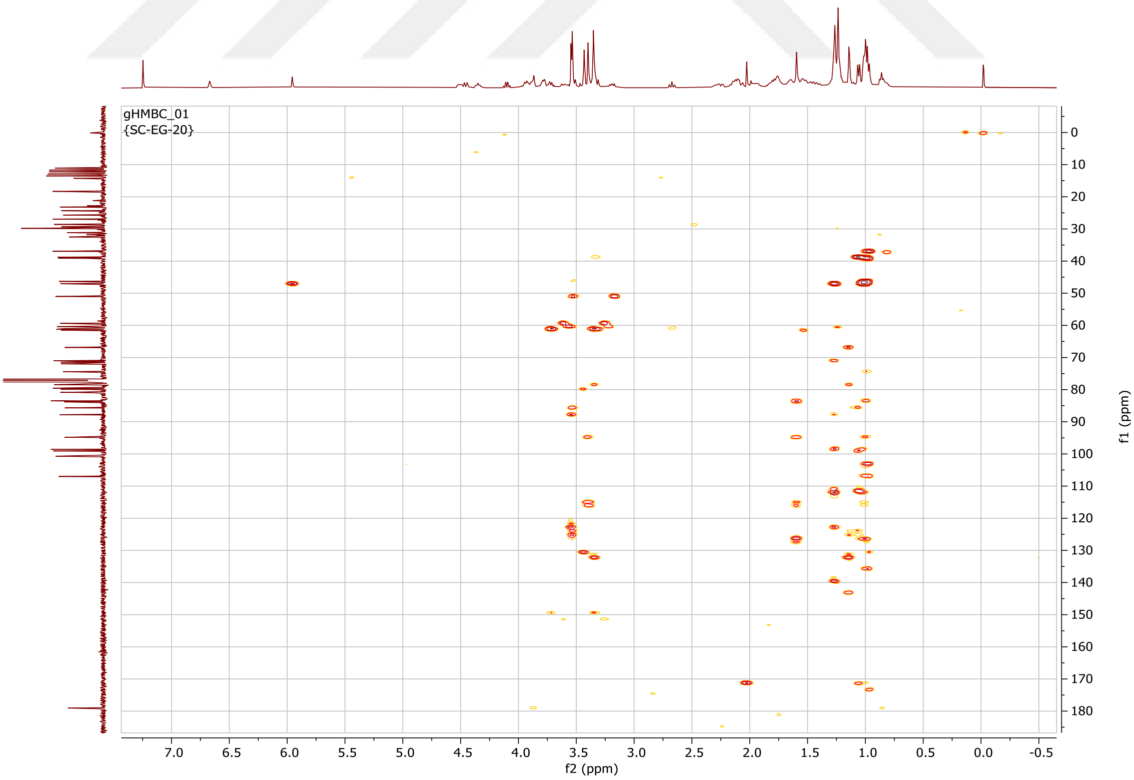

Spectrum 3.22. HMBC spectrum of **SC-EG-20** (in $CDCl_3$, ^{1}H: 400 MHz, ^{13}C:100 MHz)

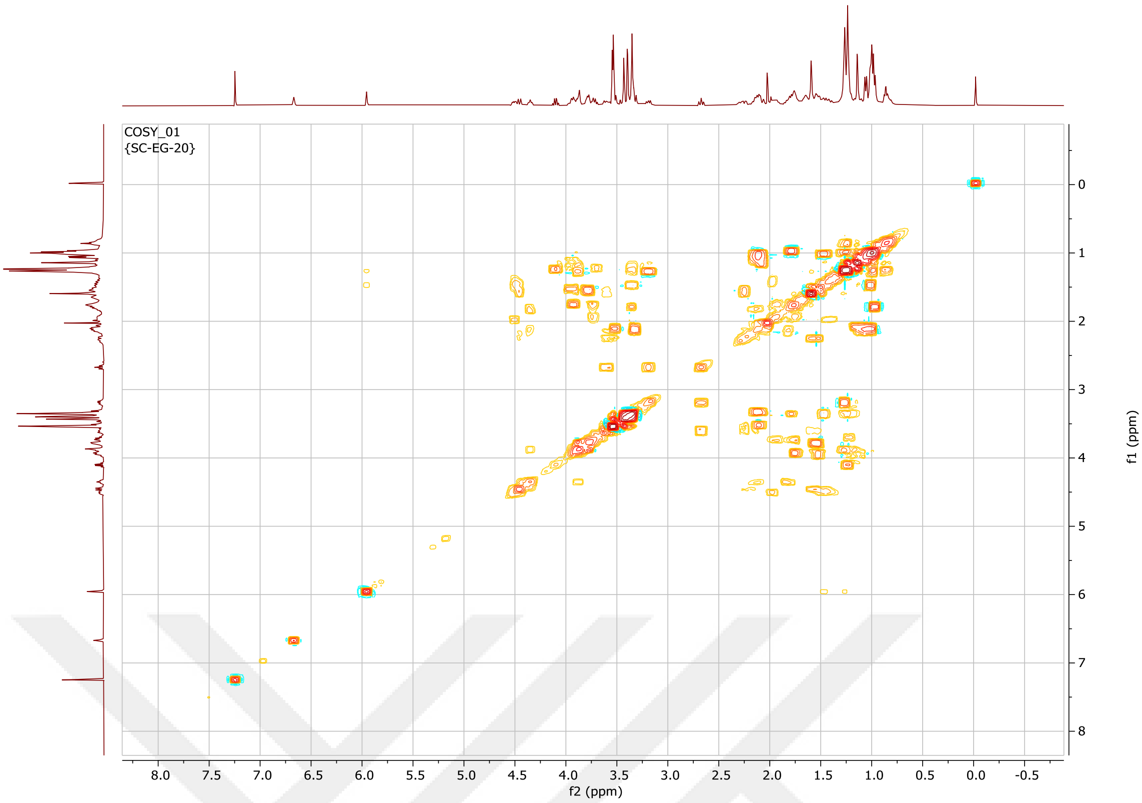

Spectrum 3.23. COSY spectrum of **SC-EG-20** (in $CDCl_3$, ^{1}H: 400 MHz, ^{13}C:100 MHz)

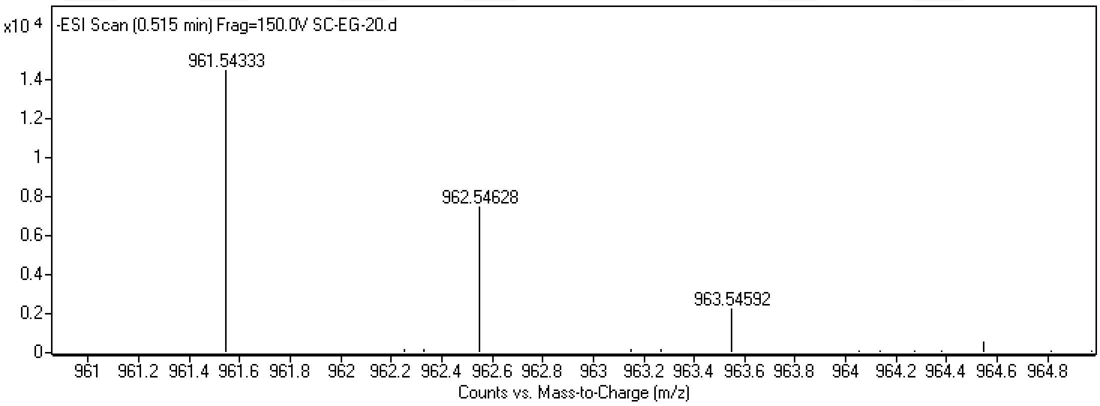

Spectrum 3.24. HR-ESI-MS spectrum of **SC-EG-20** (negative mode)

3.6.1.5. Structure Elucidation of SC-EG-13

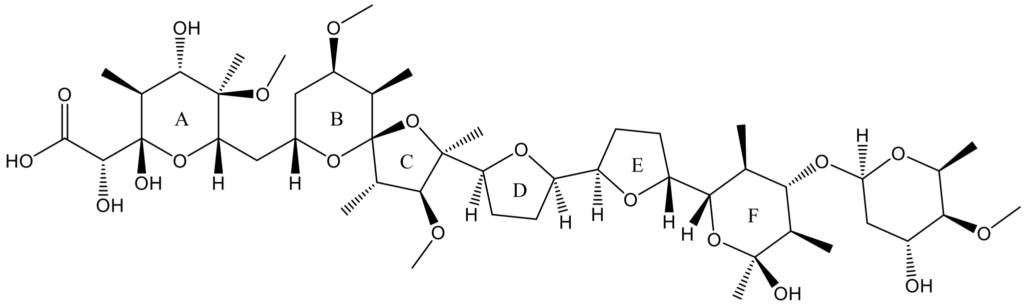

Chemical Formula: $C_{47}H_{80}O_{19}$
Exact Mass: 948.52938

Figure 3.31. Chemical structure of **SC-EG-13.**

The HR-ESI-MS analysis of **SC-EG-13** gave a major peak at *m/z* 947.52614 [M-H]$^-$ (calculated: 947.52156) revealing the molecular formula as $C_{47}H_{80}O_{19}$.

The ^{1}H and ^{13}C NMR spectra of **SC-EG-13** and **SC-EG-20** were almost superimposable for the B→F rings and sugar moiety, suggesting another b-olivose metabolite. Additionally, 5-*O*-methyl resonances in **SC-EG-13** [δ_H 3.56, s; δ_C 61.2, q for **SC-EG-20**] was lacking in the ^{1}H and ^{13}C NMR spectra. This observation was also explained the 14 amu decrease compared to **SC-EG-20**. Inspection of the COSY spectra revealed the spin systems as identical to **SC-EG-20**. Besides, the lacking HMBC correlation between C-5 and *O*-methyl protons confirmed *O*-demethylation at C-5. Thus, the structure of **SC-EG-13** was elucidated as C5-*O*-demethyl derivative of **SC-EG-20**.

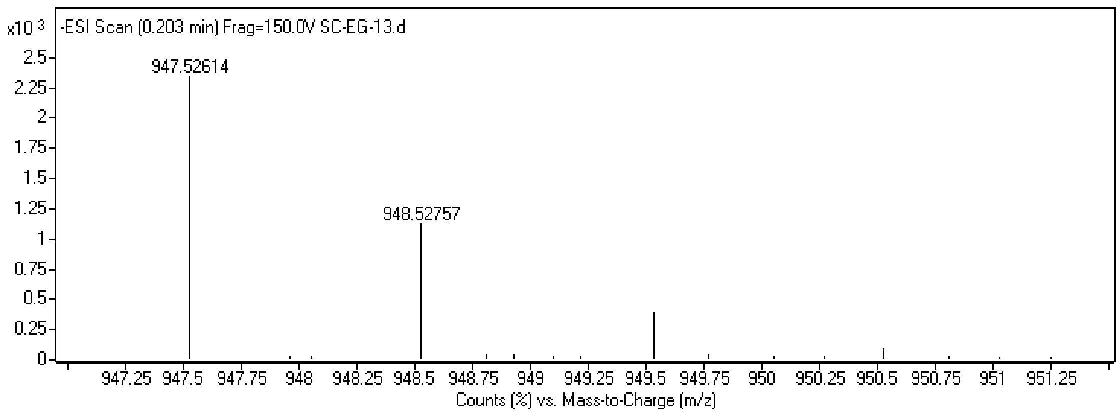

Spectrum 3.25. HR-ESI-MS spectrum of **SC-EG-13** (negative mode)

Table 3.22. ^{1}H and ^{13}C NMR spectroscopic data of **SC-EG-13** a) (in $CDCl_3$, ^{1}H: 400 MHz, ^{13}C:100 MHz)

H/C	δ_C (ppm)	δ_H (ppm), J (Hz)
1	178.9 s	-
2	71.9 d	3.89 s
3	99.1 s	-
4	38.3 d	2.18 b)
5	73.8 d	3.89 b)
6	78.0 s	-
7	65.7 d	3.92 b)
8	32.8 t	1.53 b)
9	61.3 d	4.00 b)
10	31.2 t	2.09 b); 1.16 b)
11	79.8 d	3.38 b)
12	36.9 d	1.83 b)
13	107.0 s	-
14	46.3 d	2.13 dd (9.7, 6.0)
15	94.8 d	3.54 d (9.7)
16	83.5 s	-
17	83.8 d	3.74 b)
18	25.7 t	1.96 b); 1.80 b)
19	23.2 t	1.78 b)
20	79.4 d	3.96 b)
21	79.5 d	4.52 b)
22	29.4 t	2.00 b); 1.44 b)
23	24.4 t	2.19 b); 1.85 b)
24	80.9 d	4.36 b)
25	74.4 d	3.90 b)
26	39.1 d	1.27 b)
27	83.4 d	3.37 b)
28	47.0 d	1.49 b)
29	98.5 s	-
1’	100.7 d	4.47 dd (8.0, 1.8)
2’	38.9 t	2.27 b); 1.56 b)
3’	71.4 d	3.64 b)
4’	87.8 d	2.69 t (8.9)
5’	71.0 d	3.21 dd (8.9, 6.1)
4-Me	12.2 q	1.11 d (6.6)
6-Me	11.5 q	1.14 s
6-OMe	50.7 q	3.33 s
11-OMe	59.4 q	3.45 s
12-Me	12.8 q	0.99 d (6.8)
14-Me	11.7 q	1.02 d (6.0)
15-OMe	60.4 q	3.42 s
16-Me	28.6 q	1.61 s
26-Me	13.5 q	0.99 d (6.8)
28-Me	12.9 q	1.03 d (6.8)
29-Me	27.0 q	1.29 s
4’-OMe	61.0 q	3.56 s
5’-Me	18.3 q	1.28 d (6.1)
3-OH	-	6.73 s
27-OH	-	5.94 s

a) Assignments were confirmed by COSY, HSQC, and HMBC experiments.
b) Signal pattern was unclear due to overlapping

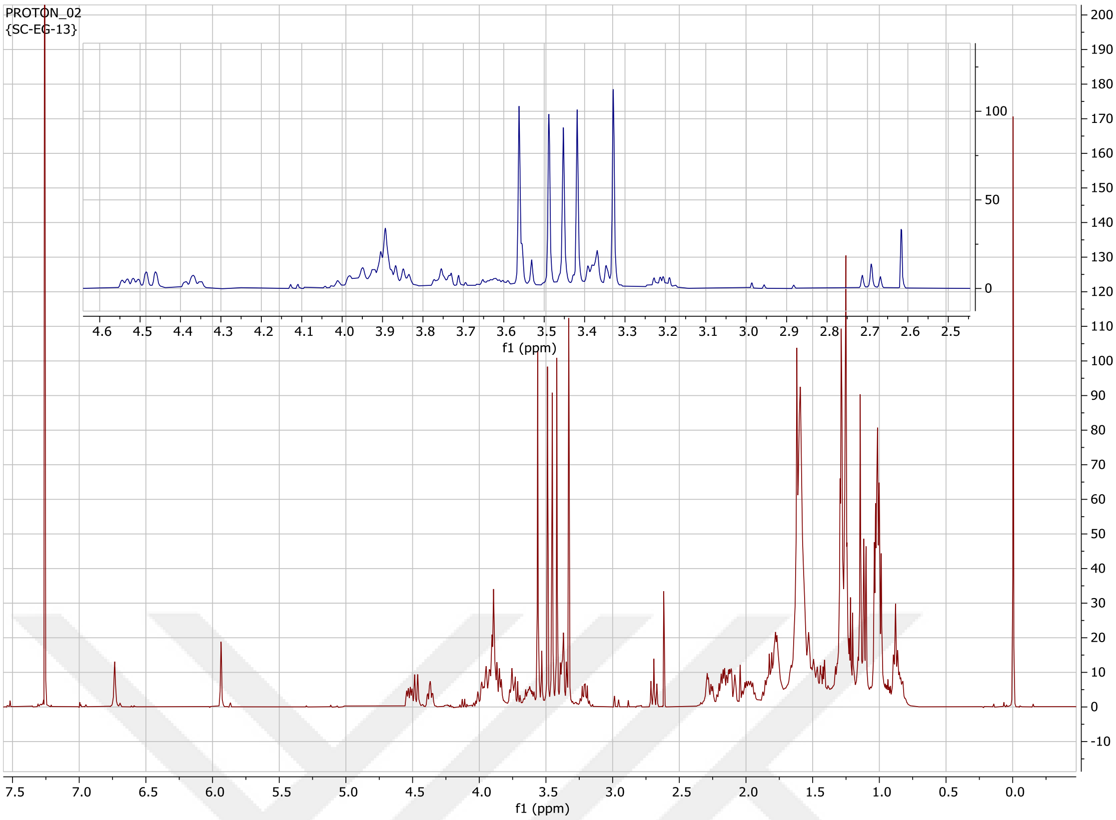

Spectrum 3.26. ^{1}H-NMR spectrum of **SC-EG-13** (in $CDCl_3$, ^{1}H: 400 MHz, ^{13}C:100 MHz)

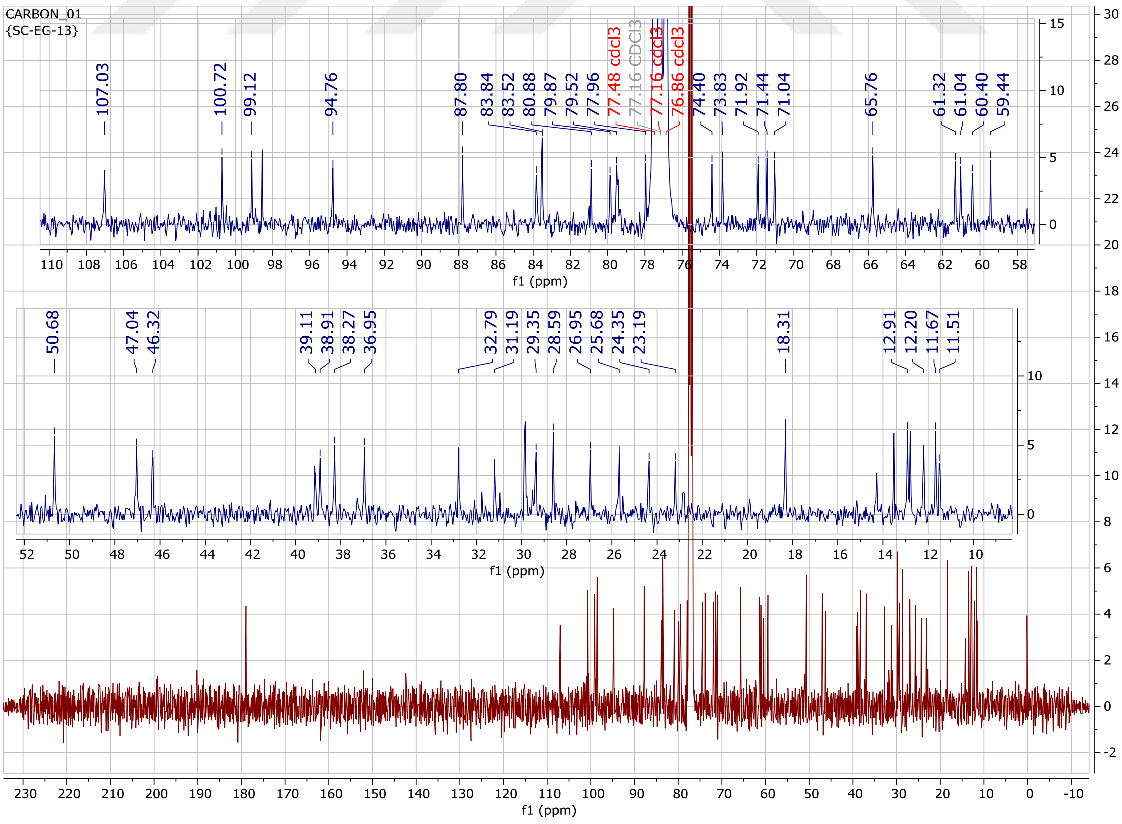

Spectrum 3.27. ^{13}C-NMR spectrum of **SC-EG-13** (in $CDCl_3$, ^{1}H: 400 MHz, ^{13}C:100 MHz)

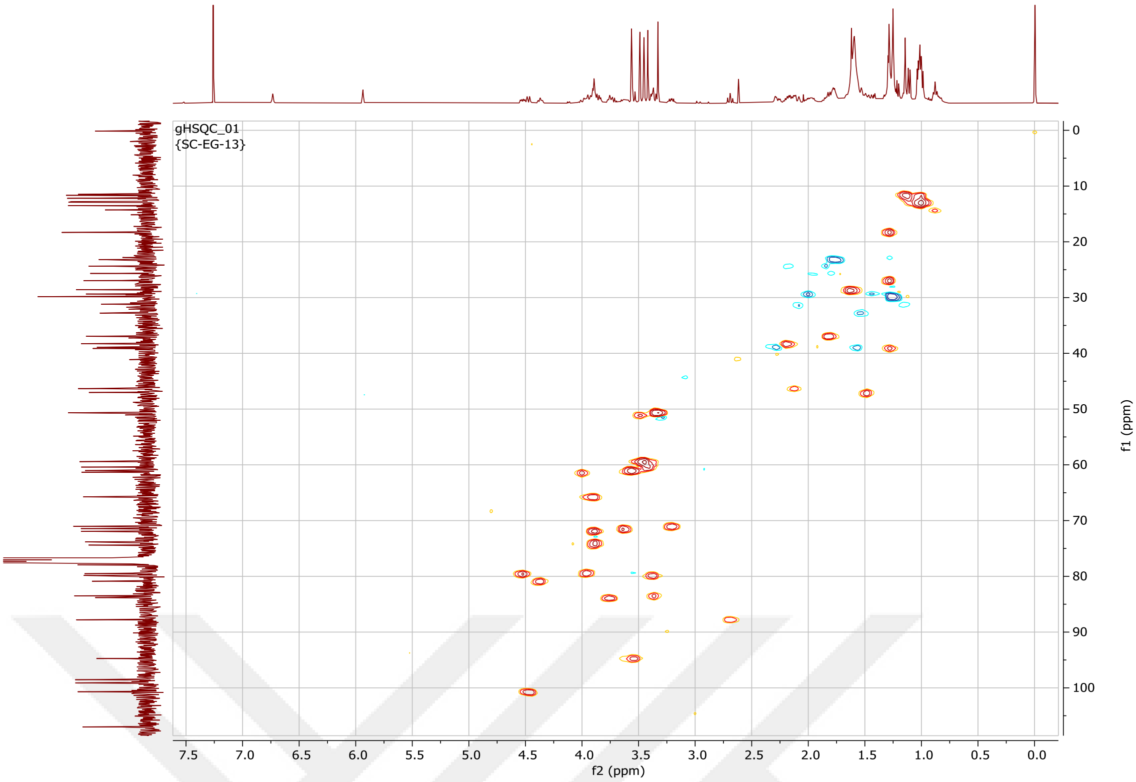

Spectrum 3.28. HSQC spectrum of **SC-EG-13** (in $CDCl_3$, ^{1}H: 400 MHz, ^{13}C:100 MHz)

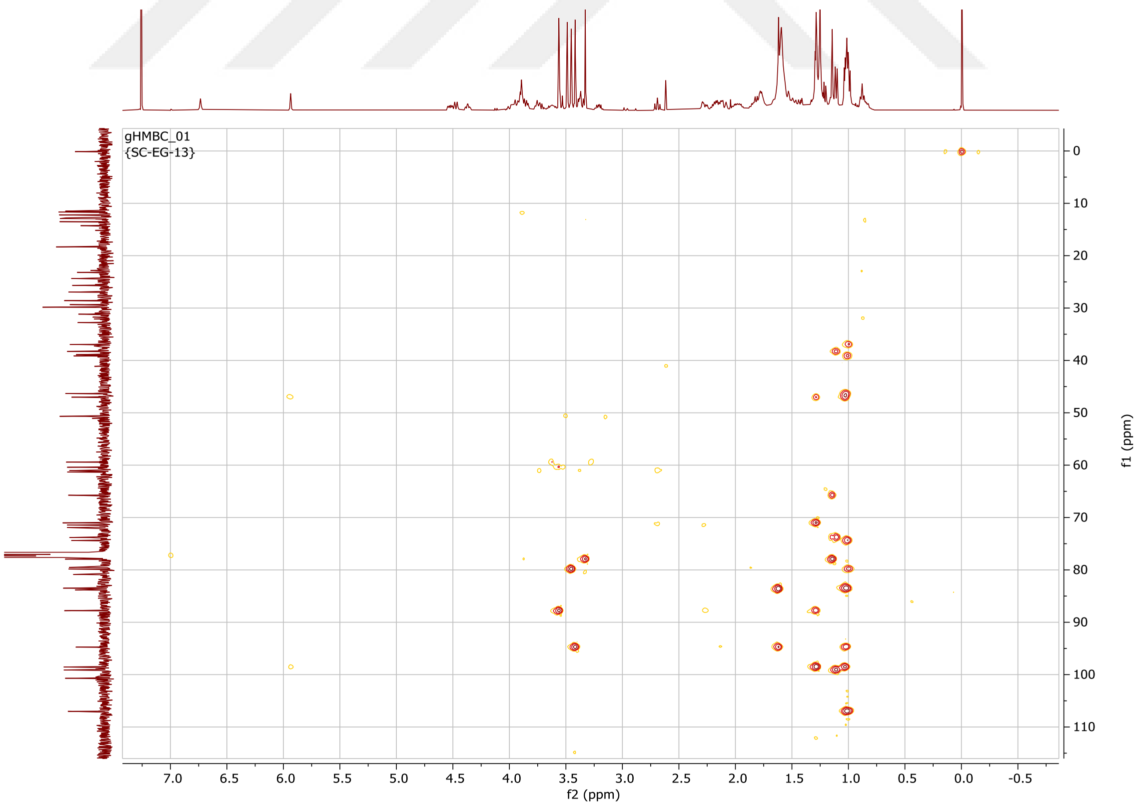

Spectrum 3.29. HMBC spectrum of **SC-EG-13** (in $CDCl_3$, ^{1}H: 400 MHz, ^{13}C:100 MHz)

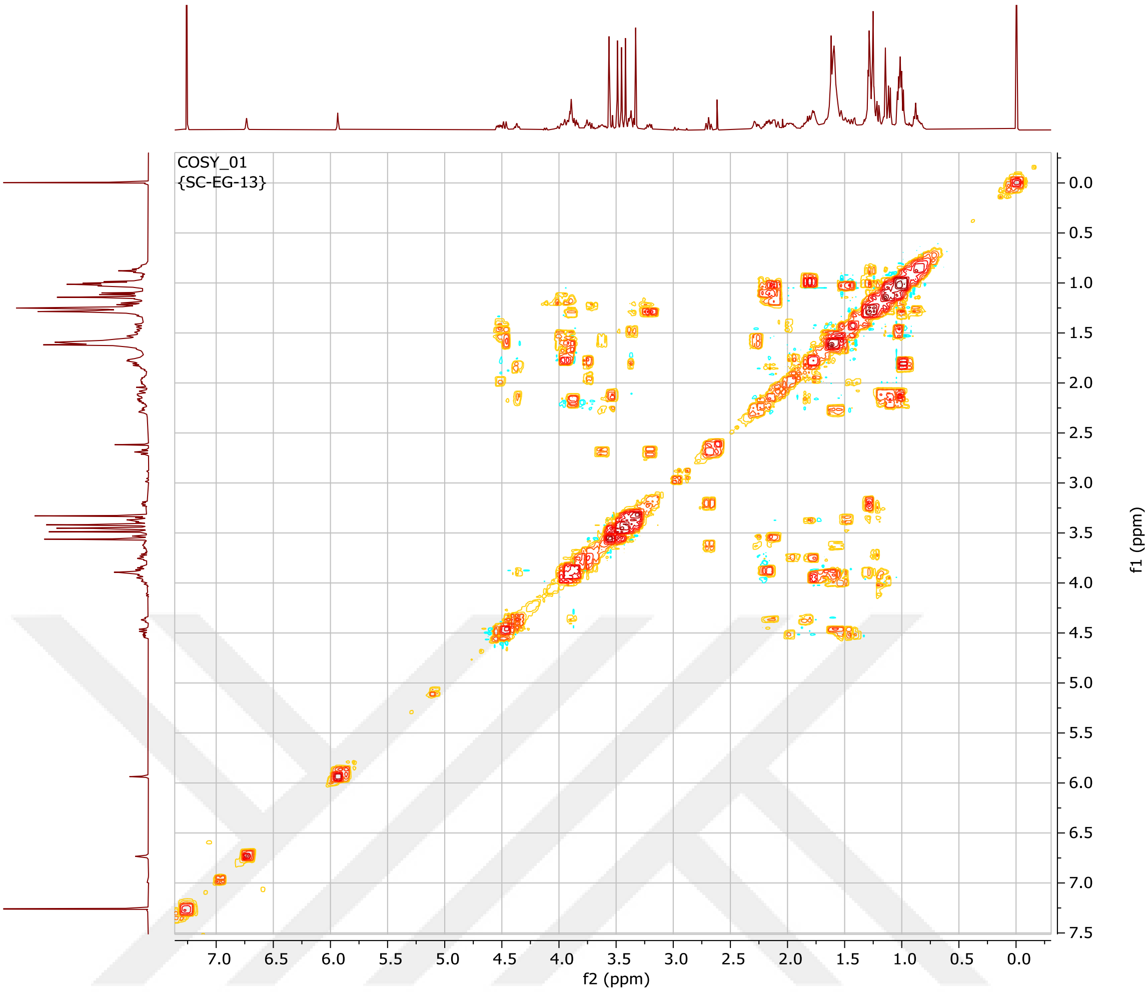

Spectrum 3.30. COSY spectrum of **SC-EG-13** (in $CDCl_3$, ^1H: 400 MHz, ^{13}C:100 MHz)

3.6.1.6. Structure Elucidation of SC-EG-07

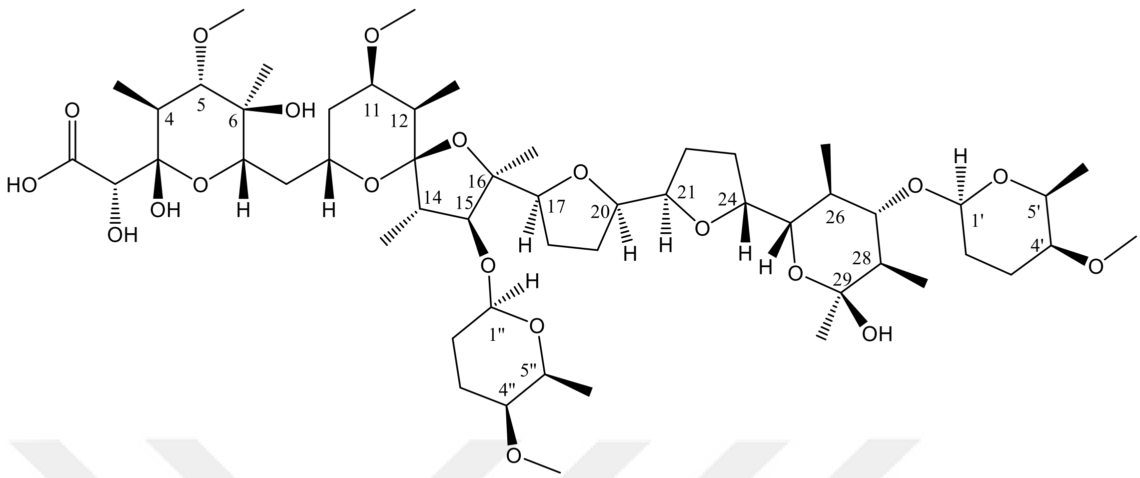

Chemical Formula: $C_{53}H_{90}O_{20}$
Exact Mass: 1046.60255

Figure 3.32. Chemical structure of **SC-EG-07.**

In the HR-ESI-MS of **SC-EG-07**, the major ion peak was observed at *m/z* 1045.5947 $[M-H]^-$ (calculated: 1045.5947) corresponding to a molecular formula of $C_{53}H_{90}O_{20}$, amu difference compared to **SC-EG-19** suggested the presence of an additional sugar moiety.

Accordingly, an examination of the ^1H and ^{13}C NMR spectra showed additional anomeric proton and carbon resonances at δ 4.34 and 103.6, respectively. The $^3J_{H\text{-}C}$ correlation from H-15 (δ 3.71) to the new anomeric carbon signal at δ 103.6 in the HMBC spectrum verified the glycosidation site as C-15. A further inspection of the resonances arising from the new sugar demonstrated a second D-amicetose unit in **SC-EG-07**. A literature survey revealed that **SC-EG-0**7 was similar to a known diglycoside polyether K41-B.[96] HR-ESI-MS result of **SC-EG-07** suggested an *O*-demethyl derivative of K41-B, and examination of the 2D NMR spectra verified an *O*-demethylation at C-6 position. Thus, the structure of **SC-EG-07** was elucidated as C6-*O*-demethyl K41-B.

Table 3.23. ^{1}H and ^{13}C NMR spectroscopic data of **SC-EG-07** [a] (in $CDCl_3$, ^{1}H: 400 MHz, ^{13}C:100 MHz)

H/C	δ_C (ppm)	δ_H (ppm), J (Hz)
1	178.9 s	-
2	72.0 d	3.90 s
3	99.3 s	-
4	38.6 d	2.13 dd (11.2, 6.6)
5	88.5 d	3.17 d (11.2)
6	74.9 s	-
7	68.8 d	3.73 dd (7.2, 4.4)
8	32.2 t	1.59 [b]
9	61.4 d	3.98 [b]
10	31.1 t	2.09 [b], 1.14 [b]
11	79.9 d	3.37 [b]
12	37.0 d	1.78 [b]
13	106.4 s	-
14	46.3 d	2.13 dd (9.4, 6.7)
15	93.1 d	3.71 d (9.4)
16	84.0 s	-
17	84.2 d	3.93 [b]
18	25.4 t	1.94 [b], 1.75 [b]
19	23.2 t	1.74 [b]
20	79.2 d	3.93 [b]
21	79.5 d	4.52 ddd (10.8, 5.2, 1.2)
22	29.4 t	1.96 [b], 1.41 [b]
23	24.4 t	2.15 [b], 1.87 [b]
24	80.8 d	4.37 [b]
25	74.4 d	3.91 dd (6.0, 2.5)
26	39.2 d	1.27 [b]
27	83.1 d	3.39 [b]
28	47.1 d	1.48 [b]
29	98.5 s	-
1’	102.8 d	4.44 dd (8.8, 1.6)
2’	30.6 t	1.94 [b], 1.46 [b]
3’	27.4 t	2.19 [b]
4’	80.4 d	2.79 ddd (10.4, 9.6, 4.8)
5’	74.6 d	3.28 dd (9.6, 6.0)
1’’	103.6 d	4.34 dd (9.2, 2.0)
2’’	30.6 t	1.94 [b], 1.46 [b]
3’’	27.2 t	2.19 [b]
4’’	80.2 d	2.79 ddd (10.4, 9.6, 4.8)
5’’	74.8 d	3.28 dd (9.6, 6.0)
4-Me	12.4 q	1.09 d (6.6)
5-OMe	62.6 q	3.59 s
6-Me	14.8 q	1.15 s
11-OMe	59.4 q	3.45 s
12-Me	12.8 q	0.99 d (7.0)
14-Me	11.1 q	0.96 d (6.7)
16-Me	26.0 q	1.59 s
26-Me	13.6 q	1.02 d (6.6)
28-Me	12.9 q	1.04 d (7.0)
29-Me	26.9 q	1.28 s
4’-OMe	57.0 q	3.35 s
4’’-OMe	57.1 q	3.35 s
5’-Me	18.4 q	1.24 d (6.0)
5’’-Me	18.4 q	1.24 d (6.0)

a) Assignments were confirmed by COSY, HSQC, and HMBC experiments.
b) Signal pattern was unclear due to overlapping

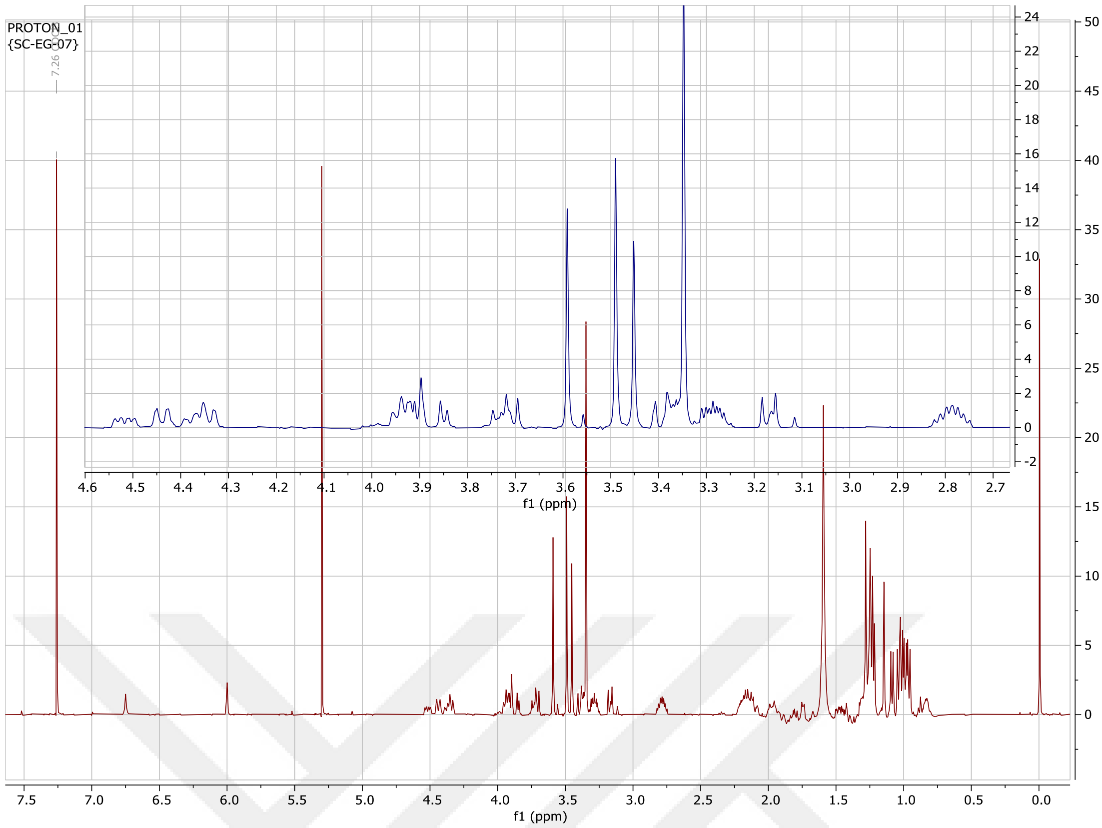

Spectrum 3.31. ^{1}H-NMR spectrum of **SC-EG-07** (in $CDCl_3$, ^{1}H: 400 MHz, ^{13}C:100 MHz)

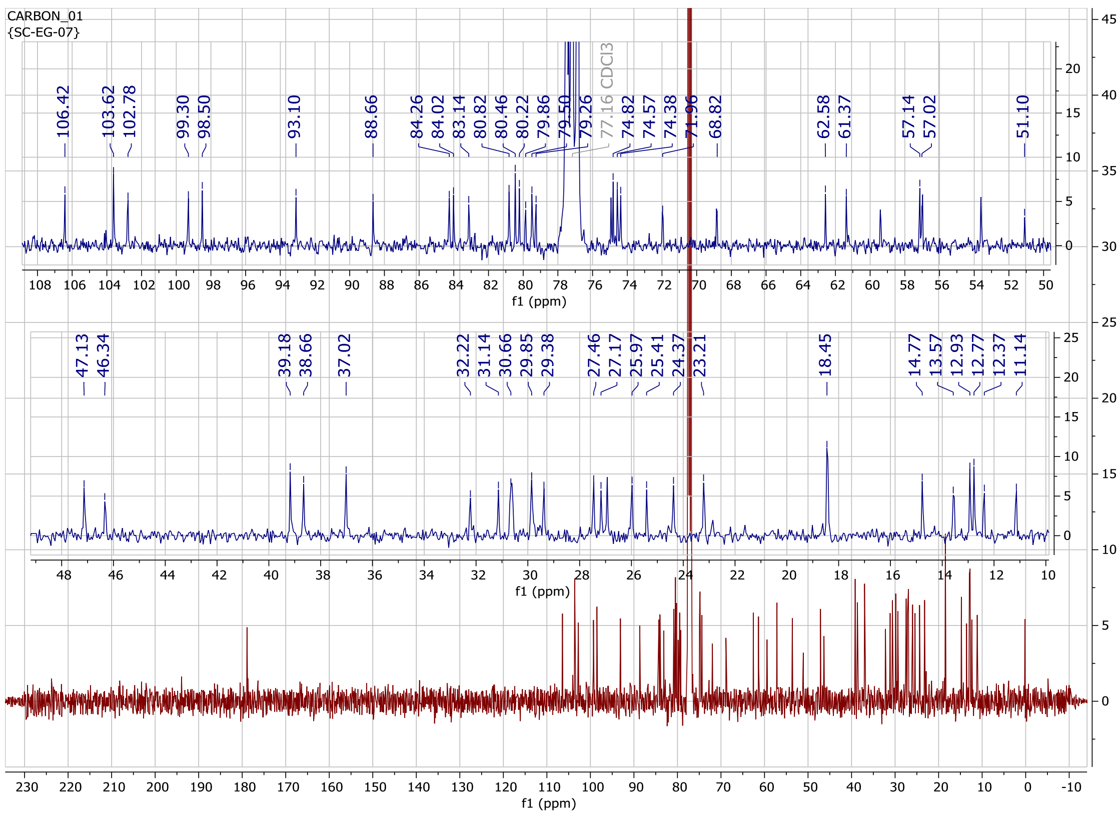

Spectrum 3.32. ^{13}C-NMR spectrum of **SC-EG-07** (in $CDCl_3$, ^{1}H: 400 MHz, ^{13}C:100 MHz)

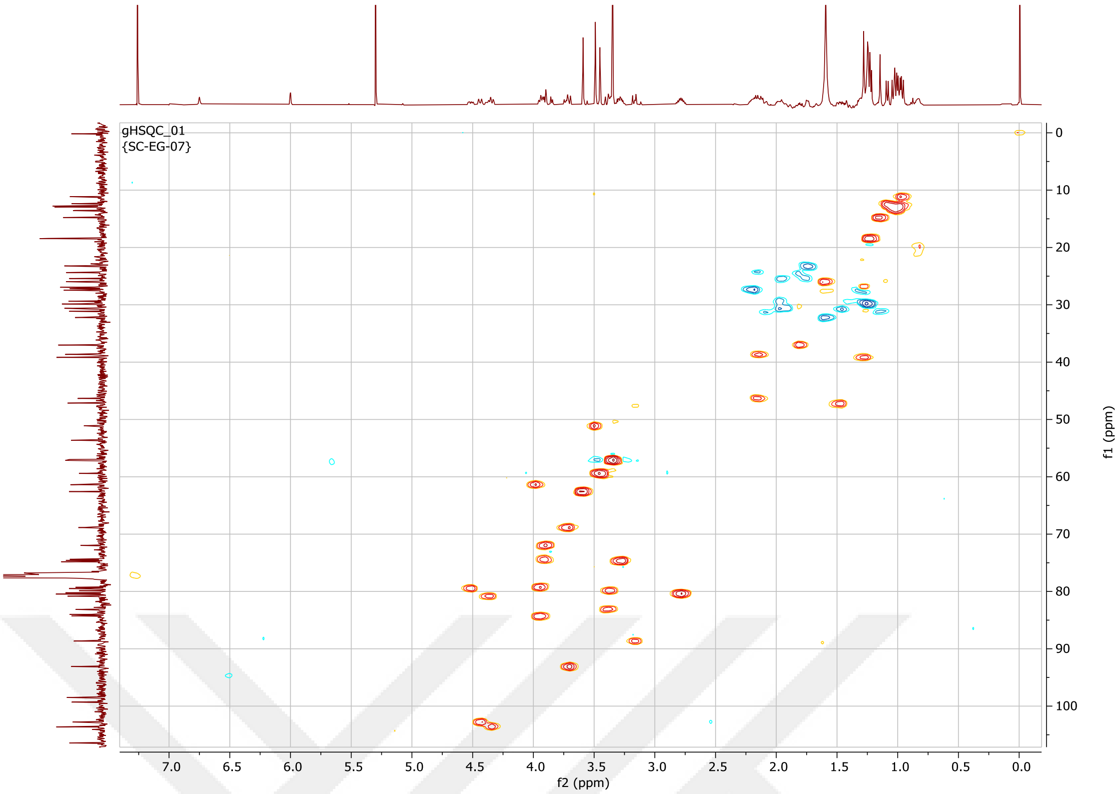

Spectrum 3.33. HSQC spectrum of **SC-EG-07** (in $CDCl_3$, ^{1}H: 400 MHz, ^{13}C:100 MHz)

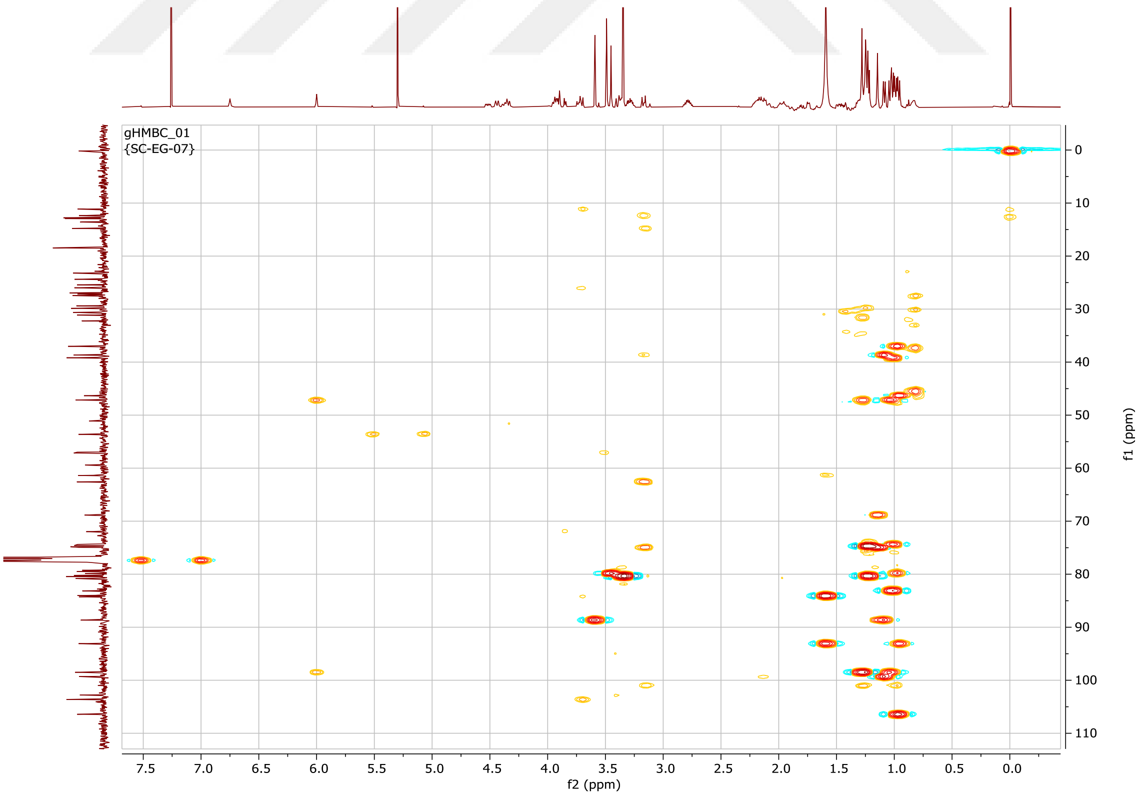

Spectrum 3.34. HMBC spectrum of **SC-EG-07** (in $CDCl_3$, ^{1}H: 400 MHz, ^{13}C:100 MHz)

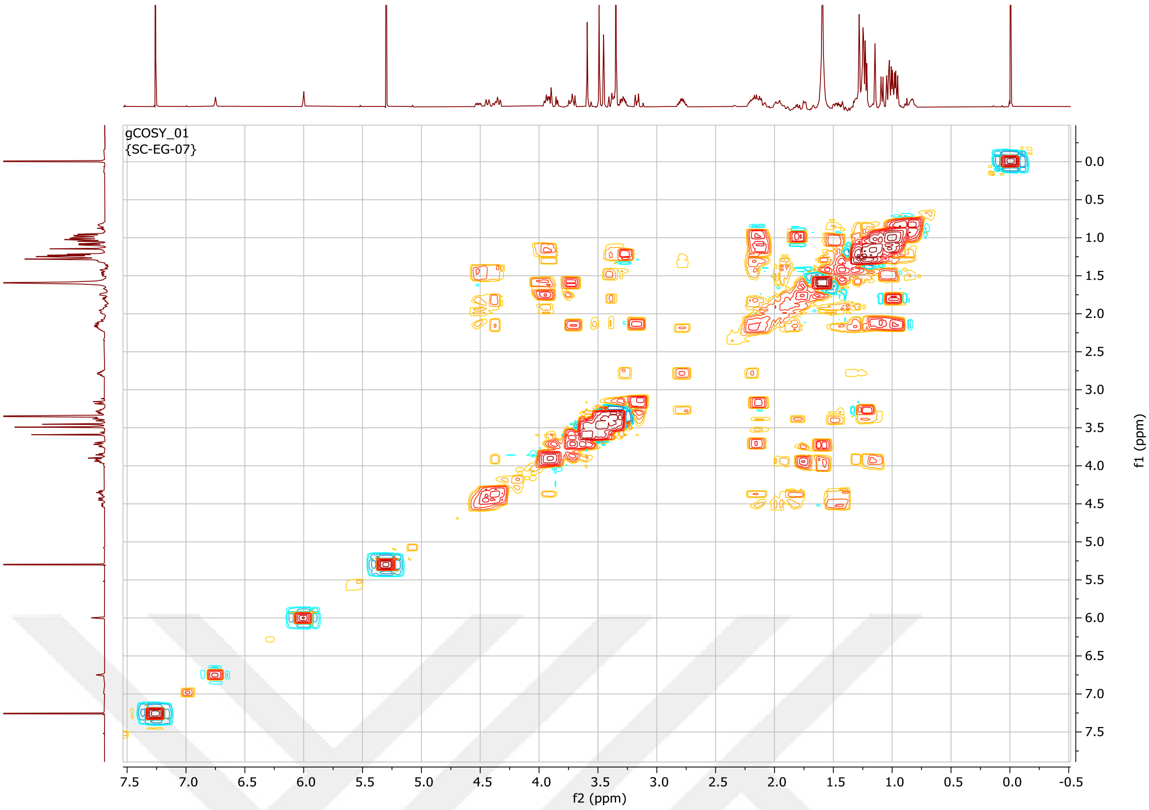

Spectrum 3.35. COSY spectrum of **SC-EG-07** (in $CDCl_3$, ^{1}H: 400 MHz, ^{13}C:100 MHz)

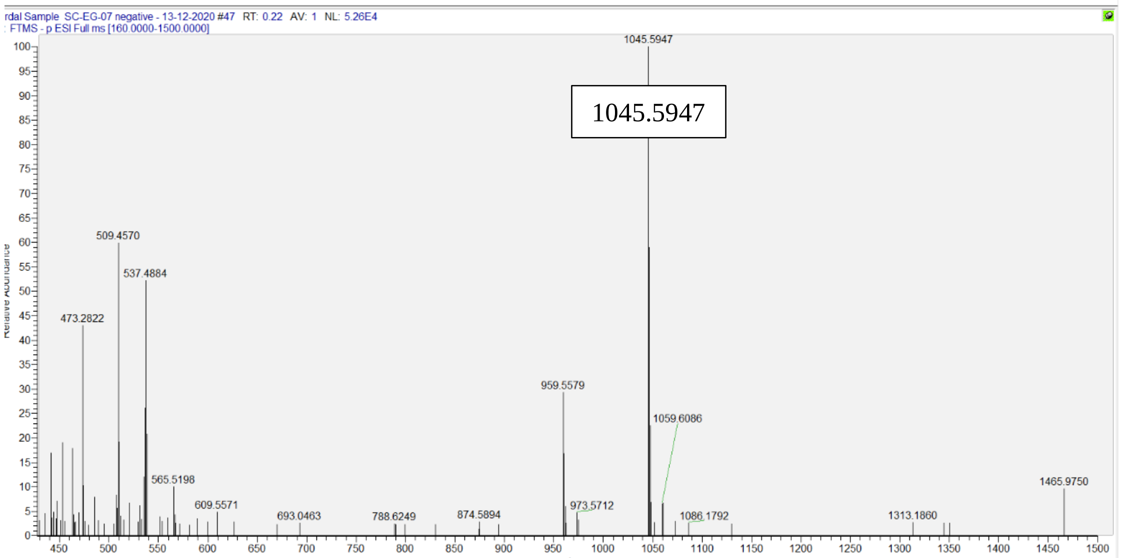

Spectrum 3.36. HR-ESI-MS spectrum of **SC-EG-07** (negative mode).

3.6.1.7. Structure Elucidation of Known Polyethers

In addition to **SC-EG-19** (K41-A), seven more known polyether molecules were identified.

SC-EG-01 was C6-*O*-demethyl derivative of K41-A; **SC-EG-02** was C27-*O*-deglycosyl derivative of K41-A; **SC-EG-03** was C5-*O*-demethyl derivative of K41-A; **SC-EG-08** was C27-*O*-deglycosyl, C29-*O*-methyl derivative of K41-A; and **SC-EG-12** was C27-*O*-deglycosyl, C5-*O*-demethyl derivative of K41-A. All these derivatives have recently been reported from four different mutant strains of a *Streptomyces* species.[97]

SC-EG-06 was identified as C29-*O*-methyl derivative of K41-A, reported in 2019 with antitumoral activity.[94]

SC-EG-18 was identified as arenaric acid, which was first isolated from a marine actinobacterium in 1999.[98]

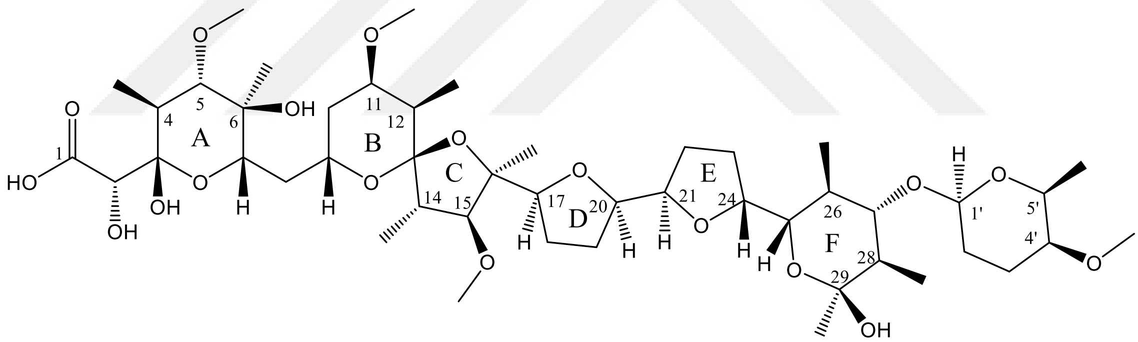

Chemical Formula: $C_{47}H_{80}O_{18}$
Exact Mass: 932.53447

Figure 3.33. Structure of **SC-EG-01.**

Table 3.24. ^{1}H and ^{13}C NMR spectroscopic data of **SC-EG-01** (in $CDCl_3$, ^{1}H: 400 MHz, ^{13}C:100 MHz)

H/C	δ_C(ppm)	δ_H (ppm), J (Hz)
1	179 s	-
2	71.9 s	3.91 m
3	99.3 d	-
4	38.7 d	2.13 m
5	88.6 d	3.17 d (11.2)
6	74.9 s	-
7	68.8 d	3.73 m
8	32.2 t	1.58 m
9	61.4 d	3.99 m
10	31.1 t	1.14 m, 2.10 m
11	79.8 d	3.38 m
12	36.9 d	1.79 m
13	107 s	-
14	46.3 d	2.12 m
15	94.7 d	3.53 d (9.3)
16	83.4 s	-
17	83.4 d	3.73 m
18	25.7 t	1.78 m, 1.95 m
19	23.2 d	1.77 m
20	79.4 d	3.95 dd (7.7, 1.5)
21	79.5 d	4.52 ddd (11.0, 5.3, 1.8)
22	29.4 t	1.43 m, 1.99 m
23	24.4 t	1.84 m, 2.13 m
24	80.9 d	4.37 td (8.5, 2.7)
25	74.4 d	3.91 dd (5.6, 2.7)
26	39.2 d	1.27 m
27	83.0 d	3.38 m
28	47.1 d	1.48 m
29	98.5 s	-
1’	102.8 d	4.44 dd (9.5, 2)
2’	30.6 t	1.49 m, 1.96 m
3’	27.4 t	2.19 m
4’	80.4 q	2.78 ddd (10.6, 9.1, 4.5)
5’	74.6 d	3.28 dd (9.0,6.1)
4-Me	12.4 q	1.09 d (6.7)
5-OMe	62.6 q	3.59 s
6-Me	14.7 q	1.14 s
11-OMe	59.4 q	3.45 s
12-Me	12.8 q	0.99 d (7.2)
14-Me	11.7 q	1.02 d (6.4)
15-OMe	60.4 q	3.41 s
16-Me	28.6 q	1.6 s
26-Me	13.6 q	1.02 d (6.4)
28-Me	12.9 q	1.04 d (6.4)
29-Me	27.0 q	1.28 s
4’-OMe	57.0 q	3.35 s
5’-Me	18.4 q	1.22 d (6.1)

*Assignments are confirmed by COSY, HSQC, and HMBC experiments.

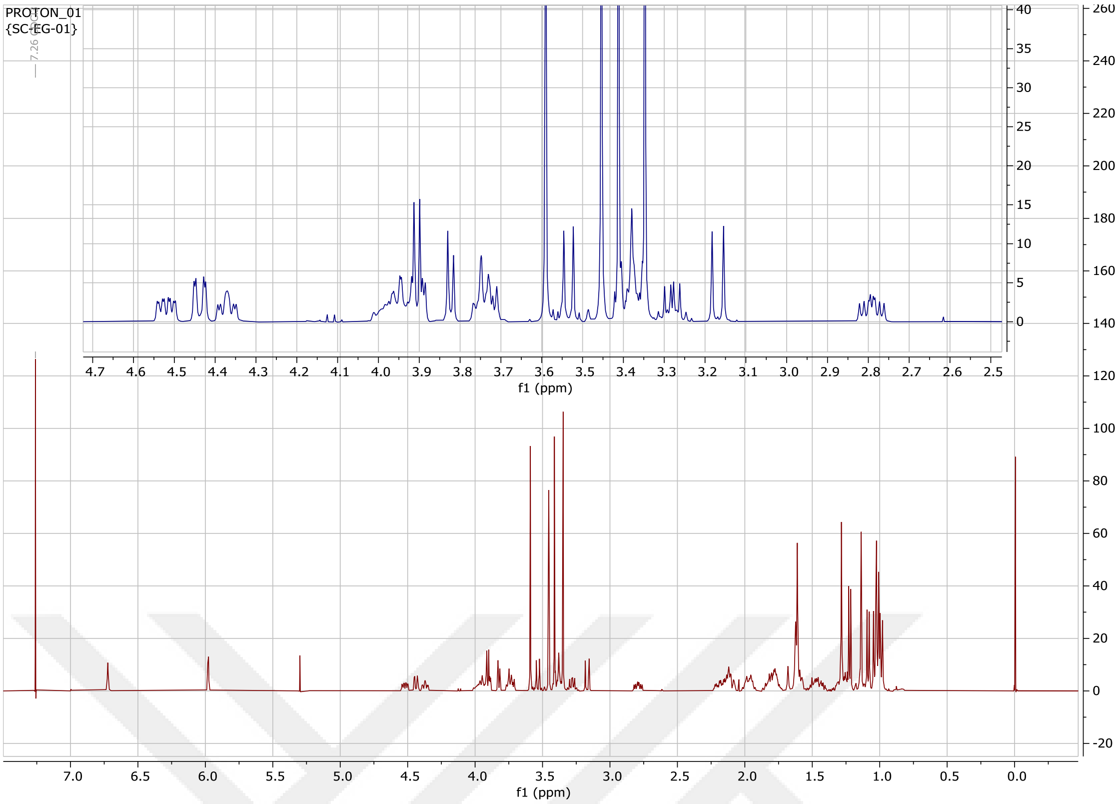

Spectrum 3.37. [1]H-NMR spectrum of **SC-EG-01** (in $CDCl_3$, [1]H: 400 MHz, [13]C:100 MHz)

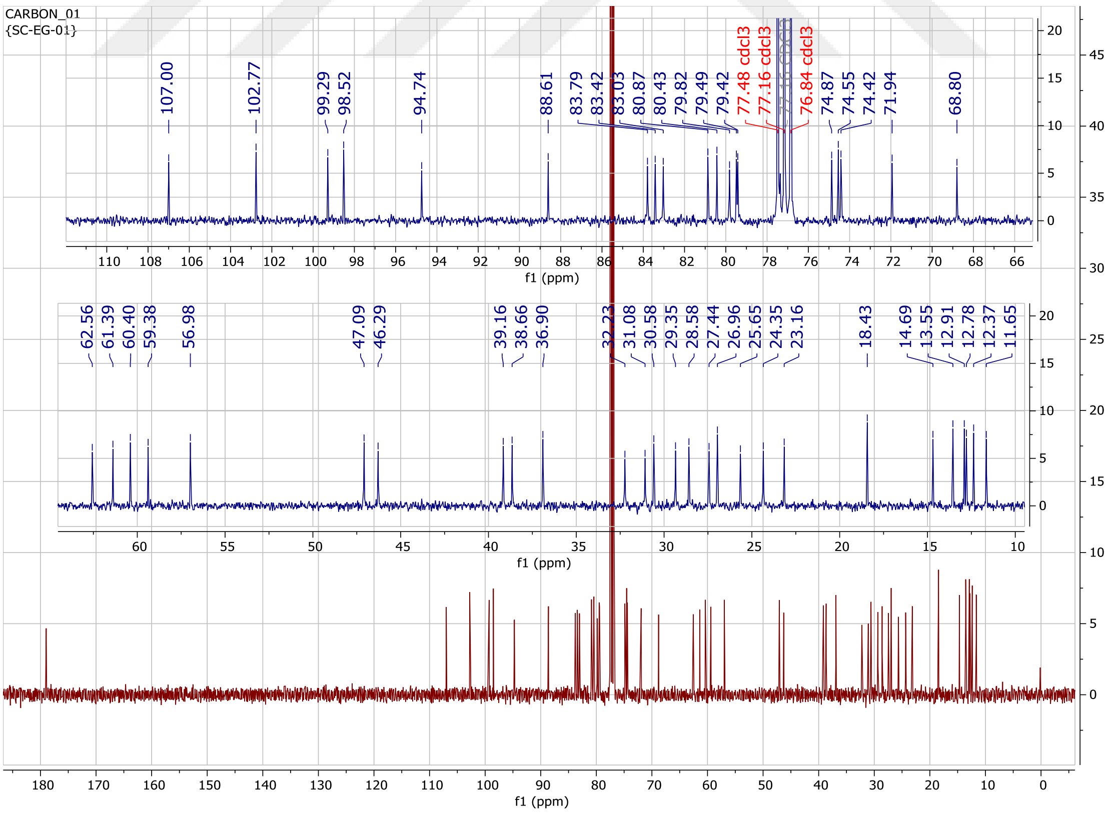

Spectrum 3.38. [13]C-NMR spectrum of **SC-EG-01** (in $CDCl_3$, [1]H: 400 MHz, [13]C:100 MHz).

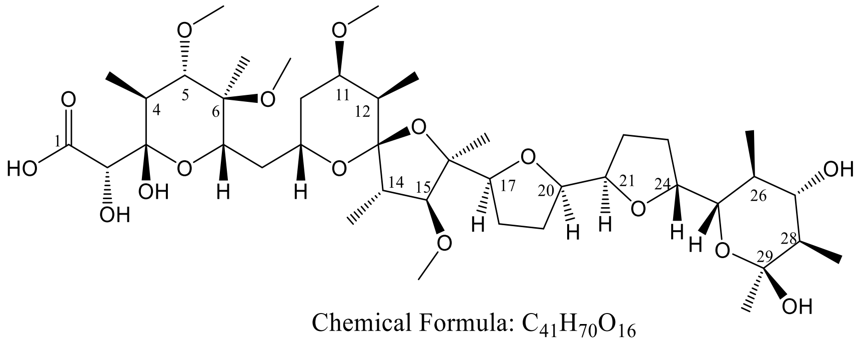

Chemical Formula: $C_{41}H_{70}O_{16}$
Exact Mass: 818.46639

Figure 3.34. Structure of **SC-EG-02.**

Table 3.25. ^{1}H and ^{13}C NMR spectroscopic data of **SC-EG-02** (in $CDCl_3$, ^{1}H: 400 MHz, ^{13}C:100 MHz)

H/C	δ_C (ppm)	δ_H (ppm), J (Hz)
1	179.0 s	-
2	71.9	3.90 s
3	99.1 s	-
4	38.8 d	2.13 m
5	85.5 d	3.32 m
6	78.4 s	-
7	66.8 d	3.81 m
8	32.4 t	1.54 m
9	61.5 d	3.94 m
10	31.1 t	2.09 m; 1.13 m
11	79.8 d	3.38 m
12	36.9 d	1.78 m
13	107.0 s	-
14	46.3 d	2.10 dd (10.3, 6.7)
15	94.7 d	3.53 d (10.3)
16	83.5 s	-
17	83.8 d	3.73 m
18	25.7 t	1.94 m; 1.77 m
19	23.2 t	1.76 m
20	79.4 d	3.94 m
21	79.5 d	4.52 dd (10.7, 5.1)
22	29.3 t	1.99 m; 1.43 m
23	24.3 t	2.16 m; 1.83 m
24	80.8 d	4.34 td (7.5, 2.4)
25	73.6 d	3.89 d (7.5)
26	40.4 d	1.19 m
27	75.1 d	3.30 m
28	47.0 d	1.34 m
29	98.3 s	-
4-Me	12.3 q	1.00 d (4.8)
5-OMe	61.2 q	3.54 s
6-Me	11.2 q	1.15 s
6-OMe	51.0 q	3.36 s
11-OMe	59.2 q	3.43 s
12-Me	12.8 q	0.99 d (6.7)
14-Me	11.7 q	1.02 d (6.7)
15-OMe	60.4 q	3.41 s
16-Me	28.6 q	1.61 s
26-Me	13.3 q	0.97 d (5.8)
28-Me	12.5 q	1.07 d (6.3)
29-Me	27.0 q	1.28 s
27-OH	-	5.82 s

*Assignments are confirmed by COSY, HSQC, and HMBC experiments.

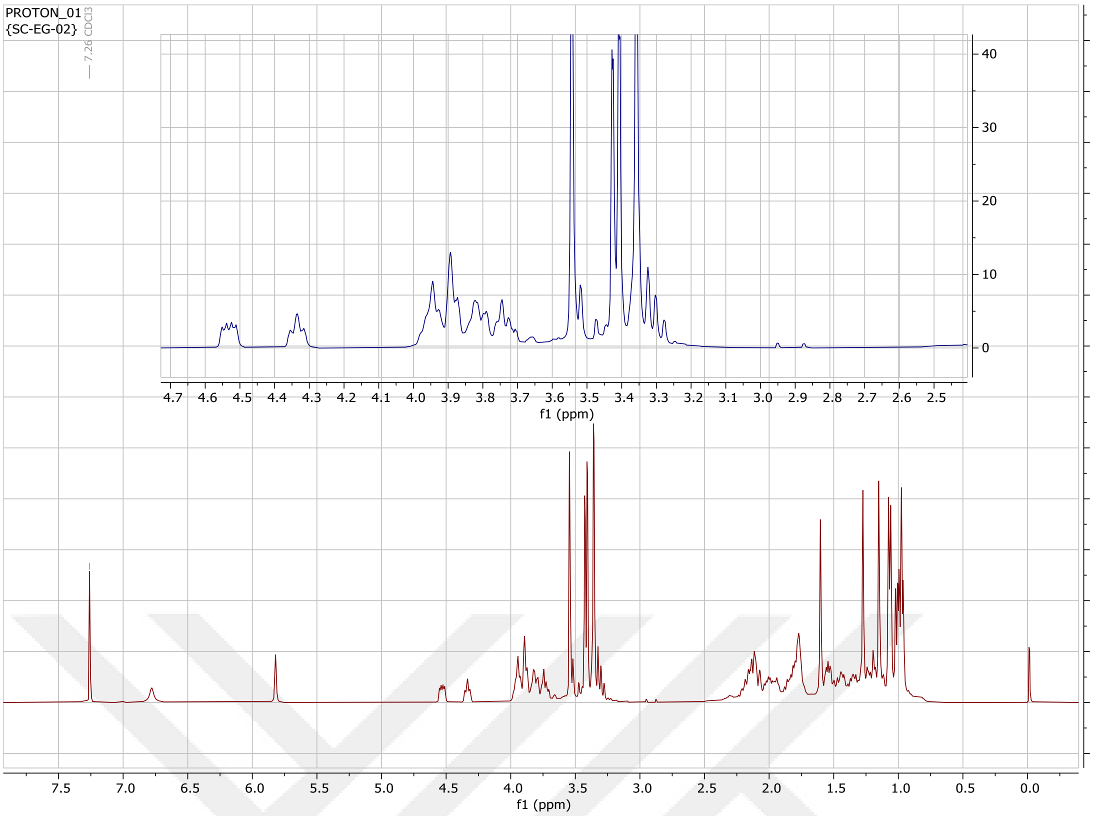

Spectrum 3.39. [1]H-NMR spectrum of **SC-EG-02** (in $CDCl_3$, [1]H: 400 MHz, [13]C:100 MHz)

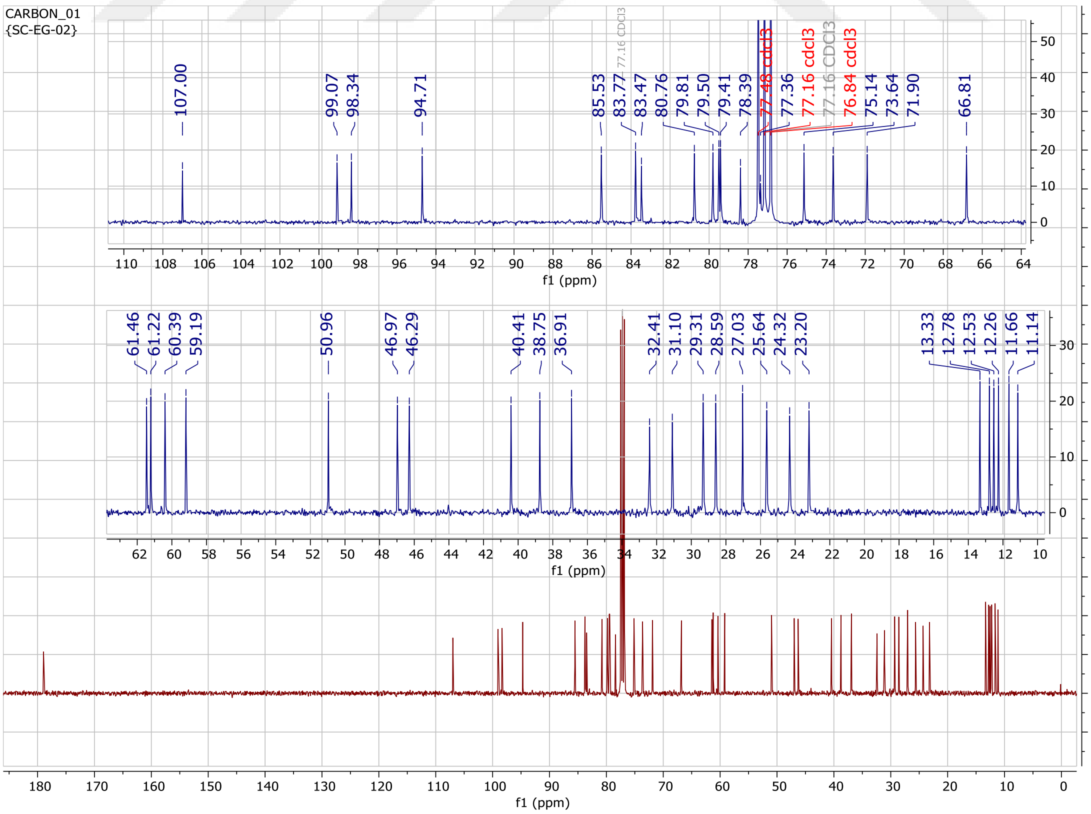

Spectrum 3.40. [13]C-NMR spectrum of **SC-EG-02** (in $CDCl_3$, [1]H: 400 MHz, [13]C:100 MHz).

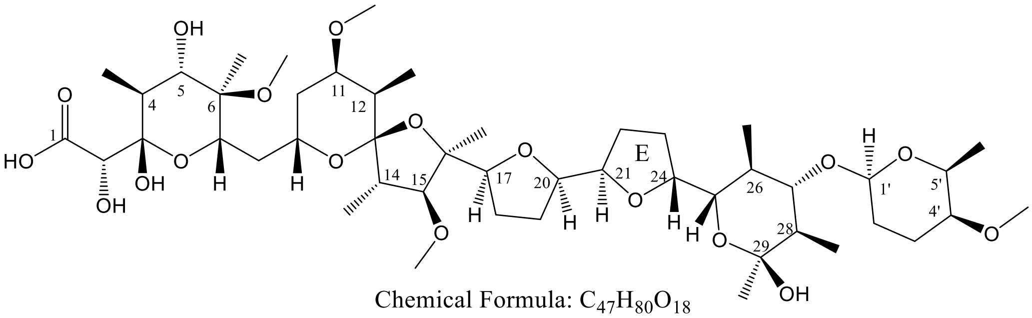

Chemical Formula: $C_{47}H_{80}O_{18}$
Exact Mass: 932.53447

Figure 3.35. Structure of **SC-EG-03.**

Table 3.26. ^{1}H and ^{13}C NMR spectroscopic data of **SC-EG-03** (in CDCl3, 1H: 400 MHz)

H/C	δC (ppm)	δH (ppm), J (Hz)
1	178.2 s	-
2	71.1 d	3.85 m
3	99.0 d	-
4	38.3 d	2.16 m
5	72.9 d	3.88 m
6	77.8 s	-
7	65.6 d	3.92 m
8	33.3 t	1.60 m,1.53 m
9	61.2 d	3.78 m
10	31.3 t	1.08 m, 2.10 m
11	78.9 d	3.34 m
12	36.9 d	1.78 m
13	106.5 s	-
14	45.9 d	2.00 m
15	94.5 d	3.53 d (9.8)
16	82.2 s	-
17	83.6 d	3.57 m
18	25.8 t	1.69 m, 1.86 m
19	22.8 t	1.70 m, 1.82 m
20	78.3 d	3.91 m
21	79.7 d	4.21 dd (11.8, 4.1)
22	29.5 t	1.35 m, 1.89 m
23	24.3 t	1.82 m, 2.06 m
24	79.3 d	4.32 td (8.9, 2.5)
25	75.1 d	3.75 dd (10.7, 2.8)
26	38.9 d	1.27 m
27	82.3 d	3.26 m
28	47.7 d	1.46 m
29	99.0 s	-
1’	102.6 d	4.42 dd (9.4, 2)
2’	30.6 t	1.44 m, 1.95 m
3’	27.4 t	1.28 m, 2.17 m
4’	80.4 d	2.78 ddd (10.4, 9.0, 4.4)
5’	74.5 d	3.25 m
4-Me	12.3 q	1.11 d (6.6)
6-Me	11.9 q	1.13 s
6-O-Me	50.3 q	3.29 s
11-O-Me	57.9 q	3.36 s
12-Me	12.96 q	0.96 d
14-Me	11.5 q	0.96 s
15-O-Me	60.6 q	3.39 s
16-Me	28.5 q	1.49 s
26-Me	13.5 q	1.00 d
28-Me	12.93 q	1.00 d
29-Me	26.8 q	1.42 s
4’-O-Me	56.9 q	3.31 s
5’-Me	18.4 q	1.21 d (6.0)

*Assignments are confirmed by COSY, HSQC, and HMBC experiments.

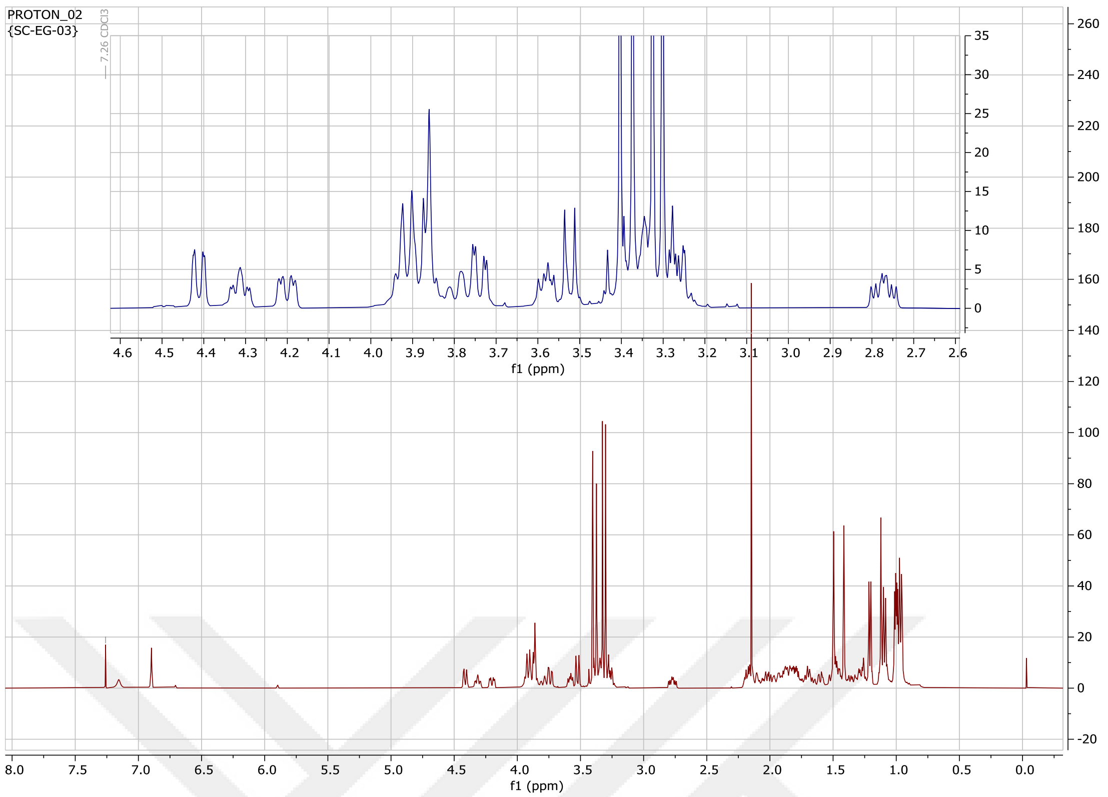

Spectrum 3.41. [1]H-NMR spectrum of **SC-EG-03** (in $CDCl_3$, [1]H: 400 MHz, [13]C:100 MHz)

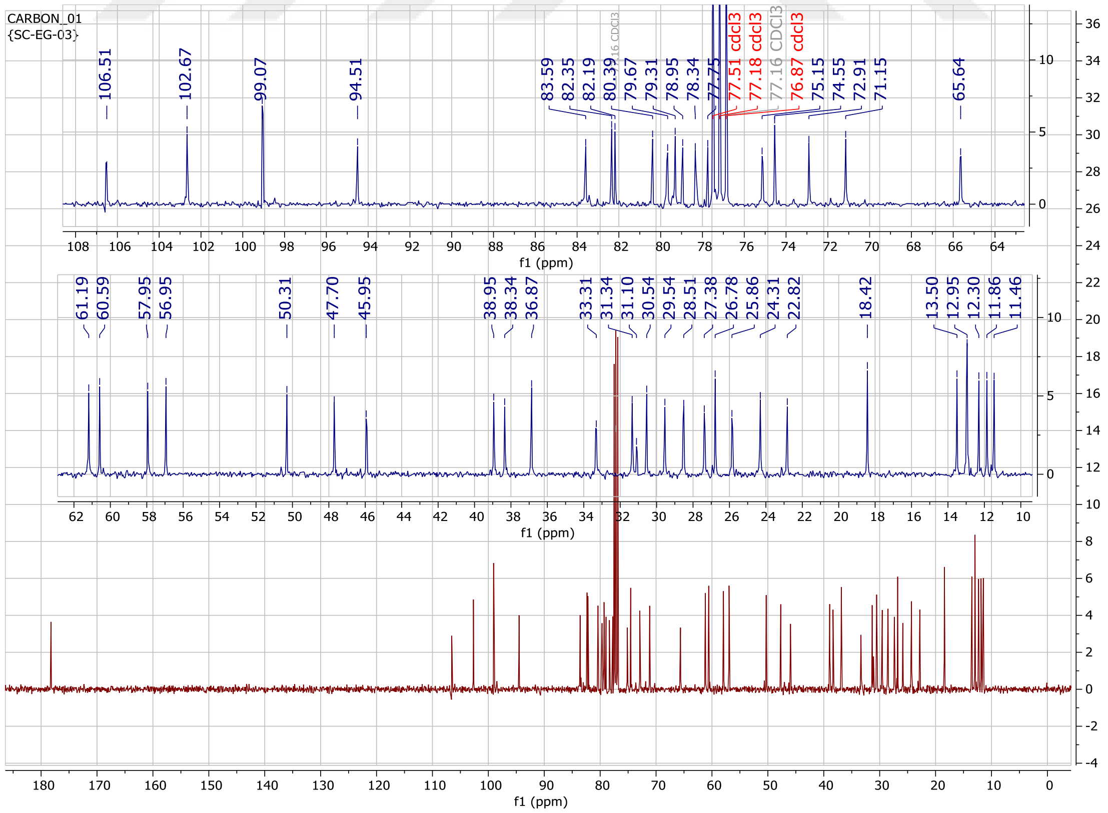

Spectrum 3.42. [13]C-NMR spectrum of **SC-EG-03** (in $CDCl_3$, [1]H: 400 MHz, [13]C:100 MHz).

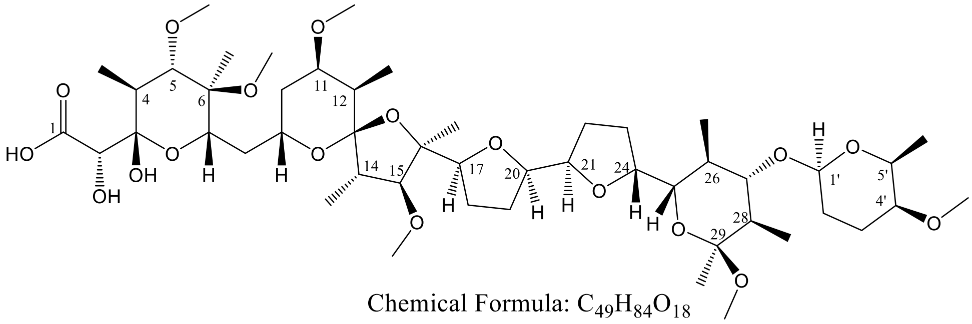

Figure 3.36. Structure of **SC-EG-06.**

Table 3.27. ^{1}H and ^{13}C NMR spectroscopic data of **SC-EG-06**

H/C	**δ_C (ppm)**	**δ_H (ppm), J (Hz)**
1	178.4 s	-
2	71.3 d	3.87 s
3	99.2 s	-
4	38.6 d	2.14 dd m
5	85.5 d	3.34 m
6	78.5 s	-
7	66.5 d	3.80 m
8	32.4 t	1.54 m
9	61.9 d	3.97 m
10	31.2 t	1.16 m, 2.15 m
11	79.5 d	3.35 m
12	37.1 d	1.79 m
13	107.2 s	-
14	46.7 d	2.16 m
15	95.1 d	3.53 d (9.1)
16	84.3 s	-
17	83.3 d	3.82 m
18	26.1 t	1.82 m, 1.92 m
19	23.3 t	1.51, 1.72 m
20	81.4 d	3.75 ddd (10.1, 5.1, 2.3)
21	78.7 d	4.84 dt (8.4, 3.1)
22	28.6 t	1.49 m, 2.29 m
23	24.6 t	1.78 m, 2.04 m
24	81.6 d	4.45 d (8.3)
25	78.1 d	3.60 d (10.8)
26	38.7 d	2.18 m
27	82.8 d	3.38 m
28	47.7 d	1.51 m
29	100.9 s	-
1’	102.9 d	4.41 dd (9.4, 1.8)
2’	30.6 t	1.95 m, 1.47 m
3’	27.4 d	1.3. m, 2.14 m
4’	80.4 d	-
5’	74.7 d	3.28 m
4-Me	12.2 q	1.07 d (6.6)
5-OMe	61.2 q	3.54 s
6-Me	11.2 q	1.16 s
6-OMe	50.8 q	3.33 s
11-OMe	59.0 q	3.41 s
12-Me	12.5 q	0.99 d (6.4)
14-Me	11.8 q	1.02 d (6.8)
15-OMe	60.3 q	3.39 s
16-Me	28.5 q	1.61 s
26-Me	13.6 q	1.00 d (6.4)
28-Me	12.9 q	0.98 d (6.4)
29-Me	22.1 q	1.24 s
29-OMe	48.6 q	3.11 s
4’-OMe	56.9 q	3.35 s
5’-Me	18.4 q	1.23 d (5.5)

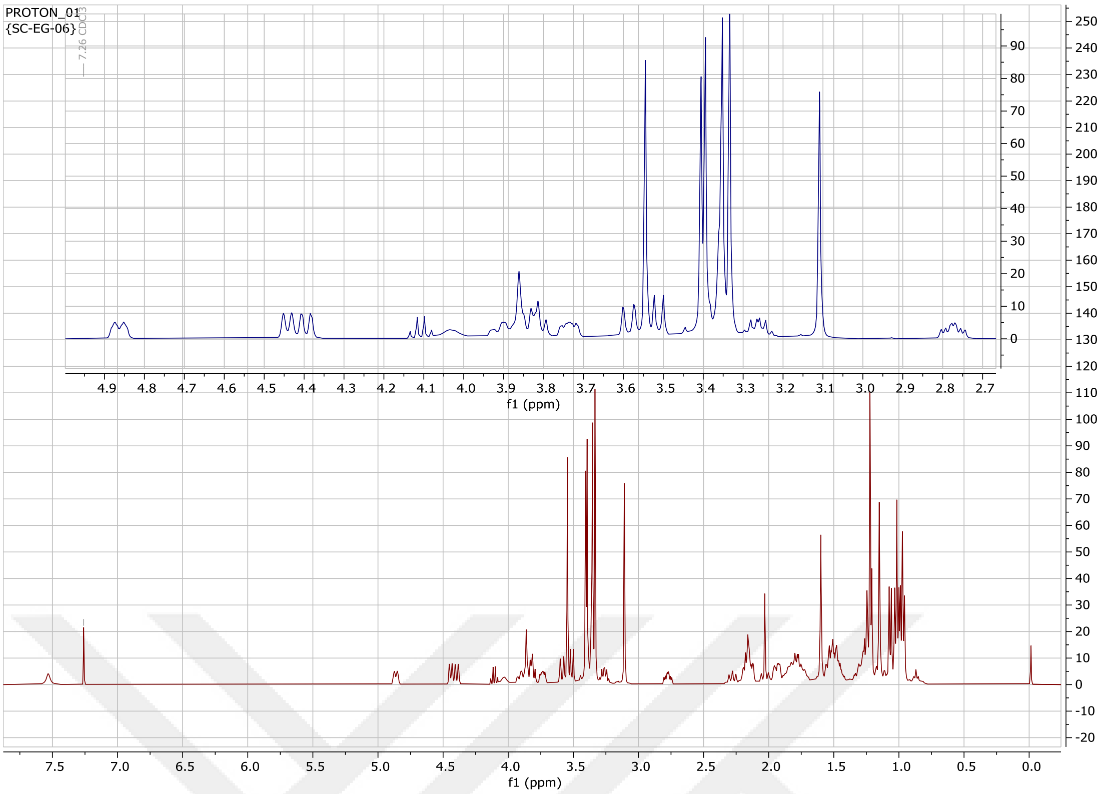

Spectrum 3.43. ^{1}H-NMR spectrum of **SC-EG-06** (in $CDCl_3$, ^{1}H: 400 MHz, ^{13}C:100 MHz)

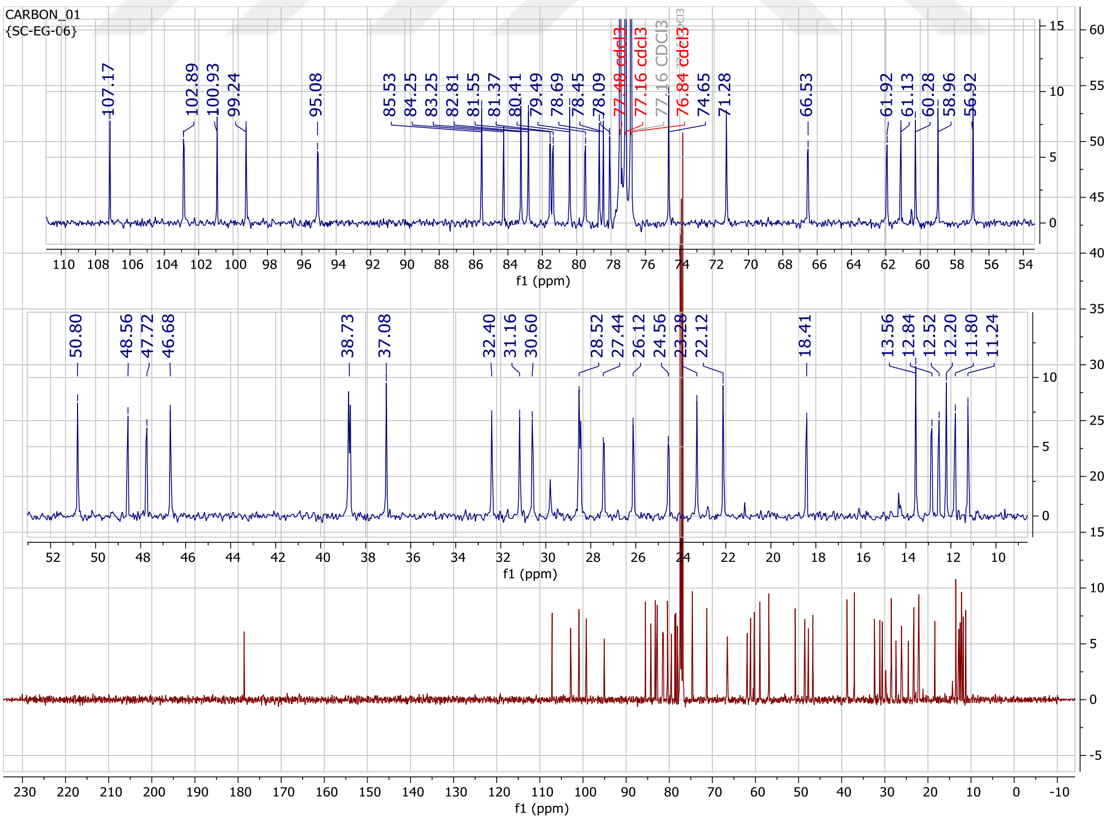

Spectrum 3.44. ^{13}C-NMR spectrum of **SC-EG-06** (in $CDCl_3$, ^{1}H: 400 MHz, ^{13}C:100 MHz)

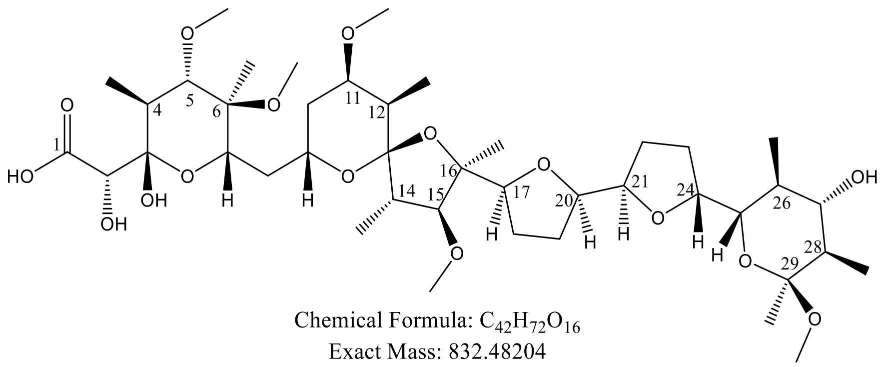

Figure 3.37. Structure of **SC-EG-08.**

Table 3.28. ^{1}H and ^{13}C NMR spectroscopic data of **SC-EG-08** [(a)] (^{1}H: 400MHz, ^{13}C:100 MHz)

H/C	δ_C(ppm)	δ_H (ppm), J (Hz)
1	178.6 s	-
2	71.3 d	3.86 s
3	99.2 s	-
4	38.7 d	2.17 dd (6.6, 1.4)
5	85.6 d	3.36 d (1.4)
6	78.4 s	-
7	66.6 d	3.83 [b)]
8	32.4 t	1.56 [b)]
9	62.0 d	3.92 [b)]
10	31.1 t	2.16 [b)]; 1.15 [b)]
11	79.5 d	3.36 [b)]
12	37.1 d	1.81 [b)]
13	107.2 s	-
14	46.7 d	2.15 dd (9.1, 6.0)
15	95.0 d	3.53 d (9.1)
16	84.3 s	-
17	83.3 d	3.82 [b)]
18	26.1 t	1.91 [b)]
19	23.3 t	1.76 [b)]; 1.51 [b)]
20	81.4 d	3.74 [b)]
21	78.7 d	4.88 d (9.4)
22	28.6 t	2.31 [b)]; 1.49 [b)]
23	24.8 t	2.07 [b)]
24	81.5 d	4.42 d (8.3)
25	79.5 d	3.36 [b)]
26	39.8 d	1.25 [b)]
27	74.8 d	3.31 d (9.8)
28	47.6 d	1.40 [b)]
29	100.8 s	-
4-Me	11.9 q	1.08 d (6.6)
5-OMe	61.2 q	3.56 s
6-Me	11.3 q	1.16 s
6-OMe	50.9 q	3.37 s
11-OMe	58.9 q	3.40 s
12-Me	12.3 q	0.99 d (6.8)
14-Me	12.2 q	1.04 d (6.0)
15-OMe	60.3 q	3.40 s
16-Me	28.5 q	1.61 s
26-Me	13.5 q	0.99 d (6.8)
28-Me	12.9 q	1.02 d (6.2)
29-Me	22.1 q	1.24 s
29-O-Me	48.6 q	3.11 s
27-OH	-	5.84 s
3-OH	-	6.78 s

a)Assignments are confirmed by COSY, HSQC, and HMBC experiments.
b) Signal pattern was unclear due to overlapping

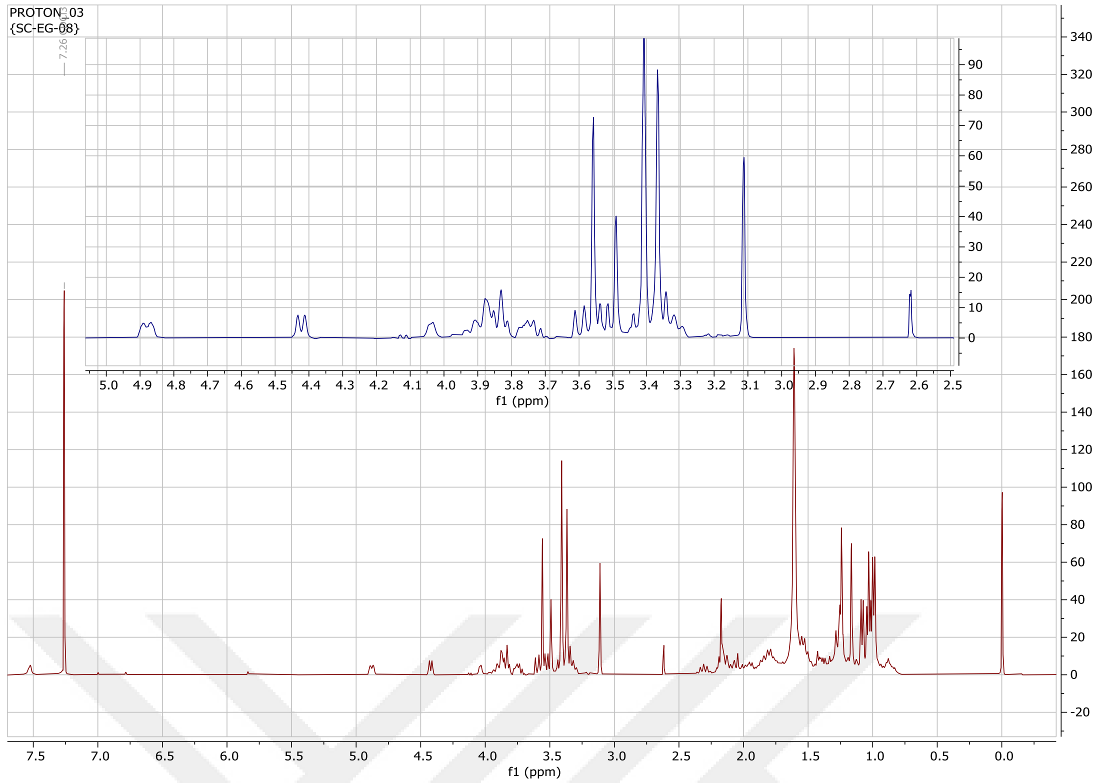

Spectrum 3.45. ^{1}H-NMR spectrum of **SC-EG-08** (in $CDCl_3$, ^{1}H: 400 MHz, ^{13}C:100 MHz)

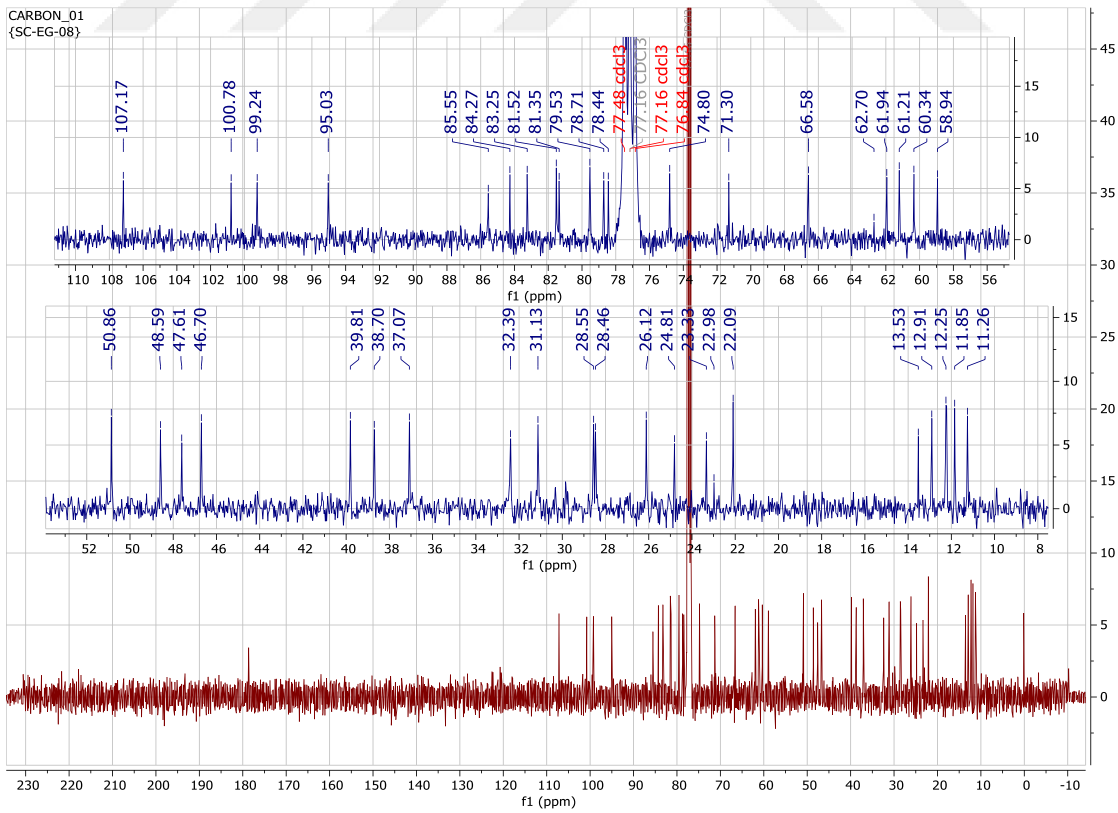

Spectrum 3.46. ^{13}C-NMR spectrum of **SC-EG-08** (in $CDCl_3$, ^{1}H: 400 MHz, ^{13}C:100 MHz).

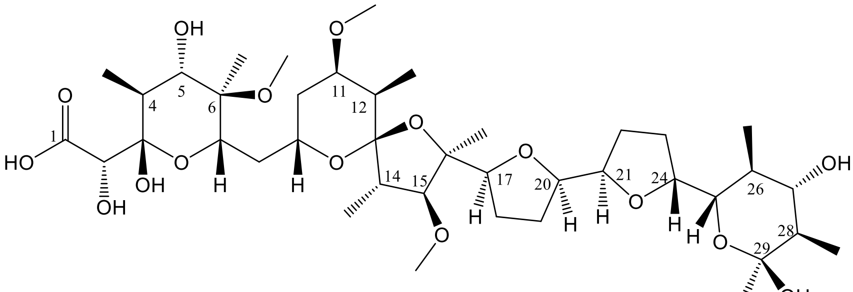

Chemical Formula: $C_{40}H_{68}O_{16}$
Exact Mass: 804.45074

Figure 3.38. Structure of **SC-EG-12.**

Table 3.29. ^{1}H and ^{13}C NMR spectroscopic data of **SC-EG-12** (^{1}H: 400 MHz, ^{13}C:100 MHz)

H/C	δ_C (ppm)	δ_H (ppm), J (Hz)
1	178.9 s	-
2	71.9 d	3.86 s
3	99.1 s	-
4	38.3 d	2.18[b)]
5	73.8 d	3.90 [b)]
6	77.9 s	-
7	65.7 d	3.87 dd (7.2, 2.4)
8	32.7 t	1.63 [b)]; 1.51 [b)]
9	61.3 d	3.99 [b)]
10	31.2 t	2.11 [b)]; 1.15 [b)]
11	79.8 d	3.37 [b)]
12	36.9 d	1.81 [b)]
13	107.0 s	-
14	46.3 d	2.13 dd (9.2, 6.8)
15	94.7 d	3.54 d (9.2)
16	83.5 s	-
17	83.8 d	3.76 d (7.0)
18	25.7 t	1.96 [b)]; 1.78 [b)]
19	23.2 t	1.77 [b)]
20	79.4 d	3.94 [b)]
21	79.5 d	4.54 ddd (11.1, 5.4, 1.8)
22	29.3 t	2.0 [b)]; 1.43 [b)]
23	24.3 t	2.20 [b)]; 1.86 [b)]
24	80.8 d	4.34 ddd (9.0, 6.9, 2.7)
25	73.7 d	3.90 [b)]
26	40.4 d	1.23 [b)]
27	75.2 d	3.29 d (9.6)
28	47.0 d	1.35 dd (9.6, 6.6)
29	98.4 s	-
4-Me	12.2 q	1.11 d (6.7)
6-Me	11.5 q	1.14 s
6-OMe	50.6 q	3.32 s
11-OMe	59.3 q	3.44 s
12-Me	12.8 q	0.99 d (7.8)
14-Me	11.7 q	1.02 d (6.8)
15-OMe	60.4 q	3.41 s
16-Me	28.6 q	1.62 s
26-Me	13.3 q	0.97 d (6.8)
28-Me	12.5 q	1.07 d (6.6)
29-Me	27.1 q	1.28 s
27-OH	-	5.78 s
3-OH	-	6.82 s

a)Assignments are confirmed by COSY, HSQC, and HMBC experiments.
b) Signal pattern was unclear due to overlapping

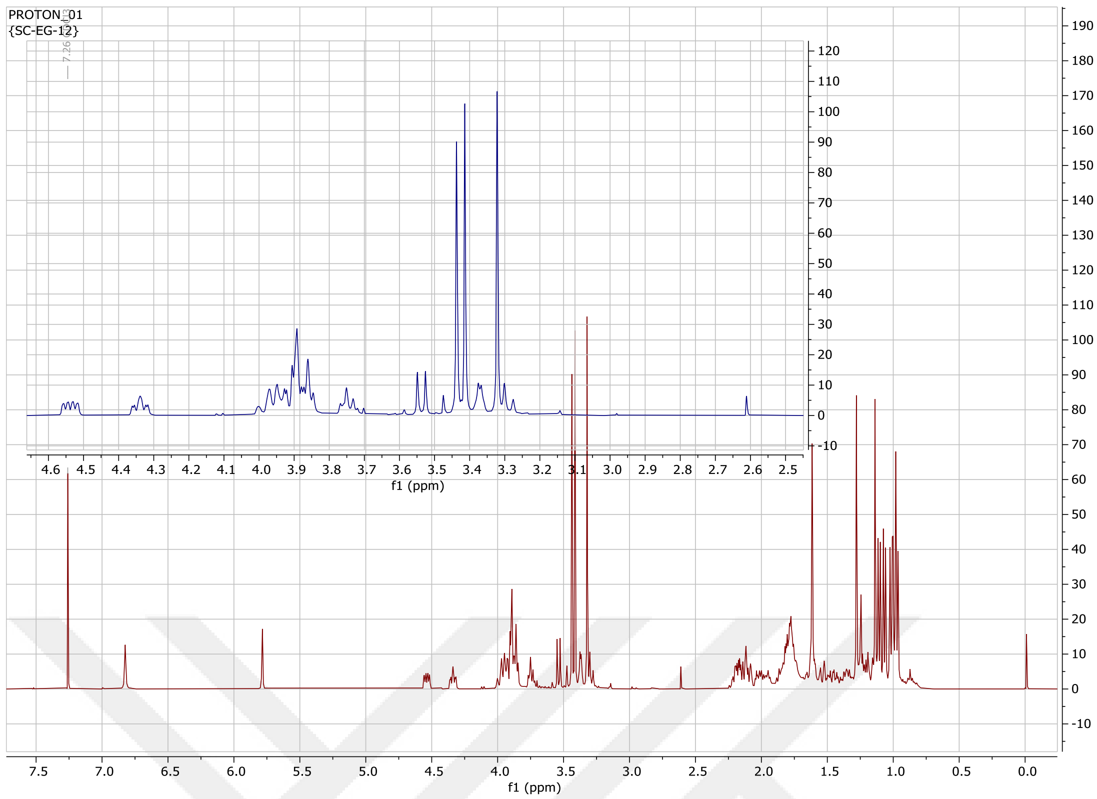

Spectrum 3.47. ^{1}H-NMR spectrum of **SC-EG-12** (in $CDCl_3$, ^{1}H: 400 MHz, ^{13}C:100 MHz)

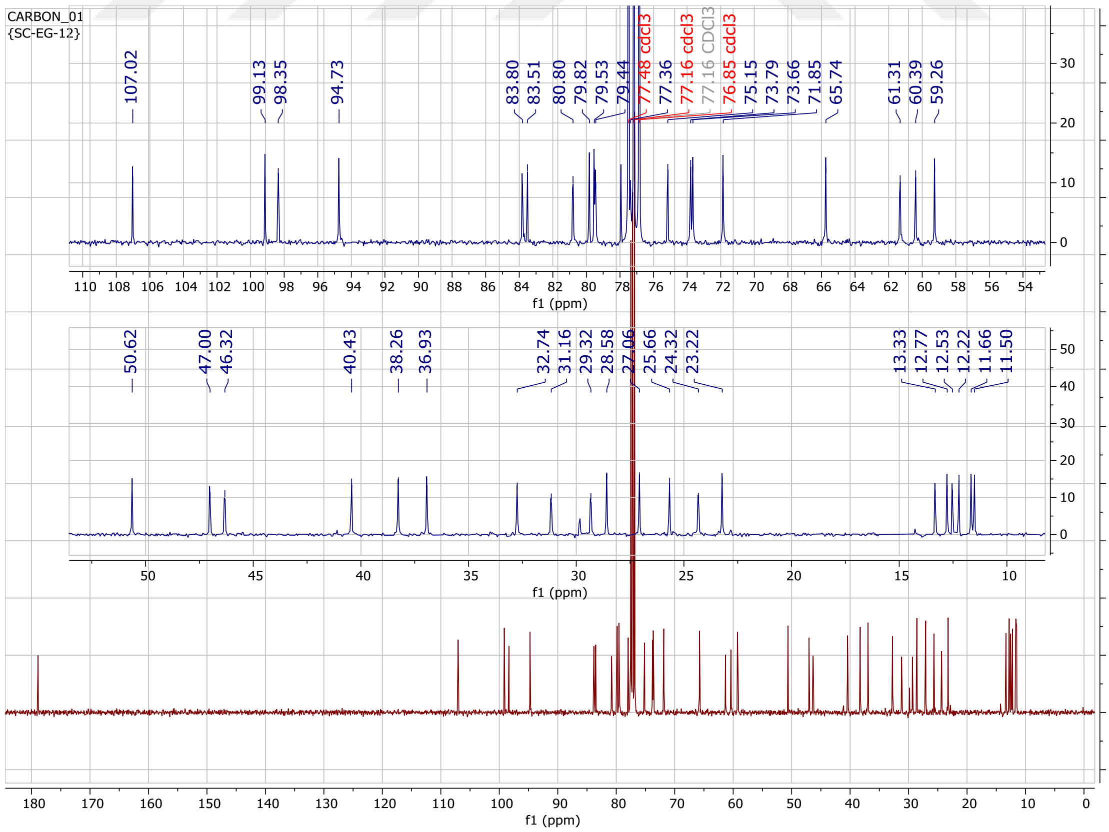

Spectrum 3.48. ^{13}C-NMR spectrum of **SC-EG-12** (in $CDCl_3$, ^{1}H: 400 MHz, ^{13}C:100 MHz).

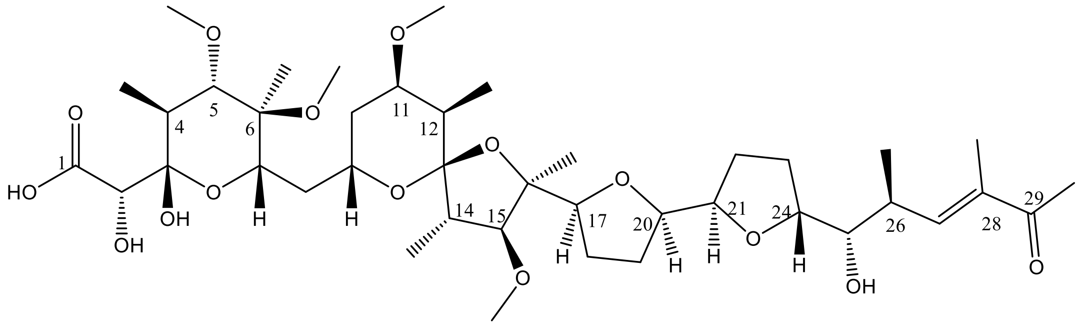

Chemical Formula: $C_{41}H_{68}O_{15}$
Exact Mass: 800.45582

Figure 3.39. Structure of **SC-EG-18.**

Table 3.30. ^{1}H and ^{13}C NMR spectroscopic data of **SC-EG-18** (^{1}H: 400 MHz, ^{13}C:100 MHz)

H/C	δ_C(ppm)	δ_H (ppm), J (Hz)
1	180.0 s	-
2	71.4 d	3.96 m
3	99.4 s	-
4	38.7 d	2.19 m
5	85.9 d	3.30 dd (11.1;1.8)
6	78.2 s	-
7	67.6 d	3.77 m
8	31.8 t	1.56 m
9	61.8 d	3.83 m
10	31.1 t	2.16 m
11	79.8 d	3.41 d (1.8)
12	37.2 d	1.84 m
13	107.5 s	-
14	47.0 d	2.13 m
15	94.6 d	3.50 dd (8.7,1.8)
16	84.7 s	-
17	83.0 d	3.80 m
18	25.9 t	1.84 m, 1.97 m
19	23.2 d	1.74 d (1.9)
20	79.4 d	3.92 m
21	78.8 d	4.57 m
22	29.7 t	1.46 m, 2.04 m
23	24.6 t	1.71 m, 2.07 m
24	83.4 d	4.08 m
25	74.6 d	4.04 m
26	36.5 d	2.61 m
27	145.5 d	6.74 d (9.4)
28	136.9 s	-
29	200.5 s	-
30	25.8 q	2.30 s
4-Me	12.3 q	1.06 d (1.7)
5-OMe	61.2 q	3.54 s
6-Me	10.9 q	1.15 s
11-OMe	58.7 q	3.44 s
12-Me	12.9 q	1.00 dd (7.0, 1.8)
14-Me	12.0 q	1.06 d
15-OMe	60.3 q	3.40 s
16-Me	28.5 q	1.60 s
26-Me	17.8 q	1.08 d (1.7)
28-Me	11.2 q	1.74 d (1.9)
29-Me	26.9 q	1.26 s

*Assignments are confirmed by COSY, HSQC, and HMBC experiments.

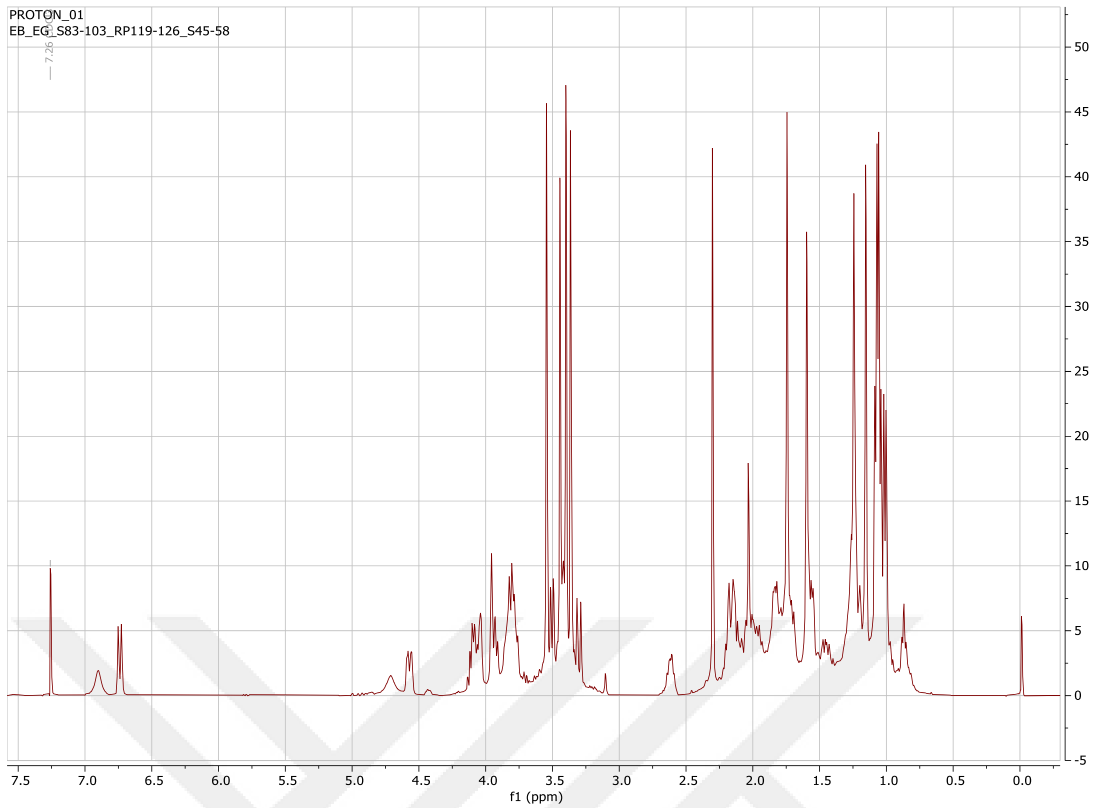

Spectrum 3.49. ^{1}H-NMR spectrum of **SC-EG-18** (in $CDCl_3$, ^{1}H: 400 MHz, ^{13}C:100 MHz)

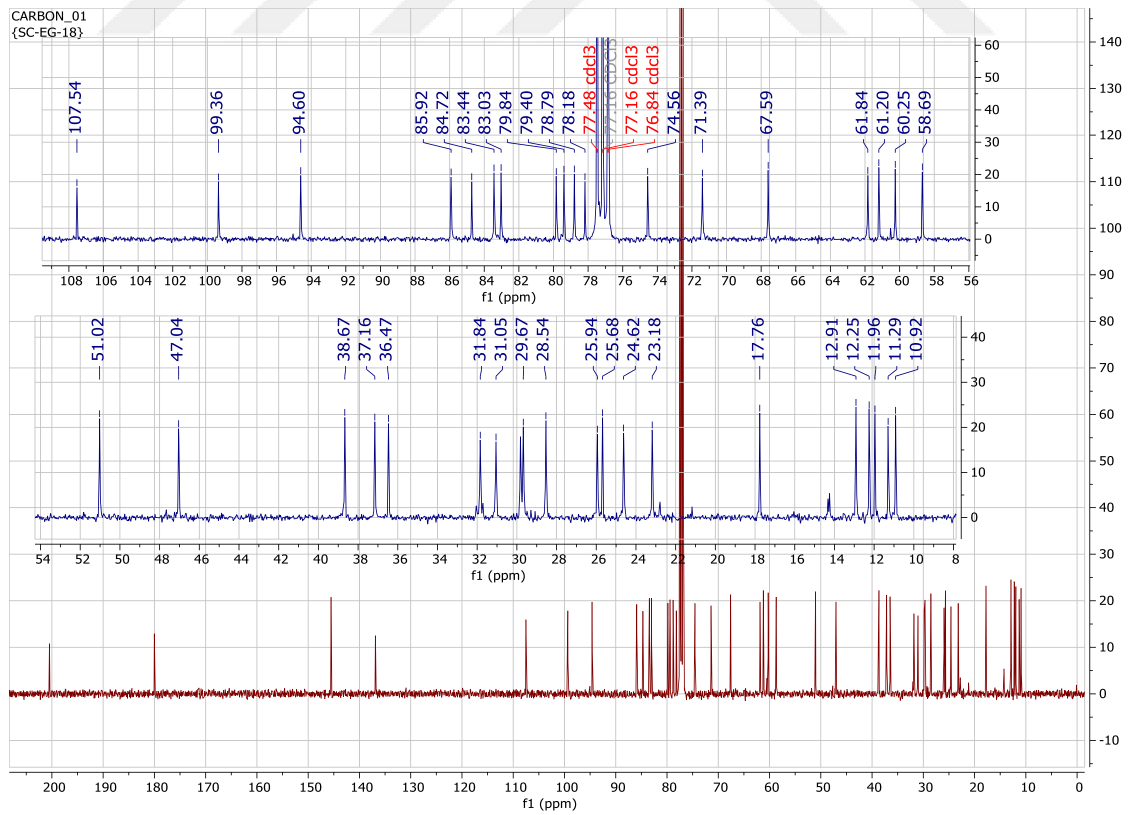

Spectrum 3.50. ^{13}C-NMR spectrum of **SC-EG-18** (in $CDCl_3$, ^{1}H: 400 MHz, ^{13}C:100 MHz)

Table 3.31. All elucidated polyether molecules. **A**: arenaric acid, **B**: C5-demethoxy derivative of K41-A, **C:** *O*-methyl and/or glycosyl derivatives of K41-A.

A

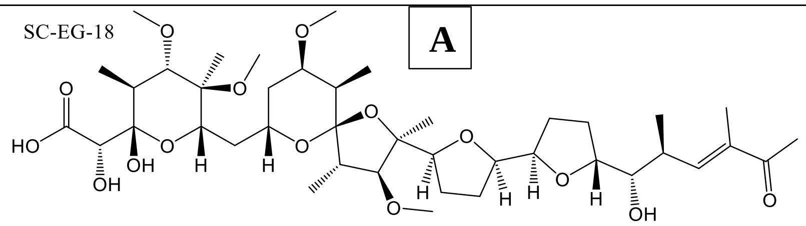

Chemical Formula: $C_{41}H_{68}O_{15}$
Exact Mass: 800.4558

B

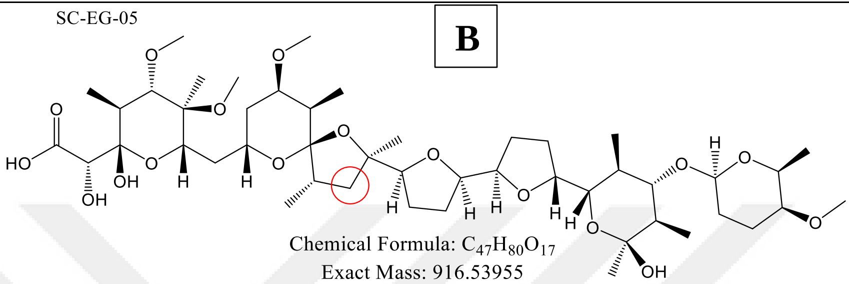

C

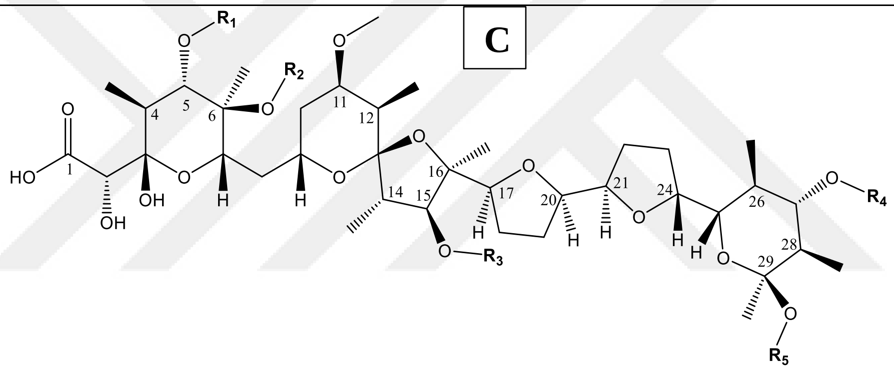

Molecules	R_1	R_2	R_3	R_4	R_5
SC-EG-01	Me	H	Me	4-*O*-Me amicetose	H
SC-EG-02	Me	Me	Me	H	H
SC-EG-03	H	Me	Me	4-*O*-Me amicetose	H
SC-EG-06	Me	Me	Me	4-*O*-Me amicetose	Me
SC-EG-07	Me	H	4-*O*-Me amicetose	4-*O*-Me amicetose	H
SC-EG-08	Me	Me	Me	H	Me
SC-EG-12	H	Me	Me	H	H
SC-EG-13	H	Me	Me	4-*O*-Me olivose	H
SC-EG-14	H	H	Me	4-*O*-Me amicetose	H
SC-EG-19	Me	Me	Me	4-*O*-Me amicetose	H
SC-EG-20	Me	Me	Me	4-*O*-Me olivose	H

4-*O*-Me amicetose:

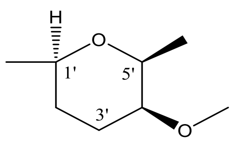

4-*O*-Me olivose:

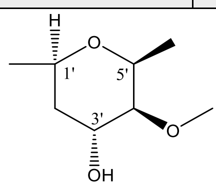

In this study, 13 polyether molecules were obtained from *S. cacaoi* (Table 3.31). The majorly produced polyether, **K41-A (SC-EG-19)**, was first obtained from *Streptomyces hygroscopicus* in 1976, and its potent activity against Gram-positive bacteria was demonstrated in the same study.[95] In 2002, *in vitro* and *in vivo* studies have shown that it has antimalarial activity against drug resistant strains of Plasmodia.[99] In 2019, its cytotoxic activity on some cancer cells by inhibiting autophagy was reported.[94] Such polyethers are called multi-target molecules because of their wide range of bioactivities. These promising bioactivities have led some scientists to try to obtain new derivatives of polyether molecules with semi-synthetic approaches.[100]

In this thesis, 11 different K41-A derivative polyethers were obtained as natural products. Among these molecules, **SC-EG-05**, **SC-EG-07**, **SC-EG-13**, **SC-EG-14** and **SC-EG-20** were found as new molecules.

SC-EG-06, a 29-*O*-methyl derivative of K41-A, was obtained semi-synthetically in the 1970s and patented for its potent anti-dysenteric and anti-coccidiosis activity. As a natural product, it was first reported in 2019, and its cytotoxic activity on some cancer cells was shown in the same study.[94]

The other known K41-A derivative polyethers coded as **SC-EG-01**, **SC-EG-02**, **SC-EG-03**, **SC-EG-08** and **SC-EG-12** were first reported in 2020. In the study of Jiang Chen *et al*., five different mutant strains of marine-derived *Streptomyces* species were obtained by disrupting the genes related to methylation. Each strain was cultured separately, and these five molecules were obtained from the fermentation of four different mutant strains. In the same study, the antiviral (anti-HIV) activity of the molecules was also examined and **SC-EG-01** showed the best activity among these five molecules. In particular, a serious decrease in antiviral activity was observed for **SC-EG-02**, **SC-EG-08** and **SC-EG-12** molecules, which are 27-deglycoside derivatives of K41-A.[97] This result indicates that sugar moiety on the structure is very important for the anti-HIV activity.

In this thesis, all molecules were obtained from the wild strain of *Streptomyces cacaoi*. Obtained molecules were tested for their antimicrobial activities (see Section 3.8) and the results were found consistent with the anti-HIV study mentioned above. Also, when the literature is evaluated, it can be predicted that the obtained new molecules have not only antimicrobial activity, but also different activities such as antiviral and antitumor.

3.6.2. Structure Identification of Other Type Molecules

Apart from polyethers, three different type metabolites, coded as **SC-EG-09**, **SC-EG-10** and **SC-EG-17**, were elucidated (Figure 40, 41 and 43).

3.6.2.1. Structure Elucidation of SC-EG-09

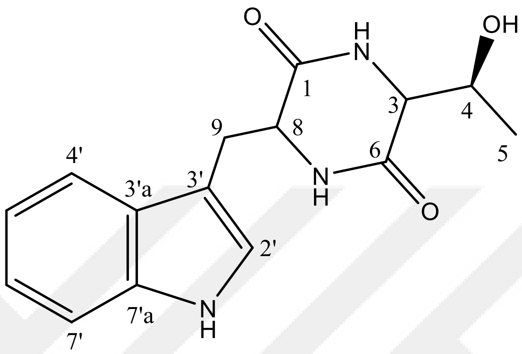

Chemical Formula: $C_{15}H_{17}N_3O_3$
Exact Mass: 287.12699

Figure 3.40. Chemical Structure of **SC-EG-09.**

The HR-ESI-MS analysis of **SC-EG-09** gave a major peak at *m/z* 310.11867 $[M-Na]^+$ (calculated: 310.11676) revealing the molecular formula as $C_{15}H_{17}N_3O_3$.

In the 1D NMR spectra, the presence of two α-proton signals (δ_H 3.66 and 4.14) and two characteristic carbon signals for the amide carbonyl groups (δ_C 168.9 and 170.9) were observed. This observation suggested a dipeptide structure. The presence of aromatic signals in the ^{1}H NMR spectrum (δ_H 7.01, 7.08, 7.12, 7.33, 7.62) revealed a tryptophan residue readily. Threonine residue in the structure was also verified by inspecting 1D and 2D NMR spectra, which was consistent with the literature.[101] Also, the hydrogen deficiency number of nine derived from molecular formula together with the key HMBC correlations from C-1 to H-3 and C-6 to H-8 verified the diketopiperazine ring in accordance with MS data. As a result, the structure of **SC-EG-09** was identified as cyclo(Thr-Trp).[102,103]

Based on the searches in *PubChem* and *SciFinder* databases, **SC-EG-09** was found to be a new cyclic dipeptide. However, determination of the absolute configurations of amino acid residues via hydrolysis were not established due to scarcity of the compound. Various cyclic dipeptides were detected as quorum sensing molecules in some marine derived microorganisms.[104] Such molecules have been reported to show potent antitumor and antifungal activities.[105]

Table 3.32. ^{1}H and ^{13}C NMR spectroscopic data of **SC-EG-09** a) (in CD_3OD, ^{1}H: 400 MHz, ^{13}C:100 MHz)

H/C	δ_C (ppm)	δ_H (ppm), J (Hz)
1	170.9	-
2 (NH)	-	-
3	62.2 d	3.66 dd (5.1, 1.1)
4	69.5 d	3.65 dd (6.5, 5.1)
5	19.8 q	1.04 d (6.5)
6	168.9 s	-
7 (NH)	-	-
8	57.7 d	4.14 dd (6.9, 5.7)
9	32.5 t	3.37 d (6.9)
1' (NH)	-	-
2'	125.2 d	7.12 s
3'	110.5 s	-
3'a	128.8 s	-
4'	119.7 d	7.62 d (8.0)
5'	120.0 d	7.01 dd (8.0, 7.0)
6'	122.5 d	7.08 dd (8.5, 7.0)
7'	112.3 d	7.33 d (8.5)
7'a	138.2 s	-

a) Assignments are confirmed by COSY, HSQC, and HMBC experiments.

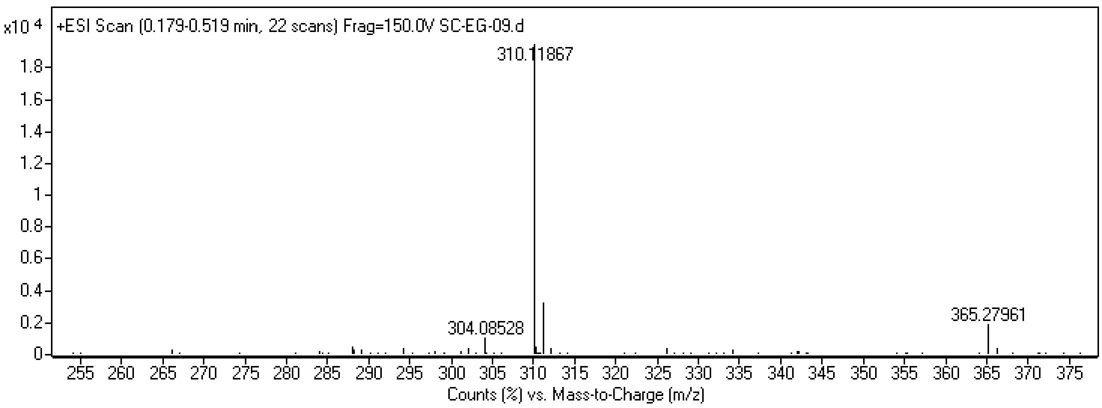

Spectrum 3.51. HR-ESI-MS spectrum of **SC-EG-09** (positive mode, $[M-Na]^{+}$)

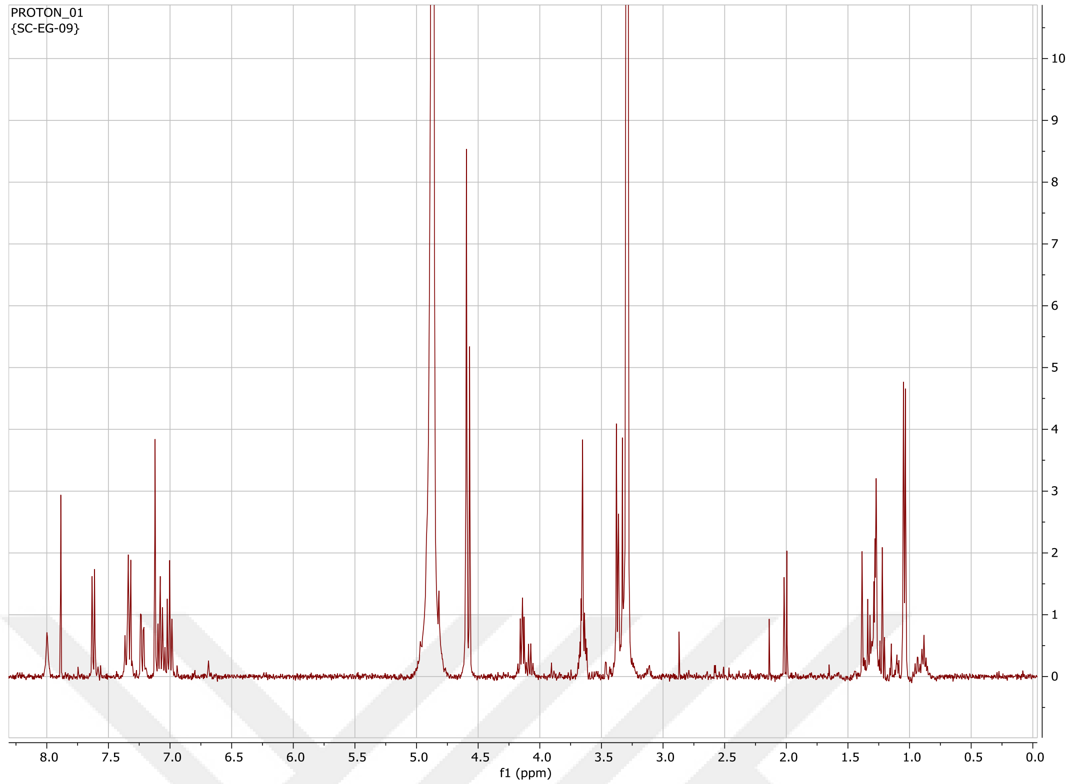

Spectrum 3.52. ^{1}H-NMR spectrum of **SC-EG-09** (in CD_3OD, ^{1}H: 400 MHz, ^{13}C:100 MHz)

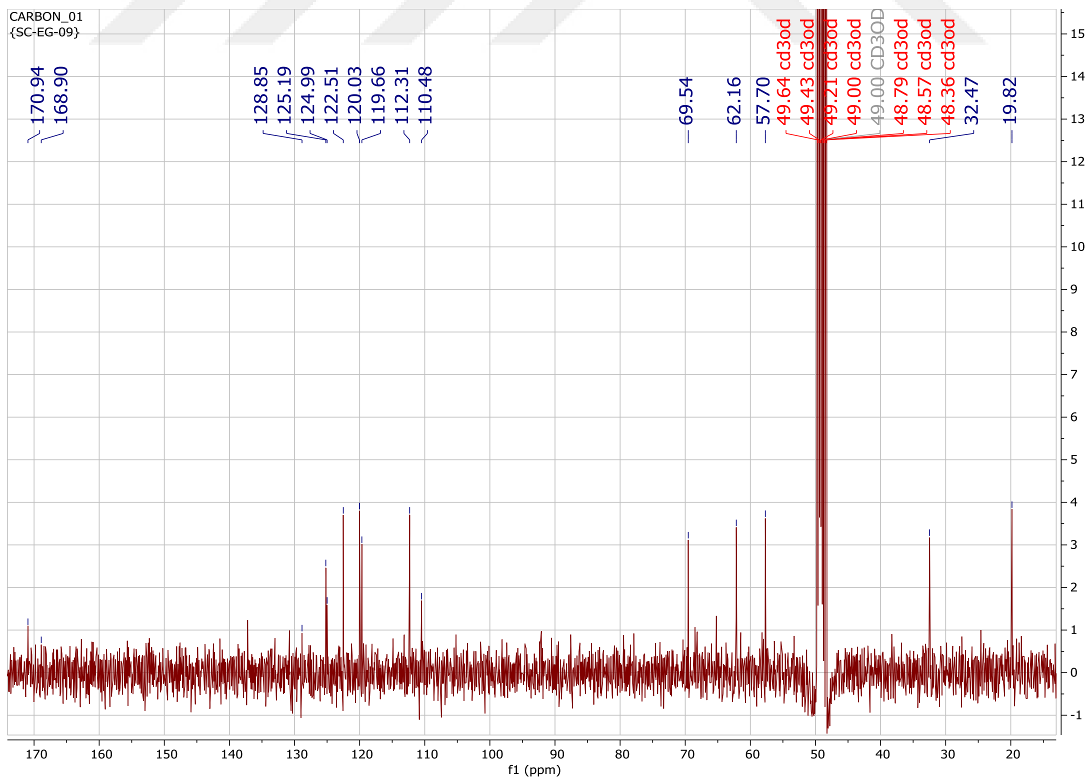

Spectrum 3.53. ^{13}C-NMR spectrum of **SC-EG-09** (in CD_3OD, ^{1}H: 400 MHz, ^{13}C:100 MHz)

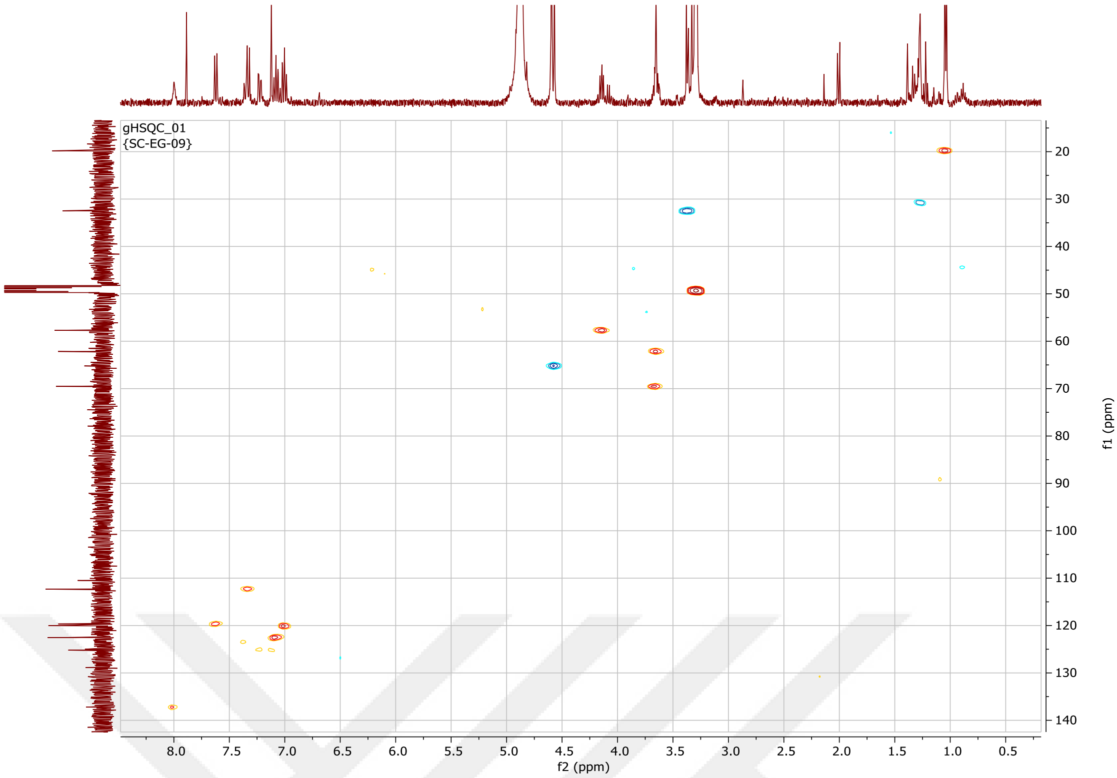

Spectrum 3.54. HSQC spectrum of **SC-EG-09** (in CD_3OD, ^{1}H: 400 MHz, ^{13}C:100 MHz)

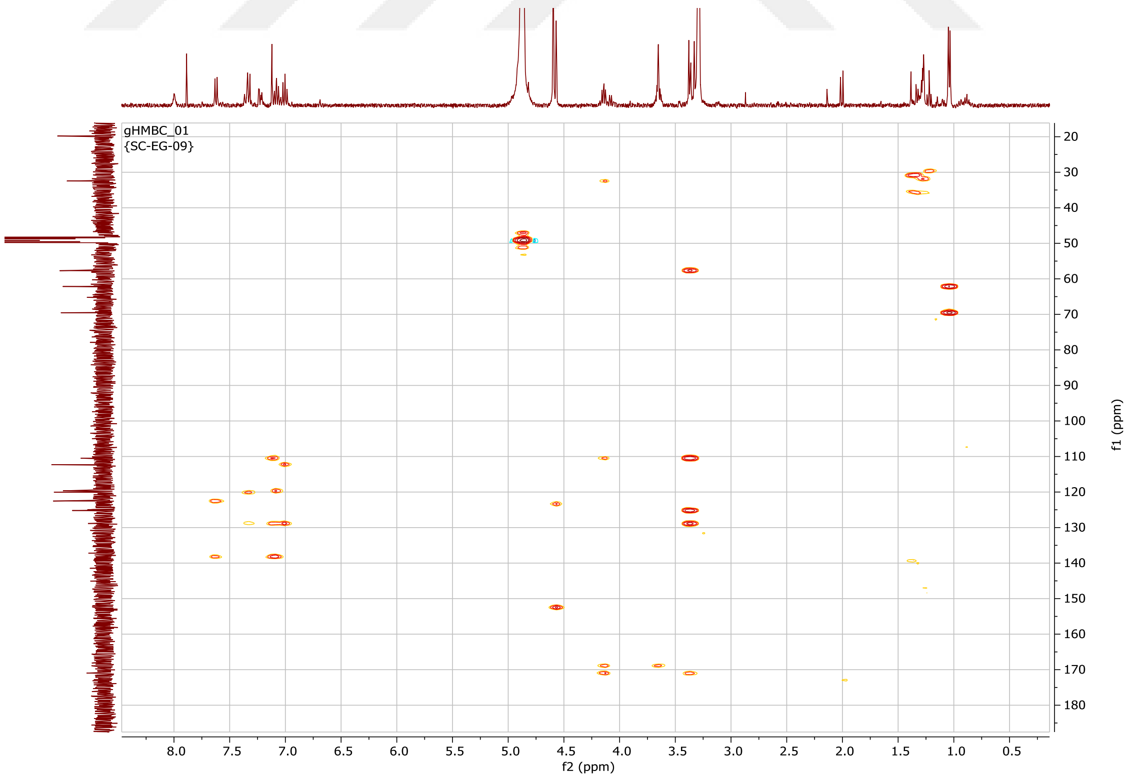

Spectrum 3.55. HMBC spectrum of **SC-EG-09** (in CD_3OD, ^{1}H: 400 MHz, ^{13}C:100 MHz)

Spectrum 3.56. COSY spectrum of **SC-EG-09** (in CD_3OD, ^1H: 400 MHz, ^{13}C:100 MHz)

3.6.2.2. Structure Elucidation of SC-EG-10

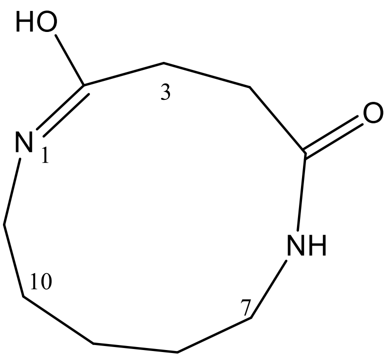

Chemical Formula: $C_9H_{16}N_2O_2$
Exact Mass: 184,12118

Figure 3.41. Chemical Structure of **SC-EG-10.**

In the HR-APCI-MS spectrum of **SC-EG-10**, a major ion peak was observed at *m/z* 185.12835 $[M+H]^+$ (calculated: 185.12900) indicative of a molecular formula of $C_9H_{16}N_2O_2$. The presence of two nitrogen atoms and unsaturation number of three suggested another dipeptide structure different from **SC-EG-09** with no aromaticity.

The 1D NMR spectra of **SC-EG-10** interestingly revealed the presence of seven methylenes and two low field carbons (δ_C 171.5 and 172.1) suggesting two carbonyls. The latter functionality accounted for two out of three unsaturation numbers indicating that **SC-EG-10** possessed a monocyclic skeleton. Inspection of the COSY spectrum revealed two spin systems: SS1) H_2-3 to H_2-4; SS2) N(H)-6 to H_2-11. The chemical shifts of the SS1 (H_2-3: δ 2.25, t; H_2-4: δ 2.56, t) and their corresponding carbons deduced from the HSQC spectrum suggested that the spin system was located between the proposed carbonyl carbons. On the other hand, terminal carbons of the SS2 viz. CH_2-7 (δ_C 38.4, δ_H 2.98) and CH_2-11 (δ_C 46.9, δ_H 3.44) were in the lower field implying their direct attachment to nitrogen atoms. This data was also suggesting that the carbonyl carbons were part of two amide functionalities forming the bridge between two spin systems and monocyclic skeleton. In this case, the finalized structure of **SC-EG-10** was pointing a symmetrical framework. However, the observed NMR data was inconsistent with such structural motif (*see* spectra 3.57-3.62 and Table 3.33). When two key observations were considered in the COSY spectrum together with the unsymmetrical nature of **SC-EG-10** [i) one of the exchangeable protons resonated at δ_H 9.57 was not part of a spin system; ii) the other exchangeable proton at δ_H 7.70 (N$\underline{H}$-6) was correlating with H_2-7 (δ 2.98, q)], an iminol functionality that is a tautomeric form of amide was proposed. Additionally, the main cross peaks observed in the HMBC spectrum from C-5 and C-7 to NH-6, C-2 and C-5 to H_2-3 and H_2-4 (δ 2.56, t) verified the linkages.

Based on this evidence, the structure of **SC-EG-10** was established as 5-hydroxy-1,6-diazacycloundec-5-en-2-one.

SC-EG-10 was probably a cyclic dipeptide deriving from deamination and decarboxylation of two aminoacids, respectively aspartic acid and lysine. A tentative pathway was proposed for the formation of **SC-EG-10** precursor (Figure 3.42). This new iminol derivative is unusual for nature, though some macrocyclic dipeptides are found in marine derived *Streptomyces*.[106]

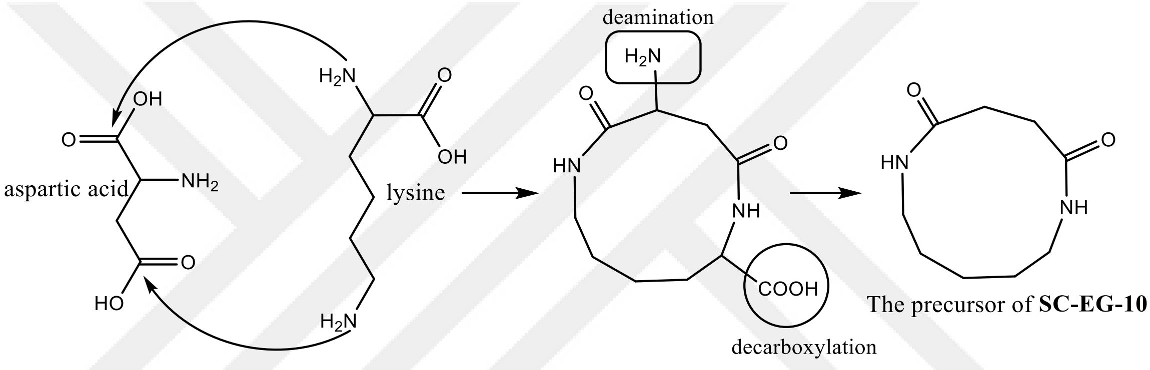

Figure 3.42. A tentative pathway for the biosynthesis of **SC-EG-10**

Table 3.33. ^{1}H and ^{13}C NMR spectroscopic data of **SC-EG-10** $^{a)}$(in $CDCl_3$, ^{1}H: 400 MHz, ^{13}C:100 MHz)

H/C	δ_C (ppm)	δ_H (ppm), J (Hz)
1(N<u>H</u>)	-	
2	172.1	9.57 s
3	30.0*	2.25 t (7) ‘
4	27.5*	2.56 t (7.3) ‘
5	171.5	-
6(N<u>H</u>)	-	7.70
7	38.4	2.98 q (6.3)
8	28.6	1.35 p (6.9)
9	23.2	1.18 m
10	25.8	1.48 p (7.3)
11	46.9	3.44 t (6.7)

a) Assignments are confirmed by COSY, HSQC, and HMBC experiments.
*,’ exchangeable

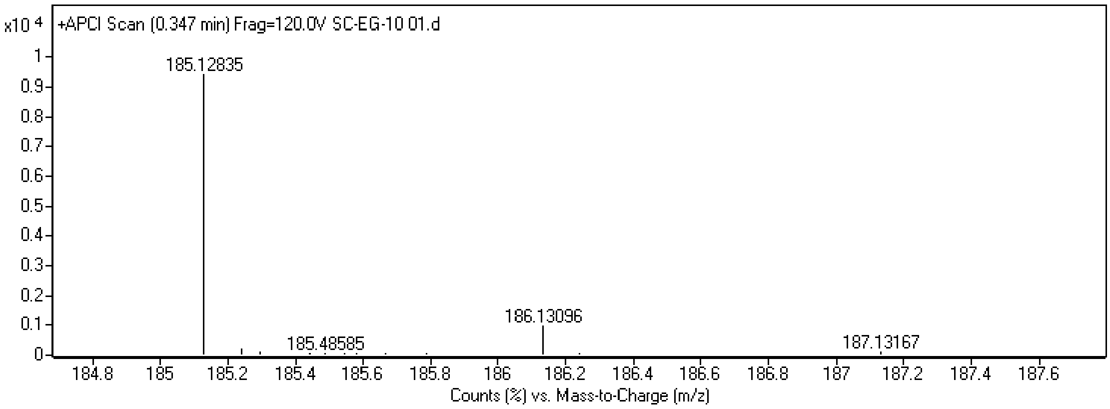

Spectrum 3.57. HR-APCI-MS spectrum of **SC-EG-10** (positive mode, $[M^+]^+$)

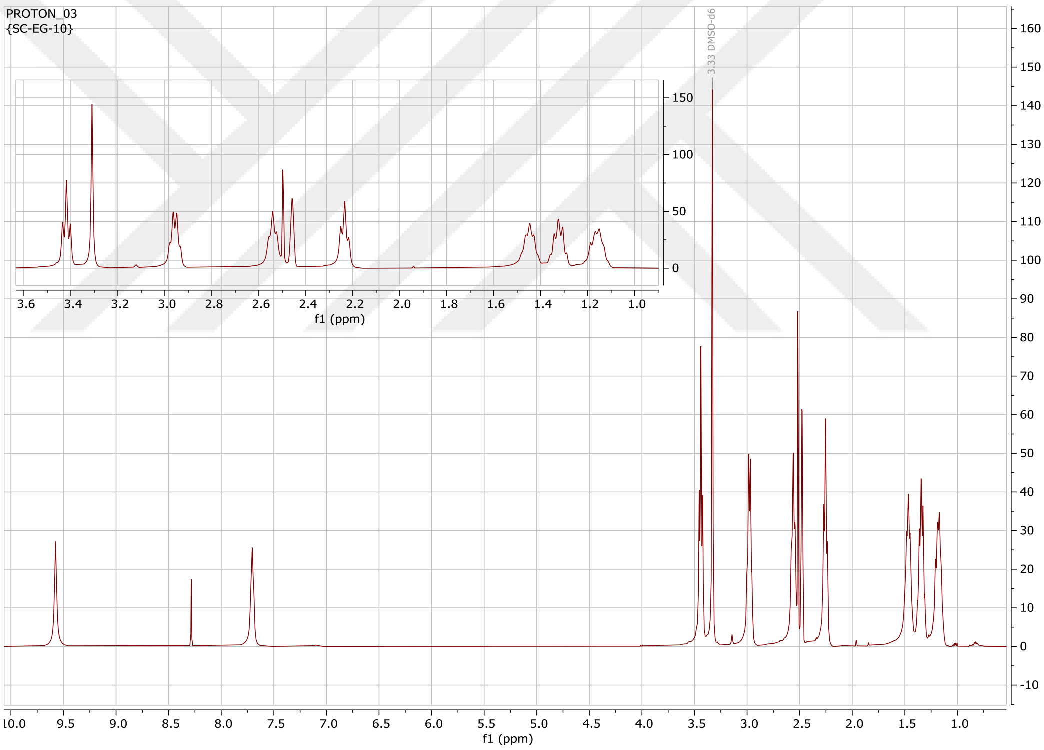

Spectrum 3.58. H^1 NMR spectrum of **SC-EG-10** (in DMSO, ^{1}H: 400 MHz, ^{13}C:100 MHz)

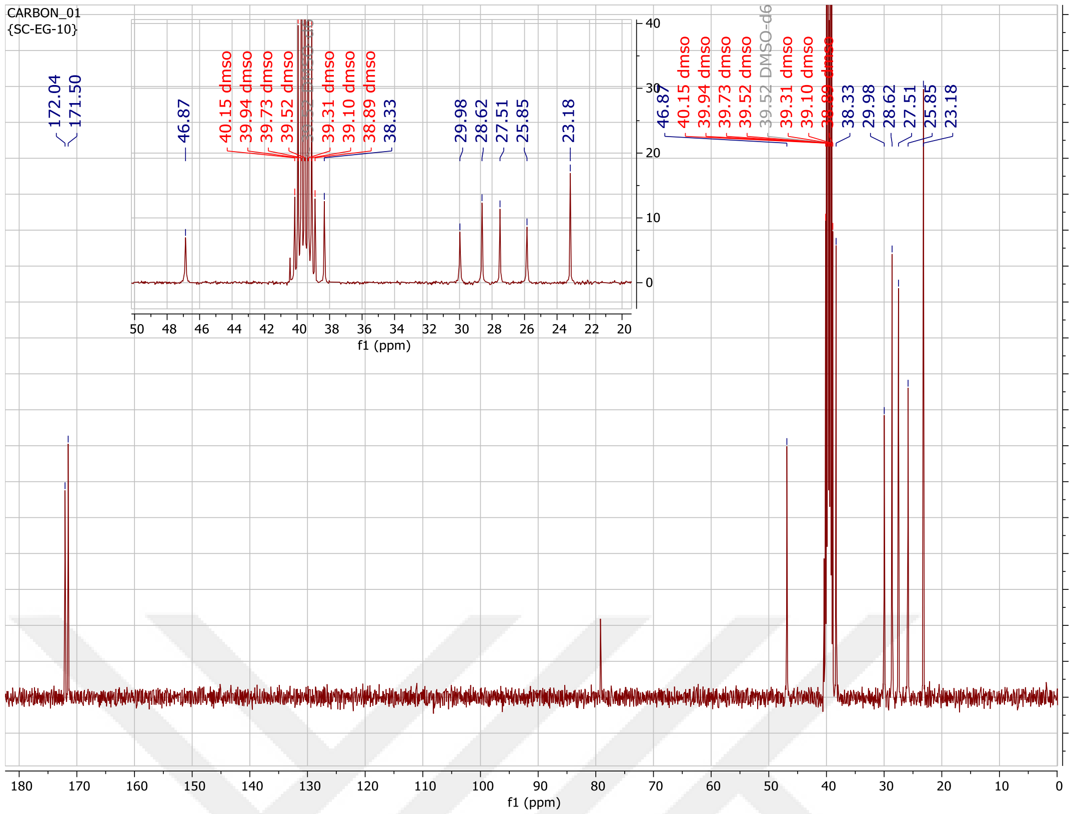

Spectrum 3.59. C^{13} NMR spectrum of **SC-EG-10** (in DMSO, ^{1}H: 400 MHz, ^{13}C:100 MHz)

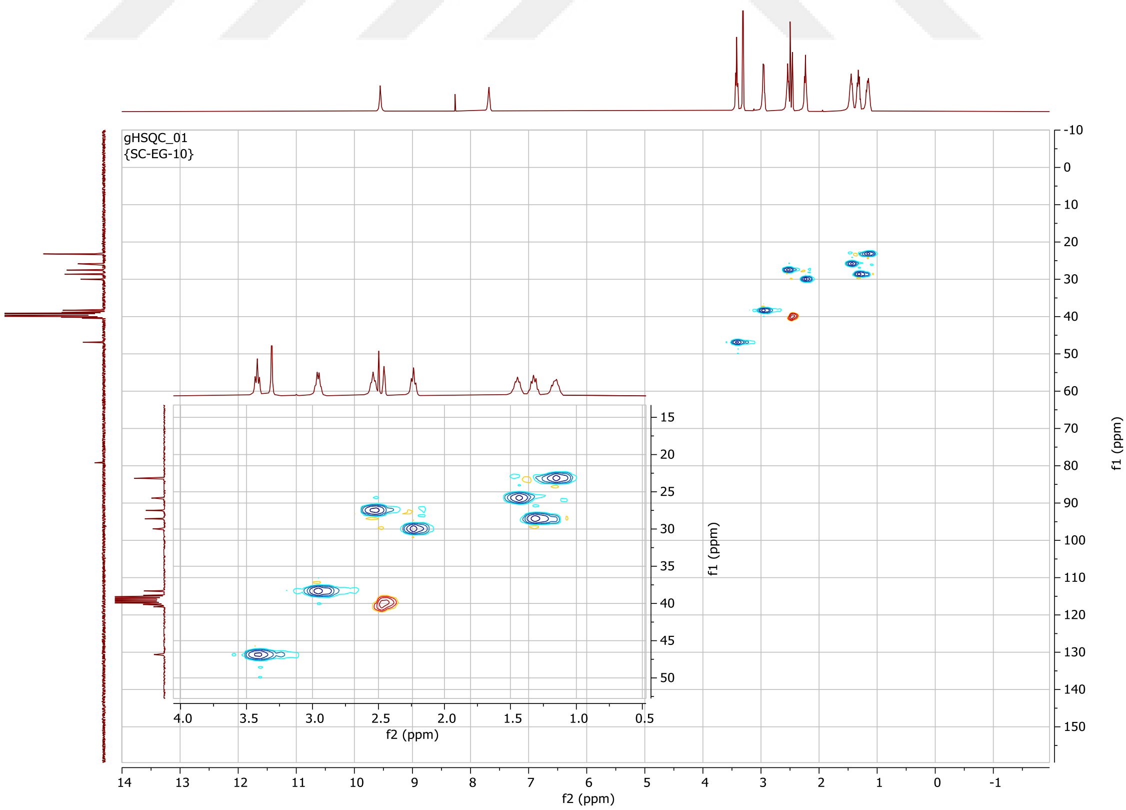

Spectrum 3.60. HSQC spectrum of **SC-EG-10** (in DMSO, ^{1}H: 400 MHz, ^{13}C:100 MHz)

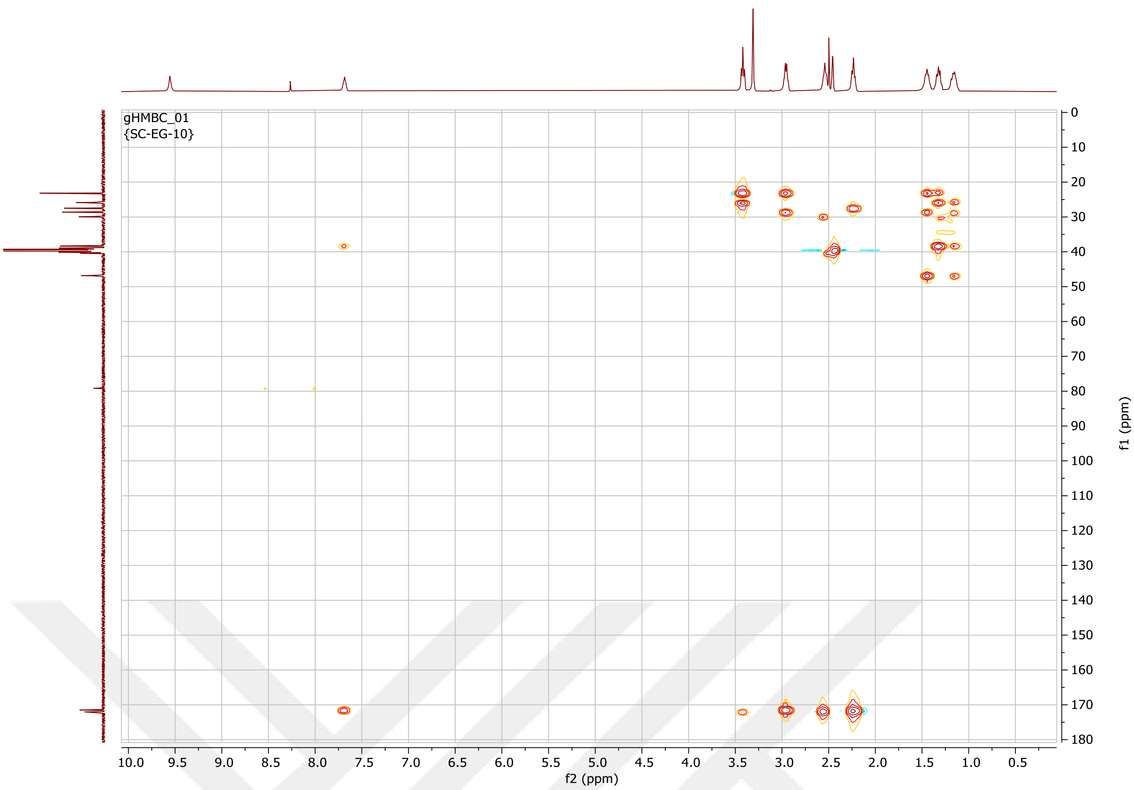

Spectrum 3.61. HMBC spectrum of **SC-EG-10** (in DMSO, ^{1}H: 400 MHz, ^{13}C:100 MHz)

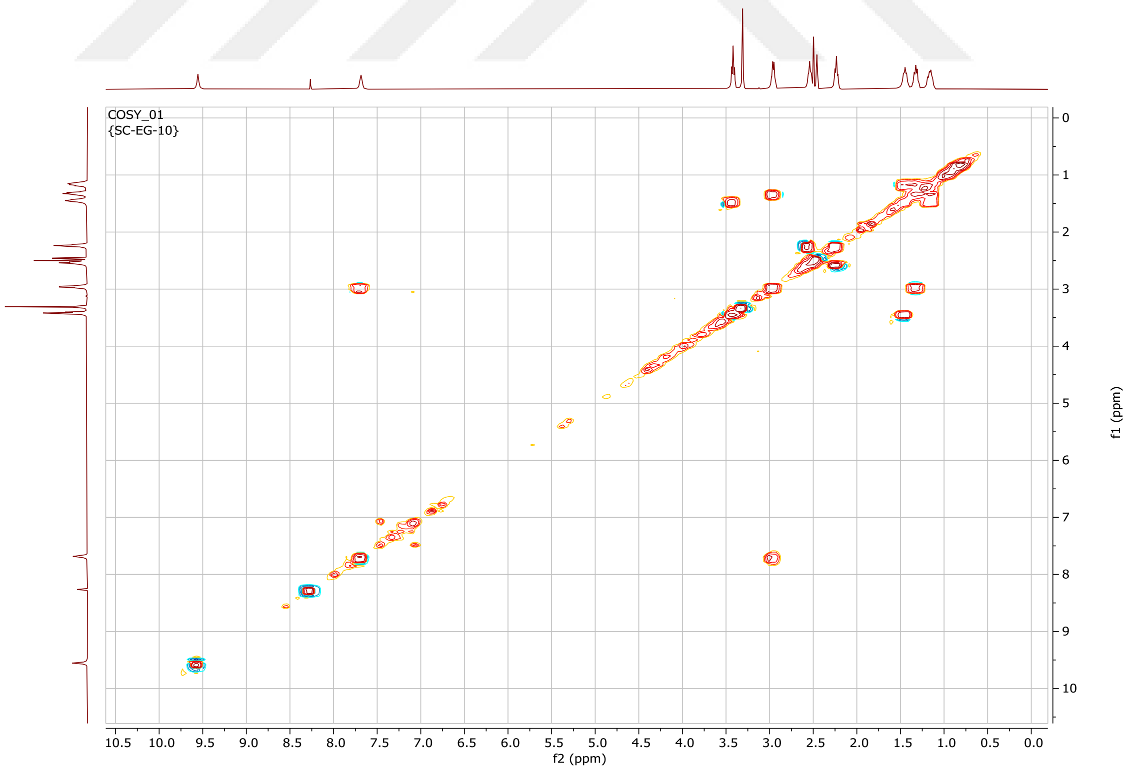

Spectrum 3.62. COSY spectrum of **SC-EG-10** (in DMSO, ^{1}H: 400 MHz, ^{13}C:100 MHz)

3.6.2.3. Structure Elucidation of SC-EG-17

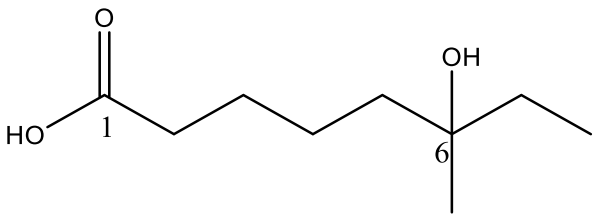

Chemical Formula: $C_9H_{18}O_3$
Exact Mass: 174.12559

Figure 3.43. Chemical Structure of **SC-EG-17.**

The HR-ESI-MS analysis of **SC-EG-17** showed a major peak at *m/z* 173.11900 $[M\text{-}H]^-$ (calculated: 173.11777) suggesting the molecular formula as $C_9H_{18}O_3$.

A detailed examination of the ^1H, ^{13}C and HSQC spectra revealed five methylenes, two methyls and two quaternary carbons. Only two down-field carbon resonances at δ_C 177.8 and 73.4 displaying no cross peak with any proton in the HSQC spectrum, and unsaturation number of one derived from the molecular formula were evident for the presence of a carboxylic acid and a tertiary-alcohol functionalities as well as acyclic nature of **SC-EG-17**. From the COSY spectrum, a terminal ethyl group was deduced (δ 0.83, t, CH_3-8; δ 1.42, q, CH_2-7). This spin system and key long-range correlations from carbon at δ_C 73.4 to the methyl protons (δ 0.83 and 1.06) in the HMBC spectrum verified that the ethyl and methyl groups were substituting from the tertiary alcohol carbon, and four methylene groups were connecting the seco-butanol moiety to the carboxyl carbon. Thus, the structure of **SC-EG-17** was elucidated as 6-hydroxy-6-methyloctanoic acid.

Octanoic acid, also known as caprylic acid, is in clinical trials for essential tremor and chronic heart failure.[107] Many hydroxylated derivatives of octanoic acids are used widely in industry.[108] 6-hydroxy-6-methyloctanoic acid is a synthetic compound, but it was reported for the first time in this thesis as a natural product.

Table 3.34.^{1}H and ^{13}C NMR spectroscopic data of **SC-EG-17,** [a)] (in CD_3OD, ^{1}H: 400 MHz, ^{13}C:100 MHz)

H/C	δC (ppm)	δH (ppm), J (Hz)
1	177.8 s	-
2	35.0 t	2.25 t (7.3)
3	26.8 t	1.55 p (7.3)
4	24.5 t	1.33[b)]
5	41.8 t	1.38 [b)]
6	73.4 s	-
6-OH	-	3.30 s
6-Me	26.2 q	1.06 s
7	34.9 t	1.42 q (7.5)
8	8.5 q	0.83 t (7.5)

a) Assignments are confirmed by COSY, HSQC, and HMBC experiments.
b) Signal pattern was unclear due to overlapping

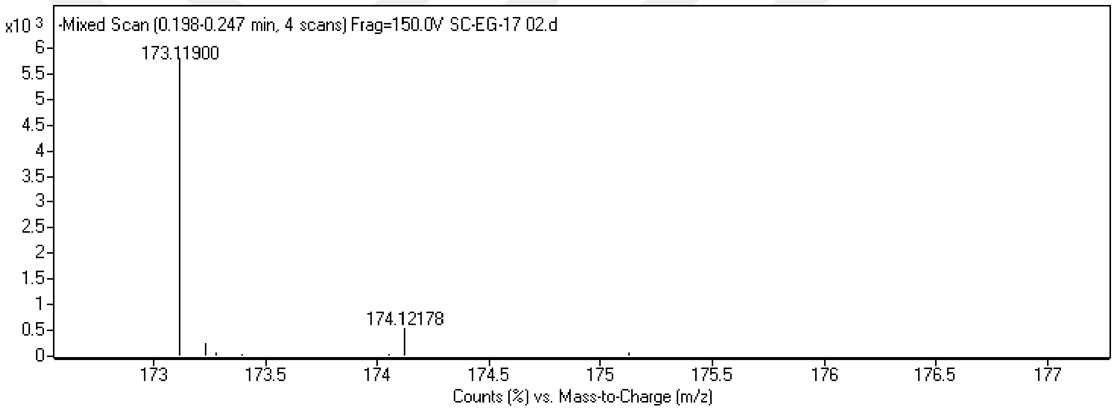

Spectrum 3.63. HR-ESI-MS spectrum of **SC-EG-17** (negative mode, $[M-H]^-$)

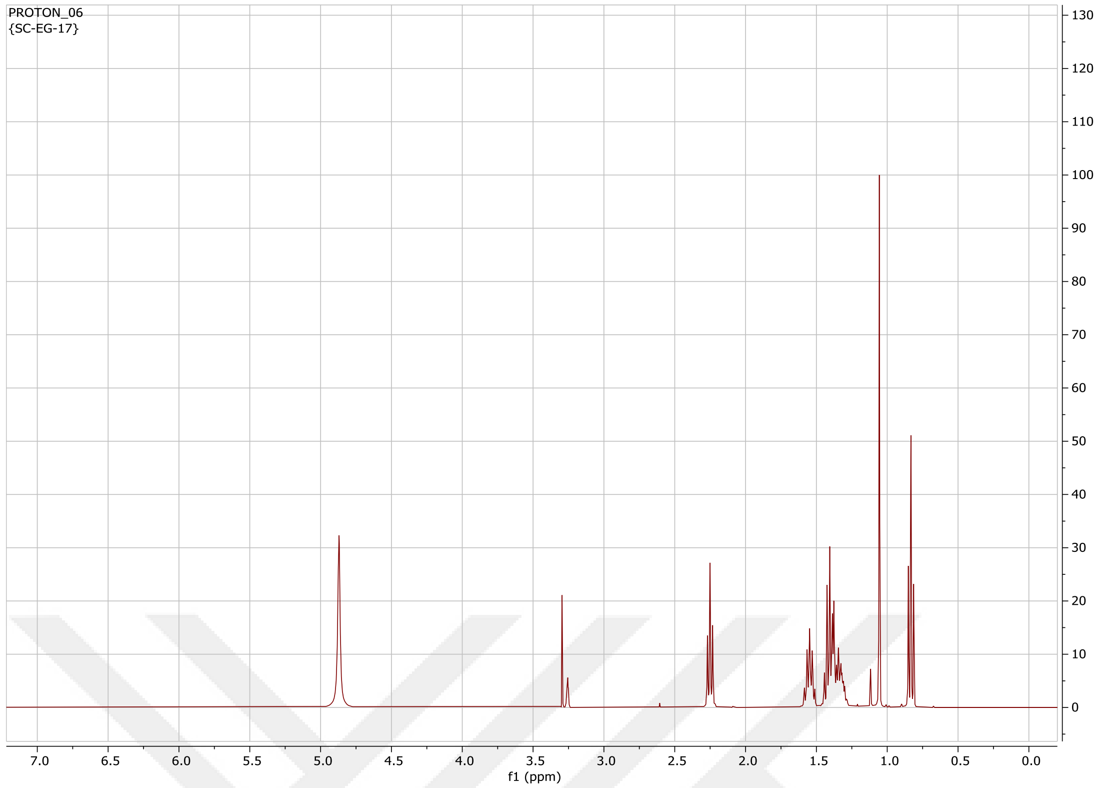

Spectrum 3.64. H^1 NMR spectrum of **SC-EG-17** (in CD_3OD, ^1H: 400 MHz, ^{13}C:100 MHz)

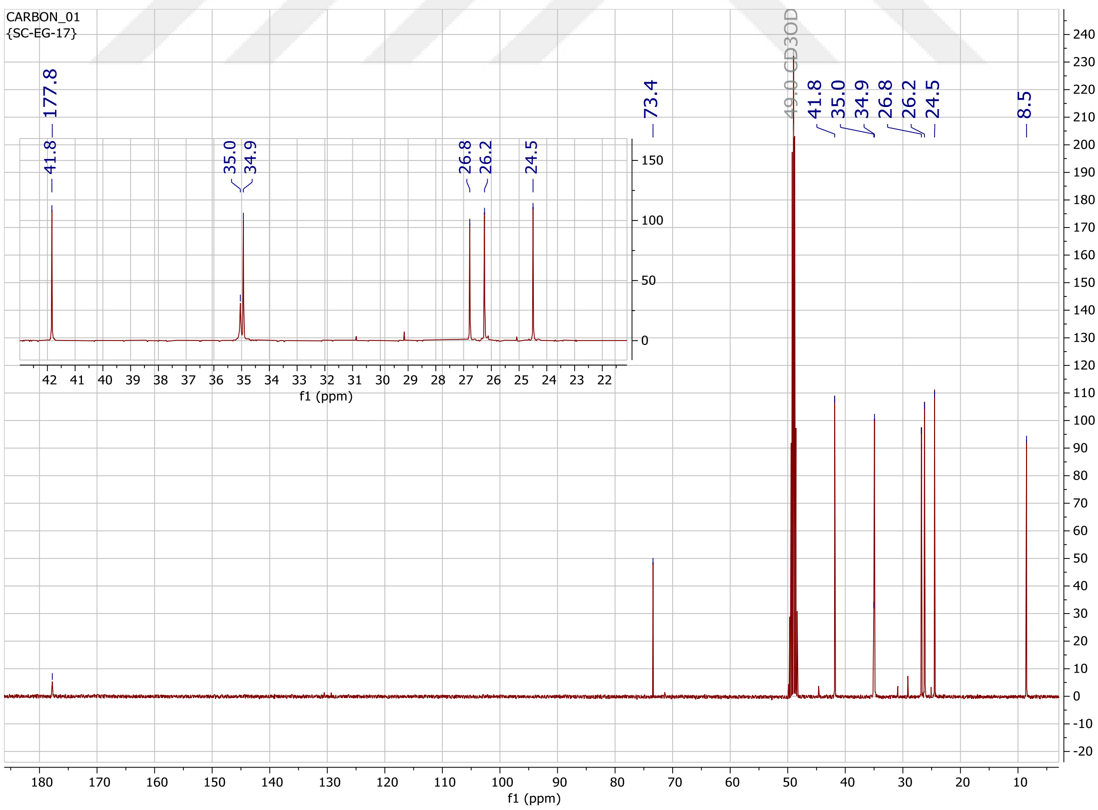

Spectrum 3.65. C^{13} NMR spectrum of **SC-EG-17** (in CD_3OD, ^1H: 400 MHz, ^{13}C:100 MHz)

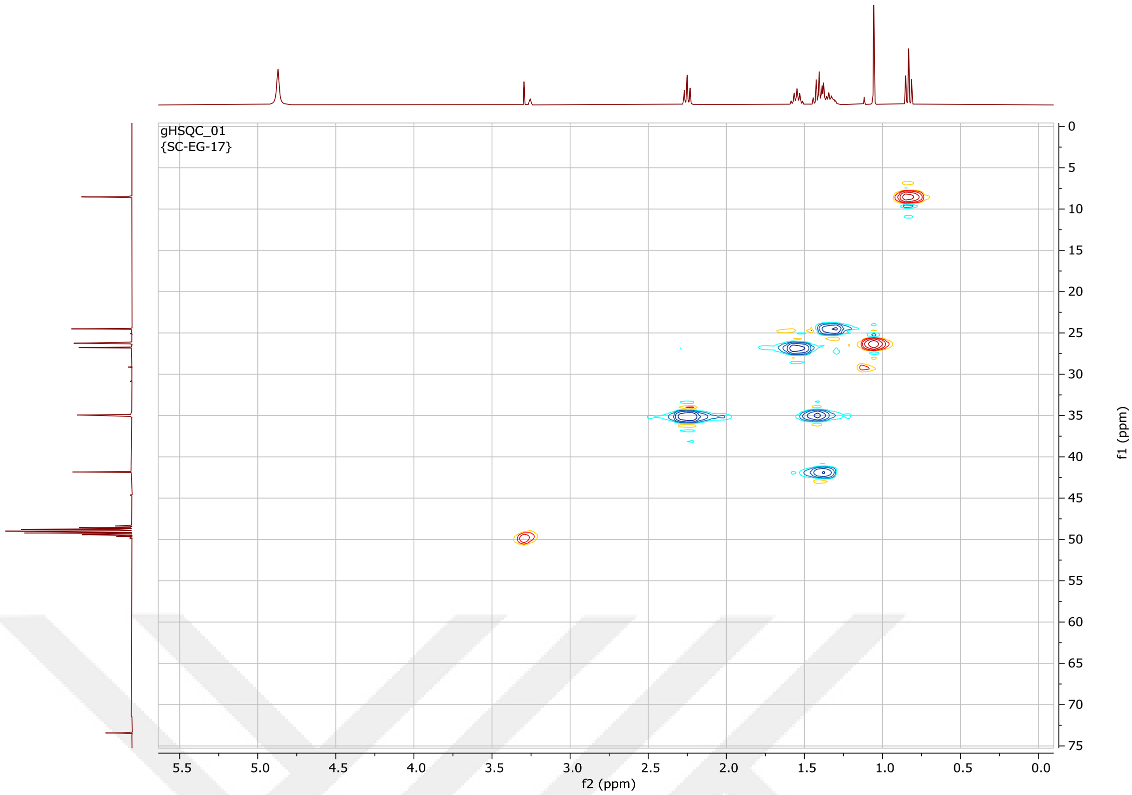

Spectrum 3.66. HSQC spectrum of **SC-EG-17** (in CD_3OD, ^1H: 400 MHz, ^{13}C:100 MHz)

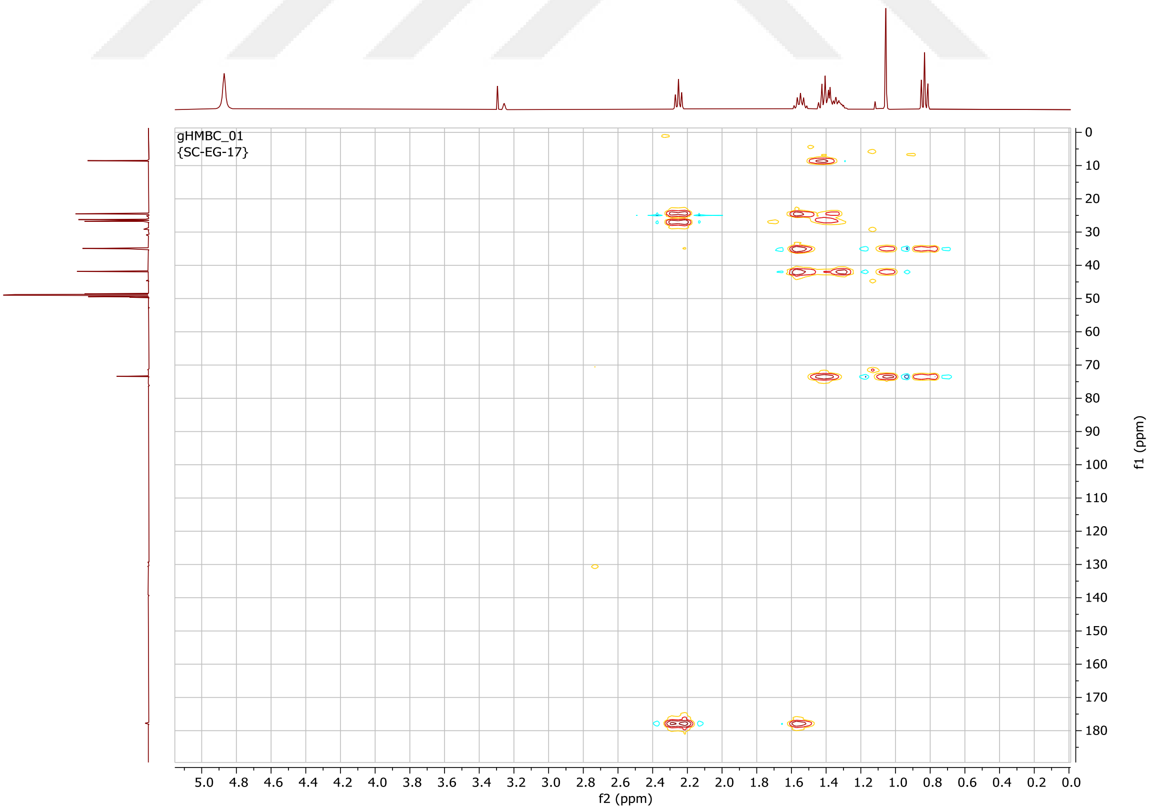

Spectrum 3.67. HMBC spectrum of **SC-EG-17** (in CD_3OD, ^1H: 400 MHz, ^{13}C:100 MHz)

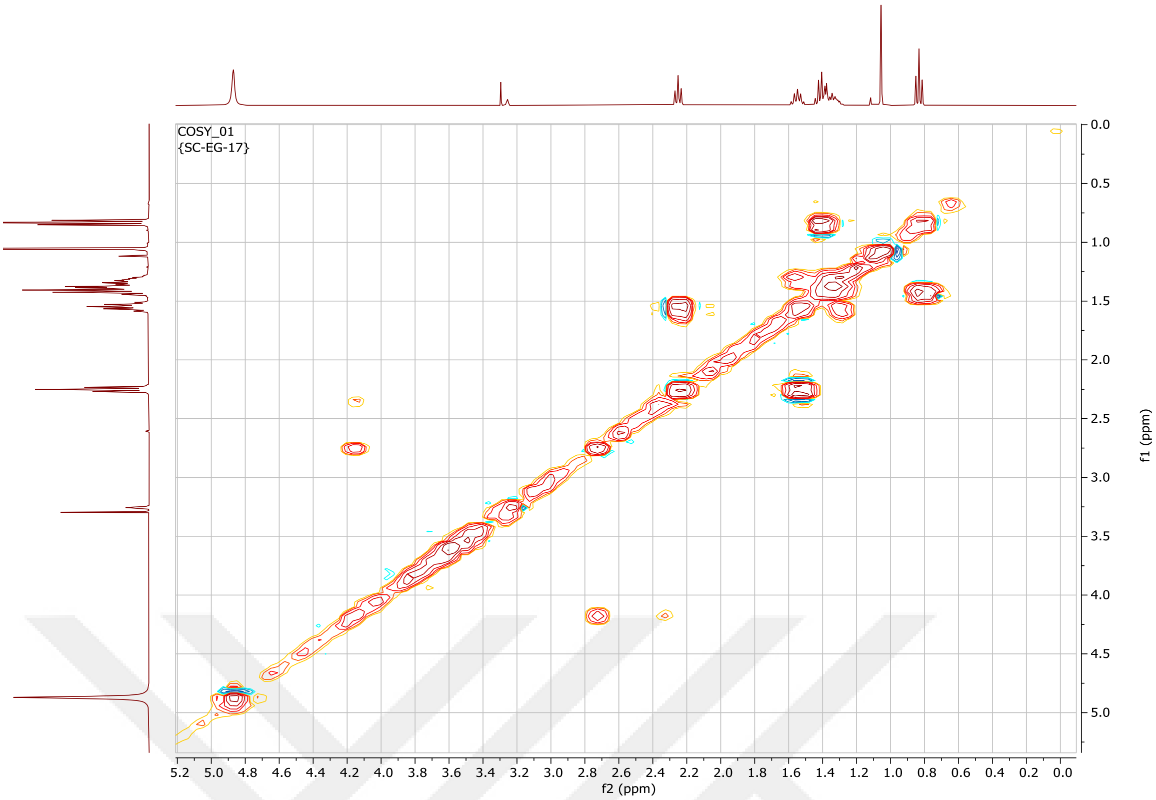

Spectrum 3.68. COSY spectrum of **SC-EG-17** (in CD_3OD, ^1H: 400 MHz, ^{13}C:100 MHz)

3.7. Bioactivity Studies

During the optimization and induction studies, it has been observed that *S. cacaoi* can produce different secondary metabolites according to incubation conditions, thus displaying different activities. The incubation conditions for production were determined such that *S. cacaoi* would produce a rich variety of secondary metabolites with high antimicrobial activity against *B. subtilis*. Therefore, it was predicted that some of the obtained molecules would have potent antimicrobial activity, especially against Gram-positive pathogenic bacteria.

3.7.1. Antimicrobial Activity Screening

Elucidated molecules were subjected to antimicrobial test against three Gram-positive (*B. subtilis*, MRSA, *L. innocua*) and one Gram-negative (*E. coli* JM 109) bacteria. The antimicrobial activities of the molecules were determined by Disc Diffusion Assay. Each molecule was loaded to the discs at an amount of 50 µg, and after 24 hours, the diameters of the inhibition zones were measured. Most of the polyether molecules showed antimicrobial activity against three Gram-positive bacteria.

In addition, with the approach called Tdtest[109], it was observed that those bacteria were susceptible to the tested molecules (50 µg), not tolerant or persistent. At the 24th hour of incubation, inhibition zones were measured and photographed. The discs were then replaced with glucose-loaded (2 mg) ones and incubated for an additional 24 hours. After 48 hours in total, no colony growth was detected inside the inhibition zones (Figure 3.44). This result indicates that the detected inhibition zones are not caused by dormancy so that the tested bacteria are killed by the molecules.[109]

Table 3.35. Result of Disc Diffusion Assay. All molecules, including positive control (vancomycin), were tested in an amount of 50 µg.

Molecules	**Diameters of Inhibition Zones (mm)**			
	B. subtilis	MRSA	*L. innocua*	*E. coli*
SC-EG-01	23	21,5	17	-
SC-EG-02	17	12	12	-
SC-EG-03	22	20,5	15	-
SC-EG-05	28	25	22	-
SC-EG-06	24	22	20	-
SC-EG-07	26	25	20	-
SC-EG-08	12	11	-	-
SC-EG-09	-	-	-	-
SC-EG-10	-	-	-	15
SC-EG-12	-	-	-	-
SC-EG-13	-	-	-	-
SC-EG-14	12	-	-	-
SC-EG-17	-	-	-	-
SC-EG-18	12	-	-	-
SC-EG-19	28	27	23	-
SC-EG-20	18	12	12	-
Vancomycin	17	23	18	-

While most of the compounds showed activity against Gram-positive bacteria, only 5-hydroxy-1,6-diazacycloundec-5-en-2-one, **SC-EG-10**, showed activity against *E. coli* (Table 3.35).

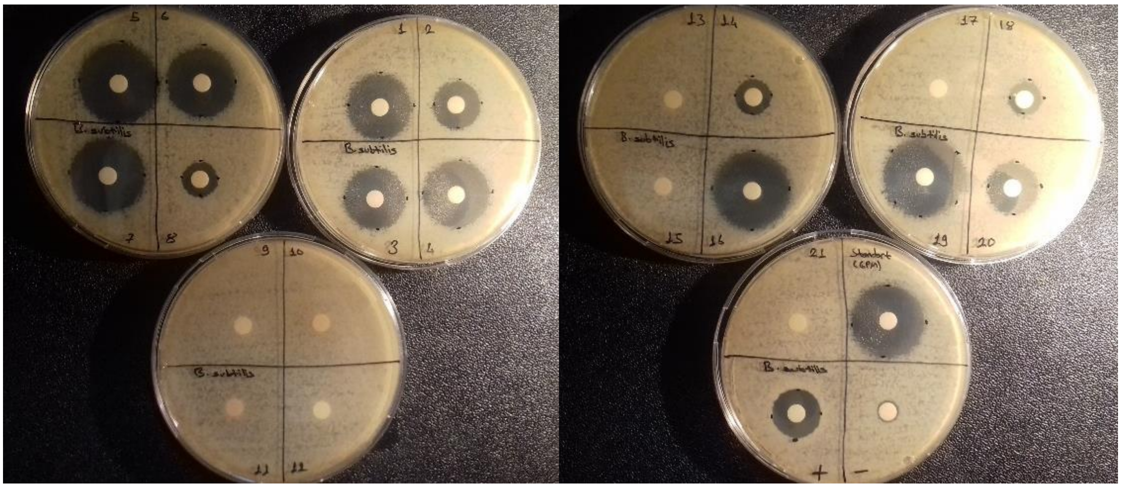

Figure 3.44. Inhibition zones at 48th hour against *B. subtilis***.**

All the bioactive molecules against Gram-positive bacteria are polyether and the diameters of the inhibition zones are in the order *B. subtilis*> MRSA> *L. innocua* for all polyethers (Table 3.35). The differences of antimicrobial activity among **SC-EG-01**, **SC-EG-02**, **SC-EG-03**, **SC-EG-08** and **SC-EG-12** molecules are fully consistent with the anti-HIV activity reported in 2020.[97]

SC-EG-19 (K41-A) and its 15-demethoxy derivative (**SC-EG-05)** exhibited the highest activity against all Gram-positive bacteria. The 27-deglycoside or 27-4-*O*-Me olivose derivatives of K41-A showed a significant decrease in activity, some of which did not even cause an inhibition zone. This observation indicates that the presence of 4-*O*-Me amicetose on the structure is crucial for antimicrobial activity. In point of the *O*-methyl groups, while a slight decrease in activity was observed for derivatives containing only one *O*-demethylation on their structure (**SC-EG-01** and **SC-EG-03**), a significant decrease in activity was detected for derivative containing two *O*-demethylation (**SC-EG-14**). This result indicates the importance of the methylation for the antimicrobial activity. Also, the decrease in activity for *O*-demethyl derivatives but not for the 15-demethoxy derivative indicates that the activity loss is due to the presence of hydroxyl groups, not absence of the *O*-methyl groups directly.

Vancomycin is a secondary metabolite first obtained from *Streptomyces orientalis*. Today, it is an FDA approved antibiotic used for infection diseases caused by MRSA.[110] When the inhibition zones against MRSA were compared, it was found that **SC-EG-05** and **SC-EG-07** molecules which were reported for the first time in this thesis showed higher anti-MRSA activity than vancomycin.

The minimum inhibitory concentrations (MIC) of the compounds were also determined by Microtitre Broth Dilution Method. Only **SC-EG-10** has a MIC value less than 32 µg/ml against *E. coli*. Polyether molecules have different MIC values ranging from 0.25 µg/ml to >64 µg/ml against Gram-positive bacteria (Table 3.36).

Table 3.36. Determined minimum inhibitory concentrations (µg/ml).

Molecules	MIC (µg/ml)	
	B. subtilis	MRSA
SC-EG-01 (C6-*O*-demethyl K41-A) 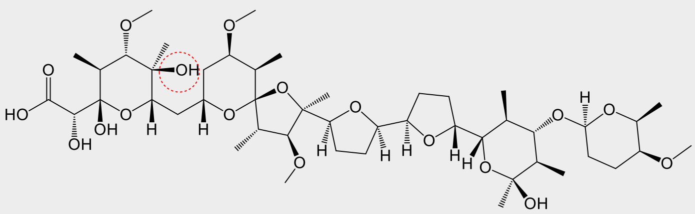	2	16
SC-EG-02 (C27-*O*-deglycosyl K41-A) 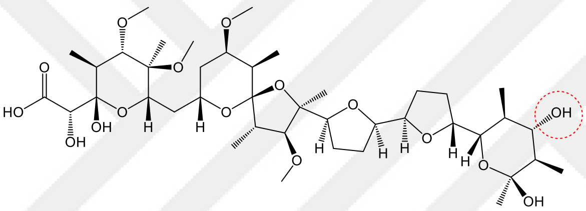	32	>64
SC-EG-03 (C5-*O*-demethyl K41-A) 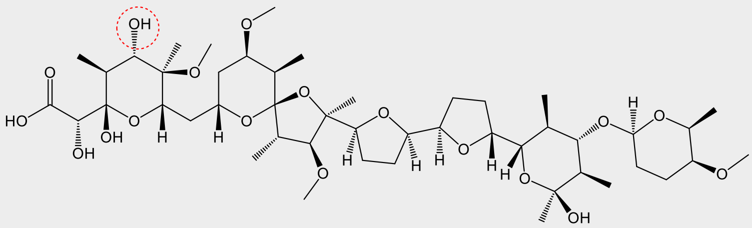	8	64
SC-EG-05 (C15-demethoxy K41-A) 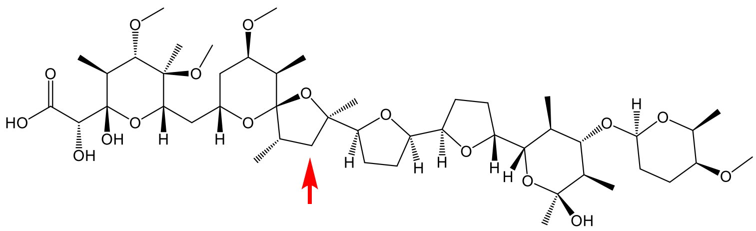	1	4
SC-EG-06 (C29-*O*-methyl K41-A) 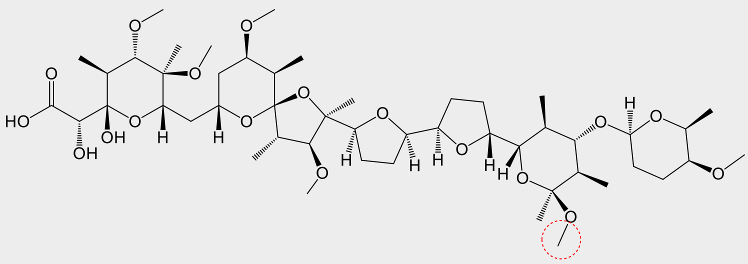	0.25	16

(cont. on next page)

cont. Table 3.36

SC-EG-07 (C6-*O*-demethyl, C15-*O*-glycosyl K41-A) 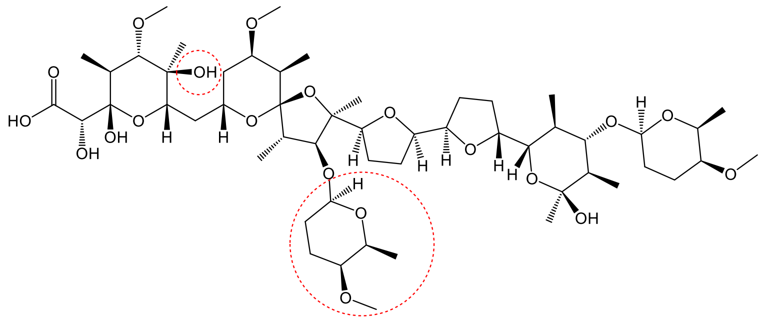	0.5	8
SC-EG-08 (C27-*O*-deglycosyl, C29-*O*-methyl K41-A) 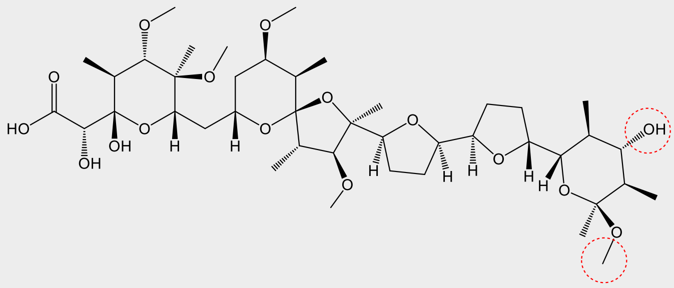	32	64
SC-EG-09 [cyclo(Thr-Trp)] 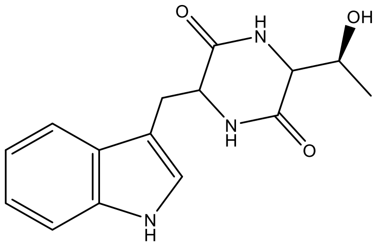	>64	>64
SC-EG-10 (5-hydroxy-1,6-diazacycloundec-5-en-2-one) 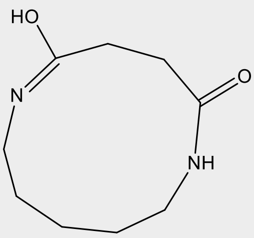	>64	>64
SC-EG-12 (C27-*O*-deglycosyl, C5-*O*-demethyl K41-A) 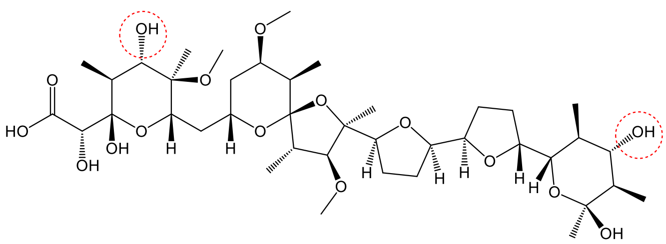	>64	>64

(cont. on next page)

cont. Table 3.36

SC-EG-13 (C5-*O*-demethyl, C27-*O*-olivose K41-A) 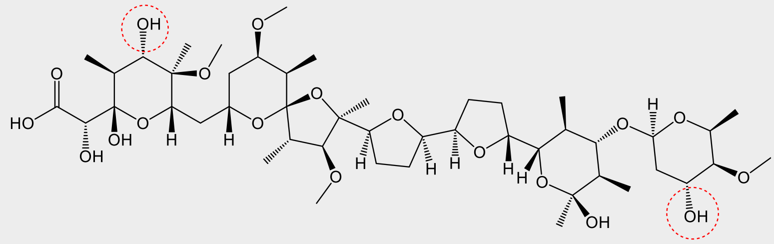	64	>64
SC-EG-14 (C5,6-di-*O*-demethyl) 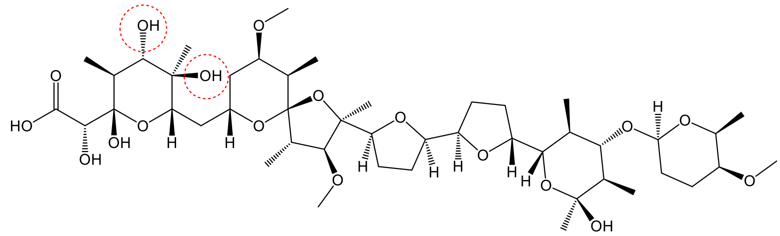	64	>64
SC-EG-17 (6-hydroxy-6-methyloctanoic acid) 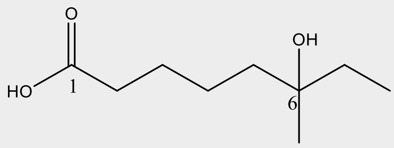	>64	>64
SC-EG-18 (Arenaric acid) 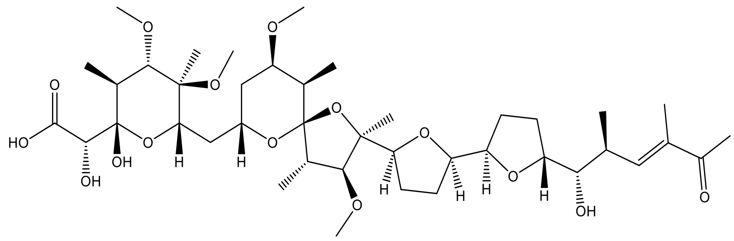	64	>64
SC-EG-19 (K41-A) 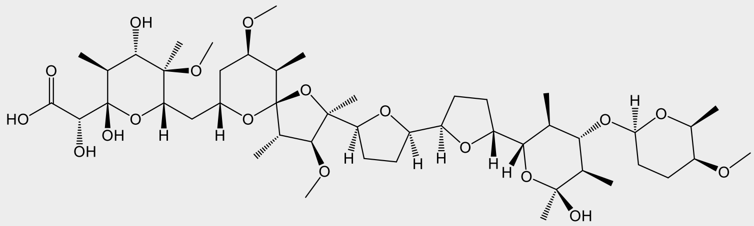	0.25	4
SC-EG-20 (C27-*O*-olivose K41-A) 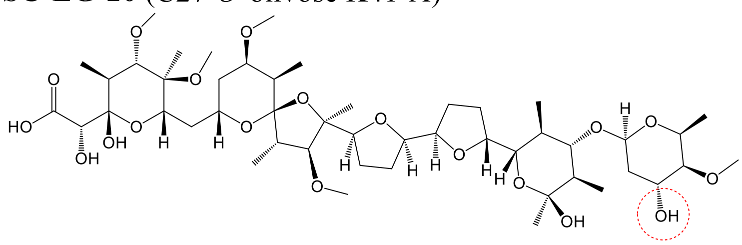	16	>64
Positive control (Vancomycin)	0.25	4

CHAPTER 4

CONCLUSION

Secondary metabolites are important sources of therapeutic agents. However, studies often result in obtaining known molecules, and due to the nature of secondary metabolism, many secondary metabolites are not produced under standard laboratory conditions. These two facts make the discovery of new/novel bioactive molecules difficult. Therefore, marine ecosystems that have quite different environmental conditions compared to terrestrial ones attract attention because they can harbor new bioactive molecule-producing organisms.

In this thesis, a marine derived actinobacterium, *Streptomyces cacaoi* was investigated in detail to determine best incubation conditions to obtain more diverse secondary metabolite profile and higher antimicrobial bioactivity. After fermentation studies in optimized conditions, 16 compounds were isolated , and their structures were determined. Nine of the isolates turned out to be new natural products. The antimicrobial activity tests revealed that 11 compounds had moderate to potent activities against Gram-positive bacteria.

Particularly, three media, which were frequently used in the fermentation of *Streptomyces* genus viz. M1, M6 (modified) and GPM, were evaluated. Based on the antimicrobial effects and chemical contents of the obtained EtOAc extracts, GPM (2% glycerol, 1% peptone water, 0.1% $CaCO_3$, 0.05% $MgCl_2$ and 0.05% $FeCl_3$) was selected for subsequent experiments. A further optimization study using Box-Behnken design with different variables was undertaken. The investigated factors (temperature, seawater ratio, and contents of GPM; glycerol, peptone water, $CaCO_3$, $MgCl_2$ and $FeCl_3$) were found to have significant effect on the chemical content, bioactivity, and amount of the EtOAc extract. Especially, it was noted that the presence of $CaCO_3$ in the medium was indispensable for higher bioactivity and yield of extract. In addition, several factors are certainly involved in multiple interactions in secondary metabolism of *S. cacaoi*. For example, while the highest bioactivity was observed at 25°C with GPM prepared in distilled water, GPM prepared in sea water showed the highest activity at 35°C. These results clearly show that microorganisms can produce different metabolites in different incubation conditions. For maximum chemical diversity and bioactivity, content of the

GPM were found to be 2.25% glycerol, 1% peptone water, 0.2% $CaCO_3$, 0.1% $MgCl_2$ in distilled water together with optimum temperature of 30 °C.

Moreover, biological and chemical induction studies were performed including co-culturing and some ionic compound supplementation. Especially, the presence of KNO_3 in the medium has prominently changed secondary metabolite production. The supplementation of KNO_3 induced biosynthesis of aromatic molecules, which were visible under 254 nm UV, and one of these compounds was found to have antimicrobial activity against *E.coli*. However, KNO_3 addition greatly suppressed the production of polyether compounds and a significant reduction in the amount of extract was observed.

A total of 25 L *S. cacaoi* fermentation experiment was carried out in optimized GPM without KNO_3. Thereafter, fractionation and purification studies were executed to obtain 16 molecules, structures of which were established by spectral methods (NMR and MS). As a result, the presence of arenaric acid, K41-A, 6 known and 5 new derivatives of K41-A, cyclo(Thr-Trp), 6-hydroxy-6-methyloctanoic acid, and 5-hydroxy-1,6-diazacycloundec-5-en-2-one were demonstrated in *S. cacaoi*.

As expected from our previous studies, polyether type polyketides were predominant compounds, especially metabolites of K41-A. To be more specific, *O*-demethyl, non-glycosidic, glycosidic (15-*O*-glycosidation) and transformed sugar moiety (alteration of 4-*O*-Me amicetose to 4-*O*-Me olivose) derivatives of K41-A were isolated. Antimicrobial activity screenings clearly showed that polyethers were major constituents in *S. cacaoi* extract for bioactivity versus Gram-positive bacteria, ranging inhibition zones from 11 mm to 28 mm for 50 µg compund. The effects of *O*-demethyl (**SC-EG-01**, **SC-EG-03**, **SC-EG-14)**, C27-*O*-deglycosides (**SC-EG-02**, **SC-EG-08**, **SC-EG-12)**, and olivose derivatives (**SC-EG-13**, **SC-EG-20)** of K41-A were lower than K41-A implying the importance of methoxy groups and amicetose moiety at C-27. Among the compounds, 15-demethoxy-K41-A (**SC-EG-05**, a new compound) exhibited the highest antimicrobial activity. It also showed higher activity than vancomycin against *B. subtilis*, MRSA and *L. innocua*.

Genetic modification studies are widely used to enhance the production of secondary metabolites. Methyl transferases genes in the SMGC of K41-A were disrupted and several *O*-demethyl derivatives of K41-A were obtained in the study of Chen *et al.* However, all *O*-demethyl derivatives showed lower anti-HIV activity than K-41A,[97] which was in accordance with our results regarding antimicrobial activity. On the other hand, the lack of oxygenation at common substitution positions may not generate activity loss as in the case of **SC-EG-05**, a demethoxy derivative of K-41A. The results suggest that a protective *O*-methyl substitution or complete removal of OH groups in the polyether framework is required for bioactivity. From biosynthetic perspective, the bioactive compound **SC-EG-05** could form via reduction of C-15 carbonyl by a ketoreductase enzyme followed by dehydration and reduction steps. Thus, based on the previous work of Chen et al.,[97] and our results it can be speculated that enhancing the expression of methyltransferase genes to mask free hydroxyl groups or complete reduction of building block carbonyl carbons may provide different bioactive demethoxy and *O*-methyl derivatives of polyethers.

In addition, due to varied bioactivities of polyethers such as antitumor, antiviral, antiparasitic, further studies are warranted to investigate actions of the obtained metabolites.

REFERENCES

1. Shewry, P.R. Biochemistry & Molecular Biology of Plants. *Plant Growth Regulation;* Buchanan, B.B., Gruissem, W., Jones R.L., Eds., 2000; Vol. 35, pp 105–106.
2. Macheleidt, J.; Mattern, D. J.; Fischer, J.; Netzker, T.; Weber, J.; Schroeckh, V.; … Brakhage, A. A. Regulation and Role of Fungal Secondary Metabolites. *Annual Review of Genetics*, **2016**, *50*(1), 371–392.
3. Bennett, J. W.; Bentley, R. What's in a Name? Microbial Secondary Metabolism. *Advances in Applied Microbiology,* **1989,** 1–28.
4. Katz, L.; Baltz, R. H. Natural product discovery: past, present, and future. *Journal of Industrial Microbiology & Biotechnology*, **2016**, *43*(2-3), 155–176.
5. Partida-Martinez, L. P.; Hertweck, C. Pathogenic fungus harbors endosymbiotic bacteria for toxin production. *Nature*, **2005,** *437*(7060), 884–888.
6. Demain, A. L.; Fang, A. The Natural Functions of Secondary Metabolites. *Advances in Biochemical Engineering/Biotechnology*, **2000,** 1–39.
7. O'Brien, J.; Wright, G. D. An ecological perspective of microbial secondary metabolism. *Current Opinion in Biotechnology,* **2011,** *22*(4), 552–558.
8. Siezen, R. J. Microbial sunscreens. *Microbial Biotechnology*, **2011**, *4*(1), 1–7.
9. Seca, A. M. L.; Pinto, D. C. G. A. Biological Potential and Medical Use of Secondary Metabolites. *Medicines,* **2019,** *6*(2), 66.
10. Yarzábal, L. A.; Chica, E. J. Role of Rhizobacterial Secondary Metabolites in Crop Protection Against Agricultural Pests and Diseases. *New and Future Developments in Microbial Biotechnology and Bioengineering*, **2019**, 31–53.
11. Sanchez, S.; Demain, A. L. Secondary Metabolites. *Comprehensive Biotechnology,* **2011,** 155–167.
12. Katz, L.; Baltz, R. H. Natural product discovery: past, present, and future. *Journal of Industrial Microbiology & Biotechnology,* **2016**, *43*(2-3), 155-176.
13. Newman, D. J.; Cragg, G.M. Natural Products as Sources of New Drugs over the Nearly Four Decades from 01/1981 to 09/2019. *Journal of Natural Products,* **2020**, *83*(3), 770-803.
14. Grienke, U.; Mihály-Bison, J.; Schuster, D.; Afonyushkin, T.; Binder, M.; Guan, S.; … Rollinger, J. M. Pharmacophore-based discovery of FXR-agonists. Part II:

Identification of bioactive triterpenes from Ganoderma lucidum. *Bioorganic & Medicinal Chemistry,* **2011**, *19*(22), 6779–6791.

15. Sparks, T. C.; Hahn, D. R.; Garizi, N. V. Natural products, their derivatives, mimics and synthetic equivalents: role in agrochemical discovery. *Pest Management Science,* **2016,** *73*(4), 700–715.
16. Laraia, L.; Waldmann, H. Natural product inspired compound collections: evolutionary principle, chemical synthesis, phenotypic screening, and target identification. *Drug Discovery Today: Technologies,* **2017,** *23,* 75–82.
17. Mishra, B. B.; Tiwari, V. K. Natural products: An evolving role in future drug discovery. *European Journal of Medicinal Chemistry,* **2011**, *46*(10), 4769–4807.
18. Marra, A. Antibacterial resistance: is there a way out of the woods? *Future Microbiology,* **2011,** *6*(7), 707–709.
19. Ali, R.; Mirza, Z.; Ashraf, G. M.; Kamal, M. A.; Ansari, S. A.; Damanhouri, G. A.; Abuzenadah, A. M.; Chaudhary, A. G.; Sheikh, I. A. New anticancer agents: recent developments in tumor therapy. *Anticancer research,* **2012**, *32*(7), 2999–3005.
20. Zhu, N.; Zhang, D.; Wang, W.; Li, X.; Yang, B.; Song, J.; Zhao, X.; Huang, B.; Shi, W.; Lu, R.; Niu, P.; Zhan, F.; Ma, X.; Wang, D.; Xu, W.; Wu, G.; Gao, G. F.; Tan, W.; China Novel Coronavirus Investigating and Research Team. A Novel Coronavirus from Patients with Pneumonia in China, 2019. *The New England journal of medicine*, **2020,** *382*(8), 727–733.
21. Puttaswamygowda, G. H.; Olakkaran, S.; Antony, A.; Kizhakke Purayil, A. Present Status and Future Perspectives of Marine Actinobacterial Metabolites. *Recent Developments in Applied Microbiology and Biochemistry,* **2019,** 307–319.
22. Bentley, S. D.; Chater, K. F.; Cerdeño-Tárraga, A. M.; Challis, G. L.; Thomson, N. R.; James, K. D.; … Hopwood, D. A. Complete genome sequence of the model actinomycete *Streptomyces coelicolor* A3(2). *Nature,* **2002,** *417*(6885), 141-147.
23. Ul-Hassan, A.; Wellington, E. M. *Actinobacteria*. *Encyclopedia of Microbiology,* **2009**, 25–44.
24. Çetinel Aksoy, S. Cultural and Molecular Characterization of Bioactive Metabolite Producing Actinomycetes From Marine Sediment Samples And Purification Of Bioactive Metabolites. Ph.D. Thesis, Ege University, 2014.
25. Barka, E. A.; Vatsa, P.; Sanchez, L.; Gaveau-Vaillant, N.; Jacquard, C.; Klenk, H. P.; Clément, C.; Ouhdouch, Y.; van Wezel, G. P. Taxonomy, Physiology, and

Natural Products of Actinobacteria. *Microbiology and Molecular Biology Reviews,* **2015,** *80*(1), 1–43.

26. Manteca, Á.; Yagüe, P. *Streptomyces* Differentiation in Liquid Cultures as a Trigger of Secondary Metabolism. *Antibiotics,* **2018,** *7*(2), 41.
27. Manteca, A.; Alvarez, R.; Salazar, N.; Yague, P.; Sanchez, J. Mycelium Differentiation and Antibiotic Production in Submerged Cultures of *Streptomyces coelicolor. Applied and Environmental Microbiology,* **2008,** *74*(12), 3877–3886.
28. Ahmed, S.; Craney, A.; Pimentel-Elardo, S. M.; Nodwell, J. R. A Synthetic, Species-Specific Activator of Secondary Metabolism and Sporulation in *Streptomyces coelicolor. ChemBioChem,* **2012**, *14*(1), 83–91.
29. Ou, X.; Zhang, B.; Zhang, L.; Dong, K.; Liu, C.; Zhao, G.; Ding, X. SarA influences the sporulation and secondary metabolism in *Streptomyces coelicolor* M145. *Acta Biochimica et Biophysica Sinica,* **2008,** *40*(10), 877–882.
30. Van der Meij, A.; Worsley, S. F.; Hutchings, M. I.; van Wezel, G. P. Chemical ecology of antibiotic production by actinomycetes. *FEMS Microbiology Reviews,* **2017,** *41*(3), 392–416.
31. Čihák, M.; Kameník, Z.; Šmídová, K.; Bergman, N.; Benada, O.; Kofroňová, O.; … Bobek, J. Secondary Metabolites Produced during the Germination of *Streptomyces coelicolor. Frontiers in Microbiology,* **2017,** *8.*
32. Bérdy, J. Erratum: Thoughts and facts about antibiotics: Where we are now and where we are heading. *The Journal of Antibiotics,* **2012,** *65*(8), 441–441.
33. Solecka, J.; Zajko, J.; Postek, M.; Rajnisz, A. Biologically active secondary metabolites from *Actinomycetes*. *Open Life Sciences,* **2012,** *7*(3).
34. Labeda, D. P.; Goodfellow, M.; Brown, R.; Ward, A. C.; Lanoot, B.; Vanncanneyt, M.; … Hatano, K. Phylogenetic study of the species within the family Streptomycetaceae. *Antonie van Leeuwenhoek,* **2011,** *101*(1), 73–104.
35. Lam, K. S. Discovery of novel metabolites from marine *Actinomycetes. Current Opinion in Microbiology,* **2006,** *9*(3), 245–251.
36. Ser, H. L.; Tan, L. T. H.; Law, J. W.; Chan, K. G.; Duangjai, A.; Saokaew, S.; … Lee, L. Focused Review: Cytotoxic and Antioxidant Potentials of Mangrove-Derived *Streptomyces. Frontiers in Microbiology,* **2017,** *8.*
37. De Lima Procópio, R. E.; da Silva, I. R.; Martins, M. K.; de Azevedo, J. L.; de Araújo, J. M. Antibiotics produced by *Streptomyces. The Brazilian Journal of Infectious Diseases,* **2012,** *16*(5), 466–471.

38. Patridge, E.; Gareiss, P.; Kinch, M. S.; Hoyer, D. An analysis of FDA-approved drugs: natural products and their derivatives. *Drug Discovery Today,* **2016,** *21*(2), 204–207.
39. Woodworth, J. R.; Nyhart, E. H.; Brier, G. L.; Wolny, J. D.; Black, H. R. Single-dose pharmacokinetics and antibacterial activity of daptomycin, a new lipopeptide antibiotic, in healthy volunteers. *Antimicrobial Agents and Chemotherapy,* **1992,** *36*(2), 318–325.
40. Chabala, J. C.; Mrozik, H.; Tolman, R. L.; Eskola, P.; Lusi, A.; Peterson, L. H.; … Campbell, W. C. Ivermectin, a new broad-spectrum antiparasitic agent. *Journal of Medicinal Chemistry,* **1980,** *23*(10), 1134–1136.
41. Schaffer, L.; Finkelstein, J.; Hohn, A.; Djerassi, I. Lincomycin-a New Antibiotic. *Clinical Pediatrics,* **1963,** *2*(11), 642–645.
42. Schildknecht, E. G.; Siegel, D.; Richle, R. W. Antiparasitic Activity of Natural and Semisynthetic Monensin Urethanes. *Chemotherapy,* **1983,** *29*(2), 145–152.
43. Barkvoll, P.; Attramadal, A. Effect of nystatin and chlorhexidine digluconate on Candida albicans. *Oral Surgery, Oral Medicine, Oral Pathology,* **1989,** *67*(3), 279–281.
44. Grassberger, M.; Baumruker, T.; Enz, A.; Hiestand, P.; Hultsch, T.; Kalthoff, F.; … Zenke, G. A novel anti-inflammatory drug, SDZ ASM 981, for the treatment of skin diseases: in vitro pharmacology. *British Journal of Dermatology,* **1999,** *141*(2), 264–273.
45. Yourassowsky, E.; Vander Linden M. P. Antibacterial activity of ribostamycin on Enterobacteriaceae. *Arzneimittelforschung,* **1976,** *26*(2), 184-5.
46. Vézına, C.; Kudelskı, A.; Sehgal, S. N. Rapamycin (AY-22,989), a new antifungal antibiotic. I. Taxonomy of the producing streptomycete and isolation of the active principle. *The Journal of Antibiotics,* **1975,** *28*(10), 721–726.
47. Calne, R. Y.; Lim, S.; Samaan, A.; Collier, D. S. J.; Pollard, S. G.; White, D. J. G.; Thiru, S. Rapamycın For Immunosuppressıon In Organ Allograftıng. *The Lancet,* **1989,** *334*(8656), 227.
48. Zhang, Y.; Wang, H.; Li, F.; Xu, X.; Chen, B.; Zhang, T. Inhibitory effects of Dulcitol on rat C6 glioma by regulating autophagy pathway. *Natural Product Research,* **2018,** *1–5.*
49. Ahmad, Z.; Pinn, M. L.; Nuermberger, E. L.; Peloquin, C. A.; Grosset, J. H.; Karakousis, P. C. The potent bactericidal activity of streptomycin in the guinea pig

model of tuberculosis ceases due to the presence of persisters. *Journal of Antimicrobial Chemotherapy,* **2010,** *65*(10), 2172–2175.

50. Moertel, C. G.; Lefkopoulo, M.; Lipsitz, S.; Hahn, R. G.; Klaassen, D. Streptozocin–Doxorubicin, Streptozocin–Fluorouracil, or Chlorozotocin in the Treatment of Advanced Islet-Cell Carcinoma. *New England Journal of Medicine,* **1992,** *326*(8), 519–523.
51. Tan, C.; Tasaka, H.; Yu, K. P.; Murphy, M. L.; Karnofsky, D. A. Daunomycin, an antitumor antibiotic, in the treatment of neoplastic disease. Clinical evaluation with special reference to childhood leukemia. *Cancer,* **1967,** *20*(3), 333–353.
52. Kasper, M.; Barth, K. Bleomycin and its Role in Inducing Apoptosis and Senescence in Lung Cells- Modulating Effects of Caveolin-1. *Current Cancer Drug Targets,* **2009,** *9*(3), 341–353.
53. Haefner, B. Drugs from the deep: marine natural products as drug candidates. *Drug Discovery Today,* **2003,** *8*(12), 536–544.
54. Carroll, A. R.; Copp, B. R.; Davis, R. A.; Keyzers, R. A.; Prinsep, M. R. Marine natural products. *Natural Product Reports.* **2020.**
55. Özcan, K.; Aksoy, S. Ç.; Kalkan, O.; Uzel, A.; Hames-Kocabas, E. E.; Bedir, E. Diversity and antibiotic-producing potential of cultivable marine-derived actinomycetes from coastal sediments of Turkey. *Journal of Soils and Sediments,* **2013,** *13*(8), 1493–1501.
56. Öner, Ö.; Ekiz, G.; Hameş, E. E.; Demir, V.; Grübe, Ö.; Özkaya, F.C.; Yokeş, M.B.; Uzel, A.; Bedir, E. Cultivable Sponge-Associated Actinobacteria from Coastal Area of Eastern Mediterranean Sea. *Advances in Microbiology,* **2014,** *4*(6).
57. Dharmaraj, S. Marine *Streptomyces* as a novel source of bioactive substances. *World Journal of Microbiology and Biotechnology,* **2010,** *26*(12), 2123–2139.
58. Feling, R. H.; Buchanan, G. O.; Mincer, T. J.; Kauffman, C. A.; Jensen, P. R.; Fenical, W. Salinosporamide A: A Highly Cytotoxic Proteasome Inhibitor from a Novel Microbial Source, a Marine Bacterium of the New Genus Salinospora. *Angewandte Chemie International Edition,* **2003,** *42(3), 355–357.*
59. Ghareeb, M. A.; Tammam, M. A.; El-Demerdash, A.; Atanasov, A. G. Insights about clinically approved and Preclinically investigated marine natural products. *Current Research in Biotechnology.* **2020.**
60. Mitchell, S. S.; Nicholson, B.; Teisan, S.; Lam, K. S.; Potts, B. C. M. Aureoverticillactam, a Novel 22-Atom Macrocyclic Lactam from the Marine

Actinomycete *Streptomyces aureoverticillatus. Journal of Natural Products,* **2004,** *67*(8), 1400–1402.

61. Bruntner, C.; Binder, T.; Pathom-aree, W.; Goodfellow, M.; Bull, A. T.; Potterat, O.; … Fiedler, H. P. Frigocyclinone, a Novel Angucyclinone Antibiotic Produced by a *Streptomyces griseus* Strain from Antarctica. *The Journal of Antibiotics,* **2005,** *58*(5), 346–349.
62. Manam, R. R.; Teisan, S.; White, D. J.; Nicholson, B.; Grodberg, J.; Neuteboom, S. T. C.; … Potts, B. C. M. Lajollamycin, a Nitro-tetraene Spiro-β-lactone-γ-lactam Antibiotic from the Marine Actinomycete *Streptomyces nodosus. Journal of Natural Products,* **2005,** *68*(2), 240–243.
63. El-Gendy, M. M. A.; Shaaban, M.; Shaaban, K. A.; El-Bondkly, A. M.; Laatsch, H. Essramycin: A First Triazolopyrimidine Antibiotic Isolated from Nature. *The Journal of Antibiotics,* **2008,** *61*(3), 149–157.
64. Waters, B.; Saxena, G.; Wangguı, Y.; Kau, D.; Wrıgley, S.; Stokes, R.; Davıes, J. Identifying Protein Kinase Inhibitors Using an Assay Based on Inhibition of Aerial Hyphae Formation in Streptomyces. *The Journal of Antibiotics,* **2002,** *55*(4), 407–416.
65. Schultz, A. W.; Oh, D. C.; Carney, J. R.; Williamson, R. T.; Udwary, D. W.; Jensen, P. R.; … Moore, B. S. Biosynthesis and Structures of Cyclomarins and Cyclomarazines, Prenylated Cyclic Peptides of Marine Actinobacterial Origin. *Journal of the American Chemical Society,* **2008,** *130*(13), 4507–4516.
66. Carlson, J. C.; Li, S.; Burr, D. A.; Sherman, D. H. Isolation and Characterization of Tirandamycins from a Marine-Derived Streptomyces sp. *Journal of Natural Products*, **2009,** *72*(11), 2076–2079.
67. Moore, B. S.; Trischman, J. A.; Seng, D.; Kho, D.; Jensen, P. R.; Fenical, W. Salinamides, Antiinflammatory Depsipeptides from a Marine Streptomycete. *The Journal of Organic Chemistry,* **1999,** *64*(4), 1145–1150.
68. Maskey, R. P.; Sevvana, M.; Usón, I.; Helmke, E.; Laatsch, H. Gutingimycin: A Highly Complex Metabolite from a Marine Streptomycete. *Angewandte Chemie International Edition,* **2004**, *43*(10), 1281–1283.
69. Itoh, T.; Kinoshita, M.; Aoki, S.; Kobayashi, M. Komodoquinone A, a Novel Neuritogenic Anthracycline, from Marine *Streptomyces* sp. KS3. *Journal of Natural Products,* **2003,** *66*(10), 1373–1377.

70. Dewick, P. D. Secondary Metabolism: The Building Blocks and Construction Mechanisms. *Medicinal Natural Products,* **2008,** 7–38.
71. Cimermancic, P.; Medema, M. H.; Claesen, J.; Kurita, K.; Wieland Brown, L. C.; Mavrommatis, K.; … Fischbach, M. A. Insights into Secondary Metabolism from a Global Analysis of Prokaryotic Biosynthetic Gene Clusters. *Cell,* **2014,** *158*(2), 412–421.
72. Osbourn, A. Secondary metabolic gene clusters: evolutionary toolkits for chemical innovation. *Trends in Genetics,* **2010,** *26*(10), 449 457.
73. Gomez, C.; Olano, C.; Mendez, C.; Salas, J. A. Three pathway-specific regulators control streptolydigin biosynthesis in *Streptomyces lydicus. Microbiology,* **2012**, *158*(Pt_10), 2504–2514.
74. Harvey, B. M.; Mironenko, T.; Sun, Y.; Hong, H.; Deng, Z.; Leadlay, P. F.; … Haydock, S. F. Insights into Polyether Biosynthesis from Analysis of the Nigericin Biosynthetic Gene Cluster in *Streptomyces* sp. DSM4137. *Chemistry & Biology,* **2007**, *14*(6), 703–714.
75. Zheng, Y.; Szustakowski, J. D.; Fortnow, L.; Roberts, R. J.; Kasif, S. Computational Identification of Operons in Microbial Genomes. *Genome Research,* **2001,** *12*(8), 1221–1230.
76. Challis, G. L.; Hopwood, D. A. Synergy and contingency as driving forces for the evolution of multiple secondary metabolite production by *Streptomyces* species. *Proceedings of the National Academy of Sciences,* **2003,** *100*(Supplement 2), 14555–14561.
77. Graham-Taylor, C.; Kamphuis, L. G.; Derbyshire, M. C. A detailed in silico analysis of secondary metabolite biosynthesis clusters in the genome of the broad host range plant pathogenic fungus *Sclerotinia sclerotiorum. BMC Genomics,* **2020,** *21*(1).
78. Palmer, J. M.; Keller, N. P. Secondary metabolism in fungi: does chromosomal location matter? *Current Opinion in Microbiology,* **2010,** *13*(4), 431–436.
79. Farman, M. L. Telomeres in the rice blast fungus *Magnaporthe oryzae:* the world of the end as we know it. *FEMS Microbiology Letters,* **2007,** *273*(2), 125–132.
80. McArthur, M.; Bibb, M. In vivo DNase I sensitivity of the *Streptomyces coelicolor* chromosome correlates with gene expression: implications for bacterial chromosome structure. *Nucleic Acids Research,* **2006,** *34*(19), 5395–5401.

81. Begani, J.; Lakhani, J.; Harwani, D. Current strategies to induce secondary metabolites from microbial biosynthetic cryptic gene clusters. *Annals of Microbiology*, **2018,** *68*(7), 419–432.
82. Nützmann, H. W.; Schroeckh, V.; Brakhage, A. A. Regulatory Cross Talk and Microbial Induction of Fungal Secondary Metabolite Gene Clusters. *Natural Product Biosynthesis by Microorganisms and Plants, Part C,* **2012**, 325–341.
83. Fu, T. J.; Singh, G.; Curtis, W. R. Plant Cell and Tissue Culture for Food Ingredient Production: An Introduction. *Plant Cell and Tissue Culture for the Production of Food Ingredients*; Fu, T. J.; Singh, G.; Curtis, W. R., Eds.; Springer Science+Business Media New York; 1999.
84. Frisvad, J. C. Media and Growth Conditions for Induction of Secondary Metabolite Production. *Fungal Secondary Metabolism*, **2012,** 47–58.
85. Baral, B.; Akhgari, A.; Metsä-Ketelä, M. Activation of microbial secondary metabolic pathways: Avenues and challenges. *Synthetic and Systems Biotechnology*, **2018.**
86. Abdelmohsen, U. R.; Grkovic, T.; Balasubramanian, S.; Kamel, M. S.; Quinn, R. J.; Hentschel, U. Elicitation of secondary metabolism in actinomycetes. *Biotechnology Advances*, **2015**, *33*(6), 798–811.
87. Chen, G.; Wang, G. Y. S.; L, X.; Waters, B.; Davıes, J. Enhanced Production of Microbial Metabolites in the Presence of Dimethyl Sulfoxide. *The Journal of Antibiotics*, **2000,** *53*(10), 1145–1153.
88. Pettit, R. K. Small-molecule elicitation of microbial secondary metabolites. *Microbial Biotechnology*, **2010,** *4*(4), 471–478.
89. Ezaki, M.; Iwami, M.; Yamashita, M.; Komori, T.; Umehara, K.; Imanaka, H. Biphenomycin A production by a mixed culture. *Appl Environ Microbiol*. **1992**, *58*, 3879-82.
90. Luti, K. J. K.; Mavituna, F. *Streptomyces coelicolor* increases the production of undecylprodigiosin when interacted with *Bacillus subtilis*. *Biotechnology Letters*, **2010,** *33*(1), 113–118.
91. Noordin, M.; Venkatesh, V.; Sharif, S.; Elting, S.; Abdullah, A. Application of response surface methodology in describing the performance of coated carbide tools when turning AISI 1045 steel. *Journal of Materials Processing Technology*, **2004,** *145*(1), 46–58.

92. Speed, T. Statistics for Experimenters: Design, Innovation, and Discovery. *Journal of the American Statistical Association,* **2006,** *101*(476), 1720–1721.

93. Kansal, H. K.; Singh, S.; Kumar, P. Parametric optimization of powder mixed electrical discharge machining by response surface methodology. *Journal of Materials Processing Technology,* **2005,** *169*(3), 427-436.

94. Khan, N.; Yılmaz, S.; Aksoy, S.; Uzel, A.; Tosun, Ç.; Kirmizibayrak, P. B.; Bedir, E. Polyethers isolated from the marine actinobacterium *Streptomyces cacaoi* inhibit autophagy and induce apoptosis in cancer cells. *Chemico-Biological Interactions,* **2019.**

95. Tsujı, N.; Nagashıma, K.; Kobayashı, M.; Wakısaka, Y.; Kawamura, Y.; Kozukı, S.; Mayama, M. Two new antibiotics, A-218 and K-41 isolation and characterization. *The Journal of Antibiotics,* **1976,** *29(1), 10–14.*

96. Tsujı, N.; Nagashıma, K.; Eruı, Y.; Torı, K. *Structure Of K-41b,* A New Diglycoside Polyether Antibiotic. *The Journal of Antibiotics,* **1979,** *32*(2), 169–172.

97. Chen, J.; Gui, C.; Wei, Q.; Liu, J.; Ye, L.; Tian, X.; … Ju, J. Characterization of Tailoring Methyltransferases Involved in K-41A Biosynthesis: Modulating Methylation to Improve K-41A Anti-infective Activity. *Organic Letters,* **2020.**

98. Cheng, X. C.; Jensen, P. R.; Fenical, W. Arenaric Acid, a New Pentacyclic Polyether Produced by a Marine Bacterium (Actinomycetales). *Journal of Natural Products,* **1999,** *62*(4), 605–607.

99. Otoguro, K.; Ishıyama, A.; U, H.; Kobayashı, M.; Manabe, C.; Yan, G.; … Omura, S. *In Vitro* and *In Vivo* Antimalarial Activities of the Monoglycoside Polyether Antibiotic, K-41 against Drug Resistant Strains of Plasmodia. *The Journal of Antibiotics,* **2002**, *55*(9), 832–834.

100. Sulik, M.; Maj, E.; Wietrzyk, J.; Huczyński, A.; Antoszczak, M. Synthesis and Anticancer Activity of Dimeric Polyether Ionophores. *Biomolecules,* **2020,** *10*(7), 1039.

101. He, R.; Wang, B.; Wakimoto, T.; Wang, M.; Zhu, L.; Abe, I. Cyclodipeptides from Metagenomic Library of a Japanese Marine Sponge. *Journal of the Brazilian Chemical Society,* **2013.**

102. Deslauriers, R.; Grzonka, Z.; Schaumburg, K.; Shiba, T.; Walter, R. Carbon-13 nuclear magnetic resonance studies of the conformations of cyclic dipeptides. *Journal of the American Chemical Society,* **1975,** *97*(18), 5093–5100.

103. Guo, J. P.; Tan, J. L.; Wang, Y. L.; Wu, H. Y.; Zhang, C. P.; Niu, X. M.; … Zhang, K. Q. Isolation of Talathermophilins from the Thermophilic Fungus *Talaromyces thermophilus* YM3-4. *Journal of Natural Products,* **2011,** *74*(10), 2278–2281.
104. Abbamondi, G. R.; De Rosa, S.; Iodice, C.; Tommonaro, G. Cyclic Dipeptides Produced by Marine Sponge-Associated Bacteria as Quorum Sensing Signals. *Natural Product Communications,* **2014,** *9*(2), 1934578X1400900.
105. Nishanth, S. K.; Nambisan, B.; Dileep, C. Three bioactive cyclic dipeptides from the *Bacillus* sp. N strain associated with entomopathogenic nematode. *Peptides,* **2014,** *53,* 59–69.
106. Hernández, I. L. C.; Macedo, M. L.; Berlinck, R. G. S.; Ferreira, A. G.; Godinho, M. J. L. Dipeptide Metabolites from the Marine Derived Bacterium *Streptomyces acrymicini. J. Braz. Chem. Soc*., **2004**, *15*(3), 441-444.
107. Lowell, S. Y.; Kelley, R. T.; Monahan, M.; Hosbach-Cannon, C. J.; Colton, R. H.; Mihaila, D. The Effect of Octanoic Acid on Essential Voice Tremor: A Double-Blind, Placebo-Controlled Study. *The Laryngoscope,* **2018.**
108. Scott, G.; Gilead, D. Degradable Polymers. Springer Science+Business Media Dordrecht, 1995.
109. Gefen, O.; Chekol, B.; Strahilevitz, J.; Balaban, N. Q. TDtest: easy detection of bacterial tolerance and persistence in clinical isolates by a modified disk-diffusion assay. *Scientific Reports,* **2017,** *7*(1).
110. Levine, D. P. Vancomycin: A History. *Clinical Infectious Diseases,* **2006,** *42*(Supplement-1), S5–S12.
111. Katahıra, R.; Uosakı, Y.; Ogawa, H.; Yamashıta, Y.; Nakano, H.; Yoshıda, M. UCH9, a New Antitumor Antibiotic Produced by Streptomyces. II. Structure Elucidation of UCH9 by Mass and NMR Spectroscopy. *The Journal of Antibiotics,* **1998,** *51*(3), 267–274.
112. Hong, J. S. J.; Park, S. H.; Choi, C. Y.; Sohng, J. K.; Yoon, Y. J. New olivosyl derivatives of methymycin/pikromycin from an engineered strain of *Streptomyces venezuelae. FEMS Microbiology Letters,* **2004,** *238*(2), 391–399.
113. Shaaban, K. A.; Srinivasan, S.; Kumar, R.; Damodaran, C.; Rohr, J. Landomycins P−W, Cytotoxic Angucyclines from *Streptomyces cyanogenus* S-136. *Journal of Natural Products,* **2011,** *74*(1), 2–11.